Optimization of minor actinides transmutation performances in GEN IV Reactors : fuel cycle and Core aspects

Timothee Kooyman

UNIVERSITE D'AIX-MARSEILLE

ED 352 – PHYSIQUE ET SCIENCES DE LA MATIERE
CEA CADARACHE – DEN/DER/SPRC/LEDC

Thèse présentée pour obtenir le grade universitaire de docteur

Discipline : Physique et Sciences de la Matière
Spécialité : Energie, Rayonnement et Plasma

TIMOTHEE KOOYMAN

AMELIORATION DES PERFORMANCES DE TRANSMUTATION DES ACTINIDES MINEURS DANS LES REACTEURS DE QUATRIEME GENERATION : ASPECTS CYCLE ET CŒURS

*Soutenue le **19/09/2017** devant le jury :*

M. Cheikh Diop	Paris Saclay/INSTN	Examinateur
M. Sylvain David	CNRS/IN2P3	Examinateur
Me Muriel Fallot	Université de Nantes	Examinateur
M. Gert Van Den Eynde	SCK-CEN	Rapporteur
Me Nuria Garcia-Herranz	Universidad Politécnica de Madrid	Rapporteur
M. Gérald Rimpault	CEA Cadarache	Directeur de thèse
M. Laurent Buiron	CEA Cadarache	Invité (Encadrant)

Numéro national de thèse/suffixe local : 2017AIXM0242/014ED352

REMERCIEMENTS

Les remerciements de thèse étant la partie la plus importante (ou du moins la plus lue) du manuscrit, il est rigueur d'y accorder une grande attention. Je vais donc commencer par remercier Laurent Buiron mon encadrant de thèse, pour avoir élevé la blague de mauvais gout au rang d'art et pour avoir toujours été disponible pour discuter sur les estimateurs de transmutation et la physique des réacteurs rapides. J'en profite pour remercier Gérald Rimpault, mon directeur de thèse pour avoir poser les bonnes questions à divers moments de ce doctorat.

Je remercie également mon premier chef de laboratoire, Bruno Fontaine, pour avoir été disponible pour relire ma prose avec des commentaires toujours pertinents et m'avoir permis de partir plusieurs fois en conférences. Profitons-en également pour remercier l'ensemble de l'équipe du SPRC, Fréderic Varaine, ancien chef de service, Jean-Christophe Bosq, nouveau chef de service, et Philippe Dardé, adjoint au chef de service et chef de laboratoire par intérim pendant la dernière année de ma thèse.

Vient ensuite traditionnellement le tour du jury et notamment celui de Gert Van Den Eynde et Nuria Garcia-Herranz pour avoir accepté d'être rapporteurs du présent manuscrit. Je remercie également Cheikh Diop d'avoir accepté de présider mon jury de thèse, ainsi que Sylvain David et Muriel Fallot pour avoir accepté d'y participer.

Et nous voila arrivés à la liste des collègues, amis et connaissances que j'ai pu rencontrer au cours de ces trois années au CEA Cadarache. Nul ordre ou hiérarchie n'est à chercher dans la liste suivante, et si d'aventure votre nom n'y figurait pas, écrivez au journal qui transmettra. Commençons par le laboratoire dans son entièreté, et plus spécifiquement David Blanchet pour m'avoir supporté comme cobureau pendant un an, Pierre Sciora pour sa connaissance de Mat4Dyn et ses remarques sur le code couleur des figures, Marc Vanier parce que c'était mieux avant, Christine Coquelet-Pascal pour toutes les questions de vecteur isotopique plutonium 20xx, et l'ensemble de l'équipe des REPs et ceux que j'ai oublié pour leur bonne humeur générale. Merci également à Benjamin Copperé de m'avoir supporté comme encadrant de stage pendant 4 mois ainsi qu'à Alexandra Herrenschmidt et Claire Boucher pour avoir fourni un support logistique de qualité pendant ces trois ans. J'en profite pour remercier Bernard Valentin du DEC pour le soutien technique sur le design des couvertures et Christine Chabert pour ses remarques sur les impacts du cycle, ainsi qu'Anne Saturnin et Alexandre Allou pour leurs informations sur les contraintes cycle.

Passons maintenant à la communauté troglodyte des doctorants de la cave (car on y vient tous un jour). La liste est également longue, commençons par Nans Odry pour le bureau partagé pendant une année difficile de rédaction pour lui ainsi que David Freynet et Maxence Maillot, ses compagnons de rédaction. Vient ensuite l'équipe des thésards de 3ème année, Valentin, Paul (enfin, seulement à moitié), Luca et Juan Pablo, toujours disponibles pour venir râler un coup sur l'avancement des travaux de thèse. Je remercie également le gang de Phelma, Ludo pour son canapé, Axel pour ses voitures souvent réparées et Virginie pour ses leçons de morale, ainsi que Paul le transfuge de Normandie. Sans les nommer un par un, je remercie également les stagiaires que j'ai vu défiler durant ma thèse ainsi que les nouveaux thésards de première année, dont Maxime Soulard qui eut également à me supporter comme encadrant de stage. La thèse au quotidien aurait surement été moins drôle sans l'ensemble des ces gens.

Un dernier merci à tous les doctorants de l'ASTHEC avec qui j'ai pu partager de bons moments hors du travail et à qui j'ai pu emprunter un canapé ou une voiture, ceux de l'Université qui étaient toujours là malgré parfois un retard dans la communication, l'équipe du NRPE/MNE pour les visites à Paris, mon ancien camarade de stage maintenant passé chez EDF pour les visites à Lyon et les sorties canoé/sous-marin. Je remercie également aussi mes différents colocataires avec une mention spéciale à Simon-François pour les canarderies diverses et variées, ainsi qu'à Lilian pour les soirées de la Bastidonne. Remercions également Pat pour sa caravane et ses fromages de chèvre, ainsi que Cathy et l'équipe du RJH pour les apéros-bricolage.

Tout le monde étant servi ou presque (mais certains ont surement été oubliés, je m'en excuse par avance), il ne me reste plus qu'à remercier Marie-Bérénice pour avoir illuminé la dernière année de cette thèse ainsi que mes parents et ma famille, puis de vous laisser lire la suite de ce manuscrit si le cœur vous en dit.

List of Figures :

List of Tables :

List of Equations:

RESUME EN FRANÇAIS : AMELIORATION DES PERFORMANCES DE TRANSMUTATION DES ACTINIDES MINEURS DANS LES REACTEURS DE QUATRIEME GENERATION : ASPECTS CYCLE ET CŒURS

Points forts :

- ✓ **La transmutation des actinides mineurs est une solution pour réduire l'impact des déchets nucléaires, tant à court terme sur le site de stockage géologique profond qu'à plus long terme vis à vis de leur radio toxicité potentielle.**
- ✓ **L'introduction d'actinides mineurs dans le cycle du combustible a des impacts négatifs tant sur les différentes étapes du retraitement et de la fabrication du combustible que sur le comportement du cœur en transitoire.**
- ✓ **Une méthodologie d'optimisation de la transmutation qui prend en compte l'ensemble de ces contraintes a été développée pendant cette thèse et appliquée aux deux principaux modes de transmutation.**
- ✓ **Dans le mode de transmutation dit hétérogène, les actinides mineurs sont chargés dans des cibles généralement situées en périphérie du cœur. Il a été démontré l'optimalité de l'ajout de modérateur dans ces cibles, ainsi que l'intérêt d'un ajout limité de matière fissile dans la couverture.**
- ✓ **Dans le mode de transmutation dit homogène, les actinides mineurs sont dilués dans le combustible, au prix d'une modification du comportement du cœur en transitoire. Il a été démontré que les cœurs de type CFV avec hétérogénéités géométriques axiales n'étaient que peu perturbés par cet ajout pour les transitoires de perte de débit, et que l'optimisation d'un cœur pour la transmutation passait par un arbitrage entre son comportement durant une perte de débit du circuit secondaire et durant une insertion de réactivité.**
- ✓ **Le mode homogène apparait comme plus prometteur du point des aspects industriels (hors aspects couts) considérés dans cette thèse.**

1) INTRODUCTION

Les réacteurs nucléaires actuels consomment environ 3 à 4 % de la masse de noyaux lourds chargés en cœur au début de cycle sous forme de fission de ^{235}U. Une partie supplémentaire du combustible est utilisé sous forme de ^{239}Pu lui-même produit par capture sur le ^{238}U. 96 % du combustible est donc réutilisable, sous forme d'uranium ou plutonium. Une réutilisation complète de ces matières permettrait à la fois une économie en termes d'uranium fissile et une limitation de la production de noyaux lourds à vie longue dans les déchets nucléaires, ce qui est un objectif de la loi française de 2006 sur la gestion des déchets nucléaires.

Cependant, pour réutiliser efficacement le plutonium, il est alors nécessaire de recycler le combustible nucléaire, c'est-à-dire de le retirer du cœur du réacteur et de lui faire subir un traitement chimique pour séparer les constituants valorisables, uranium et plutonium, des déchets à proprement parler, à savoir les produits de fission et les actinides mineurs. On parle alors de fermeture du cycle du combustible. Les produits de fission sont des noyaux relativement légers issus de la fission des noyaux lourds tels que l'uranium ou le plutonium. Ces noyaux sont considérés comme des déchets non recyclables. Leur exutoire ultime est un site de stockage géologique profond tel que celui actuellement en projet à Bures en France. Ce site doit assurer leur confinement vis-à-vis de la biosphère durant leur décroissance radioactive.

Les actinides mineurs sont des noyaux produits par capture successives sur les isotopes de l'uranium et du plutonium jusqu'à atteindre le neptunium, l'américium et le curium. Dans le cas d'un cycle fermé, ces noyaux lourds sont les principaux contributeurs à la radio toxicité[1] à long terme des déchets nucléaires. Ceci est illustré sur la Figure 1, où l'on voit que, abstraction faite du plutonium, qui est considéré absent des déchets en cycle fermé, les actinides mineurs constituent le contributeur majoritaire à la radio toxicité des déchets à vie longue. Leur élimination totale permettrait de diminuer la radio toxicité à mille ans d'environ 4 ordres de grandeur dans l'exemple donné ici.

Or, il apparait que ces éléments présentent comme tous les actinides une probabilité de fission non nulle. Il est donc possible de les transformer en produits de fission, à durée de vie notablement plus courte, en les soumettant à un flux de neutrons. On parle alors de **transmutation des actinides mineurs**. Plusieurs options existent pour implémenter cette technique mais on s'intéressera principalement à la solution apparaissant la plus réaliste au vu des contraintes techniques actuelles et attendues dans le futur proche, à savoir la transmutation avec multi recyclage des actinides mineurs dans des réacteurs à neutrons rapides. Contrairement à l'exemple illustré précédemment, les actinides mineurs ne vont pas être considérés comme des déchets ultimes lors du retraitement du combustible, mais vont être séparés pour être ensuite rechargés dans le cœur du réacteur.

[1] La radio toxicité d'un élément radioactif est obtenue en pondérant son activité par l'impact biologique des radiations émises par la désintégration de cet élément sur les tissus humains. C'est un indicateur de la dangerosité des déchets nucléaires à vie longue.

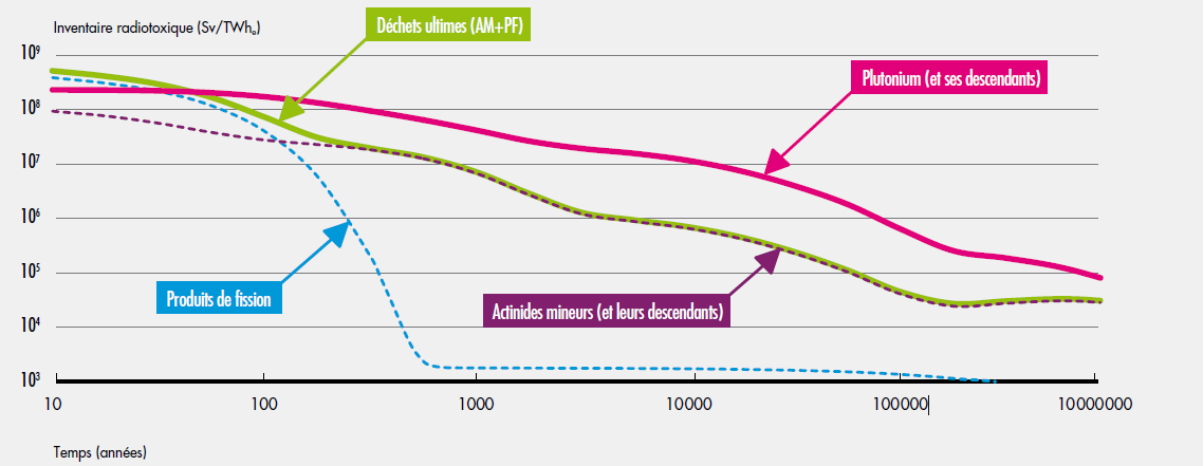

Figure 1 : Evolution dans le temps de la radio toxicité par ingestion d'un combustible usé (UOX 45 GWd/t). (Source : Rapport 2012 sur la gestion des déchets nucléaires, CEA)

Néanmoins, cette approche présente plusieurs inconvénients portant sur l'ensemble du cycle. En effet, les actinides mineurs et leurs noyaux fils produits par irradiation présentent une activité spécifique beaucoup plus importante que celle de l'uranium ou du plutonium, ce qui complique parfois drastiquement les opérations de manipulation, transport et retraitement associées au cycle du combustible. De plus, leur chargement dans le cœur d'un réacteur entraine à la fois une modification du comportement physico-chimique du combustible ainsi qu'une modification des coefficients de contre-réactions propres du cœur, ce qui peut perturber de manière négative le comportement du réacteur lors de transitoire accidentels.

Dans ces conditions, l'objectif de cette thèse était de mettre au point une méthodologie d'optimisation sous contraintes multicritères et multi-objectifs permettant d'optimiser le design d'un cœur de réacteur refroidi au sodium vis-à-vis de ses performances de transmutation des actinides mineurs tout en limitant les impacts à la fois sur le comportement de ce cœur et sur le cycle du combustible associé.

Après une brève analyse physique du procédé de transmutation, les deux principaux modes de transmutation envisagés dans les réacteurs de quatrième génération seront analysés et les résultats de l'optimisation correspondante discutés.

2) ANALYSE PHYSIQUE DE LA TRANSMUTATION

L'évolution du combustible nucléaire sous et hors irradiation obéit à l'équation de Bateman, qui est donnée ci-dessous. Cette équation décrit l'évolution de la concentration en noyaux *i* dans le combustible et peut être décomposée comme suit :

- Un terme de production par interaction d'un noyau *j* avec le flux Φ donnant naissance à un noyau *i*
- La décroissance d'un noyau *k* vers le noyau *i*, processus indépendant du flux
- Un terme de destruction par capture, fission ou réaction (n,xn) sur un noyau *i* vers un noyau *l*
- Un terme de destruction par décroissance du noyau *i* vers un noyau fils *n*.

$$\frac{dN_i}{dt} = \sum_j N_j \sigma_{j\to i}\phi + \sum_k \lambda_{k\to i} N_k - \sum_l N_i \sigma_{i\to l}\phi - \sum_n \lambda_{i\to n} N_i$$

Les noyaux principaux présents dans les combustibles nucléaires et formés par ces différentes réactions sont indiqués dans la Figure 2. D'une manière générale, on peut relier le terme de production d'un actinide mineur *i* à deux choses, à savoir le spectre et la composition isotopique du plutonium utilisé comme combustible. En effet, en observant la Figure 2, on s'aperçoit qu'américium et curium sont formés par capture successives sur les divers isotopes du plutonium à partir du ^{239}Pu. Plus le plutonium utilisé est de bonne qualité, c'est-à-dire riche en ^{239}Pu, plus la probabilité d'aboutir à plusieurs captures successives sans fission sera faible, donc plus la production d'actinides mineurs sera faible. Similairement, on peut définir la probabilité de capture comme le ratio de la section efficace de capture σ_c sur la somme des sections de fission et de capture $\sigma_a = \sigma_f + \sigma_c$. La section de capture diminuant avec l'énergie du neutron incident et la section de fission augmentant avec celle-ci, on voit qu'il y a tout intérêt à utiliser un spectre le plus rapide possible pour limiter la production d'actinides mineurs. Ce concept est illustré pour la section efficace de l'^{241}Am en Figure 3

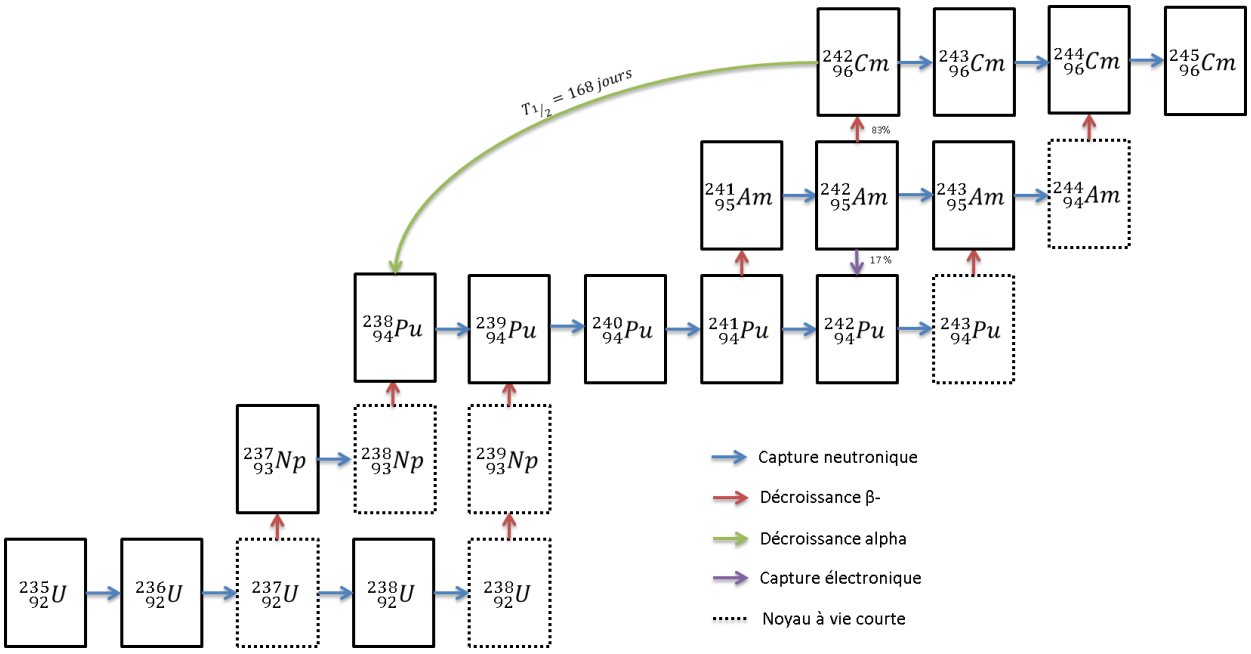

Figure 2 : Chaine d'évolution du combustible nucléaire de l'^{235}U au ^{245}Cm

Cependant, cette production ne peut pas être rendue entièrement nulle, d'où la nécessité de recourir à la transmutation des actinides mineurs et de s'intéresser aux termes de destruction $-\sum_l N_i \sigma_{i\to l}\phi$. La destruction d'un actinide mineur est obtenue une fois qu'il a subi une fission. On pourrait donc supposer qu'il y a également ici tout intérêt à minimiser le rapport capture sur fission de manière à limiter le nombre de captures secondaires pour chaque fission. En effet, on peut observer Figure 2 que la capture d'un neutron par un isotope de l'américium donne en général un nouvel actinide mineur. Cependant, ce faisant la section efficace totale d'absorption diminue, ce qui va faire augmenter le temps d'irradiation nécessaire à atteindre une consommation donnée d'actinides mineurs.

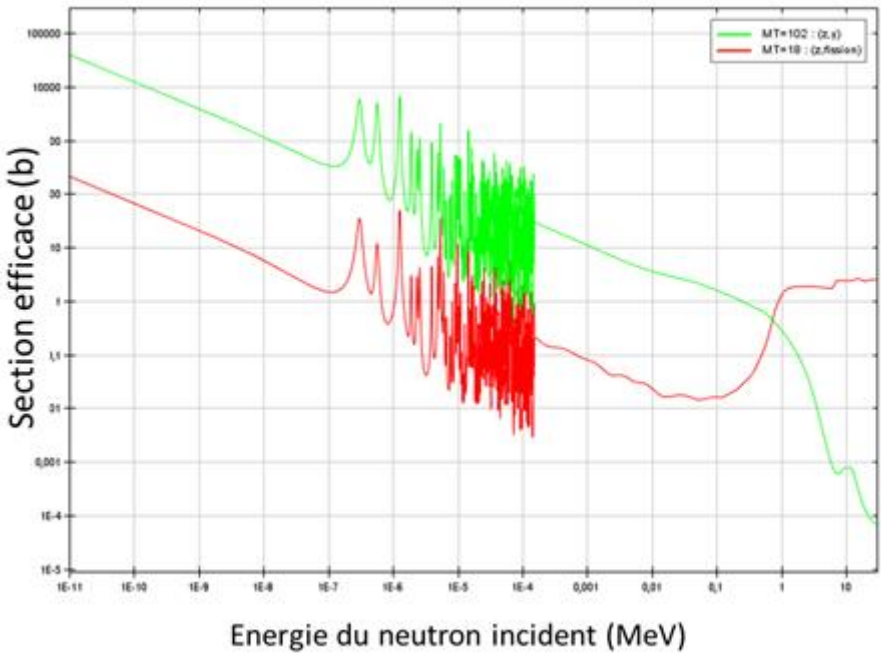

Figure 3 : Section efficace de capture (verte) et de fission (rouge) de l'^{241}Am

Une autre option est de ralentir les neutrons de manière à augmenter la section efficace totale d'absorption, en augmentant cependant le rapport capture sur fission. La consommation totale d'américium va donc augmenter, mais au détriment d'une production accrue de curium, notamment de ^{242}Cm et de ^{244}Cm, qui sont obtenus par capture sur l'^{241}Am et l'^{243}Am, ainsi que de ^{238}Pu produit par décroissance du ^{242}Cm.

Les trois noyaux fils cités ici ne sont pas anodins, car ils présentent une puissance résiduelle et une source neutron intrinsèque beaucoup plus grande que celle du combustible standard. Leur présence dans un assemblage irradié va donc augmenter fortement la charge thermique de celui-ci ainsi que le débit de dose neutron associé.

Or, les opérations de manipulation et de retraitement du combustible sont soumises à des contraintes, principalement liées à la puissance résiduelle maximale acceptable pour éviter un endommagement du combustible ou au débit de dose pendant le transport. Une production plus importante des ces isotopes va donc entrainer l'apparition d'une pénalité sur les diverses étapes du cycle du combustible, soit en augmentant le temps de refroidissement des assemblages usés pour atteindre les contraintes maximales acceptables, ou en nécessitant le développement de nouvelles technologies pour traiter ce type d'assemblage.

On peut ainsi résumer la problématique initiale de ce travail : existe-t-il un spectre et un chargement en actinides mineurs optimal, c'est-à-dire maximisant la consommation d'actinides mineurs tout en minimisant les impacts sur le cycle du combustible, et par extension sur le cœur du réacteur ?

3) OPTIMISATION DU MODE HETEROGENE

Dans le mode hétérogène, les actinides mineurs sont chargés dans des cibles dédiées, situées soit dans le cœur soit en périphérie. Dans ce dernier cas, on parle de Couvertures Chargées en Actinides Mineurs (CCAM). Cette approche présente l'intérêt de séparer physiquement le cycle du combustible électrogène de celui des CCAM, ce qui permet une plus grande flexibilité dans l'irradiation de celles-ci.

Cependant, du fait de leur position hors du cœur, elles sont soumises à un flux plus faible, ce qui réduit la consommation spécifique d'actinides mineurs. Ce faible flux est compensé par une augmentation de la teneur en actinides mineurs dans les couvertures, ce qui implique des impacts plus importants sur les différents postes du cycle du combustible nucléaire. Cette position loin du cœur a néanmoins un intérêt dans la mesure où elle limite fortement les impacts du chargement en actinides mineurs sur le comportement du cœur.

Plusieurs paramètres peuvent être variés pour optimiser la transmutation dans ces couvertures, à savoir :

- Le spectre énergétique des neutrons dans la couverture, qui est ajustable par ajout d'éléments légers qui vont ralentir les neutrons, tels l'oxyde de magnésium MgO ou l'hydrure de zirconium ZrH_2, ou par l'incorporation d'éléments fissiles dans les couvertures comme le plutonium ou l'^{235}U, qui vont entrainer un durcissement du spectre
- La teneur en actinides mineurs dans les couvertures, et principalement ici leur teneur en américium. On peut également considérer l'isotopie de l'américium chargé.
- Le temps de séjour des couvertures dans le cœur, qui est principalement limité par des considérations mécaniques liées à la résistance des matériaux de structure à l'irradiation.
- Le niveau de flux dans les couvertures, qui est fonction du cœur de réacteur considéré et du spectre neutronique.

Il a été démontré dans ce travail qu'il était possible d'évaluer l'ensemble des configurations possibles de CCAM à l'aide de ces seuls quatre paramètres. Plusieurs indicateurs sont nécessaires pour évaluer les performances de transmutation :

- La production d'Hélium dans le combustible. En effet, du fait de la forte teneur en américium, on observe une forte production d'hélium par décroissance alpha et ainsi une mise sous pression des gaines. La connaissance de cette production permet d'aboutir à un design de couvertures qui respectent les contraintes de résistance des gaines.
- Le taux de transmutation de l'américium dans la couverture, c'est-à-dire la fraction d'américium consommée durant l'irradiation.
- La puissance résiduelle et la source neutron de l'assemblage couverture usé. Ces informations permettent d'évaluer le temps de refroidissement de la couverture et donc d'estimer l'inventaire total d'américium dans le cycle du combustible.

Des méta-modèles sous la forme de réseaux de neurones artificiels ont été construits et validés dans ce travail pour prédire les indicateurs susmentionnés à partir des 4 paramètres décrits précédemment. Un outil de préconception des assemblages couvertures à partir de la donnée de

production d'hélium a également été conçu et couplé à ces méta-modèles pour aboutir à un assemblage optimisé, c'est-à-dire un assemblage respectant les contraintes de résistance associées pour lequel la quantité d'américium consommée est maximale tandis que l'inventaire dans le cycle est minimisé.

Ces méta modèles ont ensuite fait l'objet de diverses applications, avec notamment :

- Un couplage à un algorithme génétique pour évaluer l'ensemble des cas optimaux au sens de Pareto (c'est-à-dire, des cas pour lesquels il n'est pas possible d'améliorer l'ensemble des objectifs sans en dégrader au moins un). Ce couplage a permis de démontrer l'optimalité de l'utilisation de modérateurs hydrogénés comme le ZrH2 dans les couvertures.
- Une analyse des contraintes limitantes pour la transmutation en mode hétérogène. Cette analyse a permis de démontrer que le principal blocage portait sur les contraintes industrielles liées à la manipulation et au transport des assemblages couvertures frais et usés.
- Enfin, une analyse plus générale des designs possibles a été menée et est illustrée en Figure 4. Cette figure représente l'ensemble de l'espace des designs de couvertures potentiels avec en abscisses la concentration en américium dans le milieu combustible et en ordonnées la dureté du spectre neutronique. Les points verts correspondent à des assemblages non physiques, c'est-à-dire pour lesquels le spectre est trop dur par rapport à la masse chargée ou trop mou par rapport à la teneur en modérateur considérée. Les points rouges correspondent à des points non faisables par design, c'est-à-dire pour lesquels il impossible de concevoir un assemblage dont les gaines tiennent la mise sous pression due à la production d'hélium. Les points noirs sont des points pour lesquels les contraintes de fabrication ne sont pas satisfaites, et enfin les points bleus sont les points qui sont considérés comme faisables. Les deux cartes de couleur représentent respectivement l'inventaire en américium dans le cycle et la consommation d'américium par assemblage au cours de l'irradiation. On remarque notamment que la zone située en bas à droite de la partie colorée, qui correspond aux assemblages contenant de l'hydrure de zirconium présente les consommations plus élevées pour des inventaires relativement limités, ce qui confirme qualitativement l'optimalité de cette solution. On remarquera également l'illustration de l'impact négatif de la modération sur l'inventaire à la légère pente de la courbe d'iso-inventaire pour de fortes teneurs.

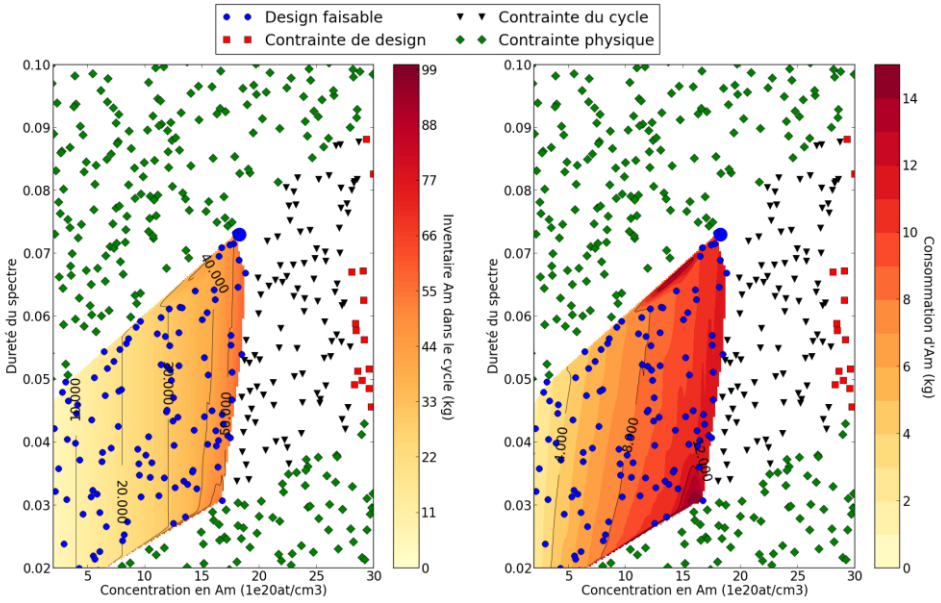

Figure 4 : Illustration des résultats de la méthodologie pour une optimisation simultanée de l'assemblage, de l'inventaire et de la consommation en américium. Une irradiation de 4100 jours à pleine puissance dans un cœur de 3600 MWTh à combustible oxyde été considérée, soit une fluence de 2.3 10^{23} n/cm^2 sur l'ensemble de l'irradiation. Une puissance résiduelle maximale de 7.5 kW a été considérée pour le retraitement des couvertures.

Une approche complémentaire basée sur l'ajout d'éléments fissiles dans les couvertures a également été faite. L'ajout de ces éléments permet à la fois de durcir le spectre neutronique, ce qui agit positivement sur la puissance résiduelle des couvertures usées mais aussi d'augmenter le niveau de flux, ce qui augmente le taux de transmutation. Il a ainsi été démontré que cette solution pouvait être équivalente, voire meilleure, que l'utilisation de modérateur hydrogéné. Les incertitudes associées à ces calculs ont également été évaluées, avec une incertitude sur la consommation de l'ordre de 3%, et de 5% sur l'inventaire.

Enfin, les performances d'une approche basée sur un cœur métal ont été également été caractérisées et comparées à celle d'un cœur de type oxyde et il apparait que le combustible métallique de type UAm10Zr pourrait être une alternative d'intérêt pour la transmutation en mode hétérogène. Ceci tient notamment au fait que la production d'actinides mineurs dans un cœur métallique est environ 2,5 fois plus faible que dans un cœur oxyde pour des consommations similaires dans les couvertures.

4) OPTIMISATION DU MODE HOMOGENE

Dans le mode homogène, les actinides mineurs sont mélangés directement dans le combustible du réacteur avec des teneurs de l'ordre de quelques pourcents. De ce fait, ils sont placés dans une zone de haut flux, ce qui améliore les performances de transmutation, mais durcit également le spectre dans le réacteur, ce qui modifie les coefficients de contre réaction du cœur tels que la vidange sodium, l'effet Doppler ainsi que les différents effets de dilatation du combustible et des structures environnantes.

Cette modification des contre réactions entraine une perturbation du comportement du cœur lors de transitoires accidentels qu'il est nécessaire d'évaluer. Pour ce faire, trois transitoires

hypothétiques supposés enveloppes du comportement réel du cœur ont été sélectionnés, à savoir :

- Une perte totale du débit sodium dans le circuit primaire sans chute des barres (ULOF).
- Une perte totale du débit sodium dans le circuit secondaire sans chute des barres (ULOHS)
- L'extraction intempestive d'une barre de contrôle sans chute des barres voisines, ce qui entraine une insertion de réactivité dans le cœur (UTOP).

De la même manière que pour le cas hétérogène, des réseaux de neurones ont été construits et validés pour évaluer les coefficients de contre réactions du cœur ainsi que ses performances de transmutation et les impacts associés sur le cycle du combustible à partir d'un nombre de variables restreints : puissance du cœur, teneur en actinides mineurs, géométrie du cœur, etc.…

Les coefficients de contre réactions ainsi calculés ont ensuite été utilisés pour évaluer le comportement du code en transitoire à l'aide d'un code de dynamique simplifié et on a cherché une nouvelle fois à obtenir l'ensemble des cas optimaux vis-à-vis à la fois des performances de transmutation et des impacts cycle et cœurs.

Une première conclusion obtenue ici est l'absence d'impacts négatifs sur le comportement d'un cœur hétérogène durant un transitoire de débit primaire ou secondaire. Un cœur hétérogène est un cœur présentant des hétérogénéités axiales telles qu'une plaque fertile interne ou un plenum sodium au dessus du combustible actif, par opposition à un cœur homogène dans lequel la structure axiale du combustible est identique.

L'addition d'actinides mineurs dans le cœur d'un réacteur homogène entraine une diminution de l'effet Doppler et une augmentation de l'effet de vidange, les deux effets contribuant à une insertion positive de réactivité lors d'un ULOF. En conséquence, l'ajout d'actinides mineurs dégrade les performances en transitoire de ce type de cœur. A l'inverse, dans un cœur hétérogène, l'effet Doppler contribue positivement à la réactivité totale lors d'une perte de débit primaire ou secondaire du fait du refroidissement du combustible. L'ajout d'actinides mineurs va donc entrainer une baisse de la valeur absolue de l'effet Doppler, qui se traduit par une diminution de la réactivité insérée par l'effet Doppler. Cette diminution est compensée par l'augmentation de l'effet de vidange, d'où l'absence d'effets importants sur la réactivité totale et donc sur le comportement du cœur. Ceci est illustré dans le Tableau 1. On peut voir que les transitoires de débit n'ont effectivement pas d'impact sur le comportement d'un cœur hétérogène mais un impact significatif sur l'UTOP.

Tableau 1: Comparaison du comportement d'un cœur homogène et d'un cœur hétérogène de 3600 MWth entre 0et 5% de teneur américium

ULOF température sodium maximale (°C)	0 % Am	5 % Am
Homogène	1332	1557
Hétérogène	1027	1026

ULOHS température sodium finale (°C)	0 % Am	5 % Am
Homogène	825	810
Hétérogène	709	703

UTOP température maximale du combustible (°C)	0 % Am	5 % Am
Homogène	2180	2330
Hétérogène	2390	2446

En effet, durant un UTOP, la contre réaction de vidange n'influe que très peu sur le transitoire, tandis que le Doppler est responsable de l'évolution du cœur. La baisse du Doppler due à l'ajout d'actinides mineurs entraine donc une augmentation plus importante de la température combustible pour compenser l'insertion de réactivité positive, et donc un échauffement plus important du combustible.

Les informations sur les transitoires à considérer pour mettre au point un cœur réaliste étant relativement limitées, il est impossible de donner une image de cœur optimale définitive, celle-ci dépendant nécessairement des transitoires considérés. Cependant, il est possible à des fins illustratives de considérer le cœur permettant de transmuter une masse d'américium maximale au vu de trois transitoires de référence :

- Une perte de débit primaire jusqu'à 10 % du débit primaire avec un temps de demi débit de 24s
- Une perte de débit secondaire linéaire jusqu'à 0 % du débit en 40 s
- Une insertion de 250 pcm en 150 s.

Les performances de cœur ainsi obtenues sont données dans le Tableau 2 et sont comparées aux performances d'une stratégie de transmutation en mode hétérogène optimisée. On constate que la consommation des deux options est quasiment équivalente, mais qu'il faut un temps deux fois plus important dans le cas du mode hétérogène, ce qui s'explique par le niveau de flux plus faible dans les couvertures. De plus, si l'on considère la consommation spécifique, c'est-à-dire ramenée à la production d'énergie pendant l'irradiation, on voit nettement apparaitre l'avantage du mode homogène. En termes d'inventaire, l'inventaire associé au cœur homogène est plus important du fait de la quantité d'américium chargée plus importante. Cependant, on aboutit à une consommation quasiment 5 fois plus élevée pour un inventaire 70 % plus élevé seulement.

Tableau 2 : Comparaison des performances de deux cœurs optimaux vis à vis du chargement en américium (5 at% en homogène, 20 at% en hétérogène)

	Hétérogène	Homogène
Consommation totale (kg)	1428	1422
Temps de séjour (JEPP[2])	5950	3019
Teneur Am dans l'assemblage (at%)	20	4,9
Chargement initial (kg)	1896	3143
Consommation spécifique (kg/TWhe)	2.68[3]	13,5
Inventaire associé (kg)	2710	4935
Température max ULOF (sans DCS[4])	/	999
Température finale ULOHS		664
Température max UTOP		2258

L'application de la méthodologie d'optimisation développée pendant cette thèse a donc permis d'évaluer un grand nombre de configurations de cœurs hétérogènes et d'obtenir des images de cœur optimales en prenant en compte un ou plusieurs transitoires. Il a été également été montré que le comportement de ce type de cœur lors d'une transitoire de débit n'était pas affecté. Enfin, l'analyse d'une configuration optimale et sa comparaison à une situation optimisée de transmutation en mode hétérogène a permis de démontrer le fort intérêt du mode homogène vis-à-vis du mode hétérogène.

5) CONCLUSIONS

La transmutation des actinides mineurs, c'est-à-dire leur transformation en produits de fission à vie courte en les soumettant à un flux de neutrons en réacteur, permettrait de réduire l'impact radiotoxique des déchets nucléaires à vie longue d'environ deux ordres de grandeurs. Cependant, leur chargement dans le cœur du réacteur ainsi que leur introduction dans le cycle du combustible présente certains aspects négatifs : modification du comportement du cœur, activité plus importante des combustibles usés et frais, etc.

Ce travail de thèse a permis de faire la synthèse de l'ensemble de ces impacts pour deux stratégies de transmutation, l'une où les actinides mineurs sont traités de manière séparée, dite mode hétérogène, et l'autre où ils sont directement mélangés avec le combustible nucléaire, dite mode homogène. Cette synthèse effectuée, une méthodologie d'analyse et d'optimisation basée sur l'utilisation de méta-modèles et d'algorithmes génétiques a été développée.

L'optimalité de l'utilisation de modérateur dans les couvertures radiales chargées en actinides mineurs a été démontrée, ainsi que l'intérêt de l'ajout de matière fissile dans les couvertures pour améliorer les performances de transmutation. Le bon comportement des cœurs hétérogènes vis-à-vis d'un chargement en cœur des actinides mineurs a été également été

[2] Jour équivalent pleine puissance

[3] Consommation de 6.90 kg/TWeh dans les couvertures pour une production de 4.22 kg/TWeh dans le cœur

[4] La température sodium ici dépasse la température d'ébullition (≈ 900 °C) mais on suppose l'utilisation de systèmes passifs non modélisés ici permettant d'obtenir une température maximale inférieure à 900 °C.

identifié, notamment en ce qui concerne les transitoires de débit. Ceci a permis de produire une image de cœur optimisée pour la transmutation homogène et de démontrer l'intérêt de la transmutation en mode homogène du fait de l'absence d'impact significatif sur les performances du cœur.

Ces résultats doivent maintenant être consolidés, notamment au niveau des calculs cœurs en sélectionnant des configurations optimales et en évaluant leurs performances en transitoire à l'aide de codes de calculs plus évolués. Il serait également nécessaire dans un second temps de coupler cette méthodologie d'optimisation à un code de scénario industriel de manière à pouvoir évaluer les impacts des différentes stratégies à l'échelle de la durée de fonctionnement d'un réacteur.

Il a également été démontré que quelque soit le mode de transmutation choisi, les contraintes liées au cycle sont prédominantes par rapport à celles liées au cœur. La R&D sur les installations du cycle est donc un préalable nécessaire à la mise en œuvre d'un scénario de transmutation quel qu'il soit.

CHAPTER 1: INTRODUCTION

Highlights:

- ✓ **It is possible to close the nuclear fuel cycle using fast reactors.**
- ✓ **In this case, minor actinides (neptunium, americium and curium) are the main contributors to long radiotoxicity of the spent fuel**
- ✓ **Fast reactors are better suited than thermal reactors to transmute these nuclei, e.g. to turn them into shorter-lived fission products by irradiation.**
- ✓ **However addition of minor actinides in the fuel cycle leads to significant penalties on manufacturing, core behavior during transient and fuel reprocessing.**

The aim of this introductory chapter is first to present some specificities of fast reactors compared to the regular LWR currently found in commercial operation. Then fuel cycle is discussed along with the possibility to move towards a sustainable use of nuclear material: the closed fuel cycle using fast reactors tuned as breeders. Considering such a long term strategy, the produced wastes are then detailed along with the classification of nuclear waste. An emphasis is then made on the specific case of High-Level Waste and the role they would play for the final repository design, which leads to introduce the concept of transmutation and its expected gains.

1) AN HISTORICAL INTRODUCTION TO FAST REACTORS

The early nuclear reactors have been fueled with natural or enriched-uranium, depending on the availability of enrichment technology for the countries aiming at starting a nuclear industry. Thus, the US started using LWR while France, Britain and Canada designed reactors which could operate using only natural uranium, such as the UNGG, MAGNOX or CANDU reactors respectively.

It had been noticed early in the nuclear era (and readily used in the nuclear weapon program) that some plutonium isotopes and especially ^{239}Pu were as good a nuclear fuel as ^{235}U. However, this element is not directly available in nature and must be "bred" in nuclear reactors by neutron capture on ^{238}U following the reaction shown in Equation 1.

$$^{238}_{92}U + ^{1}_{0}n \rightarrow ^{239}_{92}U \xrightarrow{\beta\ (23.45\ \mathrm{m})} ^{239}_{93}Np \xrightarrow{\beta(2.35\ d)} ^{239}_{94}Pu$$

Equation 1 : Production route of ^{239}Pu

It quickly appeared that, given the right conditions, a plutonium-fueled reactor could produce enough neutrons to *breed enough plutonium to replace the one it consumed.* In such a reactor, called **breeder**, the fuel is in fact ^{238}U, which is turned in ^{239}Pu and then reused. This completely

removes the need for ^{235}U enrichment which currently exists for LWR and also permits the use of the important stockpiles of depleted uranium which are accumulating in enrichment plants around the world.

By 1955, a first breeder was built in the US, called EBR-I, and it soon demonstrated that achieving a breeding gain higher than one was possible in practice at core scale. The breeding ratio or breeding gain is defined as the ratio of the mass of plutonium produced over the mass consumed. However, to achieve such a feature, specific conditions are required. A breeder core operating with the $^{238}U/^{239}Pu$ fertile/fissile couple must have a **fast** neutron spectrum, to make use of the increased neutron production from ^{239}Pu in the relevant high energy range. This means that light or heavy water cannot be used as coolant, as they are also a very efficient neutron moderator and thus would slow down the neutrons to an energy range in which breeding is not possible. Consequently, liquid metals or helium must be used. EBR-I was itself cooled with a eutectic mixture of sodium and potassium. This adds engineering constraints which proved to be difficult to handle and also modify the behavior of the core compared to a regular LWR, as it will be discussed later.

With the first oil crisis in 1973 and the consequent surge in reactor construction which followed, the perspective of a shortage of uranium in the medium term became more realistic [1] and as a consequence the breeder solution looked even more attractive. By then, the main focus for fast reactor design was to lower the so-called doubling time, which is the time necessary to produce enough plutonium in a single core to start a new reactor. Consequently, the emphasis was put on obtaining the highest achievable breeding gain, for instance by using external “blankets” of fertile material to make use of the important neutron leakage in a fast reactor. However, the combined effects of Three Mile Island, Chernobyl accidents and the discovery of new important reserves of uranium strongly played against the commissioning of breeder reactors and only a handful of reactors were ever build and operated since. Political choices regarding reprocessing also oriented research towards other fuel cycles.

However, considering the recent ramp-up in the construction program in China and around the world, the economic incentive to build fast reactors reappeared. Indeed, it is expected that breeder reactors could become competitive compared to current thermal reactors by the end of the century [2].

The design main focus point moved from doubling time to safety features. Early design required the use of numerous active safety systems to prevent core damage in case of accidents and with the evolution of safety measures, the main design consideration is now to have a core which relies as much as possible on passive safety systems than on active systems. Others goals, notably on the economic side, have been set up for next generation of commercial nuclear reactors by the Gen IV Forum [3]

The objectives set up by the GIF are the following:

- Sustainability: a Gen IV reactor should provide clean energy while minimizing the long-term stewardship burden of the nuclear waste it produces
- Economics : a Gen IV reactor should have a life-cycle cost advantageous compared to other energy sources and the same level of financial risk

- Safety and reliability : a Gen IV should have a very low likelihood of core damage, eliminate the need for offsite emergency response and have an otherwise excellent safety and reliability
- Proliferation resistance : Gen IV reactors and associated fuel cycles should made the diversion of weapons-usable materials difficult and unattractive

Any new design should focus on these goals and how to reach them. CEA is currently working on a new prototype of sodium-cooled fast reactor called ASTRID which is aimed at having a new core design featuring such advantages which should prepare the future deployment of fast reactors.

In the next part, we will introduce some specific aspects of fast reactor design, which differs from conventional LWR design.

2) AN INTRODUCTION TO FAST REACTOR DESIGN

In essence, a fast reactor is similar to a LWR, with a core in which a sustainable fission chain reaction produces power, which is extracted by the primary coolant. The heat is then used to produce steam and drive a turbine linked to an alternator producing electricity. However, some specificities exist and should be mentioned here. We will take the example of a sodium fast reactor, which is shown in Figure 5. Three reactors of this kind were built in France and thus most of the experience in fast reactors lies in this system.

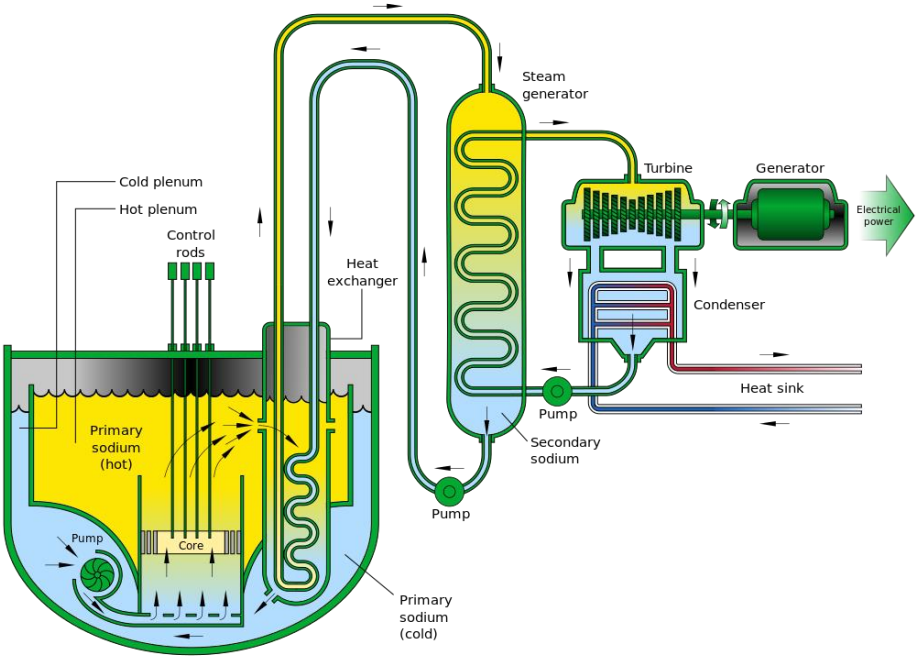

Figure 5 : Sodium fast reactor schematic

a) THE CORE

As their name suggests, fast reactors exhibit a fast neutron spectrum. This is illustrated shown in Figure 6, where a fast spectrum is compared to a thermal reactor spectrum. As cross sections globally decrease with the neutron incident energy, the level of flux must be higher than in a

thermal reactor to obtain the same reaction rate and then the same power. Consequently, a typical fast reactor flux is around 10^{15} n/cm^2/s compared to 10^{14} n/cm^2/s for a thermal one.

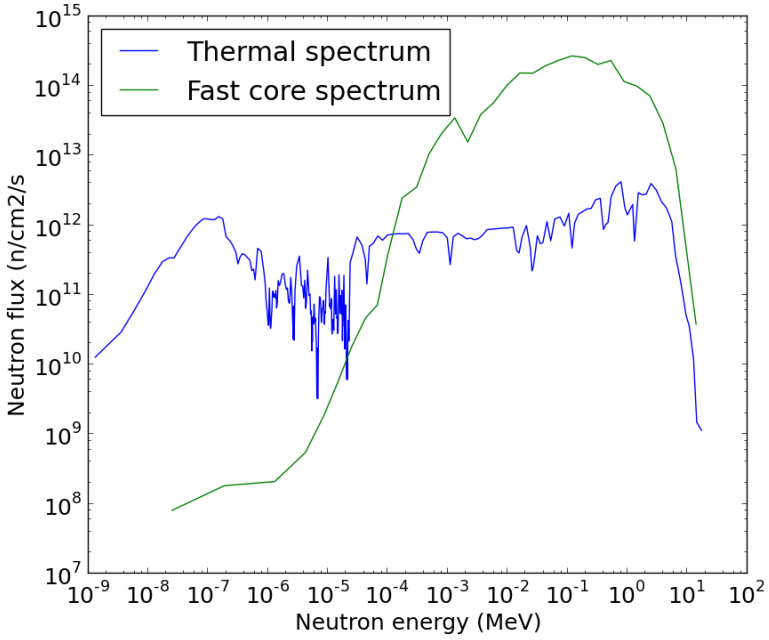

Figure 6 : Comparison of the neutron Fluxes between fast and thermal reactors

In order to minimize the cost and the overall mass of fuel to be handled, there is an incentive to minimize the core fissile inventory. This leads to smaller cores than thermal reactors. To achieve a higher packing ratio of the assemblies in the core, a hexagonal lattice is used instead of a square one.

Early design of fast reactors made use of "blankets", which are assemblies loaded with fertile material (^{238}U here), which are placed at core periphery and produce plutonium by capturing leaking neutrons. These blankets also act as neutron reflector for the core. However, such a system may lead to proliferation issues, as it can be easily diverted for military plutonium production. Consequently, new designs with internal blankets have been promoted, where the fissile and fertile fuel are axially mixed inside the assemblies to minimize the proliferation risk [4].

Several coolants can be used to extract heat from the core:

- Sodium alone, or with potassium in a NaK eutectic. This is the most common coolant used so far, as it has similar properties to water in terms of heat capacity and density. However, it is opaque and is very reactive with water and air, which complicates in service inspection and refueling and add a new hazard to reactor operation. A secondary sodium circuit is used between the primary sodium and the steam generator, to avoid the possibility of a sodium-water reaction with activated sodium from the primary circuit.
- Lead alone, or with bismuth in a lead-bismuth eutectic (LBE). This specific combination was used by Russia for nuclear submarines with a relative success. LBE is heavier than sodium and with slightly a higher melting temperature than sodium. Its high boiling

point is an asset in case of accidents. However, it requires very fine control of the oxygen concentration in the coolant to prevent aggressive oxidation effects and the high melting point means that operation at low power is less easy. Finally, bismuth yields polonium by neutron capture which is a very potent alpha emitter.

- Helium, which requires a very high pressurization of the core vessel and an important mass flow to effectively remove heat from the core. However, it is transparent, which facilities in-service inspection and repair and is totally transparent to neutron and thus not activated during irradiation.

b) THE ASSEMBLY

In order to reach a high breeding ratio, fast reactor cores should exhibit a rather large fuel volume fraction. Given the good thermal hydraulic features of the sodium used as a coolant, it is possible to choose a sub-assembly design where coolant volume fraction is limited. Therefore, liquid metal fast reactors assemblies are made of pin bundles with a diameter between 5 and 10 mm and between 169 and 397 pins per assembly. The pins are separated by a spacing wire running helicoidally around the pins. The assemblies are lined with a hexagonal duct of a few millimeters thickness and there is thus no cross-flow in a fast reactor core, as in a BWR for instance. A typical SFR assembly is given in Figure 7.

The fuel pellets inside the pins can incorporate a central hole and are clad in a stainless steel alloy which can be ferritic or martensitic steel (AIM1, ODS or 15-15 Ti) and is chosen purely on mechanical properties. Indeed, the fast spectrum obviates the need for zirconium in the cladding, as fast neutron interactions with stainless steel are very limited. The hexagonal duct is also made of stainless steel.

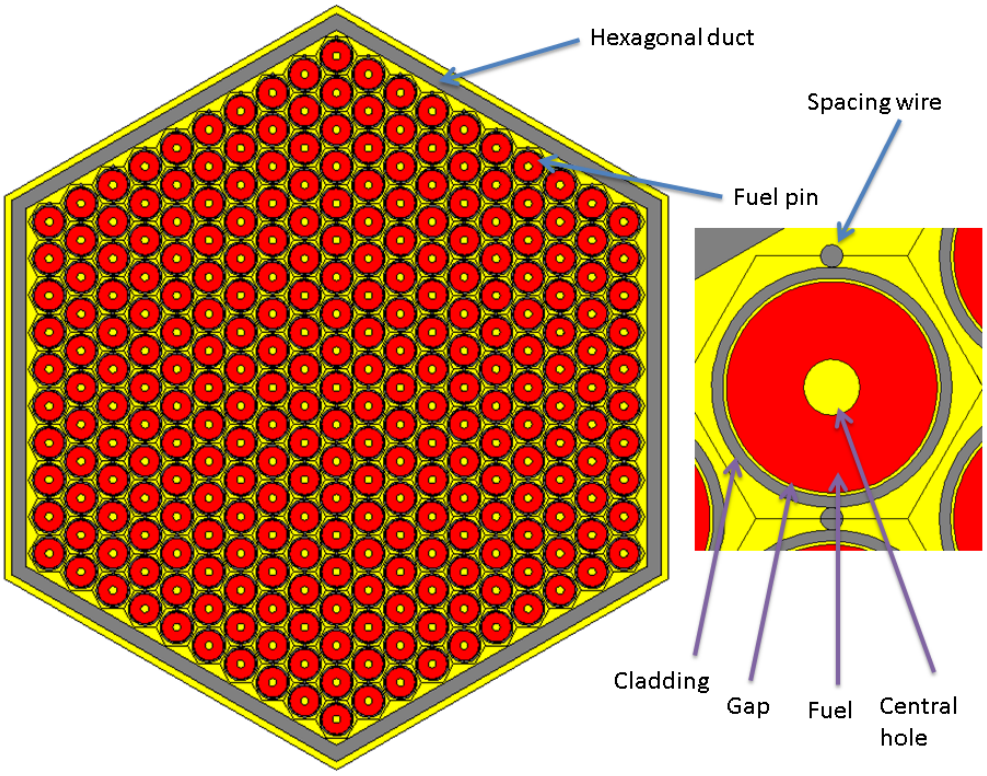

Figure 7 : SFR assembly and pin

c) THE FUEL

Different kinds of fuels have been tested for fast reactors. The first fast reactor ever built, EBR-I, was fueled with a metallic fuel, which has several advantages:

- It has the highest density of heavy nuclides, which leads to a better breeding gain.
- It gives amongst the faster neutron spectrum as there is no moderating material in the fuel, which is also beneficial to the breeding gain.
- It has a very good thermal conductivity, which allows high linear heat rating

However, early metallic fuel had a high tendency to swell under irradiation which led to fuel-cladding interaction and thus limited the achievable burn-up. This effect can be lowered by increasing the smeared density of the fuel but this offsets the density gain. Its low melting point is somehow compensated by its good thermal conductivity.

Fast reactors designed and operated in France, namely PHENIX and SUPERPHENIX have been fueled with uranium-plutonium dioxide. It has a very good radiation-resistance and can thus tolerate important burn-ups, and its high melting temperature compensates for its low thermal conductivity. However, due to the presence of oxygen in the fuel, the spectrum is slightly softened and combined with a lower density, the achievable breeding gain is lower than in the metal case. The main advantage of oxide fuel is the advantage of several decades of industrial experience on the use of this fuel, as it is also used in current thermal reactors, mostly as uranium dioxide and in selected reactors as uranium plutonium dioxide, the so-called MOX fuel.

Carbide and nitride fuels were also investigated as potential fuels for fast reactors. Like oxide, they are refractory materials with a high melting point but have both better thermal conductivity and density than oxide, which leads to a higher breeding ratio and a lower fissile inventory than for oxide. However, their development is still underway and additional irradiation experiments are required to qualify those fuels. India is one of the countries pushing in this direction, where uranium plutonium carbide fuels have been irradiated in the Fast Test Breeder Reactor and then reprocessed [5] but americium carbide remains to be produced. Similarly, nitride fuel manufacturing on a conventional production line has already been demonstrated, but americium nitride transmutation targets are still being studied. In both cases, the main hardship is the low vapor pressure of americium, which evaporates during high temperature phases of the manufacturing process [6].

d) POWER PRODUCTION

Power production in a sodium fast reactor is made with three circuits:

- The primary one with sodium which evacuates the heat from the core.
- The second one, also with sodium to prevent release of activated sodium in case of sodium/water interaction in the steam generators.
- The third one, with water, which drives a turbine for electricity production. The use of steam in the tertiary circuit can lead to damaging steam-sodium interaction in the steam generators which has a negative impact on reactor uptime and overall reliability. A new approach based on gas heat exchangers in a Brayton cycle is currently being investigated at CEA for the ASTRID reactor [7].

In opposition to the PWR case, the core vessel is not under pressure (5 bars of argon), which means the core vessel thickness is much less than in a PWR. Thermal efficiency around 40 % can be reached as the sodium outlet temperature of 550 °C is higher than in the PWR case. For lead cooled reactor, no secondary circuit is needed as lead is not reactive with water. In the helium case, the gas can be directly used to drive the turbine, thus increasing the overall efficiency of the plant.

e) SAFETY

In opposition to the PWR cores, boron dilution cannot be used to control reactivity in the core in liquid metal fast reactors. Consequently, reactivity variations are managed by controls rods and inherent core feedbacks which will be detailed later. Additionally, the fast spectrum decreases the efficiency of the control rods compared to a thermal case, which adds more constraints on their core locations and individual and global reactivity worth. This may require the use of boron-10 enriched controls rods. However, the high breeding gain in the core means that the reactivity swing is much smaller than in a PWR and no Xenon effect occurs in a fast reactor. Consequently, operation of such a reactor is somewhat simpler than the one of a PWR and does not require very efficient control rods.

Due to the fast neutron spectrum, the delayed neutron fraction in such reactors is also lower than in thermal reactor, with values generally around 370 pcm for the effective delayed neutron fraction or $ (which takes into account the spectrum of the delayed neutron source). This increases the sensitivity of the core to reactivity perturbations which however are somewhat milder.

Due to the lack of pressure in the primary circuit, the main accidental transients in a sodium fast reactor are different from the ones generally considered in a thermal reactor. Three of them will be considered in this work:

- The Unprotected Loss of Flow (ULOF), in which due to an external event the sodium flow in the primary circuit stops with the controls rods not falling. In this case, the primary sodium temperature increases and then could stabilize when a natural convection regime is reached. For an intrinsically safe core design, the aim here is to avoid sodium boiling in the core, which would strongly degrade heat exchange with the fuel and lead to potential fuel melting.
- The Unprotected Loss of Heat Sink (ULOHS), in which due to an external event the sodium flow in the secondary circuit stops with the control rods not falling. In this case, the primary and secondary sodium temperature increases and the design goal remain to avoid sodium boiling in either circuit. These two accidents can be combined in what is called a power station blackout, in which all external supply power is lost, thus leading to a stop of all forced sodium flow inside the primary and secondary circuit.
- The Unprotected Transient Over Power (UTOP), in which reactivity is inserted in the core due to various potential events: gas bubble going through the core and displacing the sodium, control rod mechanism malfunction leading to rod ejection or core compaction. In this case, the fuel temperature will mainly increase and the related design objective is to prevent fuel melting during the transient.

The severity of such transients for lead cooled fast reactor is lower thanks to the high thermal inertia and high boiling point of lead. On the other hand, for helium cooled fast reactors, due to the important pressure inside the primary circuit, the possibility of a coolant voiding due to a large break in the primary circuit piping cannot be ruled out.

When considering a given transient, the core behavior can be decomposed into several contributions:

- The Doppler Effect, which comes from the broadening of resonances in the epithermal range due to a temperature increase of the fuel. This effect leads to negative reactivity variation as it increases the neutron absorption rate. This effect is mostly due to the broadening of ^{238}U resonances. It is lower for a core with a metal fuel as the spectrum is harder in such a core and there are fewer neutrons in the lower epithermal range.
- The coolant void Effect, which is due to the removal of coolant from the core, either by thermal expansion up to sodium boiling, movement of a gas bubble in the core or leak. It can be separated in to three contributions :
    - The spectral effect, which comes from the removal of the slight moderation brought by the coolant. It leads to a hardening the spectrum. This effect in reactivity is positive as plutonium and minor actinides produces more neutrons per fission when the spectrum hardens.
    - The leakage effect, which comes from the increased mean-free-path due to the removal of the coolant. This effect is negative in reactivity as it increases the leakage.
    - The capture effect, which is positive and comes from the decrease in capture in the coolant.
- The structures thermal expansion, which decreases the steel concentration due to axial expansion and thus increases reactivity, but also decreases the sodium fraction as the pins expand and thus has the same effect than the coolant void effect.
- Fuel thermal expansion, which axial part brings a negative reactivity as it decreases the fuel density. Radial fuel expansion is neglected in general.
- The grid thermal expansion, which inserts negative reactivity as it separates the fuel assemblies from each other.
- The control rods differential expansion, which has one negative contribution on the core reactivity coming from the relative rods insertion caused by the fuel axial expansion, and one negative contribution coming from the relative rods extraction caused by the structures expansion. Each of these effects operates on a different time-scale as the materials involved are different.

It is not necessary to consider all these effects for preliminary assessment of a core design. Derivation of both the value of the Doppler Effect and of the coolant void worth is enough to obtain a decent idea of a core safety performance. Until recently, coolant void worth up to 5 $ were considered compatible with active safety systems in the core, however a new design has been proposed by CEA with a negative coolant void worth, which a significant gain in terms of passive safety.

However, for a complete “safety” analysis of a core, it is necessary to evaluate its behavior in the case of every possible transient and thus to evaluate the contribution of each of this phenomenon. This will be discussed in more details in Chapter 5.

3) THE NUCLEAR FUEL CYCLE

The nuclear fuel cycle comprises all the operations related to manufacturing, irradiation and reprocessing of the nuclear fuel. It is represented in Figure 8.

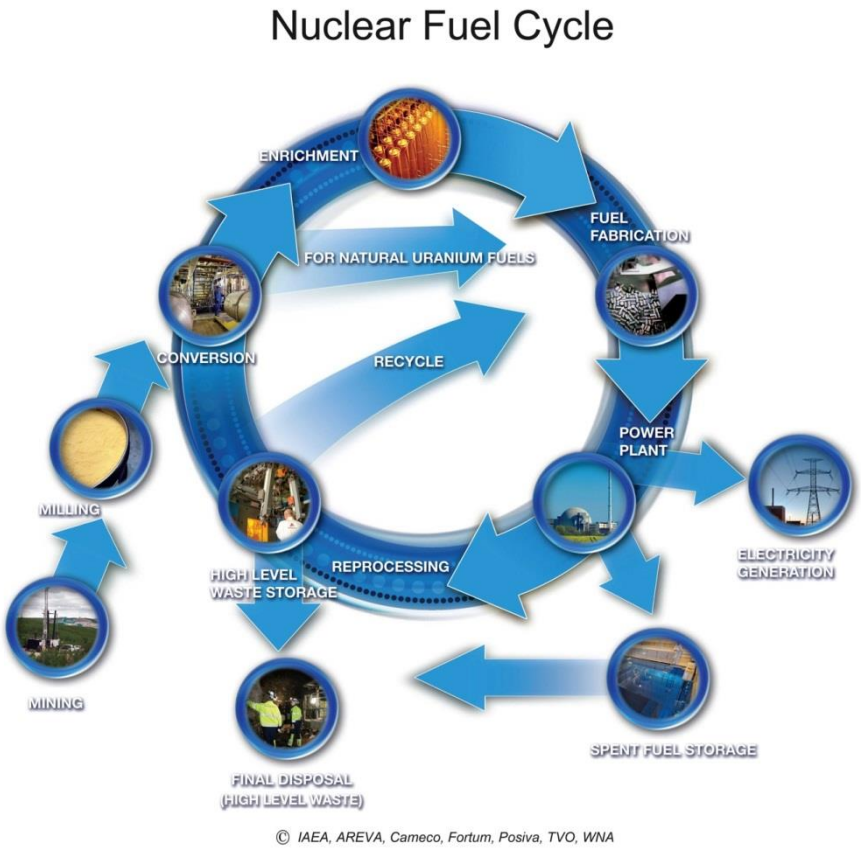

Figure 8 : The nuclear fuel cycle

a) FRONT-END

The front-end of the nuclear fuel cycle encompass all the activities related to fuel fabrication *before irradiation*. In the case of a conventional enriched uranium fuel, this represents the mining of uranium ore, its conversion into yellow cake and then uranium hexafluoride, the enrichment, the conversion into dioxide power, the fabrication of the pellets and assemblies.

When plutonium is reused, this also includes the manufacturing of new pellets from reprocessed materials and the fabrication of new assemblies.

b) BACK-END

The back-end of the nuclear fuel cycle comprises all the activities related to fuel reprocessing *after irradiation* and conversion into base materials which can be used for manufacturing new fuels assemblies. Spent fuel reprocessing is carried out in France on an industrial basis in the La

Hague plant using the PUREX process, which has been developed in the USA after the Second World War [8] and studied in Europe in the Eurochemic plant in Dessel, Belgium [9]. After being unloaded from the reactor core, the irradiated fuel assemblies are stored in cooling pools on site and allowed to decay in order to decrease their residual gamma emission and decay heat. Once cooled enough, they are transported to the reprocessing facility, where the assemblies are dismantled into pieces, dissolved in nitric acid and separation of uranium and plutonium from the fission products is carried out. Uranium and plutonium are then converted into the adequate form (powder, solution or gaseous) for re-manufacturing.

Plutonium is currently being reused once in thermal nuclear reactors as MOX fuel (mono-recycling) as performed in the French Fleet [10]. Fission products together with minor actinides from UOX-PWR fuels are vitrified into glass packages and sent to final storage while uranium is stored (and partly reused after re-enrichment).

c) CLOSING THE FUEL CYCLE

Closing the nuclear fuel cycle could remove the entire mining process from the front-end by replacing the extracted ^{235}U feed by a plutonium source. It can be achieved using breeder reactors which produce enough plutonium to replace their consumption. In a closed fuel cycle, the irradiated fuel is first allowed to cool down with typical time scales of several years before being reprocessed. The recovered uranium and plutonium are then used for manufacturing new fuel pins while fission products and minor actinides are vitrified and discarded as waste. As a consequence, continuous operation of a reactor requires more than one core in terms of total immobilized fuel. As the reactor must continuously operate, at least two cores must be available so that one is in the reactor while the other one is being reprocessed. Consequently, this implies a bigger inventory in the fuel cycle but a lower flux of waste. A closed fuel cycle is shown in Figure 9.

Closing the fuel cycle thus eliminates the mining process, which has a high environmental impact and the costly enrichment process from the fuel cycle [11]. Additionally, it leads to a sharp decrease in the production of nuclear waste as only the fission products and minor actinides, along with the small losses during reprocessing are sent to waste, plutonium and uranium being reused. However, it increases the proliferation risks as plutonium must be separated from the spent fuel and it also increases the transport of nuclear materials across the country between the various facilities. It should be mentioned here that the PUREX process can be modified into the TRUEX process [12] or the GANEX process [13] in which plutonium is extracted with the minor actinides, thus limiting the proliferation risks.

Using a simplified economic approach, closing the nuclear fuel cycle is only interesting if the price of uranium reaches a certain threshold above which fast reactors can compete with LWRs [2]. However, further considerations going beyond the scope of this study should also be taken into account, such as the CO_2 price or plutonium management schemes.

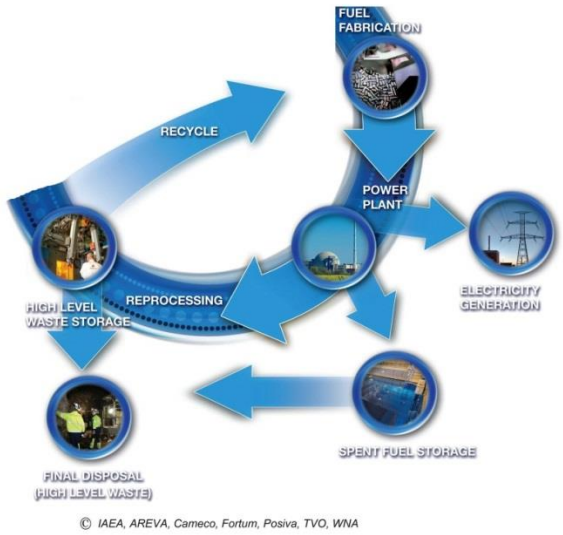

Figure 9 : Closed nuclear fuel cycle

d) WASTE MANAGEMENT

Nuclear waste is currently divided into several categories summarized in the table below. We will mainly focus here on the case of the waste with a high activity and long half-lives (HL), or HLW for High-Level waste. In a closed cycle, HLW includes all the fission products and minor actinides extracted during reprocessing, plus a small fraction of plutonium and uranium corresponding to the inherent losses during reprocessing. Currently, HLW comprises the irradiated MOX assemblies along with the uranium oxide assemblies which are not reprocessed. Only about two thirds of the spent uranium oxide fuel assemblies are currently reprocessed as only 22 reactors are fueled with MOX.

Table 1 : ANDRA nuclear waste classification from [14]

<table>
<tr><td rowspan="6">Activity</td><td></td><td colspan="3">Half life</td></tr>
<tr><td></td><td>Very short HL (< 100 days)</td><td>Short HL (< 31 years)</td><td>Long HL (> 31 years)</td></tr>
<tr><td>Very low activity</td><td rowspan="3">Radioactive decay on production site and disposal through conventional means</td><td colspan="2">Surface storage</td></tr>
<tr><td>Low activity</td><td rowspan="2">Surface storage</td><td>Low-depth storage (under review by ANDRA)</td></tr>
<tr><td>Medium Activity</td><td rowspan="2">Reversible deep geological storage (under review)</td></tr>
<tr><td>High activity</td><td></td></tr>
</table>

The 2006 French Act on Nuclear Waste mandated research on three possible options to deal with these wastes:

- Transmutation and/or partition of the nuclear waste. This is the object of the present work and will be discussed further on.
- Deep geological storage, either reversible or permanent. This is currently under study by the ANDRA in Bures [15]. In this approach, the waste is compacted and vitrified. The waste packages thus created are then stored underground so that they may not reach the biosphere.
- Interim storage on surface. This is currently under study by the ANDRA.

When discussing nuclear waste in general and HLW more specifically, several points should be kept in mind. They are listed below.

i) RADIOTOXICITY

The first hazard associated with nuclear waste that comes to mind is their high level of radioactivity. However, the simple activity of a given mass of nuclear waste is not sufficient to evaluate the harm they can cause to human beings. Indeed, damage to the human body caused by radiations depends on four factors:

- The type of radiations: generally speaking, neutrons are more damaging to biological tissues than photons.
- The energy of the particles: the higher the energy, the more damage will be created.
- The organ hit: resistance to irradiation changes depending on the organ. Thus gonads will be more affected by radiations than the skin.
- The delivery method: damage done by radiation greatly increases when radioactive particles are inhaled or ingested. For instance, local contamination of the skin by alpha particles is easily managed without health consequences while ingestion of alpha emitters leads to very high internal damage.

The quantity used for measuring the effects of radiations on a human being is called **dose** and is expressed in Sievert. For comparison purposes, the annual mean dose received by someone living in France is around 2 mSv while the limit for nuclear workers is set to 20 mSv per year. An acute dose (e.g., received in a short time) of 5 Sieverts is generally considered lethal.

The conversion between Becquerel and Sievert is done using dose factors, which take into account the four factors mentioned above. These dose factors are calculated and edited by the International Commission on Radiation Protection (ICRP) [16]. The final result is called **effective dose** and is also expressed in Sievert.

Using this tool, the radiological hazard from nuclear waste can be derived as radiotoxicity, or the effective dose received by someone interacting with the waste. Usually, the radiotoxicity is calculated considering the dose received by "ingestion" of one gram of nuclear waste and is expressed in Sv/g. For instance, the radiotoxicity from a current typical spent fuel is shown below in Figure 10. The radiotoxicity of the fission products has been omitted on this plot as its contribution decreases to zero after a few centuries. In terms of heavy nuclides, plutonium is the main contributor between 1000 and 100 000 years. This highlights the interest of recovering and reusing plutonium in order to limit the radiotoxicity of the waste.

The main approach to limit the impact of the radiological waste on the environment is to isolate them in order to prevent their release to the biosphere. The currently envisioned solution is to vitrify the HLW and then to seal the glasses obtained into metallic canisters which are then

buried into a deep geological repository in cemented chambers. This approach is being studied in France at the Bures laboratory in the Meuse department. Other countries such as Finland or Sweden have already started building deep geological repositories.

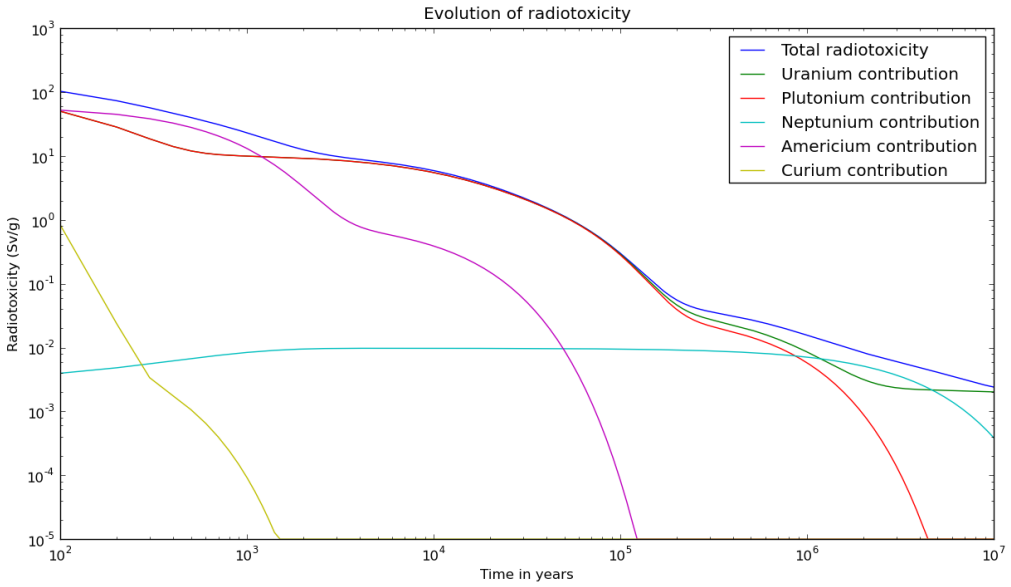

Figure 10 : Evolution of radiotoxicity of a typical UOX spent fuel from [17]

ii) VOLUME

Excavation of a deep geological repository is expensive and reducing the number of HLW packages which must be stored is beneficial in terms of cost. Reduction of the volume of HLW can be done for instance by closing the fuel cycle or by adopting the French solution of recycling once the PWR spent fuel.

iii) THERMAL ACTIVITY

HLW packages are containing several kilograms of alpha emitters which are generating heat which must be dissipated into the nearby environment. The temperature of the ground around the package in the geological repository must be kept below 90 °C [18] in order to avoid formation of cracks in the rock and infiltration of water which will attack the glass and potentially leach away radionuclides.

Heat management in the repository is done by sufficiently spacing the waste packages to avoid overheating of the walls. However, the higher the thermal emission of the individual packages, the higher the spacing required and thus the bigger the repository needed. Consequently, reducing the decay heat of the final waste which is sent to the geological repository is a good way of reducing its size and thus its cost.

A high thermal activity in the fuel will also require additional cooling equipment for both manufacturing and reprocessing of the fuel. Transportation of the fresh and irradiated fuel assemblies will also be more arduous as the still hot fuel elements will have to be cooled during transportation or a higher number of individuals transfers will have to be done.

iv) NEUTRON SOURCE

HLW and more specifically the one coming from multi-recycled fuel accumulate high mass heavy nuclides which are strong neutron emitters due to spontaneous fissions such as Curium isotopes beyond ^{244}Cm or ^{252}Cf. A high neutron source in the waste will strongly impact handling and transportation stages of HLW as they will require additional shielding. It also strongly increases the limitations on fuel reprocessing due to the low moderated critical mass of some isotopes.

4) TRANSMUTATION OF MINOR ACTINIDES

In the case of a closed fuel cycle, long-term behavior of nuclear waste is driven by a small fraction of nuclei which are called minor actinides, as it can be seen on Figure 10. When plutonium is removed from the waste, americium becomes the main contributor to long term radiotoxicity. These are nuclei formed by neutron capture on uranium and plutonium isotopes. They exhibit long half-life and high radiotoxicity by ingestion as they are mainly alpha emitters. They also exhibit high decay heat level, which is a drawback for long-term underground storage of the associated waste. Transmutation is the process of destroying these minor actinides by turning them into shorter-lived fission products. We will discuss here the interest of transmutation in general and the physics behind it and detail the physical properties of the minor actinides.

a) MOTIVATION OF TRANSMUTATION

Transmutation of nuclear waste has been defined as a possible solution to minimize the impact of nuclear waste. It does not remove the need for a final storage solution, but it can minimize the constraints on such a solution.

The principle behind transmutation is to use a neutron source to turn long-lived radionuclides into stable or shorter-lived radionuclides, either by fission or capture nuclear reaction. Theoretically, it can be done with long-lived fission products (LLFP) and minor actinides. However, as LLFP does not produce neutrons under irradiation, they require a much higher number of neutrons in order to achieve transmutation. Consequently, we only considered minor actinides transmutation in this work.

Transmutation of minor actinides could lead to a significant reduction of the waste thermal activity and thus of the final repository size along with a reduction of the total long-term radiotoxicity of the waste, fission products being shorter-lived than minor actinides.

It has to be noted that this reduction is only achievable in the case of a closed plutonium cycle. If plutonium is considered a waste, both its mass and radiotoxicity contributions will be predominant and the gain associated with minor actinides transmutation will be negligible. This also means that minor actinides currently produced are not transmuted but are slowly accumulating. As they are vitrified with fissions products, their recovery for transmutation in the future is highly unlikely. Fortunately, minor actinides are in small amount in the UOX PWR spent fuel currently reprocessed in opposition to MOX PWR spent fuel assemblies which are accumulating in spent fuel pools waiting for FR to be deployed. Consequently, the more time is spent closing the plutonium cycle, the more minor actinides will be found in the waste and will potentially have to be reprocessed again to extract the actinides and transmute them or the bigger the size of the repository will be no matter the final solution implemented.

As it will be shown in the next part, production of minor actinides and transmutation capabilities strongly depends on the type of reactor technology considered. Various approaches can be considered considering for instance dual system with PWRs purely dedicated to electricity production and a smaller number of fast reactors (or ADS) used to close the plutonium and eventually minor actinides fuel cycle (the so-called symbiotic or double strata approach [19] [20]). This approach is of interest during the early deployment of the fast reactors, as it allows a quicker closure of the fuel cycle. Such an approach was studied in the European project for scenarios studies PATEROS [21].

However, this study will focus on the longer term where the entire reactor fleet is made of SFRs, as it is the current studied scenario for nuclear energy in France [22]. In this case, closure of the fuel cycle is considered achieved and two goals can be settled in order to obtain a comprehensive transmutation strategy. The first one is the stabilization of the minor actinides inventory, e.g. the consumption of the minor actinides produced during power-generation. In this case, the total minor actinides inventory in the waste is stable and equal to the inventory at the start of transmutation. It only slightly increases due to losses during reprocessing. The second objective than can be set is the resorption of the minor actinides stockpile. This can be done only if stabilization of the inventory has been implemented. In this case, transmutation systems are used to transmute part of the legacy inventory in minor actinides. This scenario requires the development of a process to recover the minor actinides from the waste.

b) THE MINOR ACTINIDES

Let's examine now the physical characteristics of the minor actinides, their possible transmutation chain and their impact on waste management. Actinides are elements with an atomic number between 89 and 103. Uranium and plutonium (Z=92 and 94) are sometimes called "major actinides" as they are used for power production in large quantities. Excluding plutonium, elements with Z > 92 are themed "**minor actinides**" as they are produced in low quantities compared to plutonium and as they are not directly used in nuclear reactors. The three most predominant elements are neptunium, americium and curium, which we will further describe here. A mass repartition of the production of these elements in three different reactors is given in Table 2. It can be seen that minor actinides always amount to less than 1% of the total heavy nuclides content in the core.

Table 2 : Composition of various reactors spent fuel

Reactor	PWR UOX 37 GWd/t	PWR MOX 48 GWd/t	SFR MOX 100 GWd/t
Element	Fraction (wt%)	Fraction (wt%)	Fraction (wt%)
U	95,07	88,23	73,61
Pu	1,01	6,24	15,98
Am	0,05	0,52	0,35
Np	0,05	0,02	0,05
Cm	0,01<	0,11	0,02
FP	3,83	4,89	10,01
Total	100	100	100

i) NEPTUNIUM

Neptunium (Z=93) [23] has been discovered by MacMillan and Abelson in 1940 [23]. Only isotope 237 of neptunium has a half-life longer than a week, and with a half-life of 2.14 million years, its activity is low enough to allow direct manipulation by hand. It has two main production ways given in Equation 2:

- Successive neutron capture on ^{235}U, which is predominant in thermal reactors.
- (n,2n) reaction on ^{238}U, which is predominant in fast reactors, as it is a threshold reaction with a 6 MeV threshold as seen in Figure 11.

Its production is more important in thermal reactors than in fast reactors due to higher capture cross sections on ^{235}U and ^{236}U. It amounts to up to 50 % of the produced minor actinides in UOX-fueled thermal reactors while only making 10 % of the mix in a typical fast reactor.

^{237}Np decays to ^{233}Pa and emits a 5 MeV alpha particle but its activity is too low for this emission to have a significant contribution to the decay heat of the HLW and its contribution to radiotoxicity only becomes predominant after 3 10^5 years. Its neutron emission can be neglected compared to the one from Curium isotopes.

Neptunium transmutation is straightforward: it can either directly fission or capture a neutron, in which case it will promptly decay to ^{238}Pu, which itself will either fission or capture a neutron and lead to ^{239}Pu which is a very good fissile nucleus and can be reused in the nuclear fuel. Nevertheless, the relatively short half-life of ^{238}Pu will have a impact on the reprocessing part of the fuel cycle as it will generate more heat by alpha-decay compared to neptunium.

$$^{235}_{92}U + n \rightarrow {}^{236}_{92}U + n \rightarrow {}^{237}_{92}U \xrightarrow{\beta} {}^{237}_{93}Np$$
$$^{238}_{92}U + n \rightarrow {}^{237}_{93}Np + 2n$$

Equation 2: Neptunium formation reactions

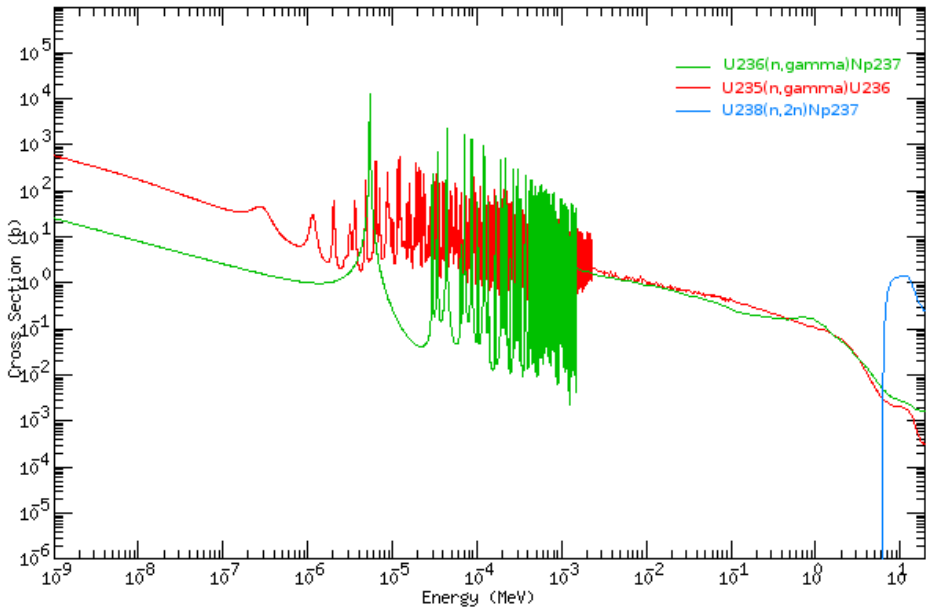

Figure 11: Neptunium formation cross sections

ii) AMERICIUM

Americium (Z=95) has been discovered in 1944 by Seaborg, James and Morgan in Berkeley [24]. It has three isotopes with significant half-lives e-g which will be found in non-negligible quantities several days after reactor shutdown, which are listed below:

Table 3 : Isotopes of americium

Isotopes	Half Life (y)	Daughter-nuclei (by α decay)	Production way
241	432.2	Np 237	^{241}Pu decay
242m	141	Pu 238	Capture on ^{241}Am
243	7370	Pu 239	Capture on ^{242}Pu

^{241}Am comes from beta decay of ^{241}Pu following Equation 3, with half-life of 14 years. Its production is strongly dependent on the isotopic vector of the plutonium used as fuel and on the reactor spectrum. Plutonium multi-recycled in SFR will have a content in ^{241}Pu as low as 3 %, which in turns leads to a low production of ^{241}Am, while current plutonium from UOX or MOX thermal reactors is closer to 8 % [25]. It makes up most of the minor actinides production in fast reactors, with generally more than 60 % of the mass. The amount of ^{241}Am in the fuel cycle is strongly dependent on the cooling and reprocessing time of the spent fuel. The longer this cooling time, the higher the fraction of ^{241}Pu that has decayed and the higher the production of ^{241}Am.

$$^{241}_{94}Pu \xrightarrow{\beta,14y} {}^{241}_{95}Am + {}^{0}_{-1}e + \bar{\nu}$$

Equation 3 : Americium 241 formation equation

Due to its alpha decay, it has a small thermal load of 0.11 W/g. This decay is accompanied with a weak gamma ray generally around 60 keV emitted by the ^{239}Np produced. Consequently, americium-containing fuels must be handled in gloves-boxes or even hot-cells, depending on the quantity considered.

^{242}Am and its more stable isomer ^{242m}Am are produced by capture on ^{241}Am (Equation 4). The actual proportion of each nuclei produced depends on the incoming neutron energy as it can be seen on Figure 12. ^{242}Am decays with a 16h half-life to ^{242}Cm in 82.7 % of the case and directly to ^{242}Pu by electronic capture in the remaining 17.3 %. ^{242m}Am is unusually a metastable state more stable than its related ground state and it nearly always transition to ^{242}Am by gamma emission. ^{242m}Am has a very high fission cross-section which means it is found in relatively low quantity in the minor actinides production of a reactor, between 1 and 2 %.

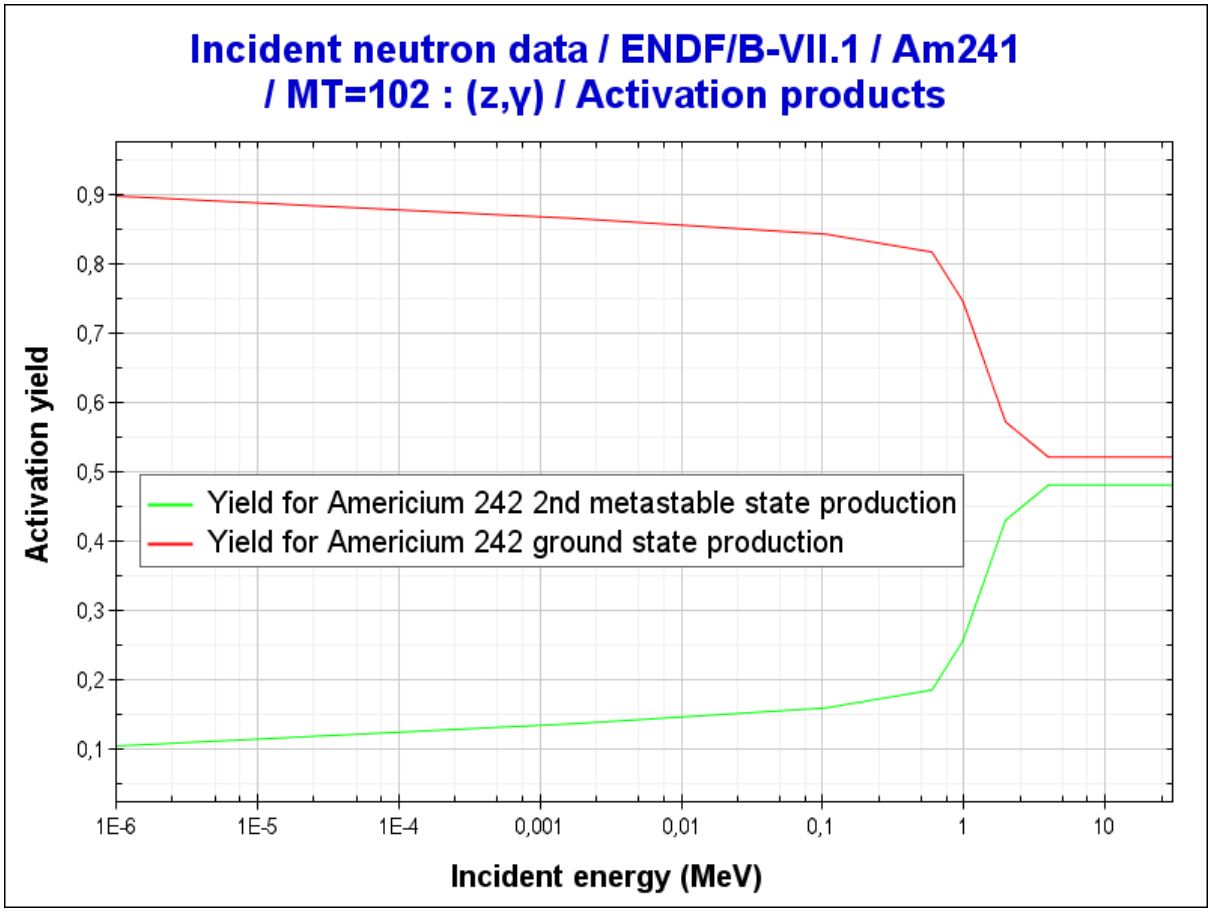

Figure 12 : Capture yields on ^{241}Am. Red : Am242, Green : ^{242m}Am

$$^{241}_{95}Am + ^{1}_{0}n \rightarrow ^{242(m)}_{95}Am$$

Equation 4 : Americium 242 formation equation

Finally, ^{243}Am is the longest lived isotope of Americium and is produced by neutron capture and subsequent decay on ^{242}Pu (Equation 5). Consequently and similarly to the ^{241}Am case, its production can vary by up to a factor two depending on the plutonium isotopic vector of the fuel. By alpha decay, ^{243}Am yields ^{239}Np which is a strong gamma emitter and thus contributes to the radiotoxicity of americium.

$$^{242}_{94}Pu + ^{1}_{0}n \rightarrow ^{243}_{94}Pu \xrightarrow{\beta,5h} ^{243}_{95}Am + ^{0}_{-1}e + \bar{\upsilon}$$

Equation 5 : Americium 243 formation equation

Americium is the main contributor both to minor actinide fuel cycle inventory and medium-term (between 100 and 10 000 years approximately) radiotoxicity in the case of a closed fuel cycle. Consequently, Americium transmutation is a good option to reduce both parameters. However, it is less straightforward than neptunium transmutation as it leads to Curium by neutron capture, which is also a minor actinide and is less convenient to handle.

iii) CURIUM

Curium (Z=96) is the last minor actinide which is produced in significant quantities in nuclear reactors. It has been discovered in 1944 by the team of Glenn Seaborg along with Americium [26]. The curium isotopes that can be found in the spent fuel are given below:

Table 4 : Isotopes of curium

Isotopes	Half Life (y)	Daughter-nuclei (by α decay)	Production way
242	0.45	Pu238	^{242}Am decay
243	29.1	Pu239	Capture on ^{242}Cm
244	18.1	Pu 240	Capture on Am 243
245	8.5e3	Pu241	Capture on ^{244}Cm
246	4.8e3	Pu242	Capture on ^{245}Cm
247	1.6e7	Am243	Capture on ^{246}Cm
248	3.5e6	Pu240	Capture on ^{247}Cm

^{242}Cm is found in kilogram quantities in the spent fuel due to the decay of ^{242}Am produced by capture on ^{241}Am (Equation 6). However, its half-life is significantly short which leads to a significant thermal and neutron emission with a specific heat load of 121.4 W/g during its decay to ^{238}Pu which has itself a high heat load of 0.57 W/kg. This important decay heat translates into additional constraints for handling of the spent fuel during refueling operations. This issue can be simply solved by letting the fuel cool down for several decay period of ^{242}Cm but at an economic cost, as this either means a decrease in the plant load factor or an increase in the total fuel inventory. ^{243}Cm inventory is very limited due its high fission cross section and to its production mode which is capture on the relatively short-lived ^{242}Cm.

$$^{242}_{95}Am \xrightarrow{\beta} {}^{242}_{95}Cm + {}^{1}_{0}n \rightarrow {}^{243}_{95}Cm$$

Equation 6 : Cm242 and Cm243 formation equations

^{244}Cm is the main curium isotope found in the spent fuel, as it is produced from ^{243}Am which is readily available for neutron capture and as its absorption cross-section is low leading to its accumulation in the fuel (Equation 7). Similarly to ^{242}Cm, it is a strong thermal and neutron emitter with a specific heat load of 2.84 W/g. With its longer half-life, it is going to be more of an issue with regards to the storage in the final repository. It also has a high spontaneous fission probability, leading to a high intrinsic neutron source.

$$^{243}_{95}Am + {}^{1}_{0}n \rightarrow {}^{244}_{95}Cm + {}^{1}_{0}n \rightarrow {}^{245}_{95}Cm + {}^{1}_{0}n \rightarrow {}^{246}_{95}Cm + \cdots$$

Equation 7 : Curium 244 and above formation equation

^{245}Cm is also produced in kilogram quantities as it comes from ^{244}Cm which is present in significant quantities in the fuel. It shares a significant neutron emission with its parent isotope ^{244}Cm However, heavier isotopes of Curium are not found in significant quantities in general (up to a few grams each in fast reactors) as they require numerous successive captures to be produced. Nevertheless, they have a non-negligible contribution on the neutron source of the spent fuel as they usually have a high spontaneous fission rate.

Curium production is less than 10 % of the total minor actinides production but it drives the short-term radiotoxicity along with fission products (up to a few hundred years) and is the main contributor to decay heat and neutron source.

iv) Berkelium, californium, etc..

There are several other minor actinides which are produced in microgram quantities in nuclear reactors, namely berkelium and californium (Z= 97 and 98). Though they have a very low production rate, they can have a significant contribution to neutron source. Thus, ^{252}Cf specific neutron source is 10^5 times higher than ^{244}Cm neutron source. Consequently, the production of these elements must be taken into account during calculations in order to correctly estimate the neutron source of the waste [27].

c) Physics of transmutation

i) Minor actinides transmutation

As shown in Figure 13, a minor actinide nucleus submitted to a neutron flux can either fission or capture a neutron. In the former case, effective transmutation has been achieved as the fission products decay is faster than minor actinides decay in general. However, capture can also happen and it simply leads us back to the initial issue as the new nucleus is generally also a minor actinide.

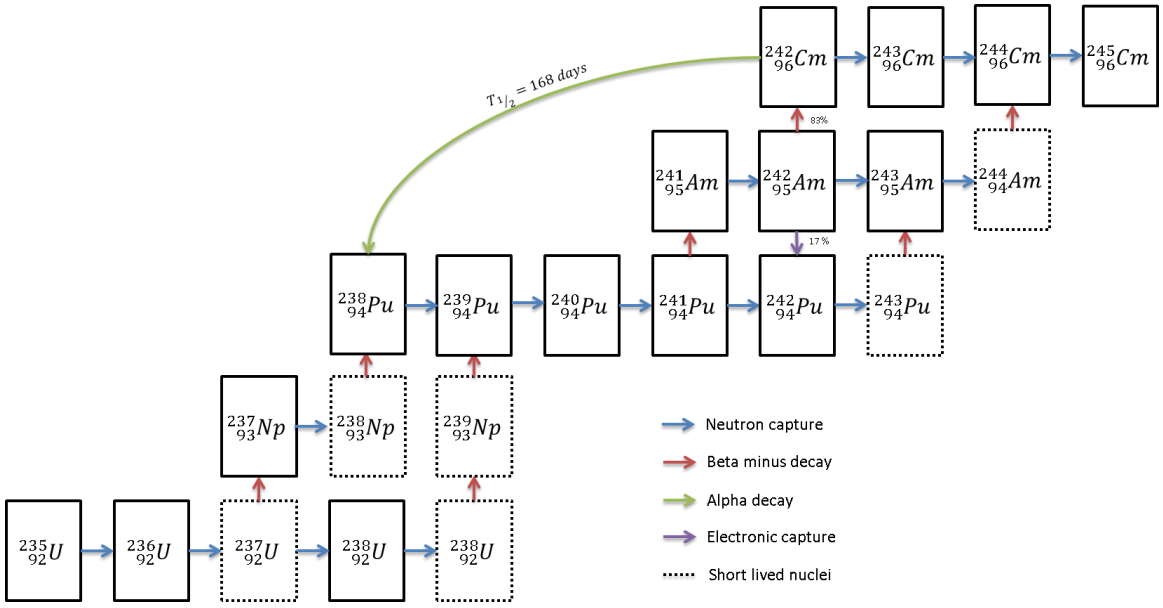

Figure 13 : Transmutation chain of minor actinides

It appears from this that an efficient transmutation system must maximize the number of fissions while minimizing the number of captures, in order to « burn » as many minor actinides nuclei as possible while saving as many neutrons as necessary. However, many other parameters must be taken into account for designing a transmutation system as it will be detailed in the next chapters.

The capture to fission ratio, usually written α, depends on the neutron spectrum inside the reactor. This ratio indicates the number of capture for each fission of a given nuclei. There is an

interest in lowering it in order to make the better potential use of the available neutrons. As capture cross sections varies with 1/E while fission cross section is more or less constant, there will be more fission per capture in a fast spectrum than in a thermal spectrum, which will be beneficial for transmutation.

This ratio has been estimated using typical neutron spectrums (see Table 5). For instance, it can be seen that the for one fission of Americium 243, one hundred and eleven captures leading to curium 244 will occur in a thermal spectrum system versus only 8.6 in a fast spectrum one. This means that, even though minor actinides consumption in a thermal reactor is possible, it is going to lead to a very high total inventory in curium isotopes or plutonium 238 in the case of neptunium, which may create challenging, if not unacceptable constraints on the fuel cycle. Regardless of the necessity to achieve a closed fuel cycle, this constitutes one of the main arguments for minor actinides transmutation in fast reactors

Furthermore, loading of plutonium and minor actinides in a thermal reactor is limited by the increase in coolant void feedback. Due to strong resonances in the low-energy range, the addition of plutonium shifts the spectrum towards higher energy and thus decreases the efficiency of the boron in the primary circuit water. Consequently, a maximal content of 12 % of plutonium per MOX assembly is authorized.

As minor actinides have the same impact on the neutron spectrum as plutonium, their content was also limited and an equivalence formula was devised: 1 % of plutonium loaded is equal to 3 % of minor actinides loaded. This only allows a limited loading of minor actinides in thermal reactors. The various approach developed to solve this problem are discussed in Annex 3.

Table 5 : Capture to fission ratio for most minor actinides in a thermal and fast spectrum from [28]

Isotope	REP-UOX			REP-MOX			RNR-MOX		
	σ_f	σ_c	α	σ_f	σ_c	α	σ_f	σ_c	α
^{237}Np	0.52	33	63	0.6	18	30	0.32	1.7	5.3
^{241}Am	1.1	110	100	0.8	35.6	44.5	0.27	2.0	7.4
^{242m}Am	595	137	0.23	126.6	27.5	0.2	3.3	0.6	0.18
^{243}Am	0.44	49	111	0.5	31.7	63.2	0.21	1.8	8.6
^{242}Cm	1.14	4.5	3.9	0.96	3.45	3.6	0.58	1.0	1.7
^{243}Cm	88	14	0.16	43.1	7.32	0.2	7.2	1.0	0.14
^{244}Cm	1.0	16	16	1	13.1	13.1	0.42	0.6	1.4
^{245}Cm	116	17	0.15	33.9	5.4	0.2	5.1	0.9	0.18

Transmutation physics can also be understood using the so-called D-Factor approach as exposed in [29]. This parameter quantifies the number of neutrons required to achieve total destruction of a given nuclei by successive captures or fission until short-lived fission products only remain. It is defined below in Equation 8 with D_J the neutron consumption to fully incinerate the nuclide J, $\{J_{1i}\}$ the set of nuclides that can be obtained by neutron reaction on the nuclide J, $P_{J\rightarrow J1i}$ being the probability to obtain each nuclide and R_{J1i} the neutron loss corresponding to the creation of the nuclide J_{1i}.

$$D_J = \sum_{J1_i} P_{J \to J1i} \left\{ R_{J1i} + \sum_{J2_k} P_{J1i \to J2k} \left\{ R_{J1i} + \sum_{J3l} P_{J2k \to J3l} \{\dots\} \right\} \right\}$$

Equation 8: Definition of the D-factor for a given nuclide

The values of the D-factor for a thermal and fast spectrum are given in. Several comments can be made here. Firstly, it can be observed that the D-factor for most of the minor actinides is negative, which means that in a thermal spectrum, transmutation of these elements will consume neutrons and thus require an over-enrichment of the fuel in order to compensate for this increased neutron consumption. ^{243}Cm and ^{245}Cm exhibit a positive D-factor as they are fissile nuclei, while ^{244}Cm exhibits a positive D-factor even though it is not fissile as its daughter product by capture is ^{245}Cm which is an extremely good fissile nucleus. Due to the predominance of Neptunium and Americium in the initial minor actinides isotopic vector, the overall transmutation process in a thermal reactor is a net neutron consumer, while it is a small producer in a fast spectrum. Finally, it should be mentioned that over-enrichment of the fuel can also be obtained using plutonium and MOX fuels, however this will increase the corresponding production of minor actinides due to the unfavorable capture to fission ratios.

Table 6 : Table 6 : Values of the D-Factor for selected nuclides in thermal and fast spectrum from [27]

	Thermal spectrum	Fast spectrum
^{237}Np	-1.4	+0.3
^{241}Am	-1.4	+0.3
^{243}Am	-0.7	+0.3
^{243}Cm	+1.6	+1.8
^{244}Cm	+0.4	+1.1
^{245}Cm	+2.0	+2.2
All MA	-1.2	+0.4
Pu + MA	-0.2	+0.9
LLFP	-2.3	-2.2

A conclusion of this short analysis is that fast reactors are better suited to minor actinides transmutation compared to thermal reactor, the three main reasons for this being the possibility to close the fuel cycle using this kind of system, the lower inventories of minor actinides and the better neutron economy.

ii) A WORD ON FISSION PRODUCTS TRANSMUTATION

Along with minor actinides, long-lived fissions products such as ^{99}Tc or ^{129}I are also a potential source of hazard, considering that of some are highly mobile in the environment with significant half-lives, especially halogens, Technetium and Cesium. LLFP transmutation could then be a solution to lower this burden. Two main long-lived isotopes have been identified as targets for fission products transmutation: ^{99}Tc and ^{129}I. [30].

^{99}Tc yields ^{100}Ru after a capture and a subsequent decay of ^{100}Tc. It also has the interest of exhibiting resonances in the low epithermal range which are going to increase the efficiency of the Doppler Effect it is added to the fuel (a potential design can be found in [31]). ^{129}I, which is

highly mobile in the biosphere and is readily absorbed in the thyroid, can be transmuted to stable ^{130}Xe following a neutron capture and decay.

LLFP transmutation is however complicated by the fact that this process is a net consumer of neutrons, contrary to minor actinides transmutation, which means it will require more neutrons for completion. This is all the more true that capture cross sections of these two elements are roughly ten times lower than those of ^{241}Am for instance. However, as it can be seen in **Erreur ! Source du renvoi introuvable.**, the D factor for LLFP transmutation does not change with the spectrum. This is explained by the increase in the total flux by a factor ten in a fast reactor, which counterbalances the decrease in cross section thus leading to a nearly constant reaction rate. Designs such as moderated targets as hydride in fast reactors or in ADS have been proposed to optimize the transmutation of LLFP [32]. However this being not the object of this work, we will not further detail this point. Further information can be found in [33] and [30] detailed studies about this issue.

d) IMPACT OF MINOR ACTINIDES LOADING ON FAST REACTORS AND ON FUEL CYCLE

The higher the neutron flux available for transmutation, the better the performances will be as more neutrons will be available to "burn" the minor actinides. Consequently, it would seem that loading minor actinides-bearing assemblies directly near the core center, where the neutron flux is the highest, would be the best transmutation option.

However, the introduction of minor actinides in a nuclear reactor has negative effects on both the reactor natural behavior (feedback coefficient, delayed neutron fraction) and on the fuel cycle, which will be detailed below and which limits the possibilities with regards to their transmutation. The magnitude of both these effects depends on the way the minor actinides are loaded in the core.

i) IMPACTS ON THE CORE

Minor actinides, and especially americium, have important capture cross sections level below 30 keV which is going to lower the neutron population in the keV range where the Doppler contribution is dominant. Consequently, fast reactors loaded with minor actinides will exhibit a decreased Doppler effect compared to "regular" fast reactors.

Minor actinides fission cross sections are also more sensitive to the hardening of the neutron spectrum between 0.2 and 0.8 MeV and they also produce more neutrons per fission. This can be seen looking at the evolution of the fission probability of ^{241}Am and ^{238}U vs the energy as shown in Figure 14. In the case of a coolant voiding, the reactivity increase will be higher compared to "regular" fast reactors as more neutrons will be produced due to fissions on minor actinides nuclei.

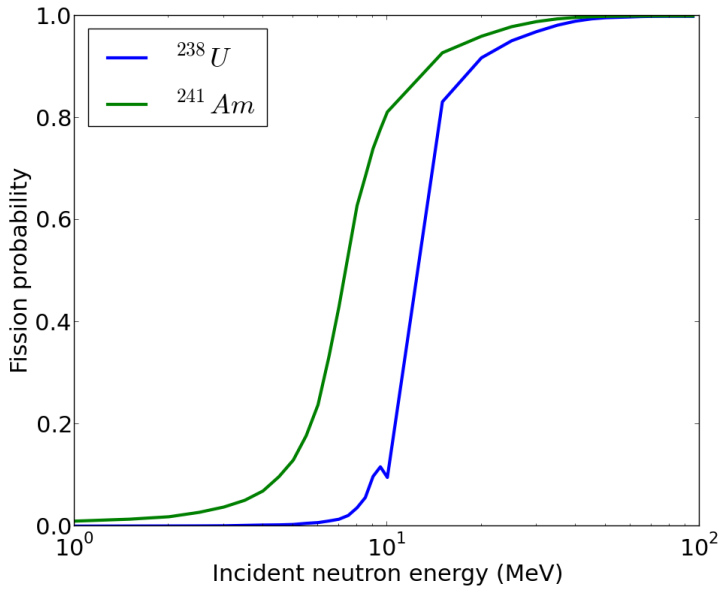

Figure 14 :Fission probability of ^{238}U and ^{241}Am in the fast energy range

The introduction of minor actinides in the core in significant amount also decreases the delayed neutron fractions as the production of delayed neutrons precursors is lower for heavier nuclides. Additionally, the high capture cross sections of americium below 0.5 MeV leads to the capture of more delayed neutrons, which are born with a slightly less energetic spectrum than fission neutrons. These neutrons also generate fewer neutrons per fission due to their lower energy, thus lowering the effective delayed neutron fraction. This furthermore decreases the effective delayed neutrons fraction. A more detailed breakdown of these spectrum impacts can be found in [34]

Minor actinides addition to the fuel also modifies the behavior of the fuel pin under irradiation. More specifically, it leads to an increased production of helium from alpha decay (mainly of ^{242}Cm from capture on ^{241}Am) which requires a larger expansion plenum and leads to modification of the fuel properties under irradiation. Minor actinides atoms in the fuel also impact the melting point and thermal conductivity which increases the sensitivity of the core to transient by reducing the safety margins [35]. The high helium production is especially important to take into account during shutdown, where helium is produced in a cold fuel, which may induce cracking or other mechanical modifications of the fuel. High solid swelling may also be observed in fuel with a high fraction of minor actinides.

Finally, an effect on the breeding gain and reactivity swing during cycle can be observed due to the substitution of uranium by minor actinides which have a different of breeding behavior. The breeding gain will generally increase compared to a pure uranium-plutonium situation, both as more plutonium is produced and as some minor actinides produced by capture such as ^{242m}Am or ^{245}Cm are more “reactive” than plutonium (higher fission cross section compared to ^{239}Pu).

It appears that additional care has to be taken in designing a transmutation system in order to accommodate minor actinides in the core. Possible solutions to this problem are discussed in Annex 3..

ii) IMPACTS ON THE FUEL CYCLE

If minor actinide loading modifies the core behavior, it also has non-negligible impacts on the fuel cycle. First, after unloading, the fuel assemblies will have a higher decay heat and gamma and neutron emission due to the important contribution of Curium isotopes and to a lower extent ^{238}Pu. This will impact the handling and transportation of spent fuel assemblies during refueling and temporary storage. This can be seen in Figure 15 which shows the neutron source and decay heat of MOX fuel without minor actinides and with 3 % of americium (in substitution to uranium). The impact of minor actinides on these two parameters can be clearly seen here. The impact of minor actinides loading is limited for short term cooling times as the early decay heat is dominated by fission products. However, this impact increases with the cooling times due to the shorter half-lives of fission products compared to minor actinides.

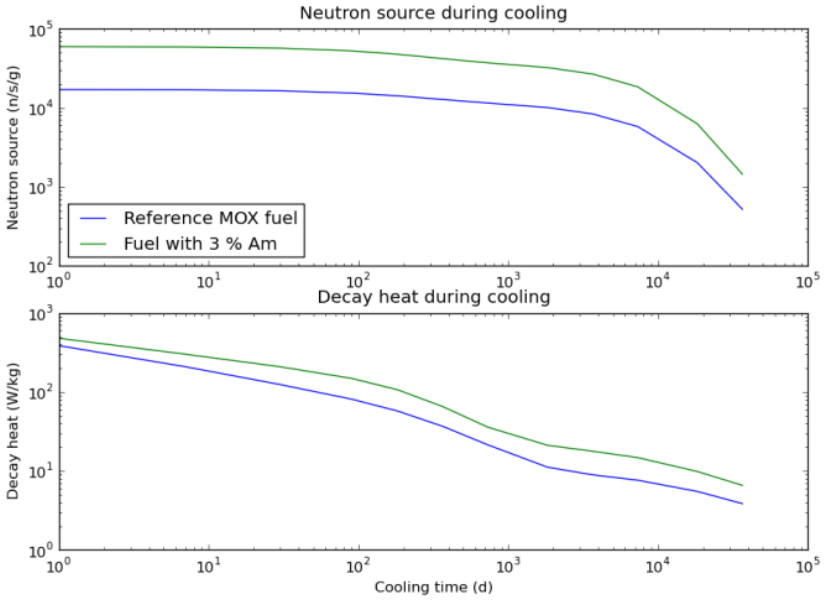

Figure 15 : Comparison of neutron source and decay heat between standard and transmutation fuel

This higher residual activity will also have an impact on reprocessing, as the spent fuel will have to be more diluted in solvent to abide by safety rules. Consequently, reprocessing will take a longer time and will probably be more expensive. In the case where minor actinides are only irradiated once and then sent to the final repository, an interim storage of several decades will be necessary to allow cooling of the waste packages until ^{244}Cm contribution has significantly decreased.

In the case where multi-recycling of minor actinides is implemented in a fashion similar to what is done with plutonium, additional “costs” and complications will arise from the necessity to shield the fabrication chain due to the high activity of the fresh fuel. This will also complicate transportation of the fuel assemblies to the power plant. It should also be noted that fabrication of minor actinides bearing fuels with the traditional powder metallurgy technic is not acceptable as it would lead to very high levels of contamination of the fabrication chain due to the volatility of the powders used in this process. New solutions are currently being developed to solve this issue. Extensive characterization of the microstructures of transmutation fuels is also underway. This is detailed in Annex 3.

In conclusion, one can see that minor actinides incorporation in the fuel has an impact on every single step of the nuclear fuel cycle, which means that the transmutation process must be thought with the entire fuel cycle in mind and not only the irradiation part. The various impacts exposed here are summarized in Figure 16. The orange colored impacts are related to the core transient behavior while the green ones are related to the fuel cycle penalties introduced by minor actinides loading. The blue ones correspond to the necessary modification in assembly design resulting from this loading.

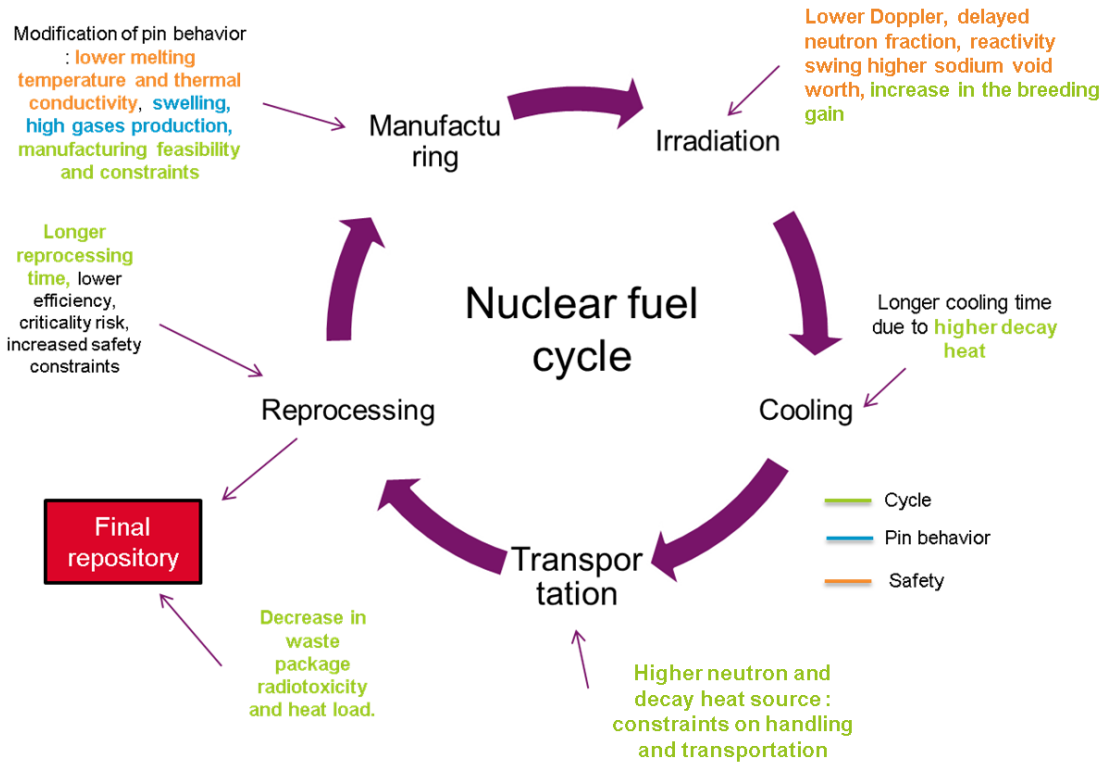

Figure 16 : Summary of minor actinides impacts on a closed fuel cycle

5) Conclusions

Fast reactors are adequate tools for minor actinide transmutation, which in turn appears as a potential solution to reduce the volume of HLW produced by nuclear energy. The specificities of fast reactor design have been introduced in this chapter, along with the main difficulties of HLW storage. Transmutation objectives and methods were broadly discussed. It appears than a successful implementation of a working transmutation strategy requires R&D on numerous aspects of the nuclear fuel cycle, from the fabrication to the reprocessing along with potentially significant changes in the reactor design to accommodate the impacts of minor actinides on the core behavior.

CHAPTER 2: OBJECTIVES, METHODS AND TOOLS

Highlights:

- ✓ **The goal of this work is to build a methodology for minor actinides transmutation optimization under constraints.**
- ✓ **Constraints from the fuel cycle and the core transient behavior will be considered.**
- ✓ **To keep the computation time reasonable, meta-models will be used to replace complete core calculations.**
- ✓ **Genetic algorithms will be used as optimization algorithms.**
- ✓ **A second part of this work will be dedicated to analyzing innovative transmutation strategies such as the use of thorium or additional fissile material loading in radial blankets.**

The purpose of this chapter is to detail the objectives of this work along with the methods and tools which will be used here. The approach used to complete this study will also be detailed.

1) OBJECTIVES AND APPROACH USED

As mentioned in Chapter 1, the objectives of this work are dual. The first and main one is the development of an optimization methodology of minor actinides transmutation in a fast reactor which takes into account constraints coming from the fuel cycle and reactor behavior during incidental transients. The second and complementary objective is the design and development of innovative systems in order to improve transmutation performances.

The design of the optimization methodology was performed using a three-tiered approach. In a first time and in order to be as exhaustive as possible, a physical analysis of the transmutation process independently of the assembly or core design was carried out. This preliminary work is detailed in Chapter 3 and led to the identification of physical limitations of the transmutation process and of directions of research to be followed.

Considering the research avenues highlighted during the physical analysis, technological constraints were then added to the problem. These constraints can roughly be separated into three main categories, as it was done in Chapter 1:

- Assembly design constraints, which are dependent on the type of fuel, coolant and cladding considered and on the transmutation process itself through the irradiation time and the isotopic vector of the minor actinides considered

- Fuel cycle constraints which are generally expressed using estimators built on the decay heat or activity of an assembly. Consequently, the evaluation of these constraints requires the prior evaluation of the assembly design constraints in order to obtain geometrical data on the assembly itself.
- Core behavior constraints, which can be reduced to margin to sodium boiling or fuel melting during a selection of unprotected transients. This information also depends on the actual geometrical design considerations.

It can be seen here that it is necessary first to consider mechanical and thermal constraints on the assembly design before implementing additional constraints. Considering the two modes of transmutation discussed in Annex 3, heterogeneous transmutation does not require the implementation of core behavior constraints as the impact of minor actinides loading at the core periphery on feedback coefficients is not significant. The description of the approach used and the analysis of this mode of transmutation are presented in Chapter 4.

Homogeneous minor actinides transmutation on the other hand does require taking into account “natural” core behavior. Additional input parameters related to core geometry are then necessary to consider this part of the problem. This transmutation mode analysis is detailed in Chapter 5 along with the associated results.

The completed methodology was then applied to several cases based on currently accepted industrial constraints in order to identify research avenues and highlights the necessary development necessary to achieve higher performances for minor actinides transmutation. The results of this application are described at the end of Chapter 4 and Chapter 5 respectively.

In parallel to this methodological work, innovation paths were identified and new innovative approaches were identified for minor actinides transmutation. A non-exhaustive description of the various innovations proposed during this work is presented in the annexes of the present document. The approach used is summarized in Figure 17, which shows the direction of the workflow during this work.

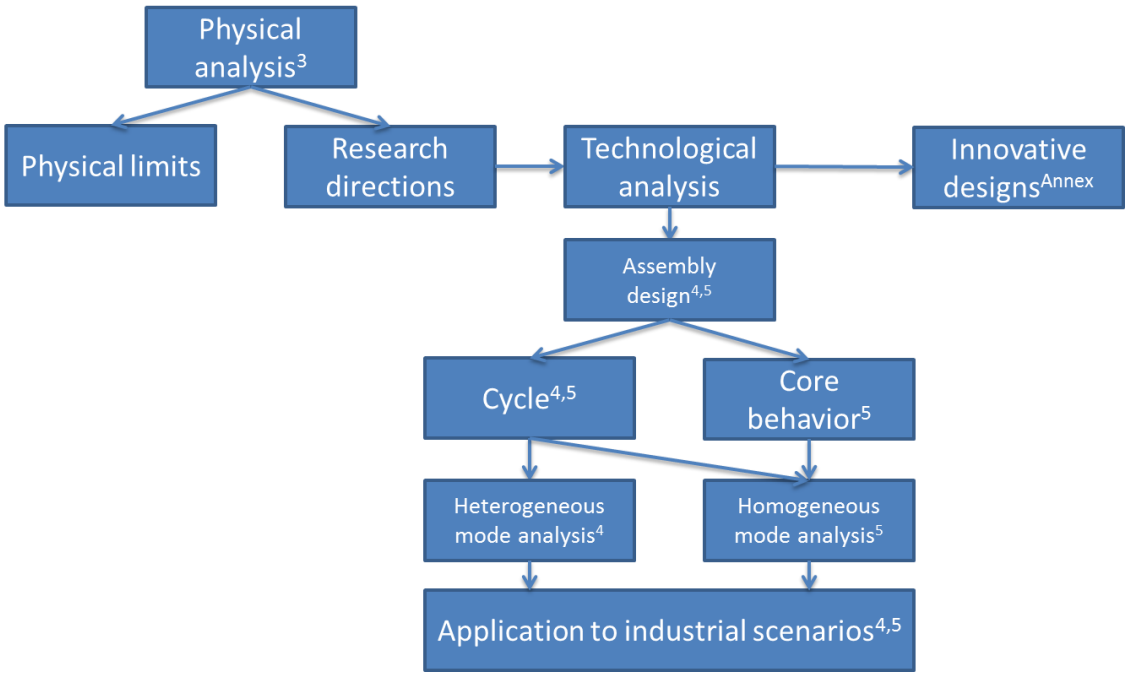

Figure 17 : Simplified diagram of the process carried out during this work. The chapter number corresponding to each box is indicated in superscript.

2) METHODS AND TOOLS USED

a) CORE ANALYSIS

Reactor analysis was carried out using the ERANOS code system [36] which is a deterministic code system which was developed by CEA to simulate fast reactors such as RAPSODIE, PHENIX or SUPERPHENIX. This code uses the classical two-step calculations (lattice/core) route to solve the neutron transport equation (or Boltzmann equation) in the reactor core.

First, the cross sections in each of the core medium (fuel, coolant, control rods, structural material) are evaluated using fundamental mode approximation. Fuel cells were described either using a complete pin-by-pin approach or were directly homogenized depending on the required accuracy. Unless otherwise mentioned, the JEFF 3.1 nuclear data library [37] was used for all the core calculations described in this work.

Then, these cross sections are used in a complete core calculation which is used to derive the state of the core and the associated neutron flux. Unless otherwise specified, a 2-D RZ description of the core was. For R-Z calculations, the finite-difference BISTRO Solver with SN angular discretization was used. 3D hexagonal calculations were also carried out, in which case the diffusion approximation of the transport equation was used to save computation time.

The PARIS platform, which a GUI developed by CEA was used to create most of the cases studied here. The core model was created using the graphical tool available and the resulting model was turned into an ERANOS input file. PARIS also features various post processing tools to evaluate core feedback coefficients and power distribution.

Depletion calculations were carried out using the DARWIN code system [38], which solves the so-called Bateman equation to compute the evolution of the number of nuclides in the fuel. Cross sections for these calculations were taken from the ERANOS calculation.

b) CORE BEHAVIOR DURING TRANSIENTS

Simulating the core behavior during a transient requires effective modelling of the various coupled phenomena occurring in the core. From the pin centerline to the coolant channel, various heat transfer mechanism must be considered along with the interaction with the coolant on the cladding boundary and the evolution of the neutron in the core.

The MAT4DYN calculation tool which was developed at CEA at the beginning of the 2000' by S. Massara [39] was used. It is a simplified tool which is coupling point-kinetics and thermal hydraulic modeling of a single channel to compute the core behavior during a given transient. To obtain a result which is representative of the core behavior, the hottest channel of the core (where the so-called hot spot is located) is modelled. If adequate safety margins are achieved for the hottest channel, the core can be considered as safe in a first approximation.

The details of the transients considered here will be exposed in Chapter 5.

c) OPTIMIZATION

The optimization process was carried out using the URANIE code system, which is the uncertainty platform of the Nuclear Energy Division at CEA [40]. This platform was developed primarily for uncertainty propagation and sensitivity calculations using various statistical tools. It also features an optimization tool which was used in this work.

Multi-criteria optimization was performed using genetic algorithms implemented into URANIE. These algorithms are numerical tools which are inspired from evolutionary process such as mutation or natural selection in order to optimize a given problem with regards to various objectives functions and constraints. One of their advantages is that they can explore a very wide range of input parameters and yield adequate results when the fitness landscape (e.g. the shape of the optimal cases distribution in the parameters phase space) is complex.

However, they tend to require a large number of evaluations of the fitness of the solutions tested, which in turn can lead to prohibitively long calculations times. Considering this, meta-models were built to reproduce the output of the calculations codes described above in order to limit the total calculation time. Artificial neural networks or ANN were created for this purpose using the built-in functionality of URANIE.

ANNs are numerical tools which can reproduce the input of a complex model at a lower cost by simulating the behavior of the brain. The network is divided into a number of artificial neurons linked together and each link can either be enforced or inhibited in order to minimize a cost function, which is usually a measure of the difference between the ANN output and the exact model. As such, the training of these ANNs requires first the creation of a series of test cases on which they can be trained and then validated. A sensitivity analysis of the various parameters of the ANN and genetic algorithms was carried out to verify that the conclusions obtained here were not dependent on numerical effects. The results of this analysis are given in Annex 4.

The general numerical process which was used in this work is summarized in Figure 18 . The actual chaining of the various steps will be discussed in details in each relevant chapter. Using

the URANIE code system, an initial set of sampling parameters is created and used to compute core feedbacks coefficients, fuel cycle parameters and transmutation performances using the ECCO/ERANOS code and the DARWIN depletion code. The outputs of these codes are used along with the initial sampling set to train the ANNs, which are then used either to generate estimators related to the fuel cycle and transmutation or to compute core parameters required to evaluate the core behavior during transient using the MAT4DYN code. Then, these estimators are used as fitness function for a general optimization process carried out with genetics algorithms coming from the URANIE code system package.

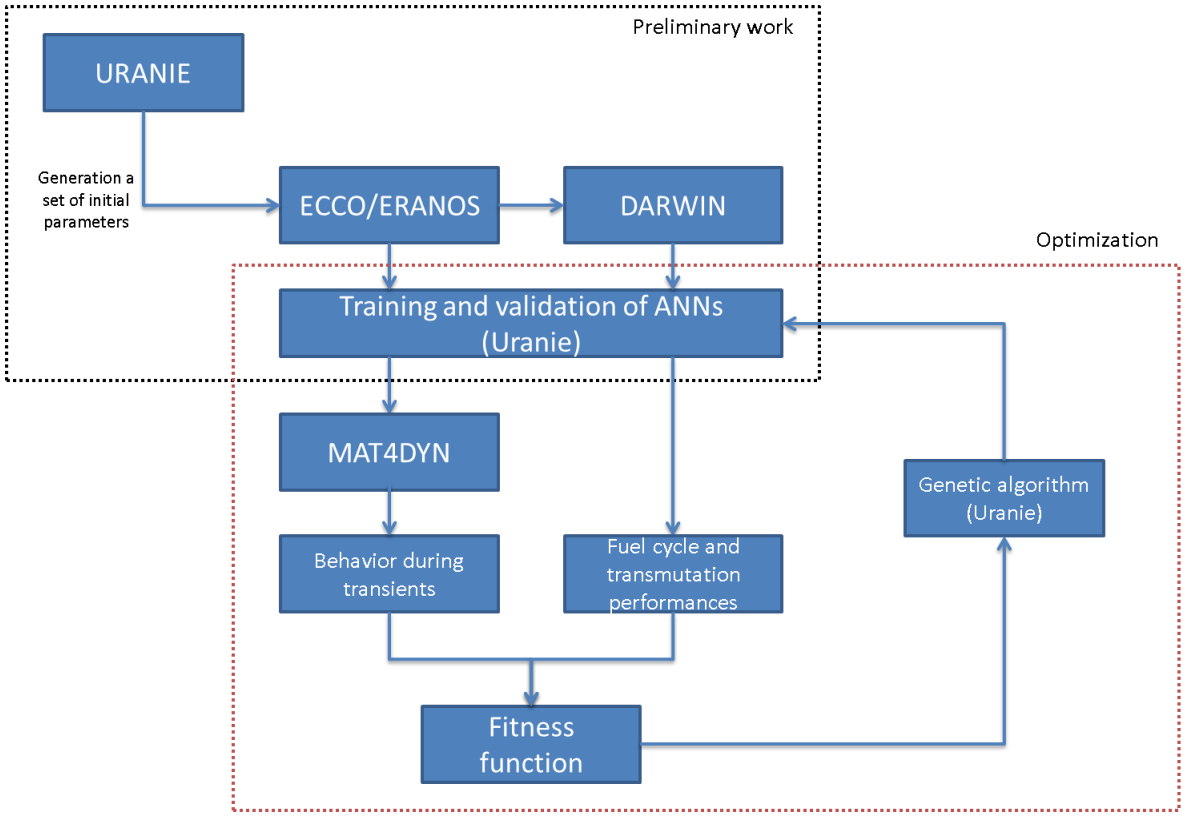

Figure 18 : Numerical process implemented in this work

3) CONCLUSION

The general objectives of this work have been discussed here and the plan used for this study was outlined. The various tools used during this work were also exposed along with the numerical methodology implemented here. A combination of calculations codes and meta-models was used to limit the computing time. The next chapter will be focused on a physical analysis of the transmutation process.

CHAPTER 3: A PHYSICAL ANALYSIS OF THE TRANSMUTATION PROCESS

Highlights:

- ✓ **The physics of the transmutation process is explained by the Bateman Equation and is thus strongly dependent on the neutron spectrum in the reactor core.**
- ✓ **Slowing down the neutrons increases the consumption of minor actinides but also increases the capture rate, thus producing more heat-emitting isotopes.**
- ✓ **The production of minor actinides in the core is significantly dependent on the plutonium isotopic vector used.**
- ✓ **It is possible to characterize the transmutation behavior of a core using a limited number of variables : the minor actinides loading, the neutron spectrum and the total fluence**
- ✓ **Artificial neural networks are trained to evaluate this behavior using these variables and are coupled to a genetic algorithm to carry out the optimization process.**
- ✓ **It is shown that a moderated approach is optimal, even when taking into account fuel cycle impacts.**

The goal of this chapter is to achieve a comprehensive analysis of the transmutation process and to use this analysis to highlight potentially interesting transmutation avenues, as well as physical limitations. In a first part the physical basis behind the transmutation process will be detailed, along with an analysis of the homogeneous and heterogeneous transmutation strategies specificities. Then the methodology used in this work will be discussed. Finally, several applications will be carried out related to the neutron spectrum, the minor actinides isotopic vector and the various constraints existing on the fuel cycle.

1) THE BATEMAN EQUATIONS

a) FUEL DEPLETION

The evolution of the isotopic composition of a given mass of heavy nuclides under a neutron flux can be computed using the so-called Bateman Equations, which is defined below in Equation 9. The change in the amount of a given nuclide *i*, by mean of number density N_i, is equal to the production rate of this nuclide coming either from neutron capture on other nuclides *j* or decay

of other nuclides *k* minus the consumption rate, which is due to neutron interaction (capture or absorption) or natural radioactive decay of the initial nuclide.

$$\frac{dN_i}{dt} = \sum_j N_j \sigma_{j\to i}\phi + \sum_k \lambda_{k\to i} N_k - \sum_l N_i \sigma_{i\to l}^{c,f,n2n}\phi - \sum_n \lambda_{i\to n} N_i$$

Equation 9 : Complete form of the Bateman Equations

Out of flux, this equation can be simplified to Equation 10, in which the flux dependent terms are equal to zero.

$$\frac{dN_i}{dt} = \sum_k \lambda_{k\to i} N_k - \sum_n \lambda_{i\to n} N_i$$

Equation 10 : Out-of-flux Bateman Equations

A given minor actinide can be considered transmuted when after a sufficient number of interactions; it has yielded fission products, either by spontaneous fission, which probability is very low, or by neutron absorption. We will thus focus here on Equation 9 where the effective destruction of heavy nuclides takes place.

Each term of Equation 9 plays a role in the transmutation process. For a given minor actinide *i* :

- $\sum_j N_j \sigma_{j\to i}\phi$ is the production term coming from capture on precursors such as ^{235}U or plutonium isotopes. There is an incentive to decrease this term in order to limit the production of minor actinides in the core.
- $\sum_k \lambda_{k\to i} N_k$ is the production term of minor actinides coming from the decay of precursors nuclides. For most cases, its contribution is limited but it plays a major role in the evolution of ^{241}Am concentration through ^{241}Pu decay.
- $-\sum_l N_i \sigma_{i\to l}\phi$ is the disappearance term through neutron interaction. This term can be divided in two parts, as shown below in Equation 11. The first term corresponds to interactions such a capture or (n,2n) reactions which yield another heavy nuclide, which can also be a minor actinides (^{244}Cm + n →^{245}Cm) for instance. In some cases, this term is a production term and it should be decreased. The second term is destruction term through fission, which is the desired goal in minor actinides transmutation. It should thus be maximized as far as possible.

$$-\sum_l N_i \sigma_{i\to l}\phi = -\sum_l N_i \sigma_{i\to l}^{c,(n,2n),\dots}\phi - N_i \sigma^f \phi$$

Equation 11 : Disappearance term of Bateman Equations

- $-\sum_n \lambda_{i\to n} N_i$ is the last term of the Bateman equation and corresponds to the natural decay of the minor actinides via various decay channels. This term is negligible for some of the minor actinides with very long half-lives such as ^{237}Np but plays an important role for relatively short lived minor actinides from ^{242}Cm with a half life of 162 days for short term cooling issues to ^{241}Am transmutation for long term storage.

It is possible to solve analytically this equation for the reduced ^{243}Am/^{244}Cm couple in a situation without initial ^{242}Pu for instance, which is representative of the transmutation process in the heterogeneous approach. In this case, Equation 9 becomes Equation 12 and Equation 13. The half life of ^{243}Am being equal to 7300 years, its radioactive decay can be neglected here. If we further neglect the production of these two nuclides coming from ^{242}Am and ^{243}Cm, which is a legitimate hypothesis considering the high fission probability of these two nuclides, we can be

obtain the functions given in Equation 14 and Equation 14, which give the evolution of the concentration of these two nuclides versus time with the hypothesis that there is no initial ^{244}Cm in the system.

$$\frac{dN_{Am243}}{dt} = N_{Am242}\sigma_c^{Am242}\phi - N_{Am243}\sigma_c^{Am243}\phi - N_{Am243}\sigma_f^{Am243}\phi$$

Equation 12 : Simplified evolution equation of ^{243}Am

$$\frac{dN_{Cm244}}{dt} = N_{Am243}\sigma_c^{Am243}\phi + N_{Cm243}\sigma_c^{Cm243}\phi - N_{Cm244}\sigma_c^{Cm244}\phi - N_{Cm244}\sigma_f^{Cm244}\phi - \lambda_{244}N_{Cm244}$$

Equation 13 : Simplified evolution equation of ^{244}Cm

$$N_{Am243}(t) = N_{Am243}(0) * e^{-(\sigma_c^{Am243}+\sigma_f^{Am243})\phi t}$$

Equation 14 : Solution of the simplified evolution equation of ^{243}Am

;

$$N_{Cm244}(t) = N_{Am243}(0)\frac{\sigma_c^{Am243}\phi}{\sigma_a^{Am243}\phi - \sigma_a^{Cm244}\phi - \lambda_{244}}(e^{-(\sigma_a^{Cm244}\phi+\lambda_{244})t} - e^{-\sigma_a^{Am243}\phi t})$$

Equation 15 : Solution of the simplified evolution equation of ^{244}Cm

Looking at Equation 14 and Equation 15 and , it is possible to draw several conclusions:

- To increase the disappearance of ^{243}Am, it is necessary to increase the term$(\sigma_c^{Am243} + \sigma_f^{Am243})\phi$. This requires either an increase of the neutron flux to which the nuclide are submitted, or in the sum of the cross sections.
- Increasing the capture cross section of ^{243}Am in turns increases the production of ^{244}Cm, thus lowering the total efficiency of the transmutation process by creating a new minor actinide nuclei.

It is also possible to plot the evolution of the concentration of ^{243}Am and ^{244}Cm during irradiation, as it is done in Figure 19. The amount of ^{243}Am in the medium decreases with the irradiation as expected, but the main point to be observed here is that the amount of ^{244}Cm increases at the beginning of irradiation, then reaches a peak value and decreases after a fluence close to the fluence obtained in a typical 3.6 GWth fast reactor as found in [41]. This effect will be referred to as “curium peak” throughout this work.

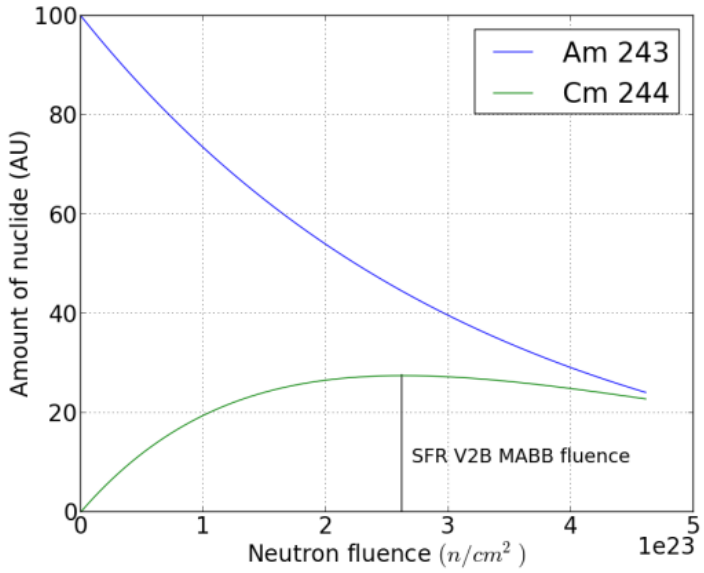

Figure 19 : Evolution of the concentration of ^{243}Am and 244Cm in the minor actinides bearing blankets of a 3.6 GW reactor taken from [41].

The transmutation process thus depends on both the neutron flux and the cross sections in the considered medium. A simplistic way of enhancing the transmutation kinetics of a given nuclide is to increase the neutron flux it "sees", however this may not always be possible. Consequently, modifying the spectrum to which it is submitted into to increase the absorption cross section appears as a solution which will be further investigated here.

b) MONO ENERGETIC NEUTRONS

One option to investigate the dependency of the transmutation process to the neutron spectrum to which it is submitted is to consider mono energetic neutrons in a simplified approach. Here, a mass unit (one kilogram for instance) of various minor actinide feeds were submitted to a mono-energetic neutron flux for an extended time period until a given percentage in mass reduction of the initial kilogram was achieved. Then, the radiotoxicity, decay heat and neutron source of the remaining percentage of heavy nuclides, including the un-transmuted minor actinides and the daughter-nuclei produced by capture or decay were computed. The latter can be linked to the impact on minor actinides transmutation in the fuel cycle on a first approximation: the higher the decay heat/neutron source, the longer the cooling time must be or the higher the constraints on the spent fuel reprocessing must be. Using this approach, it is possible to explore the behavior of transmutation with regards to the minor actinides consumption performances and the fuel cycle impacts.

The cross sections at various energies given in Table 7 were directly taken from the JEFF 3.1.1 nuclear data library [42]. Depletion calculations were carried out using a nuclide chain going from ^{234}U to ^{252}Cf. Pure feed of ^{241}Am, ^{243}Am, ^{237}Np and ^{244}Cm were considered, as well as a mixed vector named "MA2035" which is deemed representative of the minor actinides isotopic composition which will be available in 2035 in the French Fleet scenario [43]. Its composition is given in Table 8.

Table 7 : Breakdown of the neutron energy considered here

Energy	Comment
14 MeV	Fusion neutron
2 MeV	Mean energy of fission neutron
30 keV	Epithermal range
0.025 eV	Thermal range

Table 8 : Composition of the MA2035 isotopic vector

Element	Np237	Am241	Am242m	Am243	Cm242	Cm243	Cm244	Cm245	Cm246
Mass Fraction (%)	16.87	60.62	0.24	15.7	0.02	0.07	5.14	1.26	0.08

We compared the time and neutron fluence necessary to reach a 95 % reduction in mass of the initially loaded minor actinides. For the 'MA2035' case, the balance was calculated on the entire minor actinides content. The mass reduction can be achieved here either through fission or capture process. The results are given below, with a flux of 1e15 n/cm^2/s for fast to epithermal neutron and 1e14 n/cm^2/s for the thermal case. These flux levels are representative of what could be achieved in a typical fast or thermal reactor. The results are given in Table 9.

Table 9 : Neutron fluence and time necessary to reach a 95 % mass reduction in the initial mass of minor actinides

	Fluence to a reduction in original MA mass of 95 %				
Energy	^{241}Am	^{243}Am	^{237}Np	^{244}Cm	MA2035
25 meV	8.29E+21	2.53E+23	5.44E+21	2.49E+23	1.43E+23
30 keV	1.24E+24	3.27E+24	1.44E+24	2.76E+24	1.62E+24
2 MeV	1.50E+24	1.90E+24	1.73E+24	2.25E+23	1.59E+24
14 MeV	1.12E+24	1.38E+24	1.43E+24	1.99E+23	1.21E+24

	Time to a reduction in original nuclide mass of 95 % in years				
Energy	^{241}Am	^{243}Am	^{237}Np	^{244}Cm	MA2035
25 meV	0,3	8	0,2	8	45
30 keV	39	104	46	88	51
2 MeV	48	60	55	7	50
14 MeV	36	44	45	6	38

Several conclusions can be drawn from Table 9. At a first glance, it appears that thermal reactors are better suited to transmute pure minor actinides as very low fluence and corresponding irradiation time are required to remove 95 % of the initial mass. However, this is explained by the important increase in the capture cross sections in the thermal energy range, which means that for ^{241}Am or ^{237}Np among others, these elements are not effectively destroyed but turned into another heavy nuclide. This can be observed by looking at the MA2035 case, which requires more than 45 years of irradiation to achieve the required mass reduction.

It is worth mentioning that for the MA2035 case, the time required to achieve the expected mass reduction only slightly depends on the neutron spectrum considered. This is explained by the low fission rates in the thermal case, which thus requires a higher fluence to transmute all the residual Curium produced by successive captures, while in the fast case, it is explained by the lower cross sections levels, thus requiring more neutrons to achieve the same consumption. For this case, the 14 MeV case exhibits the best results but still requires around 38 years of irradiation at the required flux to turn 95% of the loaded minor actinides into fission products.

An important conclusion can be drawn from this simple analysis. Irradiation time in an industrial reactor being constrained by material resistance issue and mechanical behavior of the assemblies to around 2 10^{23} n/cm^2, it is hardly realistic to reach fluence level described in Table 9 within a single irradiation pass. **Consequently, minor actinides multi-recycling must be considered if efficient mass reduction of minor actinides is to be obtained and the irradiated mass of minor actinides must be characterized in order to assess the impacts on the fuel cycle.**

Let us now consider a reduction of 50 % of the initially loaded mass of MA2035, which can be reasonably expected to be achieved during the in-core residence time of one assembly and focus on the decay heat, neutron source and radiotoxicity of the remaining 50 % heavy nuclei, which include residual minor actinides and plutonium produced during irradiation. Decay heat and neutron source were evaluated using the nuclei given in Table 10 and Table 11, which account for more than 85 % of the decay heat after five years of cooling and 96 % of the neutron source.

Table 10 : Main heat emitting nuclei in irradiated minor actinides Obtained FROM [38]

Isotope	^{242}Cm	^{244}Cm	^{241}Am	^{238}Pu
Power density (W/g)	121.4	2.84	0.11	0.57

Table 11 : Main neutron emitting nuclei in irradiated minor actinides obtained FROM [38]

Isotope	^{244}Cm	^{245}Cm	^{248}Cm	^{252}Cf
Neutron emission (10^7n/s/g)	1.4	1.0	4.4	2.1e5

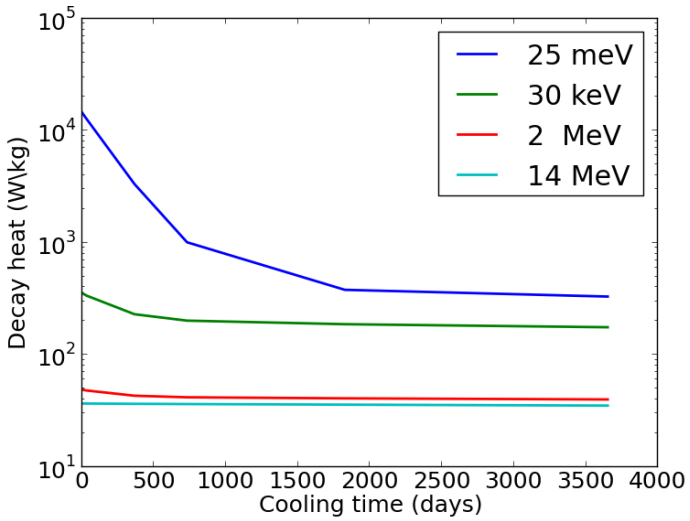

Figure 20 : Decay heat at various time steps for a 50 % reduction in MA mass as a function of the mono-energetic incoming neutron

The behavior of the remaining mass of minor actinides is similar for both decay heat (Figure 20) and neutron source (Figure 21). It can be noticed that values for the 25 meV neutron and to a lower extent for 30 keV neutrons are higher than the one for "fast" neutrons. This is explained by the higher capture cross sections in the thermal range, which increases the production of heat or neutron emitting nuclei such as ^{244}Cm or ^{238}Pu. This is shown below in Table 12, where the composition of the initial and final minor actinides isotopic vector was shown for the 4 mono energetic neutrons. It can be observed that the mass reduction for the 25 meV case is mainly obtained by turning americium into curium rather than fission of americium. The ^{238}Pu production is similarly higher in this case than in the others. For comparison purpose, orders of magnitude for currently realistic handling solutions for spent fuel assemblies are ranging from 53 to 4 W/kg of heavy nuclides, as it will be discussed later on.

Table 12 :Evolution of the composition of the minor actinides in the fuel for a 50 % mass reduction for 4 different mono energetic neutrons. ^{238}Pu was also tracked due to its contribution to decay heat.

	T = 0	25 meV	30 keV	2 MeV	14 MeV
^{237}Np	16.85	8.40	8.90	9.30	9.74
^{241}Am	60.62	4.98	27.97	30.52	30.33
^{242m}Am	0.24	0.06	1.82	0.18	0.08
^{243}Am	15.7	12.59	8.09	9.11	8.94
^{242}Cm	0.02	14.13	0.14	0.01	0.00
^{243}Cm	0.07	0.35	0.01	0.00	0.00
^{244}Cm	5.14	8.85	1.68	0.12	0.10
^{245}Cm	1.28	0.04	1.00	0.70	0.70
^{246}Cm	0.08	0.30	0.29	0.04	0.05
Total of minor actinides	100	50	50	50	50
^{238}Pu	0	17.02	20.34	0.81	0.04

Radiotoxicity (Figure 22) exhibits a slightly different behavior, where the radiotoxicity of the 25 meV irradiated fuel is notably lower than the one of the other cases. This is explained by the higher consumption of ^{241}Am in this case (cf Table 9), which has a half life of 432 years, thus contributing to most of the radiotoxicity after 1000 years. Long term radiotoxicity is also lower due to the similar behavior of ^{237}Np.

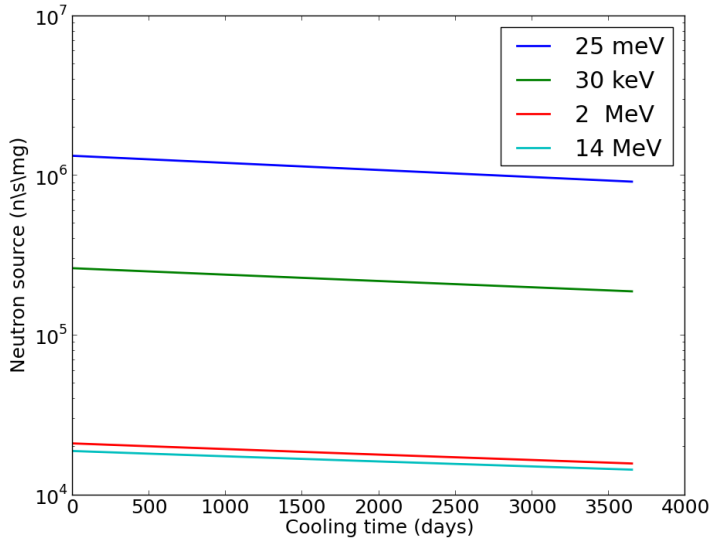

Figure 21 : Neutron source at various time for a 50 % reduction in MA mass as a function of the mono-energetic incoming neutron

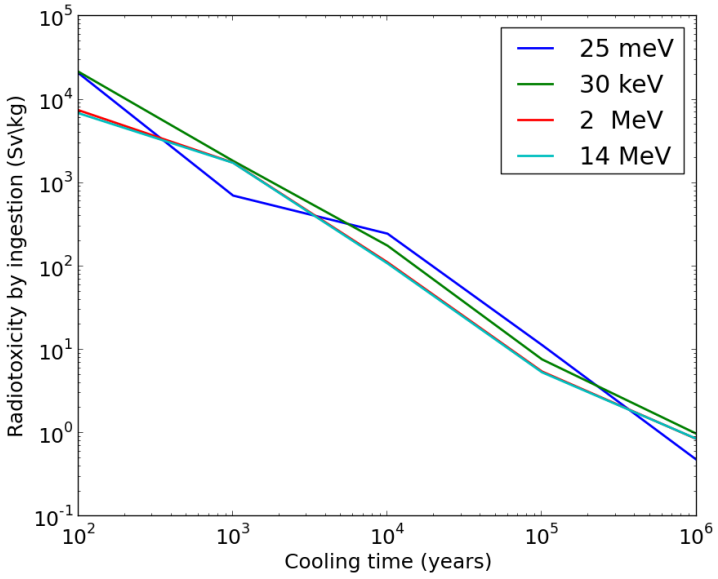

Figure 22 : Radiotoxicity at various time steps for a 50 % reduction in MA mass

This preliminary analysis confirms that multi-recycling of minor actinides in thermal reactors is less attractive than in fast reactors considering the constraints it creates on fuel cycle as already pointed out in several studies [22] [44]. It will not be further considered here. Various other features of transmutation in thermal reactors makes it unattractive, they can be found in [45]. Regardless of this conclusion, it can also be observed that there is still a factor up to 4 between

the decay heat in the 30 keV case and the 2 MeV case, both cases which are achievable in fast reactors. To adequately evaluate the problem, the study was extended in order to include a broader energy range.

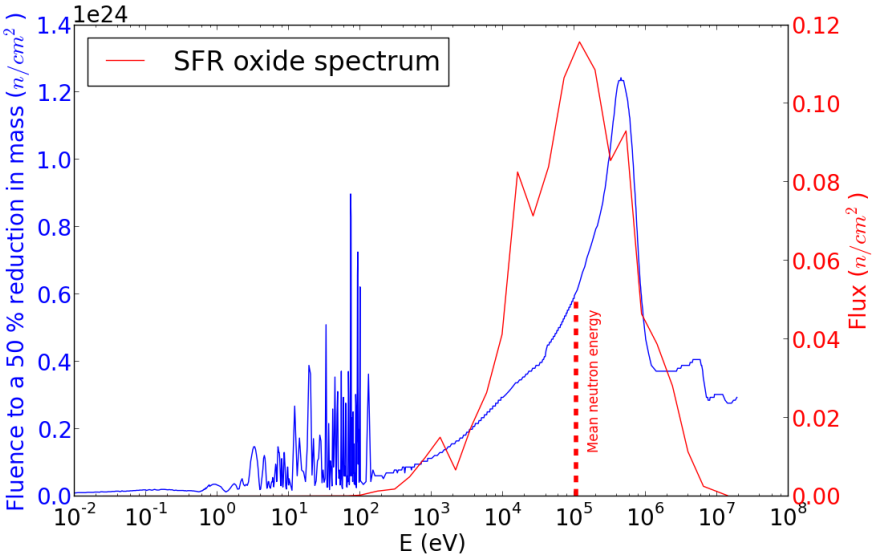

Figure 23 : Fluence necessary to obtain a 50 % mass reduction of a given mass of minor actinides. For comparison, the typical fluence of a 3600 MWth reactor is around 2 10^{23} n/cm².

This was done in Figure 23, which represents the required fluence needed to achieve a 50 % reduction in the mass of minor actinides depending on the energy of a mono-energetic neutron flux. It can be observed that the fluence level is peaked around 500 keV. This behavior is explained by the decrease in the capture cross sections, which is proportional to 1/E and the increase in the fission cross with the neutron energy, as it can be seen in Figure 24. Consequently, the total reaction cross sections decreases and the required fluence increases.

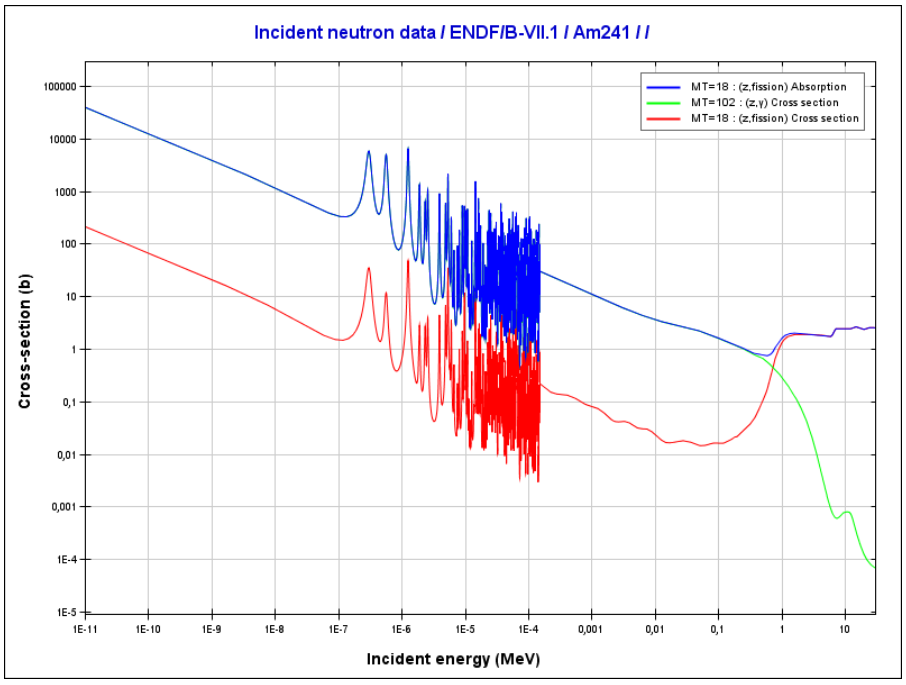

Figure 24 : Fission, capture and absorption cross sections of ^{241}Am

Rather unfortunately, the neutron spectrum of a fast reactor with an oxide core is located close to the aforementioned peak, with a mean energy of around 107 keV. It appears that hardening the neutron spectrum in a reactor will be counterproductive in terms of required fluence due to the lower reaction rate. A "pure" fission spectrum would yield better results with mean neutron energy of around 2 MeV. However, such a spectrum cannot be achieved in a realistic reactor. Consequently, the lowering of the neutron mean energy by shifting the spectrum to lower energies appears to be a relevant approach in order to enhance the transmutation kinetics. This can be achieved by adding to the fuel various materials, preferably with light elements such as beryllium, beryllium oxide, magnesium oxide or various hydrides (CaH_x,YH_x,ZrH_x,…) in order to shift the neutron spectrum by means of elastic scattering process.

However, this spectrum shift has negative impacts on the fuel cycle aspects of transmutation. As it can be seen in Figure 25, lowering the mean energy does increase both decay heat and neutron source of the remaining daughter minor actinides. Additionally, it can be observed that if hardening the spectrum decreases the transmutation performances as mentioned before, it has a strong positive impact on the spent fuel decay heat. Similar conclusions can be reached for radiotoxicity of the remaining fuel.

This last point illustrates the need for a multi-criteria optimization under constraints here: hardening the spectrum appears to limit the impact on the fuel cycle while it lowers the transmutation performances whereas moderating the spectrum has the opposite effects. The question which follows from this conclusion is: "*is there an optimum for spectrum hardness with regards to transmutation performances and fuel cycle impacts and, if yes, how does this optimum depends on the considered constraints on the fuel cycle?*".

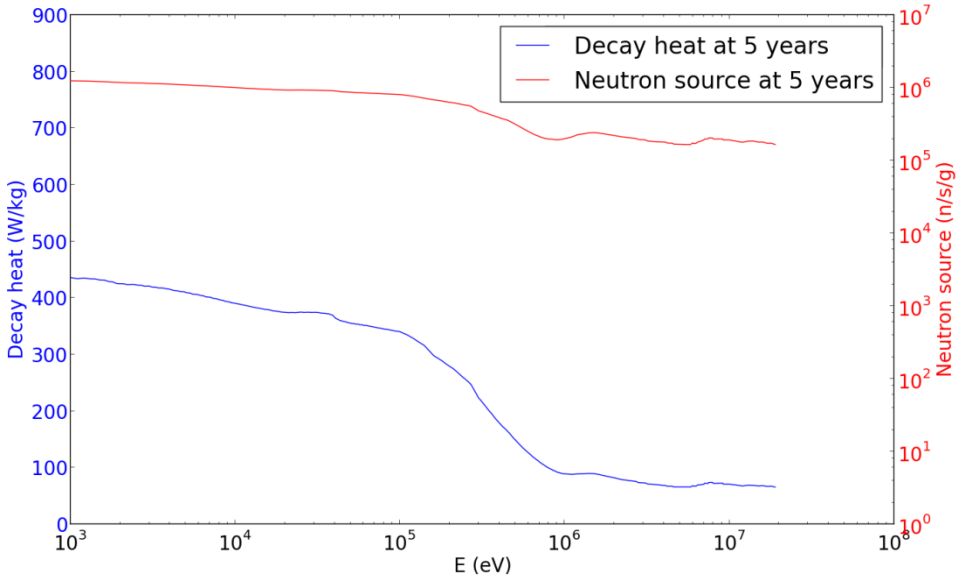

Figure 25 : Evolution of the decay heat and neutron source of the irradiated minor actinides with regards to the neutron energy considered in the epithermal to fast range

The mono-energetic approach discussed here allowed us to clearly establish the founding question and purpose of this optimization process. However, it is rather crude and must be refined for further use. This is the purpose of the next part.

2) CELL CALCULATIONS

a) APPROACH AND HYPOTHESIS CONSIDERED

As no mono-energetic neutron field can be considered realistic, it is now necessary to go into more details and to take into account a realistic neutron spectrum related to the fissile core source or target considered for minor actinides transmutation. It is also necessary to constrain the problem to what can be deemed feasible, or at least realistic. It is further necessary to consider estimators which can be used to quantify both the transmutation performances and the impact on fuel cycle.

In order to study the entirety of the physically realistic range of possible fuel assemblies here, it was decided to carry out a comprehensive sensitivity study of minor actinides transmutation to various physical and technological parameters. The list of these parameters is given below in Table 13.

Various fuel natures were considered, with different densities and support materials. Simultaneously, various coolants were considered. It should be noted here that considering the whole set of input data, only a restricted set of configurations are feasible, for instance it is hardly realistic to design a metallic-fueled helium-cooled reactor due to the non-refractory behavior of the metallic fuel. The possibility of moderating material addition in the assembly was also considered. Zirconium hydride (ZrH_2) is one of most effective candidate as it is very rich in light nuclei, but it may lead to possible worsening of accidental transients due to dissociation at high temperature and possible release of H_2 [46] which may cause over pressurization of the pin or cladding embrittlement. It should however be mentioned that such hydrides have been used in the past, for instance in the form of CaH_x during the ECRIX experiments in Phenix [47] [48]. Beryllium and Magnesium oxide (MgO) are less effective due to their higher mass but are easier to load in reactor cores due to their better stability under irradiation.

It should also be noted here that many of the configurations studied here are not feasible from a thermal point of view as it would for instance lead to very small structural volume fraction or sub-cooling of the assembly. However, it gives a complete knowledge of the physical range of achievable neutron spectrum.

Table 13 : Breakdown of the physical and technological parameters considered in this study

Physical/technological parameter	Variation range
Fuel type and volume fraction	Oxide/Nitride/Carbide/Metal between 20 to 50 %
Coolant type and volume fraction	Sodium/LBE/Helium between 20 to 50 %
Moderating material type if any and volume fraction	None/ZrH_2/Be/MgO between 0 to 20 %
Am content in the fuel	1 to 50 %
Plutonium content in the fuel	1 o 40 %
Irradiation time	300 to 10,000 EPFD
Flux level	0.1 to 10^{15} n/cm^2/s
$^{241}Am/(^{241}Am + ^{243}Am)$	60 to 90 %

For this preliminary approach, only americium transmutation was considered. Indeed, americium is the likeliest candidate for early transmutation, as it represents the bulk of the mass of minor actinides produced in plutonium fueled reactors and as it is the biggest contributor to midterm radiotoxicity in a closed fuel cycle as seen in Chapter 1. Neptunium is a very weak contributor to total radiotoxicity and behaves in a simpler manner than americium under irradiation. A more detailed analysis of neptunium transmutation can be found in Annex 1. Curium on the other hand is much more active than Americium, making manufacturing and transportation of curium loaded fuel an issue to be addressed. A short notice on the specificities and similarities of curium transmutation with americium transmutation can also be found in Annex 1.

The americium isotopic vector considered was also set as a free parameter in order to take into account the two dissimilar behaviors of americium isotopic. Indeed, ^{241}Am transmutation yields mainly the short lived ^{242}Cm ($T_{1/2}$ = 162 days) which itself decays to ^{238}Pu which has a half life of 87 years. On the other hand, ^{243}Am transmutation yields ^{244}Cm which has a half-life of 18.8 years. The evolution of the impacts on the fuel cycle of the transmutation of these two isotopes will thus be fundamentally different. This will be detailed later on in paragraph 3).1)d). Flux level and irradiation time were also used as input parameters, even though they are determined by other parameters which cannot be modeled in a cell calculation, such as the core power or of the core fuel management scheme. Considerations on core impacts in heterogeneous or homogeneous transmutation will be discussed in Chapter 4 and 5 respectively.

Considering all these parameters, URANIE [40] was used to sample a set covering the entirety of the parameter space. To simulate the irradiation, 33 group cross sections were calculated using a homogeneous cell model and the ECCO cell code [7]. These cross-sections were then collapsed into one group cross-sections for depletion calculation which were carried out with a constant flux and a depletion chain ranging from ^{234}U to ^{252}Cf. Cooling down was simulated using the same depletion calculation without flux.

The transmutation rate defined as the relative fraction of americium consumed during the irradiation time T ($\tau = \frac{Am(0)-Am(T)}{Am(0)}$) was first computed. A second rate was also considered, namely the effective destruction through fission rate, which is defined as the americium fraction which has effectively been destroyed through fission and not capture. Using this information, it was possible to identify several trends.

b) General consideration on transmutation performances

Considering the parameters discussed in Table 13, various conclusions can be reached. First, the impacts of the "technological parameters" related to the fuel and moderating material volume fraction can be observed in Figure 26. In this figure, the transmutation and fission rate for a representative fast reactor cell irradiated for 4000 EFPD in a 3600 MWth reactor are plotted. The fuel volume fraction was modified by increasing the sodium fraction for the left plot, and sodium was displaced by moderating material (here ZrH_2) in the right plot. It can be seen that when the fuel volume fraction increases (all things equal otherwise), the total transmutation rate increases while the fission rate decreases. Conversely, when the moderating material volume increases, the behavior of the two rates above mentioned is the opposite. The

explanation for this effect was already discussed in Part 1) of this chapter, as the increase of the fuel volume fraction leads to a spectrum hardening while the increase in the moderating material leads to a softening of the neutron spectrum. Considering that with the knowledge of the neutron spectrum, it is possible to design an assembly with the adequate fuel, coolant and moderating fraction to obtain this very spectrum, we can thus work using only the neutron spectrum instead of several parameters related to technological design of the assembly. Then, once an optimal neutron spectrum has been found, it is possible to design a technologically compliant assembly.

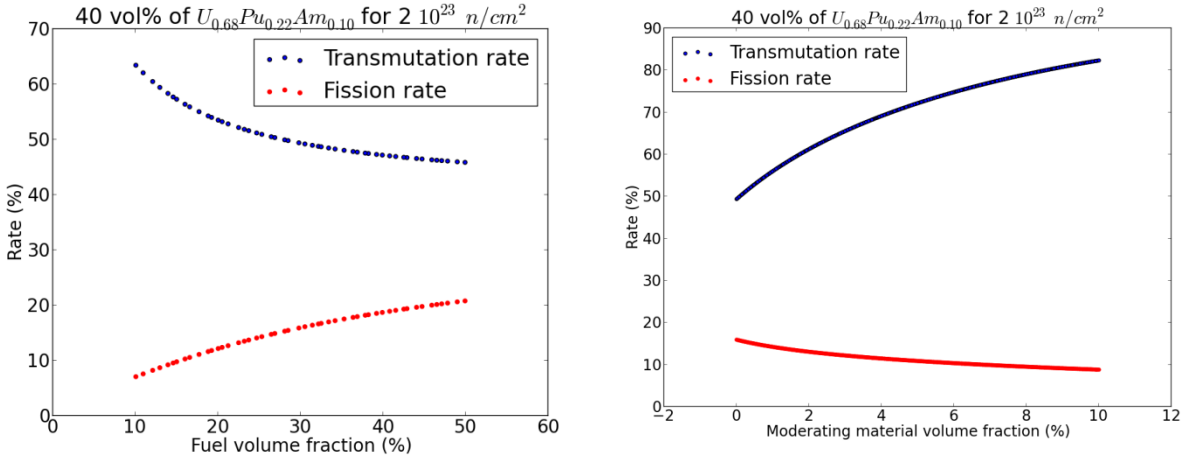

Figure 26 : Illustration of the evolution of the transmutation and transmutation rates with regards to the fuel or moderating material volume fraction. Americium fraction was set at 10 % and plutonium fraction at 22 %.

Considering now the americium content in the fuel, shown here in Figure 27, two things can be observed. First, an extrema in the transmutation rate can be reached for an initial content lying between 10 and 12 %. This extrema is explained by the initial presence of plutonium in the fuel. Indeed, if we consider for instance ^{243}Am, two opposite effects can be observed during irradiation:

- Production of ^{243}Am coming from neutron captures on ^{242}Pu
- Consumption of ^{243}Am through capture of fission

If the initial amount of ^{243}Am is too low, the production term is going to be higher than the consumption term for some time during the irradiation, which will limit the overall transmutation performances. The lower the initial amount of americium, the higher the startup production and thus the lower the final transmutation rate. This is illustrated for the ^{242}Pu/^{243}Am couple below in Figure 28, where a net production of ^{243}Am can be observed for a ratio ^{243}Am over ^{242}Pu equal to 0.10, after 2000 EFPD. If this ratio increases, actual consumption of ^{243}Am takes places, with a rate increasing with the initial amount loaded. It should also be mentioned here that, as both these phenomena depend on the neutron spectrum, the position of the extremum of minor actinides in the fuel also depends from the neutron spectrum considered. The impact of the initial amount of plutonium and its isotopic vector will be further detailed in the paragraph 2.1)c) dedicated to the homogeneous mode.

Secondly, it can be seen that for higher amount of americium loaded, an increase in the content has similar effects as an increase in the fuel volume fraction, e.g. a decrease in the transmutation rate and simultaneously an increase in the fission rate. This comes from the fact that, as it was

observed previously, adding minor actinides to the fuel hardens the spectrum. We can conclude from this that the knowledge of the minor actinides content is obviously necessary to compute the transmutation and fission rate, but also that the neutron spectrum is fraction-dependent. **We are thus confronted to a multi-variate problem with here two variables: the neutron spectrum and the initial minor actinides content.** The plutonium isotopic content must also be taken into account to compute the fuel production of minor actinides. It is consequently necessary to find one or several indicators to characterize the neutron spectrum and then to show that it is possible to build a bijective function between these indicators and the fuel and moderating material volume fraction.

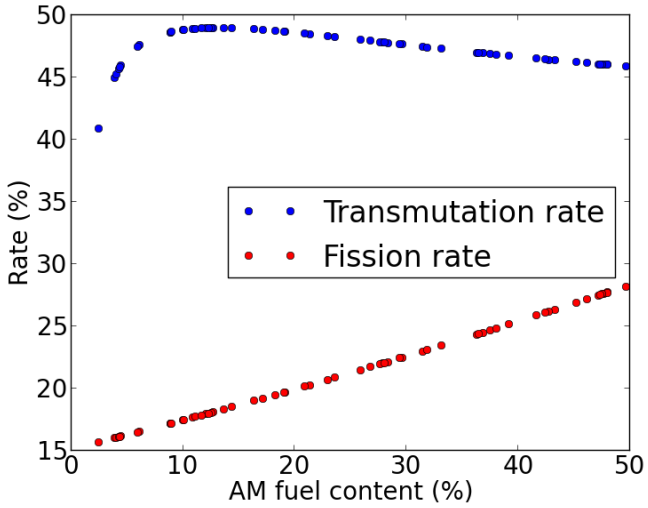

Figure 27 : Illustration of the evolution of the transmutation and fission with regards to the minor actinides content in the fuel. Fuel volume fraction was set at 40 %, with 40 % of sodium and 20 % of structural material. Plutonium content was set to 22 %.

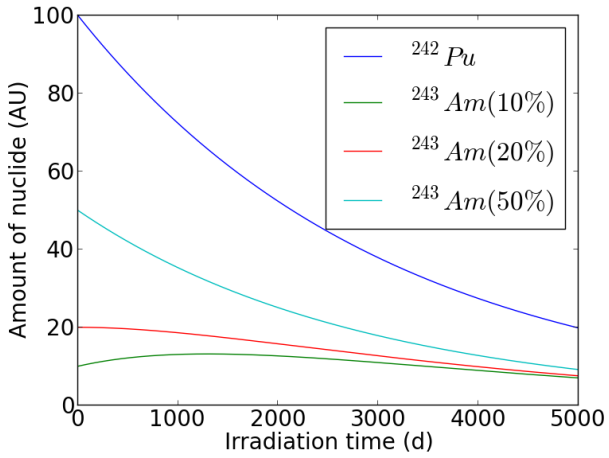

Figure 28 : Illustration of the impact of the initial amount of plutonium in the fuel with regards to americium consumption. The evolution of the ^{242}Pu amount is plotted for three different initial amounts of ^{243}Am.The percentage behind ^{243}Am corresponds to the initial amount of ^{243}Am relative to the initial amount of ^{242}Pu.

To do so, we introduce here the r-factor to characterize the neutron spectrum in the fuel. This factor is traditionally defined as the inverse of the difference of the average lethargy of

production and removal (through leakage or absorption) of the neutrons in the core, as shown in Equation 16 [49]. The value of the r-factor increases with the hardness of the spectrum, with typical values for a fast reactor being between 0.15 and 0.35 [49]. Depending on the type and amount of moderating material considered r-factor as low as 0.01 can be achieved in minor actinides bearing targets with hydrogenated moderating materials as it will be shown later. It should be mentioned here that the value of the r-factor in subcritical medium and especially radial blankets is not physical, as a r-factor of 0.01 would lead to a ratio between the neutron creation and absorption energy of 2.7 10^{43}. However, this value as computed by the ECCO cell code was found to be a good estimator of the neutron spectrum hardness in the blankets and was therefore used in this study.

$$r = \frac{1}{u_{removal} - u_{creation}}$$

Equation 16 : Definition of the r-factor

As it can be seen in Figure 29, the behavior of the r-factor with regards to the americium content and the moderating material volume fraction is smooth and predictable. The same conclusion holds for the behavior of the r-factor with regards to the fuel volume fraction. This means that it is possible to use the r-factor as a neutron spectrum indicator by itself and to carry on with the neutron analysis of the problem and then to expand the scope of the problem by matching the r-factor with the corresponding assembly design. It should be mentioned here that various assemblies may be designed for a given r-factor and americium content depending on the technologies considered. **Consequently, the multi-variate problem considered here depends for now on only two variables: the initial amount of minor actinides loaded in the fuel and the neutron spectrum inside the fuel.**

Three more variables were also considered here to obtain a full picture of the transmutation process. The first two are linked together by the fluence and the core management scheme and are the irradiation time and the flux level “seen” by the fuel or targets. The last one is the minor actinides isotopic vector to be considered.

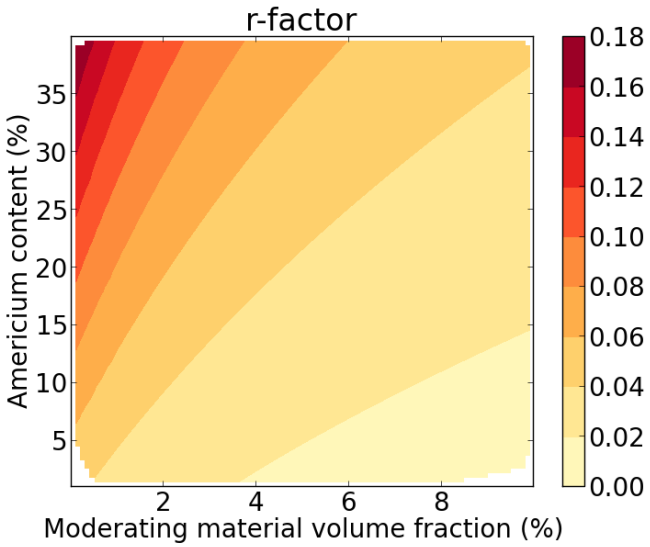

Figure 29 : Evolution of the r-factor with regards to the americium content and the moderating material volume fraction. The fuel fraction is fixed. The moderating material considered here is ZrH_2, which explains the low r-factor observed.

For comparison purposes, the neutron spectrum for four cases was plotted in Figure 30, with a thermal core spectrum, a fast spectrum, and two spectrums corresponding to Minor Actinides Bearing Blankets (MABB) with 20 at% of americium loading, with or without ZrH_2. These MABB are targets assemblies used in the heterogeneous transmutation and loaded at the core periphery in the first reflector ring. The first point to be mentioned here is that even if we somewhat abusively employ the term “moderated” to design MABB loaded with ZrH_2, the neutron spectrum in these blankets is significantly faster than a thermal spectrum. However, it effectively exhibits a “longer” thermal tail than the neutron spectrum in a standard MABB assembly. Finally, the effect of spectrum “degradation” in the blankets due to loading at the core periphery can observed here by comparing the core fast spectrum and the MABB fast spectrum.

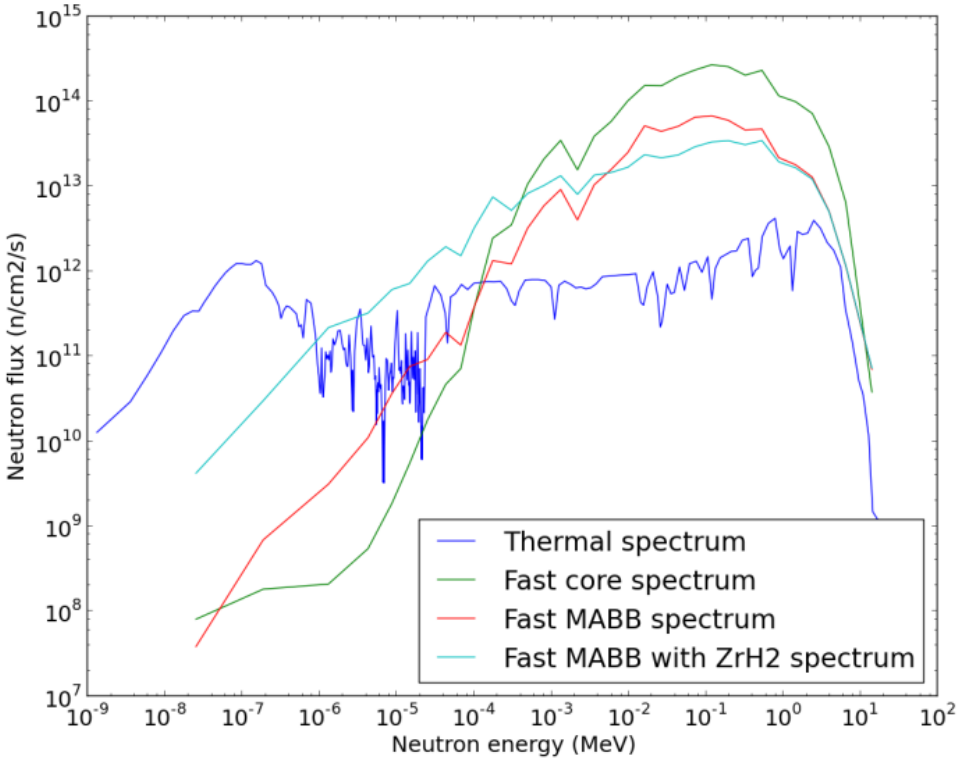

Figure 30 : Comparison of the neutron spectrum for various reactors cases

Considerations on the minor actinides isotopic vector will be limited here as further details are available in the next chapters about the impact of americium isotopic vector. The main point here is the difference between transmutation of americium only (which has been shown as the element with the most promising transmutation capability) or transmutation of the complete minor actinides isotopic vector as obtained at the end of spent fuel reprocessing. The first solution requires the separation of americium from the other minor actinides while the other requires grouped extraction or co-extraction with the plutonium in the spent fuel, as discussed in Annex 3.

The performances of two isotopic vectors will be compared here, corresponding to the isotopic vectors which are deemed available in France by 2035-2040 according to [50]. The first one is the 'MA2035' vector already described in Table 8. The second one corresponds to a similar case where only americium was considered for transmutation, with an americium isotopic vector of 75 % ^{241}Am and 25 % ^{243}Am.

In terms of neutron spectrum, it can be observed below in Table 14 that the various minor actinides have different impacts on the neutron spectrum. They can be split into two categories : the ones which harden the spectrum due mainly to captures in the epithermal range (^{237}Np,^{241}Am,^{243}Am,^{242}Cm,^{244}Cm,^{246}Cm) and the ones which harden the spectrum by fission (^{242m}Am,^{243}Cm,^{245}Cm) as the neutrons emitted by a fission have an average energy in the MeV range. These last three nuclides have a "better" hardening effect than the others. The presence of this small amount of "good" fissile nuclei in the MA2035 medium explains the harder spectrum for this isotopic vector than for the Am2040 vector. Due to this hardening of the spectrum, the americium transmutation rate for instance is slightly lower in the MA2035 case

than in Am2040 case, as it can be seen in Figure 31. It can also be further observed that the behavior of the two cases is not significantly different. In terms of transmutation performances only, the isotopic vector is thus playing a marginal role.

Nuclide	r-factor
Am 241	0,077
Am242m	0,437
Am243	0,065
Np237	0,077
Cm242	0,137
Cm243	0,475
Cm244	0,098
Cm245	0,420
Cm246	0,081
Am2040	0,074
MA 2035	0,083

Table 14 : r-factor of the neutron spectrum in a target with a 10 % content of various minor actinides. No moderating material was considered.

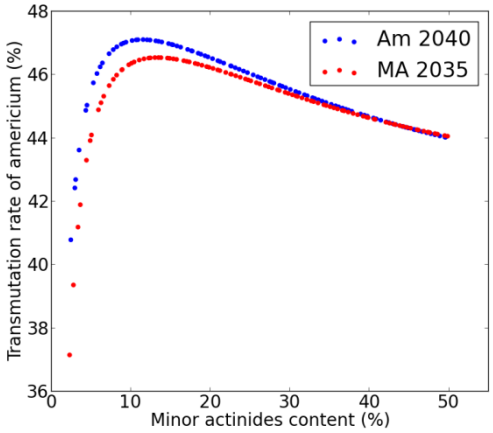

Figure 31: Comparison of the americium transmutation rate between a loading of Am2040 and Ma2035 isotopic vector

In terms of irradiation time and flux level, the example of the $^{243}Am/^{244}Cm$ is representative of what can be observed for others nuclide. Equation 14 describes the evolution of the amount of ^{243}Am in a target with no production from neutron capture from ^{242}Pu. It can be observed that the final amount of ^{243}Am at the end of irradiation depends only on the product ϕT with T the total irradiation time and ϕ the neutron flux, that is to say the total neutron fluence to which the target has been submitted. Consequently, the transmutation rate of americium in this configuration only depends on the total fluence, regardless of the irradiation time, as long as this time can be neglected compared to the radioactive half-life of ^{243}Am, which is 7300 years. Capture on ^{242m}Am will be neglected considered the high fission cross section of this isotope and its low equilibrium concentration in a reactor core.

However, the amount of ^{244}Cm at the end of irradiation can be written as shown in Equation 17. This solution depends not only on ϕT but also directly on the flux level through the $\frac{\lambda}{\phi}$ term. If we consider a flux level of 5 10^{14} n/cm^2/s and a 18.8 years radioactive period for $^{2}\phi^{44}Cm$, this term is equal to 2.4 barns, which is of the same order of magnitude than the capture or fission cross sections of ^{244}Cm. Consequently, this term cannot be neglected in the calculations in order to obtain an accurate value for the final amount of curium. The same analysis holds true for the $^{241}Am/^{242}Am$ couple, as the period of ^{241}Am is of 432 years.

$$N_{Cm244}(T) = N_{Am243}(0)\frac{\sigma_c^{Am243}}{\sigma_a^{Am243} - \sigma_a^{Cm244} - \frac{\lambda_{244}}{\phi}}\left(e^{-(\sigma_a^{Cm244}+\frac{\lambda_{244}}{\phi})\phi T} - e^{-\sigma_a^{Am243}\phi T}\right)$$

Equation 17 : Solution of Bateman Equations for the $^{243}Am/^{244}Cm$couple

As Curium is a major contributor to decay heat and neutron source of the spent fuel, it is necessary to fully take into account its production to accurately evaluate the impacts of minor actinides on the fuel cycle. Indeed, as it can be shown below in Figure 32, for a fluence equal to 2.37 10^{23} n/cm^2, which is representative of the fluence that can be seen by fast reactors blankets

over 4100 EFPD for a 3600 MWth reactor, the final ^{244}Cm content increases with the neutron flux level for a given fluence. Indeed, for low flux levels, a significant part of ^{244}Cm has time to decay during the longer irradiation time compared to a high flux level case.

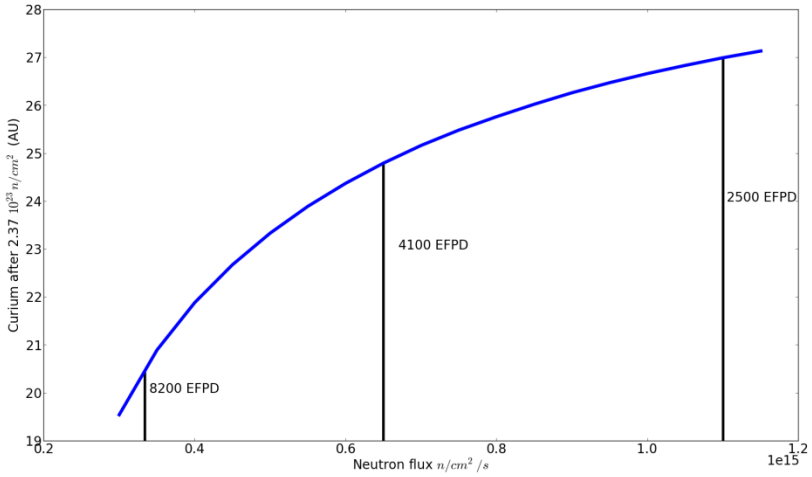

Figure 32 : Evolution of the curium concentration after 2.37 10^{23} n/cm² for various levels of flux

We can conclude from this short analysis that we can reduce the first three rows of Table 13, which were linked to technological parameters, to only one parameter, the r-factor. Along with the fluence and the americium content, these three parameters are sufficient to fully characterize the transmutation performances of a given system. However, it should be noted that the physics of the phenomenon differs depending on the initial presence minor actinides precursors or not in the fuel. This will be discussed in the next parts.

It was further shown that the fluence information only was not sufficient to characterize the behavior of curium isotopes such as ^{244}Cm or ^{242}Cm as these isotopes have periods which are of the same order of magnitude as the irradiation time considered in Table 14. Consequently, it appears that it will be necessary to use these two variables to correctly evaluate the impacts on the fuel cycle, to which curium isotopes are important contributors.

c) HOMOGENEOUS CASE

In the homogeneous approach, minor actinides to be transmuted are mixed with the fuel of the reactor. In this case, the Bateman equation for the ^{243}Am/^{244}Cm reduced system can be rewritten in Equation 18. The main difference with Equation 12 is the presence of a production term coming from the neutron captures on the ^{242}Pu in the fuel.

$$\frac{dN_{Am243}}{dt} = N_{Pu242}\sigma_c^{Pu242}\phi - N_{Am243}\sigma_c^{Am243}\phi - N_{Am243}\sigma_f^{Am243}\phi$$

Equation 18 : Solution of the Bateman Equations for the ^{242}Pu/^{243}Am couple

From Equation 18 it is clear that the production term from ^{242}Pu will itself depends on various parameters, which are the neutron spectrum, the neutron flux and the amount of ^{242}Pu in the core. These three parameters are linked together and depend on technological parameters such as core power level, the expected burn up and initial Pu content. A deeper analysis of their impact on minor actinides transmutation will be carried in more details in Chapter 5.

Nevertheless, a preliminary simplified analysis can be performed with regards to the neutron spectrum and the isotopic composition of the plutonium.

Isotopic composition of the plutonium used as nuclear fuel varies greatly depending on various factors such as the burn-up of the irradiated fuel from which the plutonium is recovered, the neutron spectrum to which it was submitted, and its cooling time. For thermal reactors, the plutonium isotopic vector usefulness is characterized using its quality, defined as the ratio of fissile isotopes (^{239}Pu and ^{241}Pu) over the total mass of plutonium and ^{241}Am. This last nuclide is taken into consideration as it is produced through decay of ^{241}Pu during cooling of the separated plutonium and thus is mixed with plutonium at loading.

However, in a fast spectrum every isotope of plutonium is "fissile" but to a different extent depending on the ratio of fission to capture cross sections and thus on the neutron spectrum. It is possible to define weights for each isotope as shown below in Equation 19 [49]. These weights are defined relatively to a reference fertile nucleus (here, ^{238}U) and a reference fissile nucleus (here, ^{239}Pu). A breakdown of the various weights of the most common isotopes in a fast spectrum is shown below in Table 15. By weighting the fuel isotopic content which the corresponding weight, it is possible to define an equivalent fuel with a given enrichment in pure ^{239}Pu, or Pu_{eq}. For instance, 1 kg of ^{238}Pu will be equivalent to 0.66 kg of pure ^{239}Pu in the spectrum corresponding to Table 15 calculated for a 3600 MWth oxide core from [51].

$$w_i = \frac{\sigma_i^+ - \sigma_{238U}^+}{\sigma_{239Pu}^+ - \sigma_{238U}^+} with\ \sigma_i^+ = \nu\sigma_f - \sigma_a \quad (10)$$

Equation 19 : Definition of a nuclide weight in a given spectrum

The plutonium isotopic vector will influence minor actinides production in two ways. First, considering the production ways of ^{241}Am and ^{243}Am (and curium isotopes beyond), high initial content in ^{241}Pu and ^{242}Pu will lead to high production rate of americium and thus degrades the transmutation performances. And the other hand, a plutonium isotopic vector with a high content in ^{239}Pu will limit the production of heavier isotopes. For comparison purpose, five equivalent plutonium isotopic vectors have been calculated and their minor actinides production after 100 GWd/t of mean burn up has been analyzed in Table 16 and Table 17. The core considered for this quick analysis will be further detailed in part 4) of this chapter.

The five isotopic vectors of Table 16 have a similar equivalent weight close to 0.668. Several comments can be made here. First, the ^{243}Am and ^{244}Cm production can be directly linked to the initial ^{242}Pu content. Similarly, ^{241}Am production can be linked to ^{241}Pu and ^{240}Pu. ^{237}Np production is nearly not impacted by the plutonium isotopic vector as it is produced through (n,2n) reactions on ^{238}U or captures on ^{235}U.

Table 15 : Weights of the most common isotopes for a fast spectrum from [51]

Nuclide	w_i
^{235}U	0.77
^{237}Np	-0.25
^{238}U	0.00
^{238}Pu	0.66
^{239}Pu	1.00
^{240}Pu	0.14
^{241}Pu	1.50
^{242}Pu	0.09
^{241}Am	-0.31
^{243}Am	-0.30
^{242m}Am	2.18
^{242}Cm	0.42
^{243}Cm	0.11
^{244}Cm	2.52
^{245}Cm	2.17
^{246}Cm	0.14

Table 16 : Composition of four plutonium isotopic vectors with a similar equivalent weight of 0.668

Mass %	^{238}Pu	^{239}Pu	^{240}Pu	^{241}Pu	^{242}Pu	^{241}Am
Reference	3.57	47.39	29.66	8.23	10.37	0.78
Vector 1	4	45	18	10	22	1
Vector 2	15	22	30	20	12	1
Vector 3	70	5	6	9.6	8.4	1
Vector 4	3.57	48.42	10	8.23	29	0.78

Table 17 : Minor actinides content of the core considered after 100 GWd/t of burn-up

Production (kg)	^{241}Am	^{243}Am	^{244}Cm	^{237}Np
Reference	171	164	54	28
Vector 1	194	342	111	27
Vector 2	313	216	66	28
Vector 3	132	123	43	27
Vector 4	156	448	145	27

It is possible to evaluate more accurately the link between plutonium isotopic vector and minor actinides production by solving the adjoint Bateman Equation and calculating the adjoint concentration at the beginning of irradiation. This was done in [52] and is shortly detailed below. The Bateman Equation from Equation 9 can be rewritten as follow in Equation 20 with R the operator describing the nuclear reactions and D the radioactive decay operator. The adjoint concentration is the solution of the adjoint Boltzmann, which is given in Equation 21. This adjoint concentration plays a similar role for the "direct" concentration as the adjoint flux for the neutron flux, that is to say for a given isotope j, the adjoint concentration represents the weights of every possible "father nuclei" leading to the isotope j. Due to the transposition of the Bateman Equation, the adjoint Bateman operator works from the end of irradiation to its beginning. Using the adjoint concentration, it is then possible to compute the sensitivities of the concentrations in minor actinides to cross sections.

$$\frac{d\vec{N}}{dt} = (R\phi + D)\vec{N} = M\vec{N}$$

Equation 20 : Matrix form of the Bateman Equations

$$\frac{d\vec{N}^{\dagger}}{dt} = -M^{t}\vec{N}^{\dagger}$$

Equation 21 : Adjoint Bateman Equations written in matrix form

For a reference core 3600 MWth oxide core, the adjoint concentrations of three minor actinides ^{241}Am, ^{243}Am, and ^{244}Cm were computed and are shown below in Table 18 to Table 20. Only significant sensitivities coefficients where shown and it can be observed that ^{244}Cm production is effectively mainly sensitive to ^{243}Am and thus to ^{242}Pu concentration since ^{243}Am production is mainly sensitive to ^{242}Pu concentration. ^{241}Am production is sensitive to ^{241}Pu but also to ^{240}Pu which is the direct source of ^{241}Pu during irradiation. ^{241}Am appears to be also slightly sensitive

to ^{244}Cm, which is due to the decay of ^{244}Cm to ^{240}Pu. This sensitivity coefficient should increase with the irradiation time.

Table 18: Sensitivities of ^{241}Am End of Life concentration to nuclear data

241Am				
Isotope	Capture	Fission	(n,xn)	Total
^{238}U	1,75E-03	-8,16E-06	-2,43E-07	1,74E-03
^{238}Pu	6,16E-03	-1,17E-03	-3,21E-07	5,00E-03
^{239}Pu	**4,73E-02**	-2,90E-03	-2,61E-06	4,44E-02
^{240}Pu	**-1,07E-02**	-5,65E-02	-4,71E-05	-6,73E-02
^{241}Am	-9,52E-02	-9,50E-02	-5,14E-05	-1,90E-01

Table 19 : Sensitivities of ^{243}Am End of Life concentration to nuclear data

243Am				
Isotope	Capture	Fission	(n,xn)	Total
^{240}Pu	6,06E-03	-2,91E-04	-2,63E-07	5,77E-03
^{241}Pu	**2,33E-02**	-7,58E-03	-6,48E-06	1,57E-02
^{242}Pu	**3,32E-01**	-2,15E-02	-5,84E-05	3,11E-01
^{241}Am	1,47E-02	-1,44E-03	-7,44E-07	1,32E-02
^{242m}Am	1,51E-02	-6,16E-03	-1,12E-06	8,92E-03
^{243}Am	-4,92E-01	-6,11E-02	-1,25E-04	-5,53E-01

Table 20 : Sensitivities of ^{244}Cm End of Life concentration to nuclear data

244Cm				
Isotope	Capture	Fission	(n,xn)	Total
^{240}Pu	2,20E-03	-8,72E-05	-7,94E-08	2,11E-03
^{241}Pu	1,06E-02	-2,82E-03	-2,44E-06	7,77E-03
^{242}Pu	**2,07E-01**	-9,36E-03	-2,57E-05	1,98E-01
^{241}Am	7,37E-03	-6,10E-04	-3,21E-07	6,76E-03
^{242m}Am	7,58E-03	-2,45E-03	-4,50E-07	5,12E-03
^{243}Am	**6,95E-01**	-3,79E-02	-7,78E-05	6,57E-01
^{242}Cm	1,76E-03	-4,80E-05	3,97E-09	1,71E-03
^{243}Cm	1,74E-03	-6,81E-04	-8,64E-08	1,06E-03
^{244}Cm	-1,62E-01	-8,01E-02	-7,95E-05	-2,42E-01

We can conclude from this that there an incentive to use a plutonium isotopic vector which is as close as possible to ^{239}Pu in order to limit the production of minor actinides. This can be achieved by instance by using as fast a spectrum as possible in order to produce good "quality" plutonium (breeding-like configuration) and then use this plutonium to transmute minor actinides. This option will be discussed in Chapter 5.

A second effect is related to the equivalent weight itself of the plutonium vector considered. The lower the weight, the higher the necessary plutonium content in the fuel to sustain the chain

reaction and thus the higher the production of minor actinides during irradiation. This is shown in Figure 33. The variability of the results for the production of minor actinides for two similar equivalent weights is directly due to the isotopic vector effect discussed in the previous paragraph. Interestingly enough, there is close to no effect on neptunium production due to the cancelling of two second order effects: an increase in the plutonium content leads to a decrease of the uranium fraction in the fuel which decreases the production rate of ^{237}Np from (n,2n) reaction on ^{238}U, but also hardens the spectrum thus increasing the (n,2n) reaction cross section.

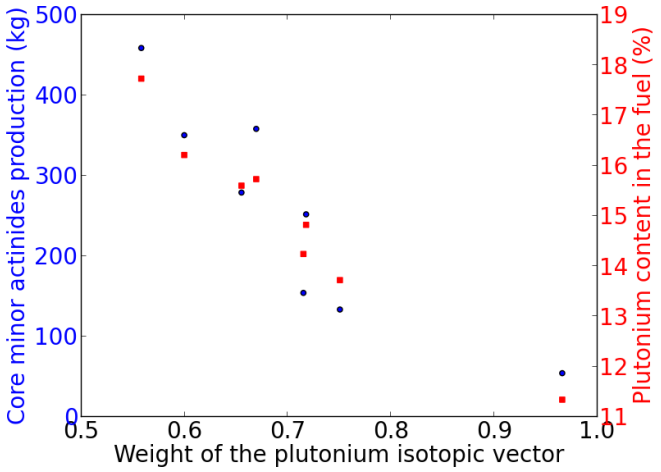

Figure 33: Evolution of the plutonium content and minor actinides production in a reactor for various plutonium isotopic vectors

Considering these specificities of the homogeneous mode, we used only one plutonium isotopic vector in this study, which is given in Table 21. This plutonium isotopic vector denominated Pu2035 thereafter is deemed representative of what would be available in France by 2035 considering the industrial scenarios discussed in [25]. This vector is of relatively bad quality with high content in ^{242}Pu and ^{241}Pu as its main component is plutonium recovered from thermal reactors fueled with MOX. Plutonium multi recycling in fast reactors leads to an improvement of the plutonium isotopic vector due to the favorable ratio of cross sections in a fast spectrum. Consequently, considering Pu2035 as the main isotopic vector can be considered as a conservative approach with regards to minor actinides production in the fuel during irradiation.

Table 21: Isotopic vector of plutonium 2035, which corresponds to plutonium coming from PWRs with UOX or MOX fuels.

Isotope	Pu238	Pu239	Pu240	Pu241	Pu242	Am241
Mass %	3,57	47,39	29,66	8,23	10,37	0,78

d) Heterogeneous case

The heterogeneous case exhibits also some peculiarities which are discussed here. First and foremost, if minor actinides are loaded inside minor actinides bearing blankets (MABB) at the core periphery, their impact on the core behavior itself is not significant in terms of feedback coefficients and transient behavior as minor actinides are loaded in a low flux zone. However,

several parameters related to breeding and reactivity swing are modified. Indeed, for a typical blanket with 20 at% of Americium irradiated during 4100 EFPD at the periphery of a 3600 MWth fast reactor, significant breeding occurs with a calculated equivalent final content in plutonium of 4.7 %. This will have an impact on the power production in the blanket region, which rises from 1.5 % to 4.9 % of the core total power output. Breeding in the blankets also leads to a small decrease of the reactivity swing in the core (-0.36 pcm/EFPD vs -0.86 pcm/EFPD for a core without MABB) and a small rise in the core breeding gain (+0.01 compared to -0.05) due to ^{239}Pu production in the blankets.

This requires a slight adaptation of the axial blankets loading in the core itself and of the control rod systems in order to achieve acceptable performances and keep the global breeding gain equal to zero. Nevertheless, this was not done here as it would require a very fine level of core design which could not be achieved with the methods developed in this work. However, it was verified for optimized designs that the breeding gain and reactivity swing remained within acceptable values.

A second approximation was done throughout the study in order to limit calculation times. A constant flux approximation was considered here, which means the depletion calculations were done using a single time step of duration T. As the final state of the system only depends on the total fluence to which it has been submitted, this allows us to consider the problem without taking into account the actual irradiation history in a “true” reactor. Indeed, two factors locally modify the flux in the blankets during irradiation:

- Breeding of ^{239}Pu and ^{238}Pu takes place from ^{238}U and ^{241}Am respectively, which increase the fission reaction rates in the blankets and thus the flux level while hardening the neutron spectrum.
- Depletion and subsequent reloading of the neighboring assemblies occurs, which modifies the source term for the flux calculation in the blankets.

Consequently, the “real” flux profile has the shape shown below in Figure 34. The flux level in the blankets gradually increases during irradiation due to production of fissile isotopes in it. Using a constant flux approximation has a very limited impact on transmutation performances, since americium half lives are much higher than typical irradiation times but it does have an impact on curium production, especially in terms of ^{242}Cm production, which has a short half live of 163 days. Indeed, its final concentration is mainly dependent on the level of flux to which the blankets is submitted during the last cycle. The higher this flux is, the higher the production of ^{242}Cm in a given time and thus the higher its final content. Consequently, the final ^{242}Cm is underestimated of about 15 % with the constant flux approximation. However, as a minimal cooling of 5 years will be considered here, ^{242}Cm will be a very minor contributor to decay heat after this period of time and the approximation of a constant flux can be used. In this regard, ^{242}Cm behaves similarly to any fission products, which were also not taken into account here. However, as ^{242}Cm decays to ^{238}Pu, this approximation will lead to a small underestimation of the long-term decay. Similarly, the neutron spectrum in the blankets changes during irradiation due to the breeding of ^{239}Pu. As for the flux, a mean value of the r-factor was considered throughout these calculations.

The approximations made for characterizing the heterogeneous transmutation mode will be further detailed in Chapter 4.

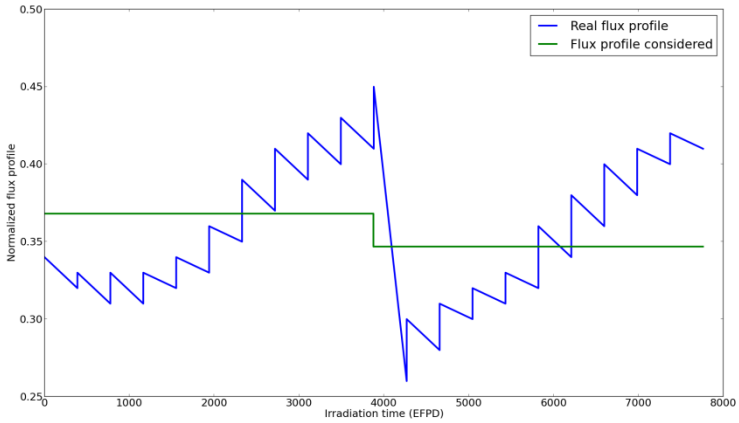

Figure 34 : Comparison of the real and considered flux profile in minor actinides bearing blankets. The irradiation time was voluntary increased to highlight the effect of breeding in the blankets.

3) PARETO FRONT ANALYSIS AND APPLICATIONS

a) METHODOLOGY AND ESTIMATORS OF INTEREST

Following this physical introduction to the physics of minor actinides transmutation, it is necessary to clearly identify the objectives and limitations of the transmutation process in order to identify research avenues. As the goal of this analysis is to derive as much information as possible while keeping the computation time reasonable, it will focus on heterogeneous minor actinides transmutation. A complete chapter of this work is dedicated to homogeneous minor actinides transmutation.

In accordance with the objectives described in Chapter 2, it is necessary to first identify the parameters and constraints of interest for the optimization process. As we consider heterogeneous minor actinides transmutation, core design constraints can be put aside and only transmutation and fuel cycle constraints remain.

Two estimators will be used to quantify minor actinides transmutation here:

- $C_1 = \Delta m$, which is defined as the mass of minor actinides consumed during irradiation. This estimator is interesting to investigate the physical or technological characteristics of the process.
- $C_2 = \frac{\Delta m}{\phi T}$, which is defined as the ratio of the minor actinides consumed during irradiation over the neutron fluence to which the blankets were submitted. This estimator is interesting as it is a metric of the overall efficiency of the transmutation process.

Unless otherwise specified, C_1 will be used as the reference estimator for calculations where the flux and irradiation time are constant.

Regarding fuel cycle constraints, it is first necessary to detail the recycling strategy considered for this study. We will consider here a scenario where fuel cycle closure is achieved using only fast reactors. This is shown in Figure 35. A fresh fuel is irradiated in a fast reactor, after what it

is cooled and reprocessed. Plutonium and uranium are recovered to be used in standard fuel assemblies, or drivers, while americium is loaded into target assemblies located at the core periphery. Similarly, irradiated targets are allowed to cool down and are then reprocessed, with plutonium being used for driver fuels and americium being re-irradiated. Curium and fission products are considered as wastes and discarded during the reprocessing step. Neptunium was not accounted for here but it can be safely assumed that it could follow the same flowsheet as plutonium here [53].

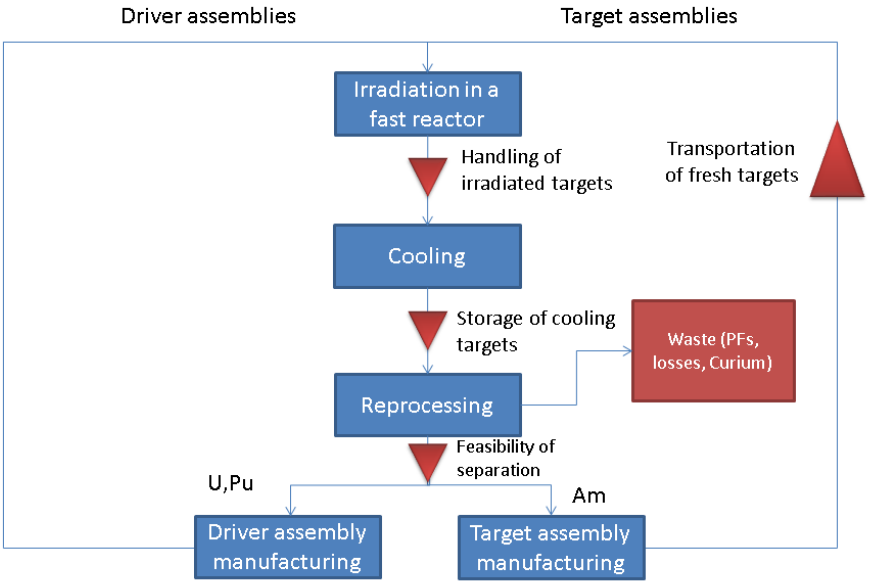

Figure 35 : Fuel cycle considered for this study. Curium was considered a waste and discarded here.

Various technological limitations can be found throughout this fuel cycle. They are shown using red arrows on the flowsheet in Figure 35. The first one is linked to transportation of fresh targets, which have a non-negligible decay heat compared to driver fuel assemblies due to their higher content in americium. The second point is the post-irradiation handling of the targets, which actually depends on the technology chosen for this operation: in-sodium handling, sodium-filled cask or in in-air cask. However, this requires precise knowledge of the short-term decay heat behavior of the irradiated assemblies, which was not computed here. Cooling and storage is dependent on the actual technology considered for removing the sodium from the assembly (or sodium-washing) before they can be safely stored in cooling pools. The length of the cooling itself is dictated by constraints on transportation of irradiated fuels, which differs from the constraints of fresh fuel. Finally, the question of the actual feasibility of the separation process remains to be addressed but this will not be treated in this study.

By considering the total inventory of americium in the fuel cycle, it is possible to take into account all those constraints in a single numerical value, which simplifies the optimization process. Indeed, if we consider an equilibrium between the production of americium in the core and its production in the blankets, an approximation of this inventory can be written as shown

in Equation 22, which m_0 the initially loaded mass of americium in the blankets and T_x the time required to accomplish the step x of the fuel cycle.

$$I = m_0(1 + \frac{T_{cooling} + T_{manufacturing}}{T_{irradiation}})$$

Equation 22 : Definition of the inventory estimator

This equation can be interpreted by considering that during the irradiation of a given set of blankets, the core produces exactly the amount of minor actinides consumed in the blankets. Consequently, at unloading, the initial mass of americium is still found, but divided between core and blankets. This formula considers that the same cooling time is applied to both fluxes of americium. At the end of cooling, reprocessing and manufacturing takes place and new blankets are irradiated. Consequently, in this approximation, the total inventory in the fuel cycle only depends on the initially loaded mass and the fuel cycle constraints which determine the cooling time.

The equilibrium hypothesis between production and consumption of americium between core and blankets is valid from a neutronic point of view, as the neutron leakage of fast reactor is generally sufficient to transmute the core production, but may not hold true due when the fuel cycle constraints are considered in, as they tend to limit the amount of americium that can be loaded in a given target and thus the amount of minor actinides that can be transmuted in the blankets.

As shown previously, it is possible to fully characterize minor actinides transmutation using the r-factor, the amount of minor actinides loaded in the blankets, the irradiation time T and flux level φ. The americium loading was characterized using the Americium concentration in at/cm^3 in the infinite medium corresponding to the targets considered. It will be denominated Am thereafter. Considering this, the following approach was used.

A first set of cell calculations for a fixed core configuration with 40 % oxide fuel, 40 % coolant and 20 % ^{56}Fe as structures material was carried out, with 22.1 % of plutonium in the fuel. These volume fractions are a good approximation of the actual volume fractions in a fast reactor. Then, these spectra and flux levels were used for source-based calculations of a blanket medium with a variable composition in terms of fuel, coolant and moderating material in order to cover as wide as possible a spectrum range. The variation ranges considered can be found in Table 13. The cell calculations were carried out using the ECCO cell code [36] and the JEFF 3.1 nuclear data library [42]. The americium vector used contained 75 % of ^{241}Am and 25% of ^{243}Am.

The minor actinides bearing blankets are depleted for 4000 EFPD using a constant flux approximation and the DARWIN code system [38]. This value was taken as it corresponds to approximately twice the residence time of the fuel in a typical SFR (4100 EFPD in the SFR V2B described in [54]). As discussed in [41] for instance, this residence time is compatible with fuel and cladding swelling due to the lower neutron flux at the core periphery. For the core mentioned here above, this corresponds to 2375 kg of Americium loaded in 84 blankets assemblies. In such a configuration, the americium consumption in the blankets is roughly equal to twice the core production, which means that the equilibrium hypothesis mentioned earlier is adequate.

Several thousand calculations (≈2500) were run to obtain a learning base for the construction of artificial neuron networks which are trained to evaluate the transmutation rate and both the neutron source and decay heat at various time steps (5/10/20/50 and 100 years) with regards to the four parameters of the problem : r, Am, T and φ. This step was done using the URANIE platform developed by CEA [40]. Multilayer perceptron (MLP) with one hidden layer were used as ANN with ten hidden neurons in the hidden layer. A representation of this approach is shown in Figure 36. Each hidden neuron is a weighting function which correlates the inputs and outputs. Training of the ANN is done by adjusting the various weights of the weighting function based on a known training base in a process known as gradient retro propagation. Further details about this approach can be found in [55].

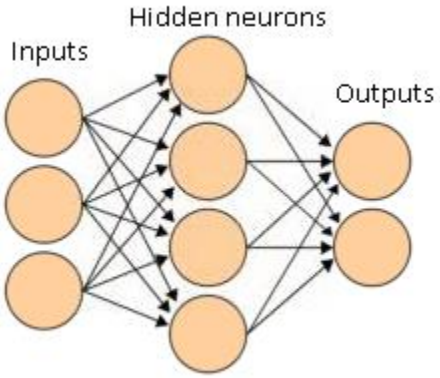

Figure 36 : Structure of the artificial neural networks used here

Training was done on half of the cases of the learning base and the validity of the artificial neural networks was checked using the other half of the training set. Using the computed values for decay heat and neutron source, the evolution of these quantities was approximated by a logarithmic law $P(t) = a * ln(t) + b$, starting from five years cooling time which is the minimum cooling time considered here. Parameters a and b were fitted for each case using scipy python package and a least-square method [56]. This approach was used instead of classical correlations such as Borst-Wheeler decay heat law due to the specificity of decay heat in MABB, above 95 % of which being due to minor actinides alpha decay and not fission products decay, as it is the case for standard spent fuel. A breakdown of the errors associated with the use of ANN is given in Table 22. It can be seen that the mean error of the meta-models is close to zero, with standard deviations around 3% for decay heat and transmutation rate. Errors for the neutron source parameter are a bit higher due to the specificities of ^{244}Cm previously described.

Table 22 : Mean error and standard deviation of the ANN used to describe the transmutation process

Parameter	Transmutation rate	Decay heat @ 5 years	Decay heat @ 10 years	Decay heat @ 20 years	Decay heat @ 50 years	Decay heat @ 100 years
Mean error (%)	0,17	-0,15	0,06	-0,21	-0,18	-0,04
Standard deviation (%)	3,24	3,08	2,73	2,61	2,13	1,68
Parameter	Neutron source @ 5 years	Neutron source @ 10 years	Neutron source @ 20 years	Neutron source @ 30 years	Neutron source @ 50 years	Neutron source @ 100 years
Mean error (%)	-0,17	-0,21	-0,27	-0,31	-0,22	-0,02
Standard deviation (%)	5,09	4,15	3,48	3,58	3,78	7,80

Beyond the simple evaluation of the mean and standard deviation of the neural networks outputs shown in Table 22, it is possible to compute the quality of the meta-models by calculating the so-called Q^2 factor [57] which is defined below in Equation 23, with y_i the value of the complete calculation at the point i, $\tilde{y}_i$ the value calculated by the artificial neural network and $\bar{y}$ the mean value of all the y_i. This factor is a measure of how well the meta-model reproduces the variance of the actual model.

A meta-model will be deemed acceptable if the Q^2 estimator is higher than 0.95 in this context. As it is shown in Table 23, it can be observed that all the estimators studied here exhibit higher than 0.95 Q^2 values, thus validating their good behavior.

$$Q^2 = 1 - \frac{\sum(y_i - \tilde{y}_i)^2}{\sum(\bar{y} - \tilde{y}_i)^2}$$

Equation 23 : Definition of the Q^2 variance estimator

Table 23 : Q^2 value for the estimators of interest modeled using ANN

Parameter	Neutron source @ 5 years	Neutron source @ 10 years	Neutron source @ 20 years	Neutron source @ 30 years	Neutron source @ 50 years	Neutron source @ 100 years
Q^2	0,9960	0,9970	0,9970	0,9970	0,9970	0,9890
Parameter	Transmutation rate	Decay heat @ 5 years	Decay heat @ 10 years	Decay heat @ 20 years	Decay heat @ 50 years	Decay heat @ 100 years
Q^2	0,9860	0,9980	0,9990	0,9990	0,9990	0,9996

A genetic algorithm was used to evaluate the Pareto-optimal cases, e.g. the cases for which it is not possible to achieve a gain in one objective without a loss in another one. Each case was characterized using a (r,Am,φ,T) quadruplet. The standard genetic algorithm available in the URANIE code package was used. This algorithm is compatible with the use of ANN and allows an efficient exploration of the entire parameter space.

A schematic explanation of the complete optimization process is given in Figure 37. ANNs are trained using input data from cell and depletion calculations. These meta-models are then used to compute the transmutation rate and decay heat rate using only the four parameters discussed previously. A genetic algorithm is then used to find the optimal solution of the problem with regards to various combinations of the parameters and objectives functions.

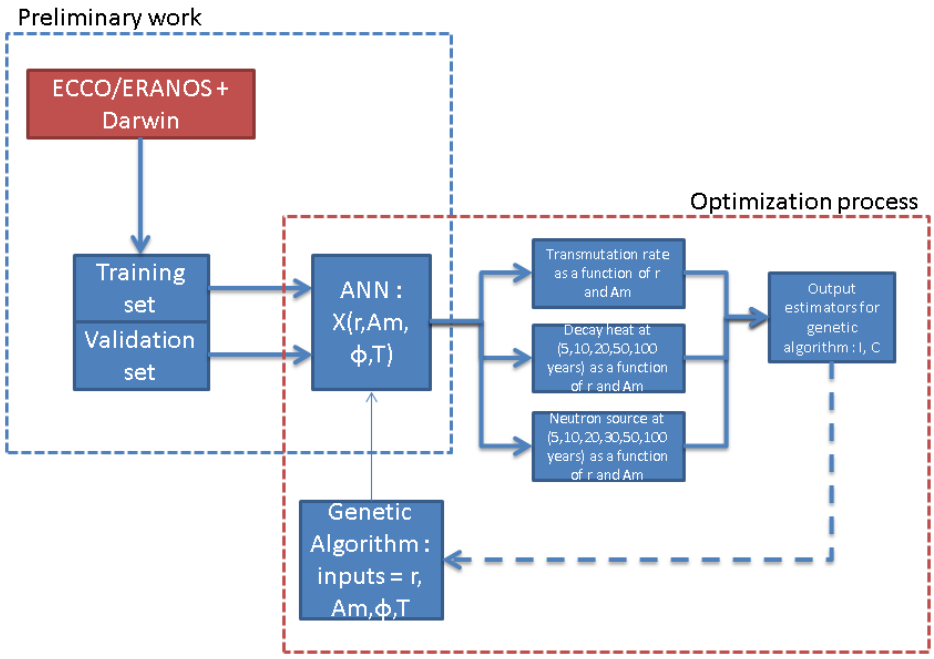

Figure 37 : Schematic description of the optimization process. ANN are trained using data obtained with the ECCO/ERANOS and Darwin code, and these ANN are then used in a genetic algorithm in the actual optimization process

Some technological approximations were made here. Indeed, the output of the depletion calculation performed in the preliminary step yields the decay heat and neutron source for one gram of initial fuel. Now, the limitation considered for washing of the irradiated target is based on the total assembly decay heat, which depends on the mass of fuel in the assembly itself. This mass depends on the assembly design, meaning that information on the geometrical design of the assembly is not considered during the optimization process. Nevertheless, this methodology allows obtaining results purely based on neutron spectrum effects, regardless of the actual geometrical design of the assembly. However, some care should be taken regarding the feasibility of the assembly designs considered here.

Before considering further calculations, it is necessary to take into account the actual technological feasibility of each case discussed before, and especially the achievability of the r-factor considered here. The data shown in Table 24 were obtained using the same models as the data for the optimization process and ECCO cells calculations. The external neutron spectrum used as a source for Minor Actinides Bearing Blankets (MABB) was calculated using the oxide fuel configuration described in the previous paragraph and it was verified that the fuel type used in the core had no impact on the blanket r-factor. We considered here the two most

"mature" fuels currently envisaged, e.g. metallic fuel and oxide fuel. In terms of intrinsic performance, the use of oxide fuel leads to slightly less energetic neutron spectrum due to the presence of oxygen nuclei scattering the neutrons. It can be seen in Table 24, for the same Am fraction, the r-factor is 0.088 for the oxide case and 0.168 for the metallic case. For the same reason, nitride and carbide fuels lie in between these two fuels in terms of performances as nitrogen and carbon are present in lower quantities in such fuel fuels. Further consideration on the role of fuels can be found in [58]. Considering that nitride and carbide fuels performances are intermediate between oxide and metallic fuels and that their industrial maturity is further away than the one of metallic and oxide, their contribution was not further detailed here.

Table 24 : r-factor versus design choices for blanket assembly. When no moderating material was used, the corresponding volume fraction was replaced by sodium.

Blanket material	AmO_2 fraction in fuel (%vol)	Moderating material (10 %vol)	r-factor
$UAmO_2$	20	None	0,088
$UAmO_2$	40	None	0,148
$UAmO_2$	20	MgO	0,062
$UAmO_2$	20	MgO (20 %)	0,047
$UAmO_2$	40	MgO	0,106
$UAmO_2$	20	ZrH2	0,016
$UAmO_2$	40	ZrH2	0,027
UAmC	20	None	0,115
UAmN[5]	20	None	0,125
UAm10Zr	20	None	0,168
UAm10Zr	40	None	0,278

As oxide fuels yield a "degraded spectrum" compared to other support, it is logical that it should be used to obtain a much degraded spectrum in blankets, using moderating materials such as MgO or ZrH_2, with the smallest r-factor being achieved using this last compound.

Using MgO only, it appears not possible to obtain low r-factor values in the blankets for high americium fraction. This is due to a competition effect between americium loading, which depopulates the epithermal range and thus hardens the spectrum and MgO which tends to slow down the neutrons. It follows from this that achieving highly moderated spectrum in the MABB will require either creative use of scattering material or adequate safety developments to allow in-pile use of hydrides. At the other extremity of the spectrum, it can be seen that even with metallic blankets and high Americium fraction, the highest value achievable for the r-factor here is 0.278, compared to 0.35 in the fuel itself.

From this analysis, it was possible to build the achievable (r,Am) domain for two cases depending on the use or not of zirconium hydride as moderating material. These domains are shown in Figure 38. The two rightmost curves delimit the allowable range while using only MgO in combination with any type of fuel, while the use of zirconium hydride extend the boundary of the allowable range to the leftmost curve, due to its better moderating properties. The ranges shown in Figure 38 corresponds to the physical boundaries of the (r,Am) domain, which are set

[5] ^{15}N-enriched [144]

by the competing effect of the moderating material and the spectrum hardening effect of the americium introduction.

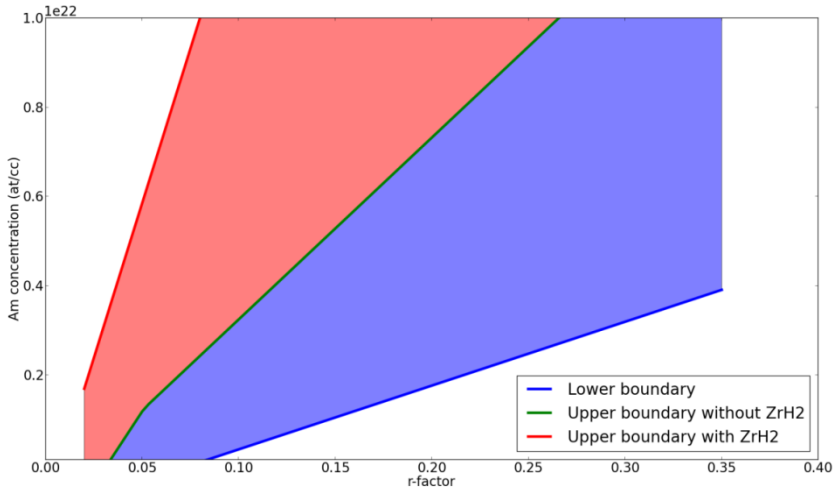

Figure 38 : (r,Am) diagram. The allowable range without ZrH_2 use is located between the two rightmost curves.

b) A CASE FOR MODERATION

As mentioned previously, "moderation" of minor actinides blankets has been proposed in the past as a potentially attractive option to improve transmutation performances in these blankets. Using the methodology discussed previously, it possible to consider this approach while taking into account both the americium consumption and the impacts on the fuel cycle using the estimators described previously.

In a first stage, an optimization is performed in order to maximize the americium consumption after a given irradiation time while minimizing the americium inventory in the fuel cycle. The parameters and constraints used here are the following:

- A fixed fluence representative of what could be found in fast reactors blankets, e.g. 4000 days at 6 10^{14} n/cm^2/s. The use of ZrH_2 is not considered here, which means that solutions of the problem will lie only in the blue zone of Figure 38.
- A reprocessing upper limit of 53 W/kg was considered along with a neutron source limit of 10^7 n/s/kg. The first value corresponds to the expected limit in the near future for reprocessing oxide fueled minor actinides bearing blankets while the second one corresponds to the intrinsic neutron source of a MOX fast reactor assembly after 5 years of cooling. These limits were taken purely as illustration purposes as industrial constraints must be expressed using integrated values over an assembly and not per kilogram. A more detailed study of their impact on the transmutation performances and fuel cycle impacts will be carried out in the next part and in the last chapter.
- Initial Americium content as well as assembly designs are considered as free parameters but not explicitly settled here. Instead their combinations are translated into r-factor as stated in previous section.

The results of this preliminary optimization are shown in Figure 39. This figure represents the Pareto Zone and Pareto Front of the problem with a cooling time corresponding to a final decay

heat of 53 W/kg and 10^7 n/s/g after 2 10^{23} neutrons/cm^2. A case is denominated Pareto-optimal when it is not possible to find a better case with regards to all the objectives functions simultaneously. Any improvement in one of the estimator considered for a Pareto-optimal case goes with a decrease in the value of a second estimator. This form is adapted to the outcome of the optimization process, as the final selection of a transmutation strategy must rely on additional choices regarding reprocessing politics and actual deployment of reactors which are not yet known.

The left part of Figure 39 corresponds to the set of optimal cases plotted in the objective phase space. The x-axis represents the amount of americium which has been consumed while the y-axis corresponds to the inventory estimator defined in Equation 22. The optimality of these cases means that for a given consumption of Am, it is not possible to obtain an inventory estimator lower than the one corresponding to the plotted points. Points located in the non-feasible zones correspond to points which are physically not realistic. On the other hand, it is possible to find cases in the so-called sub-optimal zone, e.g. cases for which the inventory associated with a given consumption is higher than the optimal one. Those were not represented here.

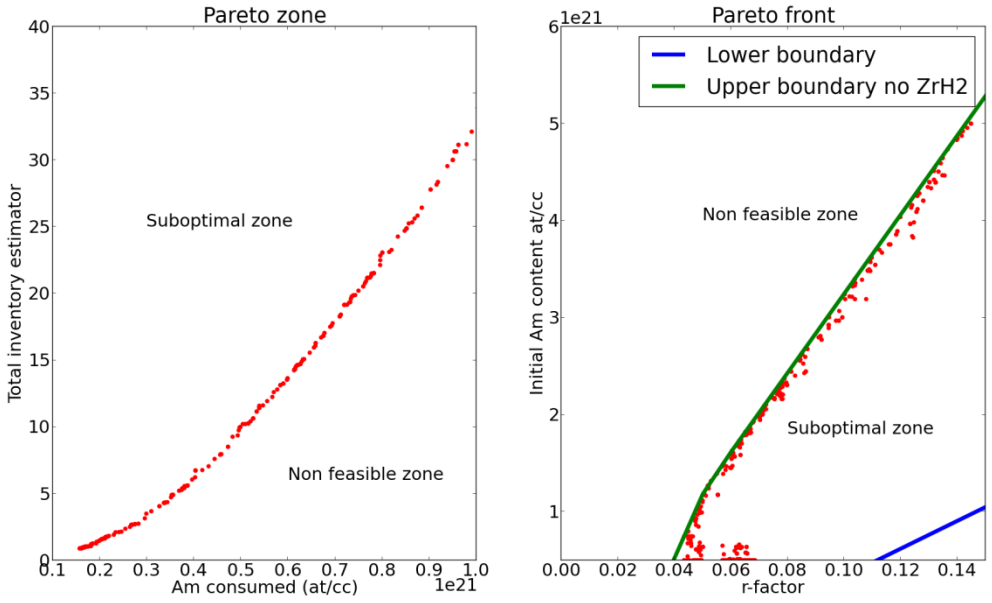

Figure 39 : Pareto zone and front for a (r,Am) optimization with a constant fluence of 2 10^{23} n/cm^2 for a scenario without the use of ZrH_2 as moderating material. Reprocessing limitS of 53 W/kg and 1e7 n/s/kg were used.

The right part of Figure 39, or Pareto Front represents the same set of optimal cases but this time plotted in the (r,Am) phase space. The x-axis corresponds to the r-factor while the y-axis is the amount of americium in the blankets. The two lines correspond to the limit of the available domain described in Figure 38. It can be observed that the optimal cases correspond to cases with a spectrum as moderated as possible, with the sub-optimal zone corresponding to the "less" moderated cases. From this, we can conclude that, for a given fluence, the increase in the decay heat of the irradiated blankets due to the enhanced curium production, as shown in Figure 25 is offset by the increase in the transmutation performances. **Even while considering**

negative impacts on the fuel cycle, it appears that the use of moderating material is beneficial to heterogeneous minor actinides transmutation.

If we further consider the use of ZrH_2 as moderating material with similar limitations on the fuel cycle as for the previous study, the available (r,Am) domain increases and it can be observed that the overall performances also increases. As it can be seen in Figure 40, for similar consumption level, the associated inventory for a case with ZrH_2 is approximately four to five times lower as in the case without ZrH_2. This is explained by the fact that, to achieve the same absolute level of consumption, it is necessary to load less minor actinides in the blankets, thus decreasing the total inventory. For illustration purpose, it is possible to consider the performances of the two cases for a consumption corresponding to Δm=1e21 at/cc. Those correspond to the intersection of the vertical black line with the two curves on Figure 40, with A the case without ZrH_2 and B the case where it is used.

The case A corresponds to a case where ZrH_2 is not used, which leads to a lower transmutation rate. Consequently, to achieve the targeted americium consumption during irradiation, the initial loading must be higher, which in turns increases the total inventory estimator. The corresponding initial loading is m_0 = 3.07 10^{21} at/cc, which for a SFR V2b blanket assembly would correspond to a 33.6 at% content of Americium. On the other hand, the use of a moderated approach with ZrH_2 increases the transmutation rate and thus decreases the initial loading to m_0 = 1.55 10^{21} at/cc, which would correspond to 16.5 at%, with a further part of the sodium being displaced to accommodate moderator loading.

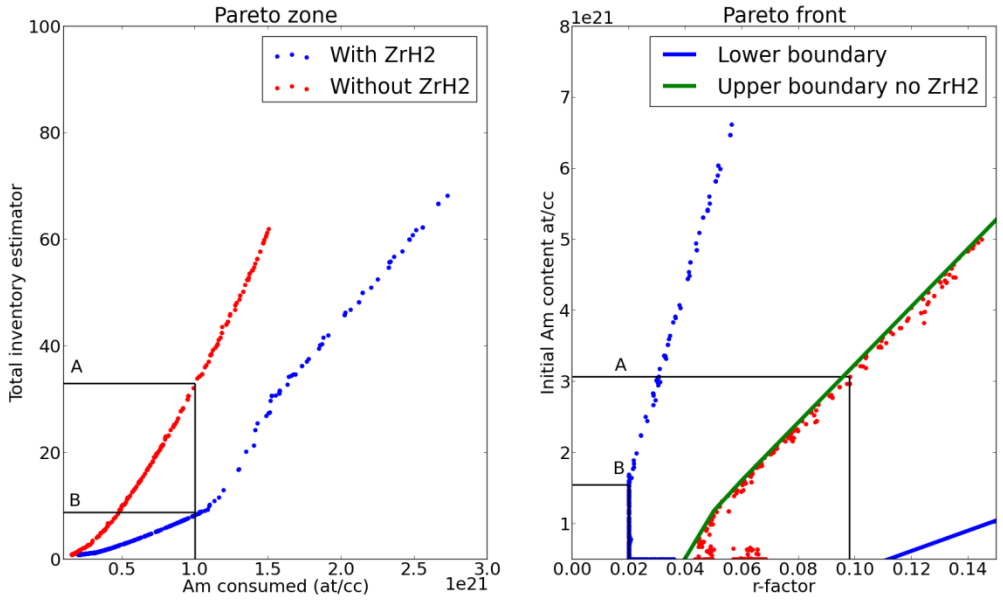

Figure 40 : Comparison of the Pareto zone and fronts depending on the use of hydrogenated moderating material for a (r,Am) optimization with an irradiation time of 4000 EFPD at 6e14 n/s/cm^2 Reprocessing limit of 53 W/kg and 1e7 n/s/kg were used. Self shielding in the blankets was not accounted for.

However, these results are preliminary and do not take into account self-shielding in the blankets, which will decrease the flux "seen" by the moderated blankets. If we apply a corrective factor for this phenomenon by reducing the flux level in the blankets in the moderated case to account for self shiedling, the results obtained can be found in Figure 41. It can be observed that

the two Pareto fronts are "closer" than in Figure 40. Indeed, due to self-shielding in the moderated blankets, the corresponding neutron flux level is lower (around 3.5 10^{14} n/cm^2/s compared to around 6 10^{14} n/cm^2/s), which in turns reduces the transmutation rate. Consequently, for a given consumption, the loaded mass must be higher, which then increases the total inventory estimator. The flux and irradiation time used in Figure 40 are close to the non moderated case, which explains why the corresponding curve is not visibly modified. As this specific study requires information on the reactor, such as the core power or geometry, it will but further detailed at the end of this chapter and in the next one.

Nevertheless, it can be concluded here that even when taking into account the self-shielding phenomenon, moderating the blankets appears to be an optimal strategy to maximize the consumption while minimizing the impacts on the fuel cycle.

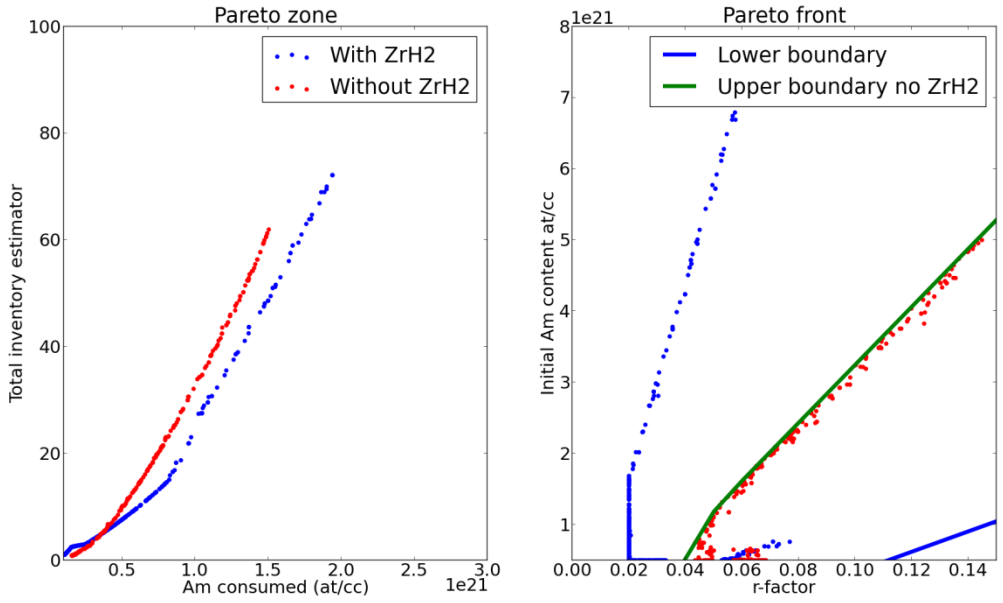

Figure 41 : Comparison of the Pareto zone and fronts depending on the use of hydrogenated moderating material for a (r,Am) optimization with an irradiation time of 4000 EFPD. Reprocessing limit of 53 W/kg and 1e7 n/s/kg were used. Self shielding in the blankets was accounted for by adapting the flux level in the blankets depending on the neutron spectrum.

c) NEUTRON SOURCE VS DECAY HEAT

Decay heat or neutron source may be leading to difficulties for handling and transportation of the spent assemblies. Considering that the shielding the spent target requires different technological solutions than removing excess decay heat, it is should be of interest to evaluate which of these two parameters is going to be the most limiting one. For comparison purposes, three limits were considered here:

- 53 W/kg for the decay heat limit
- 7784 n/s/g and 77840 n/s/g for the neutron source limit, which corresponds to the neutron source of a standard MOX assembly after 5 years of cooling and to ten times this value.

Similarly to the previous cases, the irradiated target was considered to be cooled until the corresponding value in decay heat and neutron source is reached. Similar irradiation conditions as before (6e14 n/cm^2/s for 400 EFPD) were considered here.

It can be seen in Figure 42 that the curve corresponding to 7784 n/s/g is above the two others until the americium consumption $\Delta C = 1.5\ 10^2$ at/cc, which means it is the one with the highest inventory for a given consumption. Since all the points are located in the same (r,Am) zone and thus exhibits a similar transmutation rate, the increase in the inventory is related to higher cooling times necessary to reach the neutron source limit. This means that up to this consumption, the cooling time to reach the limiting neutron source will be longer than the cooling time necessary to reach the decay heat limit, hence making the neutron source the penalizing constraint.

Above $\Delta C = 1.5\ 10^{21}$ at/cc, the curve corresponding to the 53 W/kg decay heat is the uppermost. This means that the cooling time to reach the decay heat limit is now longer than the one for the neutron source limit, making decay heat the limiting factor. We can conclude from this that, *for the constraints considered*, the limiting factor is the neutron source level for cases with low consumption and low inventories, while decay heat becomes the limiting factor for higher loaded mass.

This is explained by the differences in the half lives of the main neutron and alpha emitters. Indeed, 96 % of the neutron source of a spent assembly is due to ^{244}Cm, which has a half life of 18.1 years. On the other hand, decay heat of the spent assembly after five years of cooling can be roughly split between ^{244}Cm (≈ 40 %), ^{238}Pu (≈ 20 %) and ^{241}Am (≈ 20 %), the two last isotopes having longer half-lives than ^{244}Cm, of respectively 87.2 and 432 years. Consequently, the neutron source only increases with the ^{244}Cm production and thus with the ^{243}Am loading, which explains the quasi-linear behavior of the inventory with the mass consumed. The decay heat thus evolves with similar time kinetics than the neutron source during the early part of the cooling when the contribution of ^{244}Cm to the decay heat is still significant, but in the late stages of cooling, decay heat evolution is driven by longer-lived nuclides, thus slowing down its decrease.

Nevertheless, it should be mentioned here that relatively little information is available on effective thresholds in terms of neutron source for assembly handling and transportation, as this would require very deep levels of details about the actual technological solutions available.

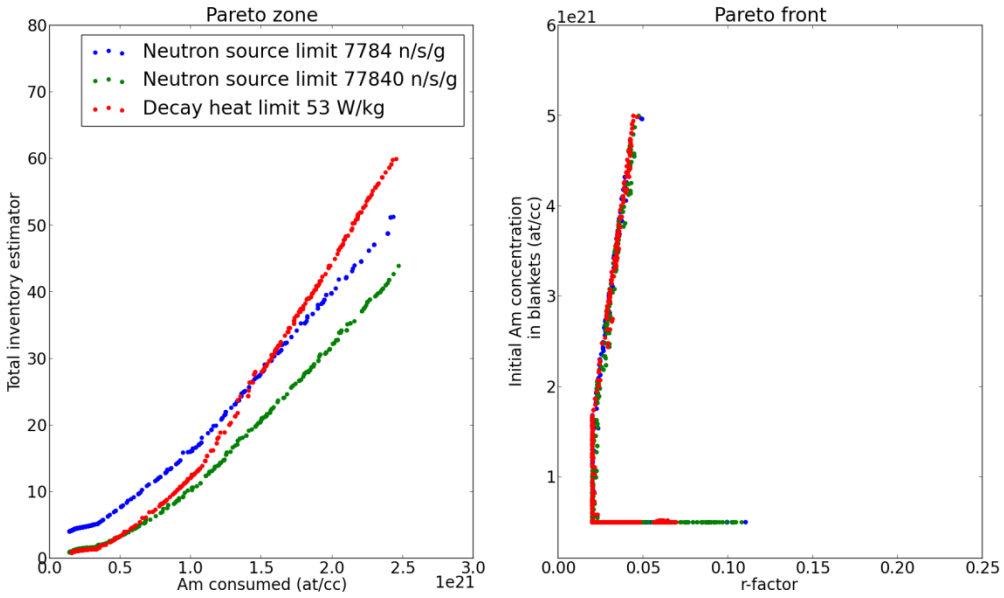

Figure 42 : Comparison of the Pareto zone and front for a washing limit of 7784 (resp. 23352) n/s/g corresponding to (resp .three times) the neutron source of a driver assembly of [51] after five years cooling and decay heat of 53 W/kg corresponding to 7.5 KW per assembly.

The impact of the considered limit can also be evaluated, as it is done on Figure 43, where the optimal cases were plotted for three reprocessing limits, 25, 53 and 75 W/kg. Here the shape of the Pareto zone or of the Pareto front does not change depending on the specific washing power considered. However, a 32 % increase in the acceptable specific washing power (from 53 W/kg to 70 W/kg) only leads to a 10 % increase in the achievable consumption at constant inventory. This is explained by the fact that, when the limit is increased, a higher initial mass of americium can be loaded. This higher initial mass will lead – with an almost constant transmutation rate, albeit slightly lower due to the small spectrum hardening – to a higher final mass and thus a higher final contribution of americium to decay heat. This means that, at equal inventory and spectrum, a relatively lower curium mass can be produced and thus a relatively lower fraction of americium can be transmuted.

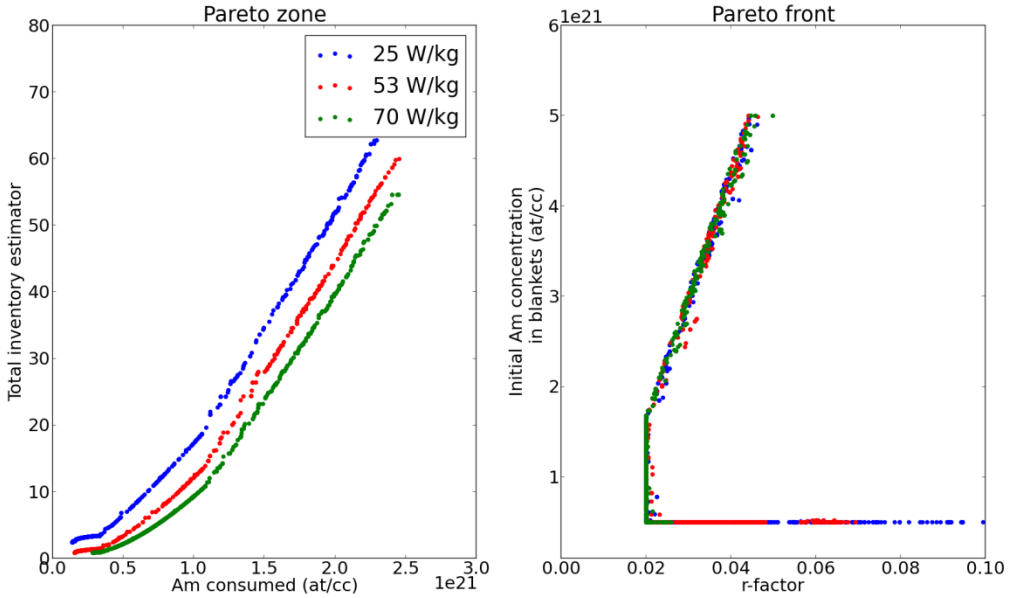

Figure 43 : Comparison of the shape of the Pareto front and domain for various washing limits

Similar consideration can be obtained for neutron source, as shown below in Figure 44. As an illustration of the flexibility of the approach, the constraint on the neutron source was moved up to one on the neutron dose rate of the spent blankets. This is made possible by the fact that as ^{244}Cm does account for more than 96 % of the neutron source at any given time, the corresponding neutron spectrum remains constant during considered cooling times and thus an adequate dose rate coefficient can be estimated from available data sheets such as [16].

This figure summarizes the optimal cases for two constraints in term of neutron dose rate of the spent blanket assembly, namely 31 mSv/s and 310 mSv/s. The 31 mSv/s limit is calculated based on the neutron dose rate of a spent MOX assembly of a 3600 MWth assembly as described in [54] after 5 years of cooling (corresponding to the 7784 n/s/g neutron source limit used before) and the 310 mSv/s is an extrapolation of the previous limit. By comparing this limit and the possible use of ZrH_2, various conclusions can be drawn here. First, similarly to the decay heat case, the total inventory in the fuel cycle decreases with the limit considered regardless of the moderator considered. Secondly, it is possible to derive the optimal strategy in order to limit the total inventory while keeping constant performances.

For small amounts of minor actinides to be consumed (corresponding to an initial loading of $m_0 = 5\ 10^{20}$ at/cm^3, or roughly below 5 at% in a UO_2 blanket), it can be observed that starting from a case with a 31 mSv/s limit and without ZrH_2, increasing the reprocessing thresholds (source and decay heat level) yields better results than using zirconium hydride (the black curve is below the blue curve for this content domain). However, above this 5 at% domain, it can be observed that using ZrH_2 is a better option than increasing the reprocessing limit to 310 mSv/s. As expected, using ZrH_2 in conjunction with an increase in the reprocessing limit yields the lowest inventory for a given consumption.

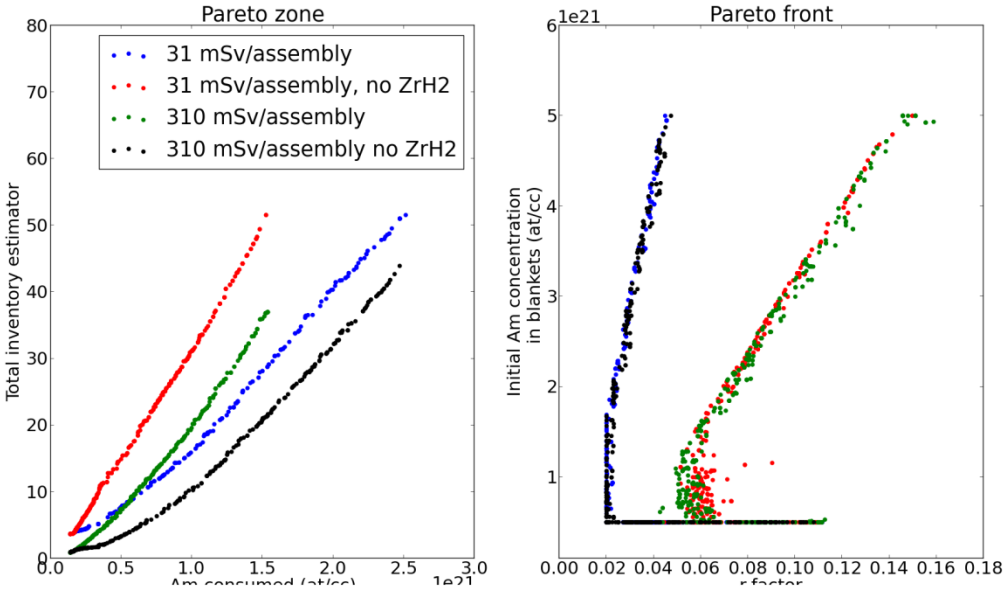

Figure 44 : Impact of the limit considered before reprocessing on the Pareto front and set.

Finally, it is possible to evaluate the optimal cases when the washing threshold is allowed to vary freely as an optimization parameter. The results of these calculations are shown in Figure 45. Similar trends as before are observed although there is a saturation of the achievable consumption when ZrH_2 is not used. It should be noted that for some cases with low americium loading (below $m_0 = 1e21$ at/cc), the optimal washing limit is below the value of 200 W/kg which was arbitrarily taken as a maximum value here. For such a limit, the neutron spectrum considered only slightly influences the total inventory, as the broader spread of the optimal cases in the acceptable domain without ZrH_2 shows. It can be concluded here that regardless of the use of zirconium hydride, the highest limit yields the best results.

Although the decay heat limit used here is based on foreseen industrial constraints, such information is not available a present time for neutron source or dose rate. However, comparison with the neutron emission of a standard fuel assembly, it can be concluded here that depending on the expected transmutation performances, the first limiting constraint may be different, but at this stage of the design process, it is not possible to give additional precisions.

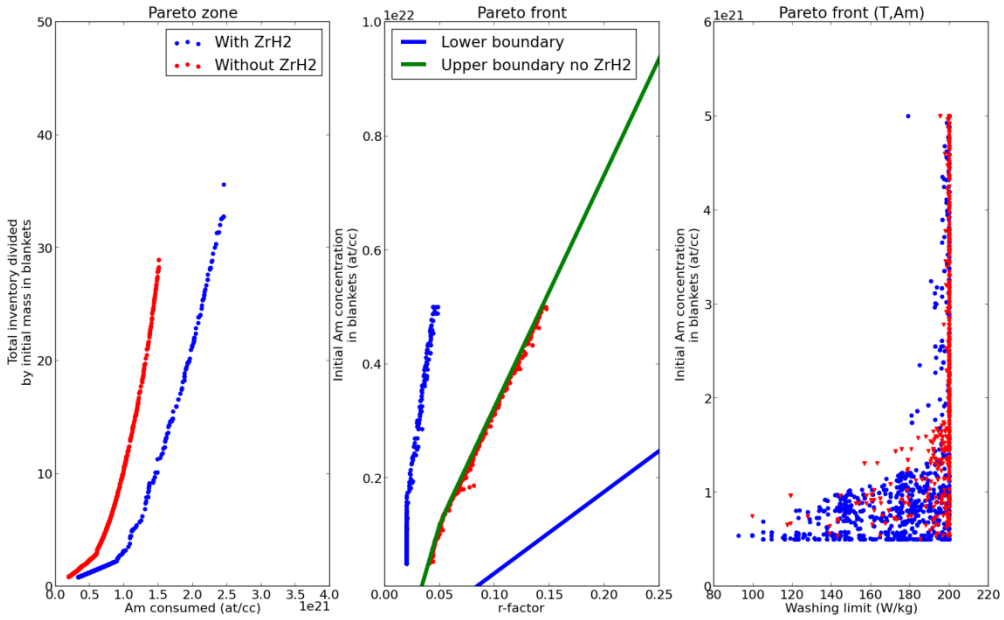

Figure 45 : Pareto zone and domains where the washing limit is set as a free parameter in the optimization process.

d) AMERICIUM ISOTOPIC VECTOR

The impact of the americium isotopic vector can also be considered here. Indeed, the production of long-term decay heat emitters can be split in two couples (^{241}Am, ^{238}Pu) and (^{243}Am, ^{244}Cm), each obtained by initial Americium loading and resulting captures on its isotopes (and eventually decay of the resulting nuclei). With a similar washing limit settled to 53 W/kg, three cases were compared, with respectively 90 %, 75 % and 60 % of ^{241}Am, the balance being ^{243}Am. Similar irradiation conditions as before (6e14 n/cm^2/s for 4000 EFPD) were considered here.

The optimal cases for each situation are shown in Figure 46. It can be seen that the slope of the increase in the total inventory decreases with the fraction of ^{241}Am in the target. This is explained by the half-lives of the various heat emitters involved in target decay heat as shown in Figure 46. Indeed, if we separate the two main contributors to decay heat at identical irradiation time, as it is done in Table 25, it can be seen that when ^{241}Am fraction increases, the contribution of this isotope and of ^{238}Pu, which are longer lived, increases while the one of ^{244}Cm decreases. However, as ^{244}Cm half-life is only 18.1 years compared to 87.2 years for ^{238}Pu, cooling down to a given level of power takes longer when the fraction of ^{241}Am is increased, which explains the behavior observed in Figure 46. It should also be mentioned here that an increase in ^{241}Am increases production of ^{242}Cm, which is strong and short-lived (160 days), which may hamper early handling of the irradiated targets.

Table 25 : Contribution of ^{244}Cm and ^{238}Pu to decay heat after five years of cooling for similar fractions loaded

Decay heat contribution (%)	60 % ^{241}Am	75 % ^{241}Am	90 % ^{241}Am
^{244}Cm	62,0	45,3	21,9
^{238}Pu	19,3	28,1	40,0
^{241}Am	15,44	22,5	32,5
Decay heat (W/g)	22,63	19,0	16,2
'Long-lived'[6] component (W/g)	7,86	9,6	11,7

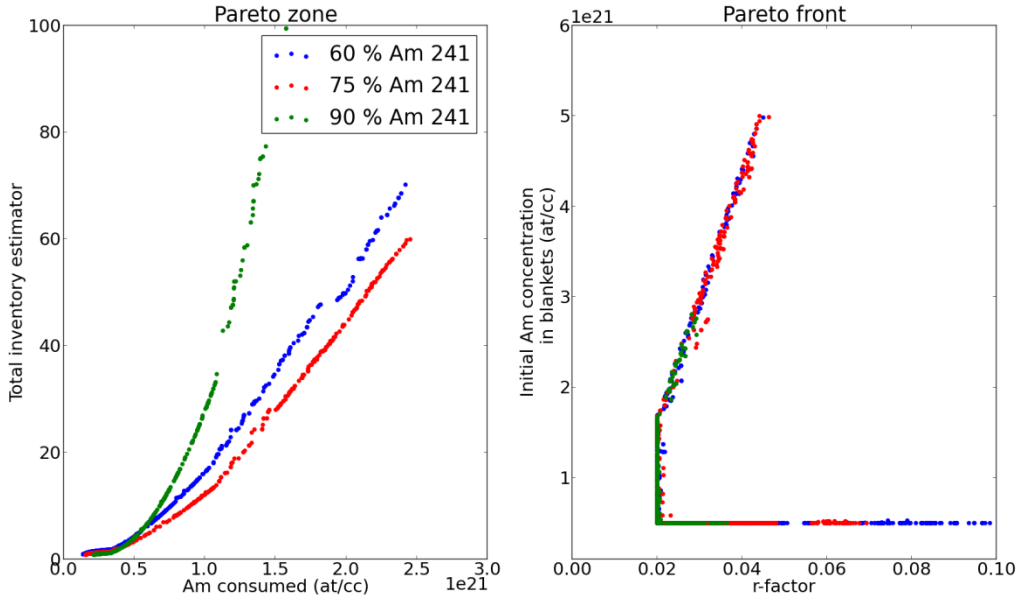

Figure 46 : Pareto front and zone for three cases with variable isotopic content for americium.

Concerning neutron source, the behavior is reversed as shown below in Figure 47. In this case the main contributor (to up to 96 %) to neutron source is ^{244}Cm, which is a direct daughter nuclei of ^{243}Am by neutron capture. Consequently, depending on the considered constraints for both neutron source and decay heat of the irradiated spent fuel, there should exist an optimal isotopic vector which complies with both constraints. For the constraints considered in the previous paragraph and the optimal cases shown in Figure 43, this optimum is obtained for a consumption of $\Delta m=15\ 10^{20}$ at/cc and a corresponding loading of 33 at% for an oxide-based target in a 3600 MWth reactor.

The position of this optimum changes with the americium isotopic vector, with an optimum around 12 at% in the blankets for the 10 % ^{241}Am case and around 18 at% for the 40 % ^{243}Am case described in Figure 46. This change is related to the different rate of increase/decrease of neutron source and decay heat with the americium isotopic vector. Increasing ^{241}Am proportion leads to a decreased neutron source during the entirety of the cooling and short term decay heat

[6] Sum of ^{238}Pu and ^{241}Am component

but also an increase in long term decay heat, while increasing ^{243}Am proportion will have the opposite effect. This effect was already discussed in part 3.1)c).

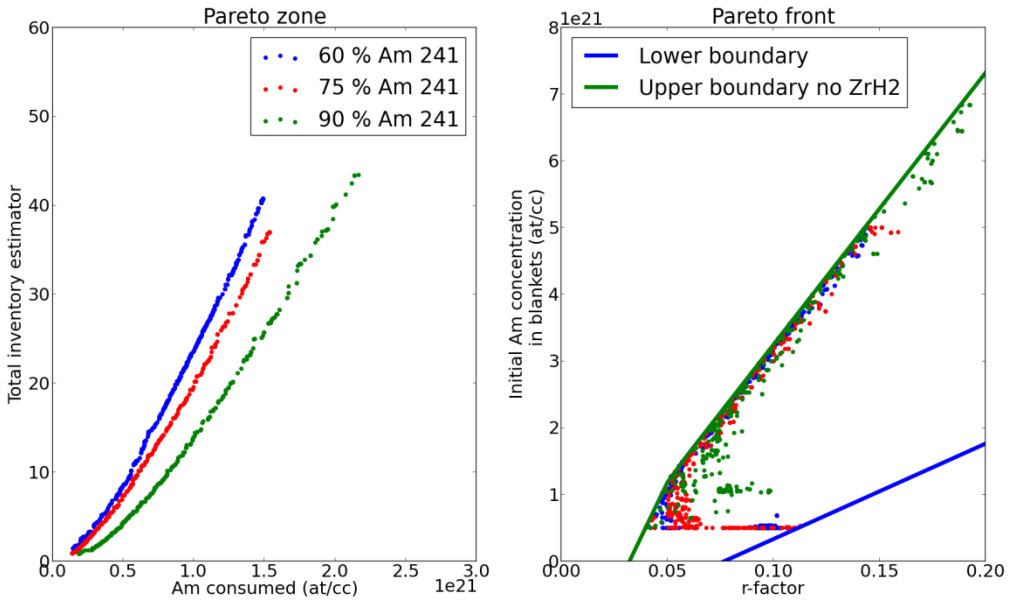

Figure 47 : Impact of the Americium isotopic vector on the Pareto front and set for cases with zirconium hydride. The results are similar when ZrH_2 is used. A limiting value of 310 mSv/s was considered here.

It is possible to illustrate the relationship between americium isotopic vector and fuel cycle constraints by considering Figure 48. It shows the evolution of the time required to reach a given decay heat limit with respect to the composition of the americium isotopic vector together with a minimal cooling time of 5 years. Here the behavior of the cooling time versus the americium isotopic changes with the considered decay heat limit. For high threshold values, the cooling time increases with the ^{243}Am concentration as ^{244}Cm is responsible for most of the decay heat for timescale between 10 and 20 years. Meanwhile, for low values, even after decay of most of the ^{244}Cm, the total decay heat is still higher than this limit and it is necessary to wait for ^{238}Pu and ^{241}Am decay to reach the limit.

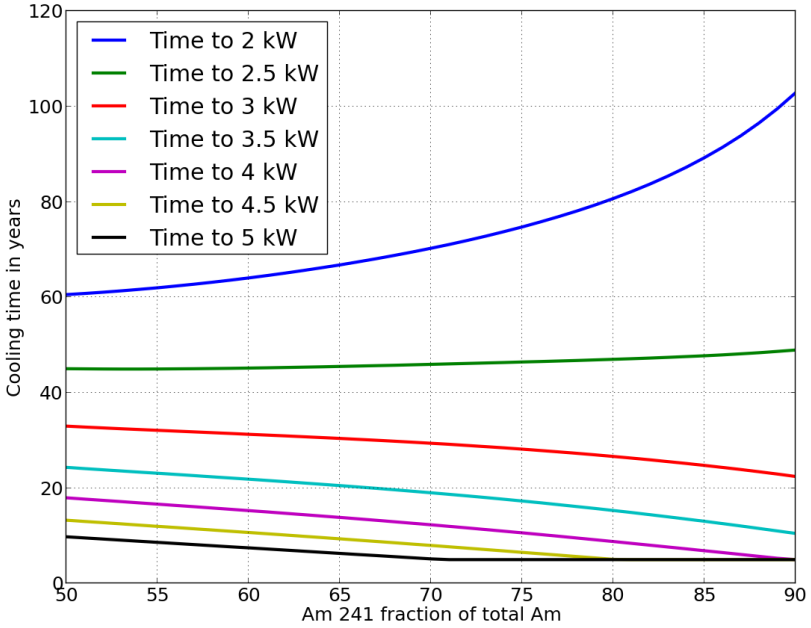

Figure 48 : Evolution of the cooling time to various decay heat limit values with regards to the americium vector for a blanket with 40 vol% of $U_{0.8}Am_{0.2}O_2$ irradiated for 4100 EFPD in a 3600 MWth fast reactor.

Several conclusions can be reached from this physics based analysis of the impact of the americium isotopic vector on the transmutation performances. The first one is that, depending on the actual vector considered, significant variations on neutron source and decay heat production can be observed, with correlated impacts on the cooling time. Secondly, we can also conclude that given the variability of the available americium isotopic vector, an optimization margin with respects to reprocessing priority and times may exist for industrial transmutation scenarios. Indeed, the americium isotopic vector can change between 25 % ^{241}Am to 90 % ^{241}Am depending on the neutron spectrum in the core, the plutonium isotopic vector considered and the cooling time.

e) FLUX LEVEL AND IRRADIATION TIME IMPACTS

Concerning the impacts of the time parameter, if we set the irradiation time as a free parameter of the optimization process, the genetic algorithm will maximize the irradiation time in order to maximize the consumption of americium as shown in Figure 49. This is consistent with the expected behavior of minor actinides transmutation, americium consumption increasing with the neutron fluence to which the fuel is submitted. **Regarding flux level, the same conclusion can be reached: the optimal cases correspond to the cases with the highest possible fluence.**

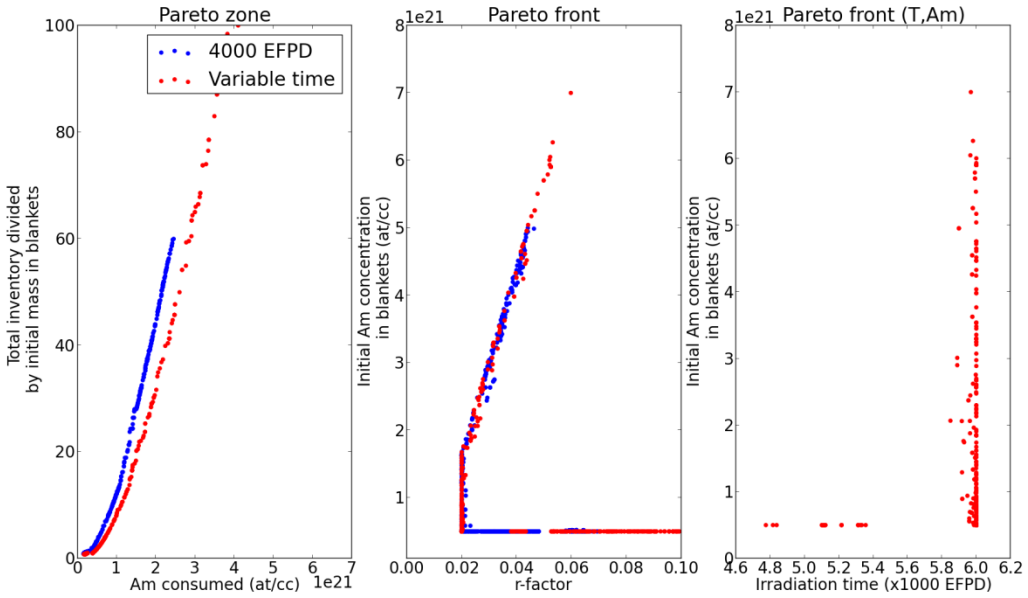

Figure 49 : Comparison of the Pareto zone and Pareto front for a case with fixed irradiation time and one where irradiation time is allowed to vary between 1000 and 6000 EPFD. A 53 W/kg reprocessing limit was considered.

If we use both the flux level and irradiation time as an input parameter, it is then of interest to use the C_2 estimator defined previously in this work as the ratio of the mass consumed over the fluence. The corresponding results are shown below in Figure 51. It can be observed that the optimal cases in the (φ,T) space are located in the upper right corner of the plot, which corresponds to a maximal flux and a maximal irradiation time. Furthermore, the case where ZrH_2 is used also exhibits better performances, as in the previous situations studied. The main conclusion that must be drawn from this figure is that for a fast neutron spectrum, **there are no threshold effects or local maximum regarding the neutron spectrum and mass to be loaded for the consumption of minor actinides and total inventory in fuel cycle.** Consequently, the only optimization margin in this regards lies with technological adaptation of the transmutation process.

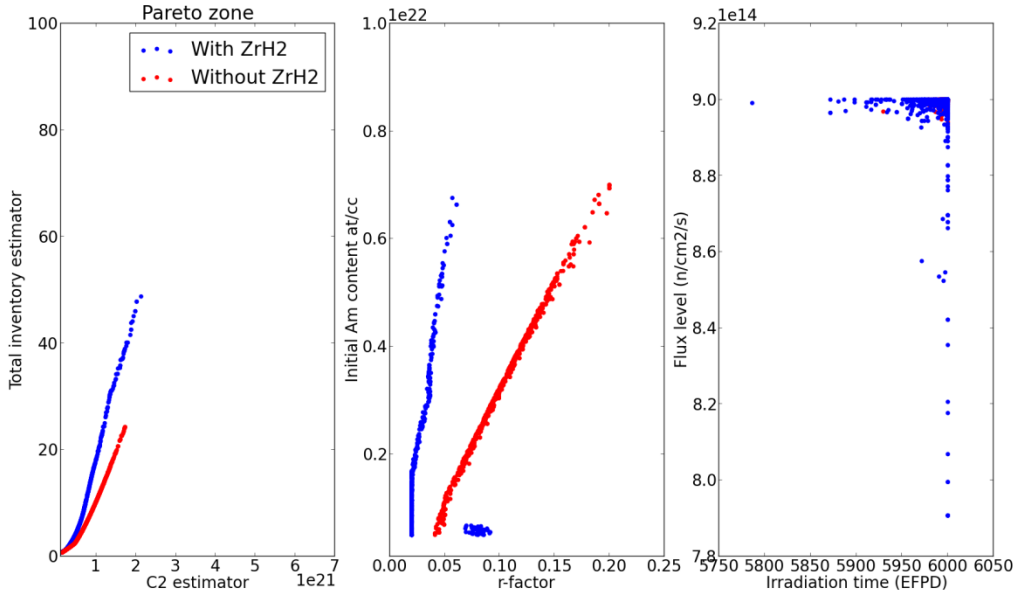

Figure 50 : Comparison of the Pareto zone and Pareto front for two cases with or without ZrH_2 where flux level and irradiation time were set as free parameters of the model and the C_2 estimator is used to evaluate the transmutation performances. A 53 W/kg reprocessing limit was considered.

4) COMPARISON TO CORE CALCULATIONS

a) GENERAL CALCULATIONS

The comparison to core calculations was carried out using the SFR V2b homogeneous core design [51] with the first reflector ring (84 positions) being substituted by transmutation blankets. This specific design was used in the transmutation studies carried out by CEA, for instance in [59]. Total irradiation time is 4100 EFPD for a core thermal power of 3600 MWth.

A reference case corresponding to 40 vol% of $U_{0.8}Am_{0.2}O_2$ with a composition of 75 % ^{241}Am and 25 % ^{243}Am diluted was selected. This corresponds to a total mass of 2375 kg of americium loaded in the blankets. The corresponding specific consumption of americium for this case is 6 kg/TWhe. This consumption rate allows transmutation of the core production and some margins for stockpile reduction. It was taken from early design of MABB as found in [41] for instance. A comparison of the activity of a spent inner driver assembly and of an irradiated target is given below in Table 26. As it can be seen, the total decay heat is increased by a factor 6.4, while the total neutron source is increased by a factor 14.4.

Table 26 : Comparison of the activity of a driver assembly and a transmutation target after five years of cooling

	Driver	MABB
Assembly mass (kg)	163	141
Decay heat (kW)	1,33	8,52
of which alpha (%)	55,4	97,7
of which beta (%)	23,7	1,4
of which gamma (%)	20,9	0,9
Neutron source (n/s)	1,22E+09	1,76E+10

This reference case was compared to three other options with a similar specific consumption of 6 kg/TWhe: one where metal fuel in the form of U10Zr was used instead of uranium oxide and two where 10 vol% of either zirconium hydride or MgO were added to the blankets as moderating material with conservation of the fuel volume fraction (e.g. by removing sodium to accommodate the moderating material, which is justified by the low power of the blanket assemblies). The fuel volume fraction in the blankets was kept constant, which explains the higher loaded mass in the metal case due to the higher density of metallic fueled (a dilution of 75 % was considered to account for high-swelling rates of this type of fuel). The americium content in the targets was modified to achieve an objective of 6 kg/TWhe.

The results of this comparison can be seen in Table 27. Similarly to what was found while using the optimization methodology, it appears that the option with zirconium hydride in the blankets yields the best results, followed by the use of MgO, then oxide and then metal fuel.

Table 27 : Comparison of the performances for the four considered cases. The total inventories are evaluated using the same approximation as in Equation 22

	Oxide	Metal	Oxide + MgO	Oxide + ZrH_2
Assembly initial heavy metal mass	141	153	141	141
Am inventory in blankets	2375	2606	2316	1699
^{244}Cm mass in the blankets at 5 years (kg)	113,2	102,6	114,3	105,6
Decay heat at 5 years (kW)	8,0	8,2	8,0	7,0
Cooling time to reach 7,5 kW (days)	2965	3251	2979	1757
Estimated americium inventory in the fuel cycle (kg)	4515	5136	4411	2757

This conclusion is explained by the fact that, even if the ^{244}Cm production rate is higher in the moderated case than in the regular case, the initial amount of americium necessary to reach the target consumption is lower due to the higher transmutation rate, thus counterbalancing the increase in ^{243}Am and ^{241}Am cross sections. This reduces the total production of curium compared to the reference cases. This combined with the lower americium mass explains the lower level of decay heat observed in this case.

The metallic spectrum case exhibits a longer cooling time due to a higher decay heat level due to the contribution of non-transmuted ^{241}Am. Even if the production level of ^{244}Cm is lower with

the metallic spectrum, the necessary increase in the loaded mass to keep similar performances leads to an increase in the long-term decay heat due to the remaining ^{241}Am at the end of irradiation, thus explaining the longer cooling time.

Considering the case with MgO as moderating material, it can be verified that this element is less effective in this role than zirconium hydride. The slight spectrum shift it brings leads to an increase in ^{244}Cm production which is counterbalanced by a decrease in the mass to be loaded to reach a specific consumption of 6 kg/TWhe, leading to a negligible difference in terms of decay heat evolution but a small 2 % decrease in the total inventory due to the lower loaded mass.

Overall, these conclusions are consistent with what was found using the methodology described in the previous parts. Core designs with MgO and ZrH_2 are lying on the Pareto Front, which means they are optimal solutions to the problem, while cores with oxide or metal fuel are outside of this optimal set. For a fixed assembly size, the americium initial concentration corresponding to a specific consumption of 6 kg/TWhe is equivalent to 0.73 10^{21} at/cc. Using Figure 51, we can estimate the ratio of the optimal inventories in both cases for such a consumption, which is equal to 12/19 = 0.632. It can be compared to ratio of inventories obtained in Table 27 for the Oxide + MgO and Oxide + ZrH_2 core, which is 2757/4411 = 0.625. These two ratios exhibit a rather good agreement, which confirms the usefulness of this methodology for comparative studies.

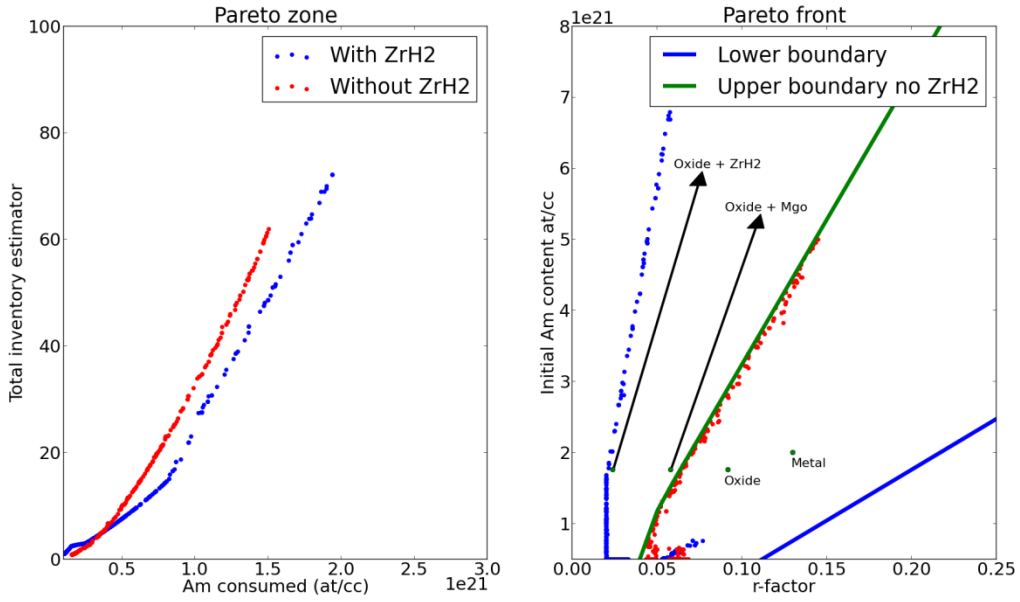

Figure 51 : Pareto zone and front for a washing limit corresponding to 7.5 kW per assembly. The upper boundary line corresponds the achievable (Am,r) range not considering the use of zirconium hydride. Green dots are corresponding to cores described in Table 27.

b) Limitations

A final limitation must still be taken into account into this calculation. When considering heterogeneous minor actinides transmutation, two major parameters must be taken into account. Firstly, since the consumption of minor actinides in the blankets must be characterized, as it was done in this chapter, the production of minor actinides in the core during the irradiation time of the blankets must also be characterized in order to have the transmutation

performances of the {core + blankets} system. Various phenomena must be taken into account to consider core minor actinides production and require a more complete description of the heterogeneous process. This will be taken care of in the next chapter. For instance, in a realistic reactor, self shielding in the blankets reduces the total neutron flux level in this region when ZrH_2 is used. This can be done by considering a case without moderation and a flux level of 6e14 $n/cm^2/s$ and a case with moderation and a flux level of 3.5e14 $n/cm^2/s$. These values were taken from core calculations mentioned above. If we plot the Pareto Front and Pareto Zone for both cases, as it was done in Figure 41, it can be seen that the ZrH_2 moderated case is still better than the non-moderated one, but the gap between the two has reduced due to a lower flux level. This illustrates the necessity of taking this parameter into account, as it will be done in the next chapter.

Secondly, as the calculations were done were based on the infinite medium corresponding to the transmutation target, it was only possible to derive decay heat and neutron per unit of mass of loaded fuel. However, technological and industrial limits for handling, transportation and reprocessing of spent fuel assemblies are expressed with regards to a complete assembly. Consequently, more information on the assembly design is required to effectively compute the fuel cycle impacts of this approach.

5) CONCLUSION

The physics of transmutation were detailed in this chapter and the various parameters impacting this process where discussed. It was shown that regardless of the actual design of the assembly to be used, transmutation could be characterized with sufficient accuracy using limited information on the actual core and assembly design. Additionally, it was shown that it possible to derive constraints linked to the fuel cycle using this simplified approach.

An optimization scheme based on these findings and artificial neural networks was used to identify trends and highlight interesting research avenues. It was found that the use of a moderated spectrum for minor actinides transmutation yielded better performances in terms of transmutation performances even when taking into account the negative impact on fuel cycle parameters associated with moderation.

However, considering the limitations of the approach, it is necessary to expand it by taking into account additional parameters related to assembly design in order to be able to correctly characterize transmutation, both in the heterogeneous and homogeneous mode. This will be done in the next chapters.

CHAPTER 4: THE HETEROGENEOUS APPROACH

Highlights:

- ✓ **Heterogeneous minor actinides transmutation requires higher care in the design of the targets due to the increased helium production during irradiation.**
- ✓ **A simplified design methodology for targets is described here.**
- ✓ **This design tool is coupled to the methodology developed in Chapter 3 for optimization of the heterogeneous transmutation.**
- ✓ **The optimality of the moderated approach is conserved when considering geometrical constraints.**
- ✓ **The use of metallic blankets is highlighted as possible alternative to moderated targets.**
- ✓ **The use of additional fissile material in the targets is also analyzed and it is shown that this approach is another alternative to the moderated one.**
- ✓ **A hierarchy of the industrial constraints related to heterogeneous transmutation is produced using the methodology. It is shown that transportation constraints for fresh assemblies are the first limiting one, followed by sodium washing of the spent assemblies.**

Considering the results obtained in the previous chapter, it is now necessary to broaden the scope of the optimization methodology to include assembly design constraints in order to be able to confidently use industrial considerations, which are expressed using the fuel assembly as unitary object, rather than the infinite homogeneous medium corresponding to the assembly.

As it will be discussed later on in this chapter, design of radial blankets for heterogeneous minor actinides transmutation exhibits various specificities compared to regular assembly designs mainly due to their position in the core and to their high minor actinide content. These particularities and the way they are addressed will be described in a first part.

A second concern regarding heterogeneous minor actinides transmutation is the production of minor actinides inside the core during irradiation. Indeed, it is necessary to evaluate this production in order to completely characterize the heterogeneous approach. A description of the approach used here and the implementation of these two points in the optimized methodology will then be discussed.

Various applications of the optimization methodology will also be discussed, and an illustration of the use which was made of this approach to highlight potentially new transmutation

approaches will be carried out. Finally, various cases with realistic constraints on the fuel cycle will be presented as well as a discussion on the impacts on each constraint.

1) SPECIFICITIES OF TRANSMUTATION TARGETS

As discussed in the previous chapters, minor actinides are loaded in dedicated targets in the heterogeneous approach. These targets can take various forms, such as specific assemblies loaded in the core or at its periphery [41]. Minor actinides can also be loaded in the axial blankets of the fuel assemblies used in heterogeneous core designs, as it was studied in [60] for instance.

However, it was shown in [60] that loading of minor actinides in targets/axial blankets inside the core yielded negative impacts on the core feedback coefficients, without significant improvements of the transmutation performances compared to a situation where radial targets at core periphery are used.

Consequently, we will consider here the loading of minor actinides bearing blankets (MABB) at the location of the first reflector ring of a given core, as shown in Figure 52. Due to their position and minor actinides content, various considerations must be taken into account to adequately design such targets, namely:

- The important gaseous production inside the targets
- The important flux gradient inside the target assembly
- The low thermal conductivity of the fuel used

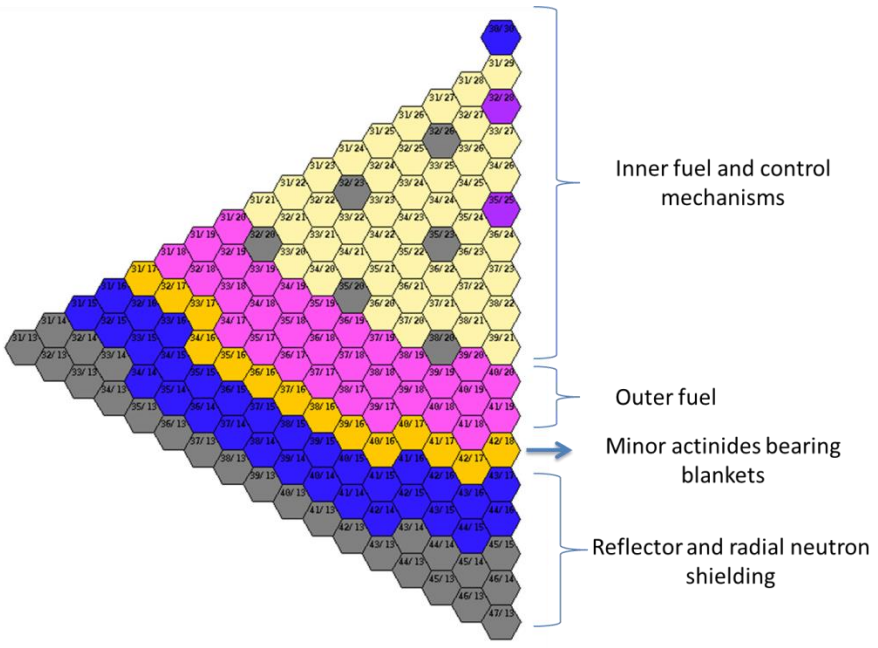

Figure 52 : Illustration on one-sixth of a core of the position of minor actinides bearing blankets

Each of this aspect of the problem will be discussed here and the approach chosen to take care of it in the calculations will be described. Finally, the optimization methodology which takes into account these additional parameters will be presented.

a) GAS PRODUCTION IN MABB

Due to their high content in minor actinides, especially in ^{241}Am, a high number of alpha decay occurs in minor actinides bearing blankets during irradiation (mainly through decay of the short lived ^{242}Cm). Table 28 below exhibits a breakdown of the production of gaseous fission products (Xenon and Krypton) and helium production for three assembly designs, one with standard MOX fuel, one with 2 at% of americium diluted in the fuel irradiated to the same burn up and one blanket assembly irradiated for 4100 EFPD in a 3600 MWth reactor with 20 at% of americium. The corresponding fluence is 2.37 10^{23} n/cm^2.

Table 28 : Comparison of the gases production for various assemblies

Fuel type	Fission gases production (cm^3/g_{HN},NTP)	Helium production (cm^3/g_{HN},NTP)	Total gases production (cm^3/g_{HN},NTP)
SFR MOX at 90 GWd/t	2.69	0.13	2.82
SFR MOX at 90 GW/d with 2 %Am	2.67	0.60	3.27
MABB at 20 % Am and 4100 EFPD	0.83	4.16	4.99

The gas production in the fuel is dominated by gaseous fission products coming from plutonium fissions while the main component of the gas production in the blankets is helium. The total production is also almost two times higher in the blankets than in the standard fuel assemblies. Consequently, if all the helium produced is released into the pin free volume, over-pressurization and subsequent rupture of the pin may result if the standard assembly design is kept unchanged. Dedicated expansion volumes located below and above the fuel stack are present in fuel assemblies to accommodate the released fraction of theses gases and to limit the increase in pin pressurization. It is then necessary to take into account the higher helium production here in order to design adequate assemblies. This requires a precise knowledge of:

- The helium and fission gases production in the blankets at the pin level
- The amount of these gases which is released in the pin free-space
- The cladding resistance to strain and maximal allowable pressure

Helium and fission gases production was computed using the DARWIN depletion code system [38] to solve the Bateman equation under irradiation. This point will be detailed the next subpart.

Due to the low linear heat rate in the blankets, behavior of the pins under irradiation is not well known. According to [61], significant helium swelling can be induced by the transmutation of ^{241}Am in the pins which may cause Fuel Cladding Mechanical Interaction. Complete characterization of this phenomenon is still underway through the MARIOS and DIAMINO experiments [62]. One option to counteract this phenomenon is to use specific fuels with tailored open-porosity in order to increase helium release in the pin free space. Given the uncertainties on the swelling behavior of the pins, it was decided to consider that **all the helium and gaseous fission products in the blankets were released into the free volume** and thus contributed to the pin pressurization. The porosity of the fuel was consequently set at

12 % (compared to 5.5 % for standard fuel) to account for the altered micro-structures. It was further supposed that, since complete release of gases from the fuel could be achieved, no significant swelling took place. A minimal gap of 0.15 mm was still considered to account for limited potential solid swelling.

Evaluation of the cladding primary strain was done using the Von-Mises stress for non-damaged material and thick tube, where the constraint is defined as $P_m = \sqrt{3}\frac{r_{int}r_{ext}}{r_{ext}^2 - r_{int}^2}\Delta p$ with $r_{int,ext}$ the internal and external radius of the clad and Δp the pressure difference on the cladding. The cladding maximal acceptable strain was compared to the ones of various Oxide Dispersed Steels (ODS). Considering the lack of available data on the resistance of these kinds of steels and their behavior under irradiation, an arbitrary value of 550 MPa was considered for the limiting primary constraint of the cladding here based on the results obtained for two steels evaluated in [63] and previous results obtained at CEA. Such kind of steels are expected to be available in the near-future and exhibit better irradiation properties than current austenitic steels such as HT9 or AIM1 [64].

Knowing the volume of gases released in the pin free space and the cladding strain resistance, it is then possible to evaluate the feasibility of an assembly design.

b) Flux gradient in MABB

However, as MABB assemblies are located at the core periphery, they are submitted to an important flux gradient, as it can be seen below in Figure 53. The neutron flux level "seen" by the pins the further away from the core is then twice as small as for the pins close the core. As the pin design in a single assembly must be unique, this implies that the outer pins will be over engineered compared to the fluence to which they will be submitted. To alleviate this effect, it has been proposed in [41] to rotate the blankets assemblies in order to flatten the irradiation profile to which they are submitted. This is illustrated below in Figure 54 which shows the radial profile of helium production with or without rotation of the assembly. In the un-rotated case, the production of helium is roughly 33 % higher in the part closest to the core than in the part the furthest away. With rotation, this effect disappears but the mean value of the helium production is conserved. The rotation of the target assembly during irradiation thus limits the total fluence gradient in the assembly.

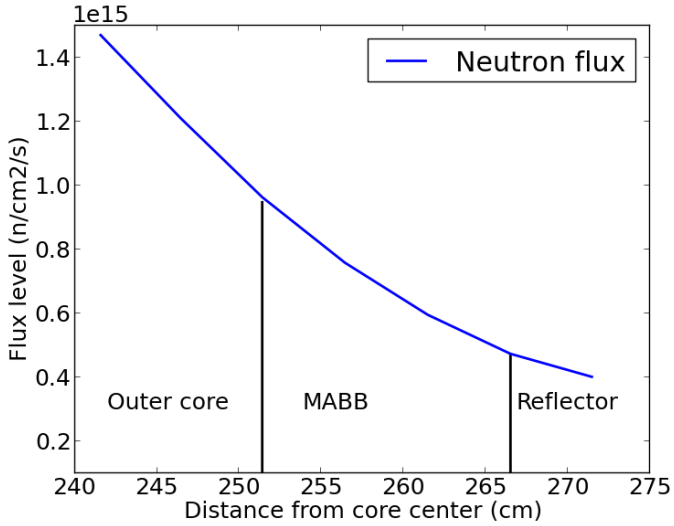

Figure 53: Evolution of the flux level in a typical blanket assembly for a 3600 MWth homogeneous fast reactor

Given the previous remarks, it was considered here that rotation of the target assembly was implemented during irradiation. To obtain gas production profiles such as in Figure 54, it is necessary to adapt the calculation scheme in order to split the blankets into an adequate number of subdivisions, nine here, and swap the concentrations and cross sections in the blankets at the middle of the irradiation in order to account for the rotation in the calculation scheme. As this would negatively impact calculation time and model complexity, a calculation scheme with a single cell medium for the blankets was used and the helium production was computed using the mean value of the flux in the blanket. This leads to a constant underestimation of the helium production of the dimensioning pin of 7 % over the entire range of Am concentration in the blanket medium as shown in Figure 54. This was accounted for in the optimization process. It was thus possible to know the helium production in the fuel while taking into account assembly rotation, and then to compute the pin pressure.

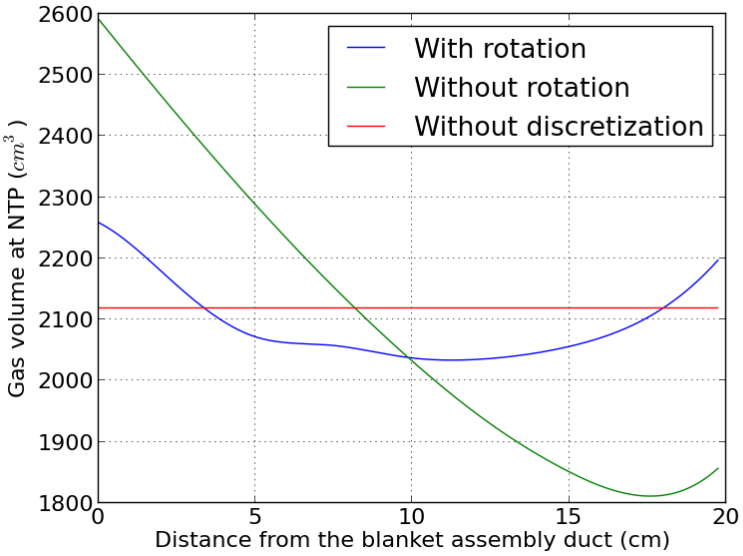

Figure 54 : Effect of rotation on gas production distribution

c) Low thermal conductivity and power of the MABB fuel

Uranium-americium oxide also exhibits a lower thermal conductivity than pure uranium oxide, as it was measured in [65] for instance. This conductivity decreases with the atomic fraction of americium in the mixed oxide. The thermal conductivity formula given in Equation 24 was used in this work, taken from [65]. At low temperatures of around 600 K, $U_xAm_{(1-x)}O_2$ has a thermal conductivity twice as low as UO_2, but this difference is much smaller at higher temperatures, with the two compounds exhibiting similar conductivities at 1000 K. However, the slightly lower thermal conductivity is offset by the lower power in the radial blankets. Due to their lack of fissile content and their position in the core, the power generated in such assemblies is generally three to five times lower than in the driver assemblies with linear heat rate being lower than 200 W/cm even for the most limiting cases considered here. An inner cladding temperature of 620 °C was considered throughout this study.

$$\lambda_{20\%Am} = \frac{1}{0.26304 + 0.97229 * 10^{-4}T}$$

Equation 24 : Thermal conductivity of Uranium-Americium dioxide

A final point which must be taken into account here is the low power level in the blankets, and its increase during irradiation. Indeed, these assemblies do not contain any "good" fissile nuclei at the beginning of irradiation, thus leading to relatively "cold" pins with centerline temperature between 600 and 800 °C at the beginning of irradiation depending on the pin diameter. This may have negative effects on the fuel behavior, all the more that due to significant breeding in the blankets during irradiation, the power level in the assemblies increases by a factor 2 to 3 over their lifetime. This power change may also lead to overcooling of the assemblies during the initial part of the irradiation. Considering the lack of available hard data on the effects of the low temperatures and undercooling, this point was not taken into consideration for the optimization process. It was however considered for a dedicated analysis which will be detailed further in this chapter.

Knowing the fuel thermal conductivity and the power in the assembly, it is then possible to compute the fuel centerline temperature for a given design and to compare it to the maximal allowable limit.

d) Boundaries of the problem and core definition

Based on the blankets assemblies previously used in past reactors, a set of boundaries for the assembly design parameters was chosen and is given in Table 29. A maximal americium content of 20 at% was considered throughout the study. A spacing wire of 1mm was considered regardless of the pin diameter. Knowing the thermal conductivity of the fuel, helium production, cladding resistance and power level, it is thus possible to design a complete assembly within the boundaries of Table 29 and with adequate pin pressurization and fuel centerline temperature.

Table 29 : Variation ranges of the parameters considered for pin design

All dimensions in mm	Lower boundary	Upper boundary	Source
Pin diameter	5.8 (PFR core)	15.8 (Superphénix blanket)	Historical review from [66]
Gap thickness	0.15	0.5	/
Cladding thickness	0.5	1.0	/
Expansion plenum height	Depends on the core considered. Here, between 98.9 cm and 168.9 cm for the core discussed in [54].		

When considering heterogeneous minor actinides transmutation, it is not only necessary to consider the efficiency of the transmutation process in the targets or blankets, but also the production of minor actinides in the core providing the neutron flux. As it was shown in Chapter 3, core production of minor actinides depends on the quality of the plutonium used as fuel and on the neutron spectrum inside the core. Regardless of these core parameters, it is also possible to cancel core production of minor actinides by loading a small fraction of minor actinides in the core corresponding to the equilibrium composition of minor actinides in the fuel. However, as this may not be adequate or feasible, two configurations were considered here. They correspond to two of the cores described in [67], which are industrial 3600 MWth cores loaded with either oxide or metallic fuel. The oxide core corresponds to the SFR V2b core described in [54]. The geometrical parameters of each core are given below in Table 30.

Table 30 : Assembly parameters of the various cores considered for heterogeneous transmutation

Parameters	Oxide	Metal
Power (MWth)	3600	3600
Fuel volume fraction (%)	43.7	40.83
Sodium volume fraction (%)	27.6	27.08
Structures volume fraction (%)	20.00	18.48
Max linear power (W/cm)	420	520
Loading frequency	5	5
Fuel residence time (EPFD)	2050	2578

Regarding core power selection, various parameters must be taken into account. The first one is core production of minor actinides, which decreases with the core power increase in terms of kg/TWhe and with the residence time. Following this tendency, high power cores with long residence time should be favored. Additionally, core production of minor actinides is inversely related to the neutron spectrum hardness, so there is an incentive to go towards the use of metallic fuel in order to achieve a very fast spectrum. Core production is also linked to the flux level in the core due to the specifics of ^{241}Am production. A higher level flux limits the production of ^{241}Am through ^{241}Pu decay and thus the production of minor actinides.

Two possibilities can be highlighted with regards to the dependency on core power. First, the impact of the geometrical core size can be analyzed. Indeed, decreasing core size while keeping the same power density would require higher plutonium content in the fuel to compensate for the increased leakage, which would in turn lead to an increased minor actinides production in the core. On the other hand, the increased leakage would slightly increase the transmutation performances. Both impacts are compared in Figure 55 , where the core power and size were

simultaneously decreased to keep a constant power density. It can be observed in this figure that the impact on blankets consumption is negligible while core production is inversely proportional to the core size.

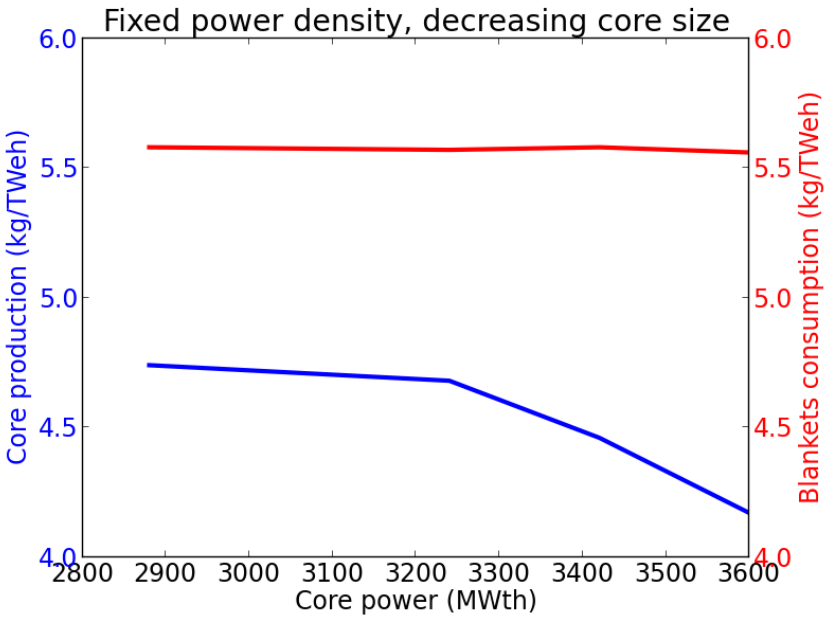

Figure 55 : Evolution of the core production and blankets consumption of americium for a nominally 3600 MWth SFR V2b core with variable core volume and fixed power density. The blankets were loaded with 20 at% Am with a design corresponding to a fuel volume fraction of 30 %.

The second possibility is to decrease the core power density by lowering the core power with a constant geometry. In this case, the lower flux level in the core will lead to a higher production of minor actinides in the core due to a lower consumption of ^{241}Pu over the irradiation. On the other hand, a slight spectrum shift will be observed at the core periphery which will decrease the r-factor in the blankets and thus increase the consumption of minor actinides. However, as it can be seen in Figure 56, the rate of increase of core production is higher than the one of blankets consumption, making this option similarly unattractive.

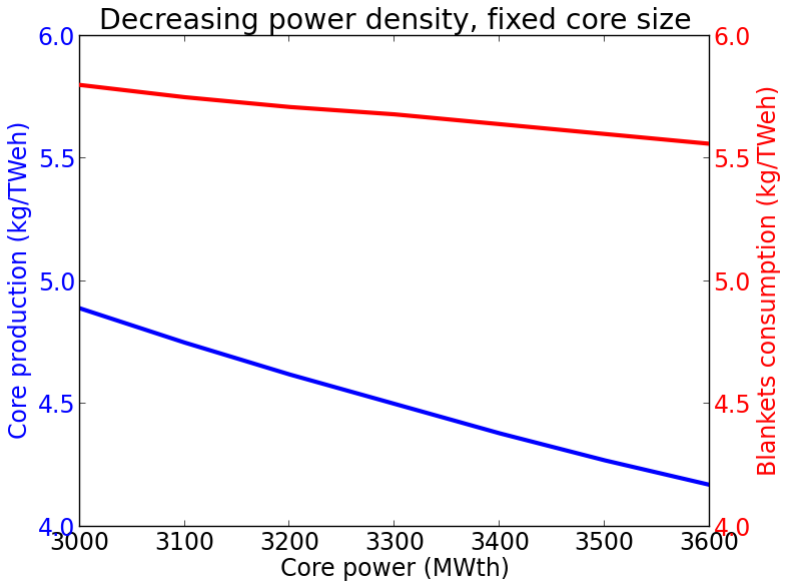

Figure 56 : Evolution of the core production and blankets consumption of americium for a nominally 3600 MWth SFR V2b core with variable power density and fixed core volume. The blankets were loaded with 20 at% Am with a design corresponding to a fuel volume fraction of 30 %.

Considering these results and that larger core designs can lead to economy of scale and lower overall costs which are beneficial from an industrial point of view, **we will only consider here 3600 MWth cores as described in Table 30.**

e) DESCRIPTION OF THE OPTIMIZATION PROCESS

A similar optimization process as used in the first part was built here, with the aim of characterizing the optimal transmutation strategies with regards to americium loading and neutron spectrum while fully specifying the corresponding assembly design. Similarly as in Chapter 3, two objectives were pursued: the maximization of the americium consumption during irradiation and the minimization of the impacts on the fuel cycle. It is summarized below in Figure 57. In addition of the tools previously used, several features were added:

- Considering that the flux level in the blankets depends on the type of core used and on the spectrum in the blankets, additional artificial neural networks were constructed in order to match flux levels in the blankets with neutron spectrum for a given core.
- Minor actinides core production was also taken into account based on the cores previously mentioned. As this production is not sensitive to the presence of blankets in the core, a constant value for each core was assumed regardless of the blanket design. Those are given in Table 34.
- Helium production in the blankets was computed and used to design viable assembly in terms of thermal and mechanical behavior. A meta-model was also used to compute the volume fraction of moderating material necessary to achieve the (r, Am) couple sampled. It was considered that the sodium volume fraction in the assembly was constant and thus that the addition of moderating material displace decreased the total mass loaded in the assembly, decreasing the absolute consumption of americium. Considering the low power level of the minor actinides bearing blankets, it would be possible to consider an alternative solution in which sodium is displaced by the moderating material instead of fuel. However, this would constitute a technological

solution to design assemblies with higher americium content rather than change the physics of the transmutation process. In order to remain conservative, it was considered throughout this study that the moderating material displaced fuel.

- Knowing the assembly design, it was possible to obtain integrated values for fuel cycle impacts and transmutation performances, which were then, used as input parameters for a genetic algorithm similarly as in Chapter 3.

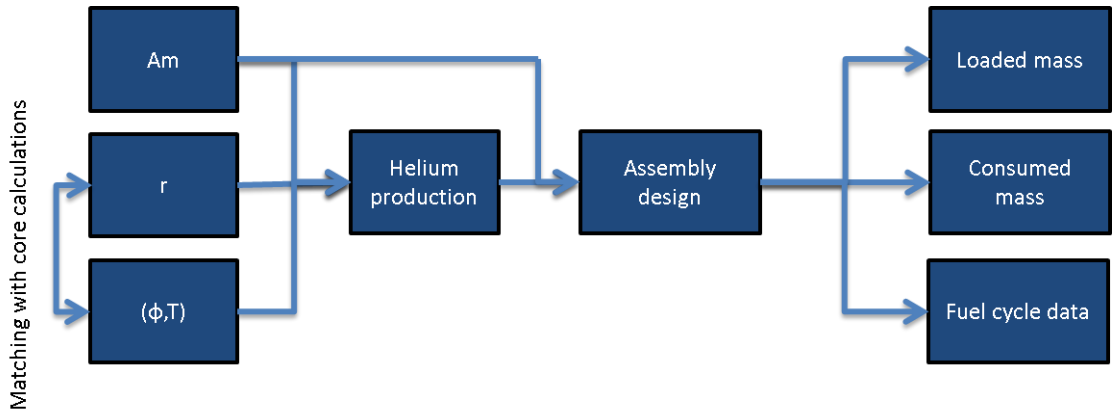

Figure 57 : Overview of the approach considered here

Considering the specificities highlighted in the previous part, the target assemblies design was done with the following objectives:

- Maximizing the fuel volume fraction in the assembly so as to minimize the Am content in the $UAmO_2$ compound. Qualitatively, this has a positive effect on the manufacturing step by reducing the specific activity of the fuel and limiting the changes in thermodynamic behavior of the fuel. In order to maximize fuel volume fraction, it is necessary to increase the pin diameter in order to increase the packing fraction.
- Keeping the pressure inside each pin below a threshold corresponding to the maximal allowable Hoop stress on the cladding. This requires either increasing the size of the expansion volume inside the pins in order to accommodate the gaseous release inside the free space, or decreasing the pin diameter in order to limit the amount of fuel inside each pin.
- Keeping fuel centerline below the melting temperature of the considered fuel, e.g. 2740 °C for oxide fuel and 1160 °C for metallic fuel. It should be mentioned here that due to the low power in the blankets, these temperatures were never reached during the optimization process.

Generally speaking, the limiting factor for assembly design was the pin pressurization and the increase in the Hoop stress in the cladding.

A breakdown of the discrepancies associated with the use of meta-models is given in Table 31. It can be seen that the mean error associated with these calculations is close to zero and that the associated standard deviation is rather limited, similarly to what was obtained in Chapter 3. In addition, the standard deviations are slightly lower here as only one combination of

fuel/coolant/moderating material was used, thus limiting the variation range of the outputs. Around 2500 calculations were used to generate the training and validation sets of the ANN.

Table 31 : Mean error and standard deviation of the artificial neural networks used for the study of the oxide core behavior.

Parameter	Transmutation rate	Decay heat @ 5 years	Decay heat @ 10 years	Decay heat @ 20 years	Decay heat @ 50 years	Decay heat @ 100 years	Moderator fraction for a given spectrum
Mean error (%)	0,06	-0,03	0,30	0,07	0,01	0,06	0,07
Standard deviation (%)	1,15	1,89	2,52	1,73	2,05	1,71	0,30
Parameter	Neutron source @ 5 years	Neutron source @ 10 years	Neutron source @ 20 years	Neutron source @ 30 years	Neutron source @ 50 years	Neutron source @ 100 years	Helium production
Mean error (%)	0,01	0,28	0,20	0,08	0,02	-0,08	-0,13
Standard deviation (%)	3,91	4,28	3,08	2,99	2,89	4,02	2,98

The Q^2 estimator defined in the previous chapter was also computed here and a very good agreement was obtained between the results calculated by ECCO and the ones obtained by the artificial neural networks, as it can be seen in Table 32.

Table 32: Q^2 estimator for the parameters of interest

Parameter	Neutron source @ 5 years	Neutron source @ 10 years	Neutron source @ 20 years	Neutron source @ 30 years	Neutron source @ 50 years	Neutron source @ 100 years	Moderator fraction for a given spectrum
Q^2	0,9996	0,9995	0,9998	0,9998	0,9999	0,9996	0,9997
Parameter	Transmutation rate	Decay heat @ 5 years	Decay heat @ 10 years	Decay heat @ 20 years	Decay heat @ 50 years	Decay heat @ 100 years	Helium production
Q^2	0,9995	0,9998	0,9998	0,9998	0,9999	0,9999	0,99998

A tentative validation of this methodology was done by comparing the results of the methodology calculated using artificial neural networks with the results of a complete core calculation carried out using ERANOS. Two cases with similar performances are presented here, one with ZrH_2 as moderating material and one without. The results are shown in Table 33. The optimization methodology exhibits a very good agreement with the ERANOS calculation for the unmoderated cases, with a slightly less good agreement in the moderated cases due to a higher calculated moderator fraction, however, the errors are within acceptable ranges. Further analysis of the associated uncertainties will be done at the end of this chapter.

Table 33 : Comparison of the outputs of a complete ERANOS calculation and the optimization methodology for two representative cases

Unmoderated V2b assembly	r = 0,073	Phi = 6,70e14
	Am = 1,82e21	T = 4100 EFPD
Calculation route	ERANOS	ANN
Consumption per assembly (kg)	11,22	11,17
Decay heat @ 5 years (kW)	8,5	8,4
Decay heat @ 50 years (kW)	4,1	4,1
Assembly mass (kg)	143,4	143,3
Moderator fraction (vol %)	0	0

ZrH_2 moderated V2b assembly	r = 0,0287	Phi = 4,90e14
	Am = 1,44e21	T = 4100 EFPD
Calculation route	ERANOS	ANN
Consumption per assembly	11,21	11,24
Decay heat @ 5 years	8,9	9,0
Decay heat @ 50 years	4,1	4,2
Assembly mass	124,9	121,2
Moderator fraction	5	5,77

For a better visualization of the results of the optimization, a different plotting strategy was also chosen here. The results are plotted using a 2d-map with the r-factor on one axis and the Am initial mass per assembly on the other one. The values of the relevant estimators are then plotted using contour plot and adequate color maps.

2) COMPLETE OPTIMIZATION PROCESS

Various applications of the complete optimization process will be discussed here.

a) VALIDATION OF THE MODERATED APPROACH

A first goal of this optimization process is the follow-up of the study developed in Chapter 3, e.g. the validation of the interest of the use of a moderated spectrum in the blankets even when taking into account the fuel cycle constraints, the lower flux associated with the moderated spectrum and the core production of minor actinides. We will thus consider here a 3600 MWth oxide core as described in [41]. The irradiation time will be set at 4100 EFPD, which amounts to 142.68 TWhe produced during the irradiation of the blankets. Oxide blankets with ZrH_2 as moderating material will be considered, where the moderating material replaces fuel in the assemblies in order to keep the coolant fraction constant.

At first stage, the Americium inventory was calculated by considering a cooling down to 7.5 kW per assembly and only an adaptation of the pellet diameter was allowed in terms of geometrical design. The same input parameters as in Chapter 3 were considered, e.g. the americium concentration in the MABB medium and the neutron spectrum. A maximal americium content of 20 at% was considered initially.

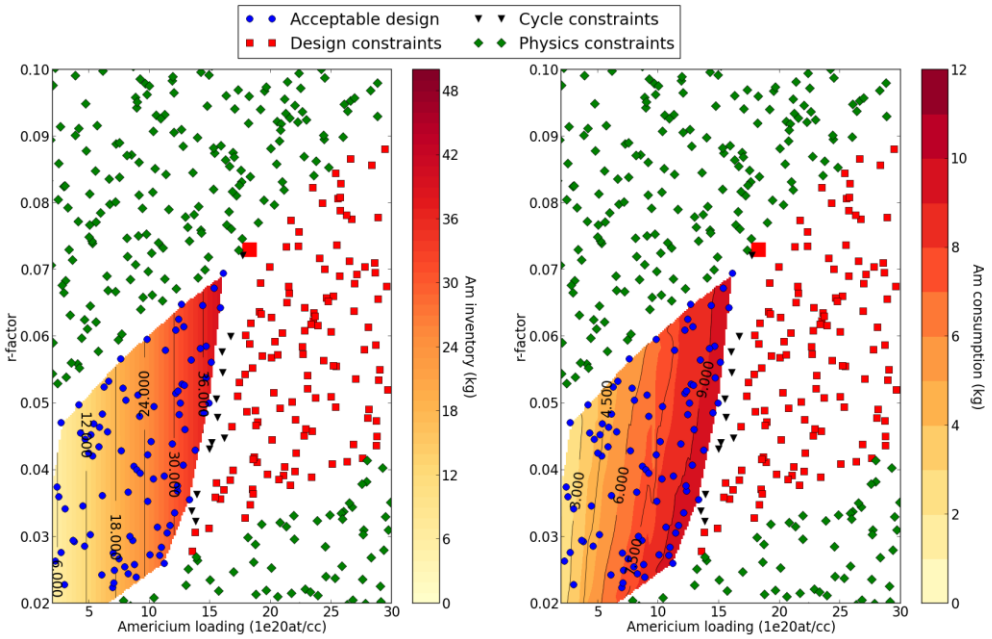

Figure 58 : Americium inventory and consumption for one blanket assembly for a 3600 MWth oxide core conditions. A 7.5 kW cooling limit was used for this calculation. Only the pellet diameter was modified in terms of geometric optimization. Zirconium hydride was used as moderating material. The big red square corresponds to SFR V2B situation.

Several comments can be done on Figure 58. The color map on the left corresponds to an estimator of the americium inventory expressed in terms of kg of americium in the cycle per blanket assembly. The color map on the right represents the evolution of the americium consumption for one assembly over the irradiation time considered, expressed in kg. It is calculated using the same approach as in the previous chapter.

The green points correspond to cases which are not physically feasible, e.g. for which the combination (r, Am) is not achievable, either because the neutron spectrum is too energetic for the amount of minor actinides loaded (upper-left part), or because it is not possible to achieve such a spectrum with a limited amount of ZrH_2 (lower-right corner).

The red points correspond to cases which are not feasible by design, mainly here because the helium production in the pins is too important for the cladding resistance and will lead to a clad rupture at the end of irradiation. The inverted black triangles correspond to cases for which the americium content in the $U_xAm_{1-x}O_2$ compound is higher than a limit set here at 20 %. Indeed, when the americium concentration in the blanket medium increases, so does the associated helium production. To accommodate this higher gas production, it is then necessary to decrease the pellet diameter, which decreases the fuel volume fraction in the assembly. To keep the americium concentration constant, the Am content in the fuel must then be raised, up to the limit of 20 %.

The blue points correspond to cases for which it is possible to design an assembly which will withstand the increase in internal pin pressurization with the required neutron spectrum and americium loading while exhibiting an americium content lower than 20 %. It can be observed that for low r values (below 0.04), which are achievable only using ZrH_2, the content limit is the first to be reached, even though assembly with the same americium content are feasible at higher r factor. This is explained by the substitution of fuel by moderating material, which requires a faster increase in the Am content in order to keep the Am concentration in the assembly constant.

It can be observed here that the inventory dependency on the neutron spectrum is inexistent. Indeed, with a washing limit set at 7.5 kW and the design limitations due to pin pressurization, it is not possible to obtain an assembly with a decay heat higher than this limit. Consequently, the cooling time is limited to its minimal value of 5 years and the inventory estimator only depends on the loaded mass, thus the vertical contour line on the inventory plot.

On the other hand, the consumption per assembly decreases with the spectrum hardening, which was expected from the results of Chapter 3. It was also found here that the point (r,Am) corresponding to SFR V2B (bigger red square) is classified as not feasible by design, which is in good agreement with previous assembly design studies [68] which have showed that it was not possible to design an assembly with 20 % Am content and 40 vol% of fuel while adapting only the pellet radius.

For illustrative purposes of the dependency of the inventory on the neutron spectrum and on the cooling limit, the evolution of the inventory with the neutron spectrum for two Am contents and two limits were plotted in Figure 59. As shown before, for the 7.5 kW limit, the inventory estimator does not vary with neutron spectrum. On the other hand, for the 2.5 kW limit, the inventory increases when the r-factor decreases. This is due to the higher production of ^{238}Pu caused by the less energetic spectrum. The effect remains relatively small, with a 10 % decrease in the inventory over the spectrum range. It is thus not very noticeable on the color maps of the next figures.

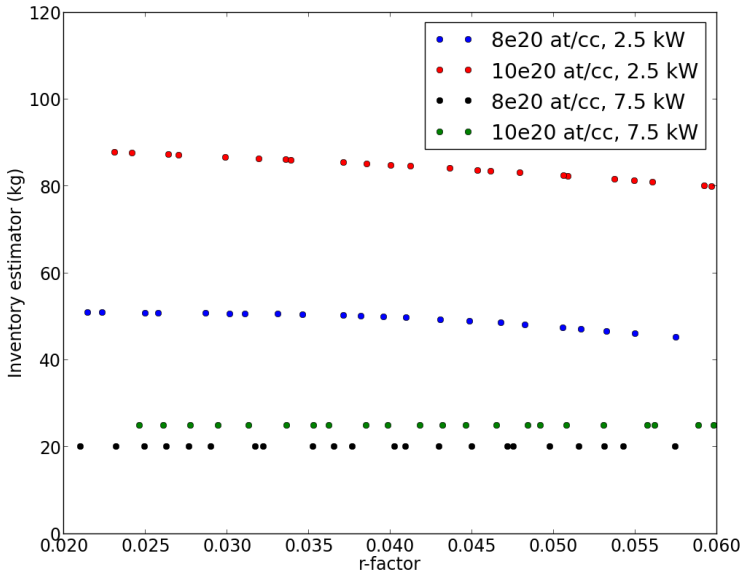

Figure 59 : Evolution of the inventory estimator with regards to the r-factor for various washing limits and americium loading. Only the pellet diameter was used as an optimization parameter for the assembly design.

If we now increase the maximal allowable height of the gas expansion plenum up to 168.9 cm, a wider domain of cases becomes accessible. The SFR V2B case also now appears to be feasible, which is in good accordance with previous studies. It further appears at the border of the feasible domain, which is coherent with the fact that it was designed with 20 at% of americium loading. Heavier assemblies' design which are feasible in terms of pin pressurization are not feasible per se as they would not be compatible with manufacturing constraints. Finally, as the loaded mass increases and despite the 7.5 kW washing limit, the dependency of the inventory on the neutron spectrum highlighted in Figure 59 starts to appears here due to the increased production of ^{244}Cm which contributes to most of the short term decay heat. Hence, the rightmost contour lines of the inventory plot are tilted to the right.

It can be qualitatively observed there that the cases with a heavily moderated spectrum yield the highest consumption with relatively limited inventories. To further refine this question, a more classical optimization based on the genetic algorithms discussed in Chapter 3 was used.

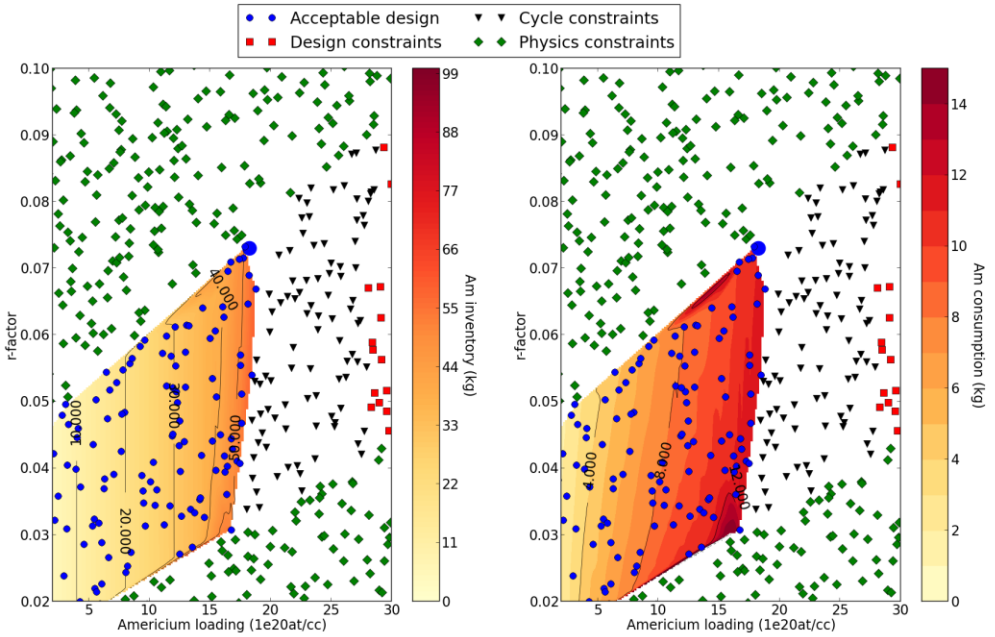

Figure 60 : Americium inventory and consumption for one blanket assembly for a 3600 MWth oxide core conditions. A 7.5 kW cooling limit was used for this calculation. Only the pellet diameter and the plenum were modified in terms of geometric optimization. Zirconium hydride was used as moderating material. The big blue circle corresponds to SFR V2B situation.

The results of the genetic algorithm optimization can be found in Figure 61 for two cases where two limits for sodium washing were considered: 2.5 and 7.5 kW. The same plots as in the previous chapter were used. The assemblies were optimized to maximize the fuel volume fraction by modifying the expansion plenum height and the pellet diameter. The irradiation time was also used an optimization parameter ranging from 2000 to 6000 EFPD; however the algorithm maximized this input parameter in order to maximize the transmutation rate. It is therefore not displayed in this figure. The results which were found in Chapter 3 regarding the interest of moderation for heterogeneous minor actinides transmutation are confirmed here, where all the optimized cases are obtained for a r-factor lower than 0.05. For very low consumption rates of americium, the inventory behaves similarly for the two limits, as the spent fuel decay heat is lower than 2.5 kW. However, above around 6 kg per assembly (2.35 kg/TWhe), the curve corresponding to the 2.5 kW limit separates from its counterpart as the irradiated blankets decay heat goes above 2.5 kW and its cooling time increases. Where equilibrium between core production and blanket consumption is required (4.22 kg/TWhe in this case, or 10.5 kg per assembly), shown as a black line on Figure 61, the inventory for the 2.5 kW limit case is 2.5 times higher than the one for the 7.5 case kW due to the longer associated cooling time. **We can therefore conclude from this that the use of a "moderated" spectrum in the blankets is optimal in terms of americium transmutation and fuel cycles impacts, even while taking into account assembly design (pin pressurization, moderator fraction and americium content).**

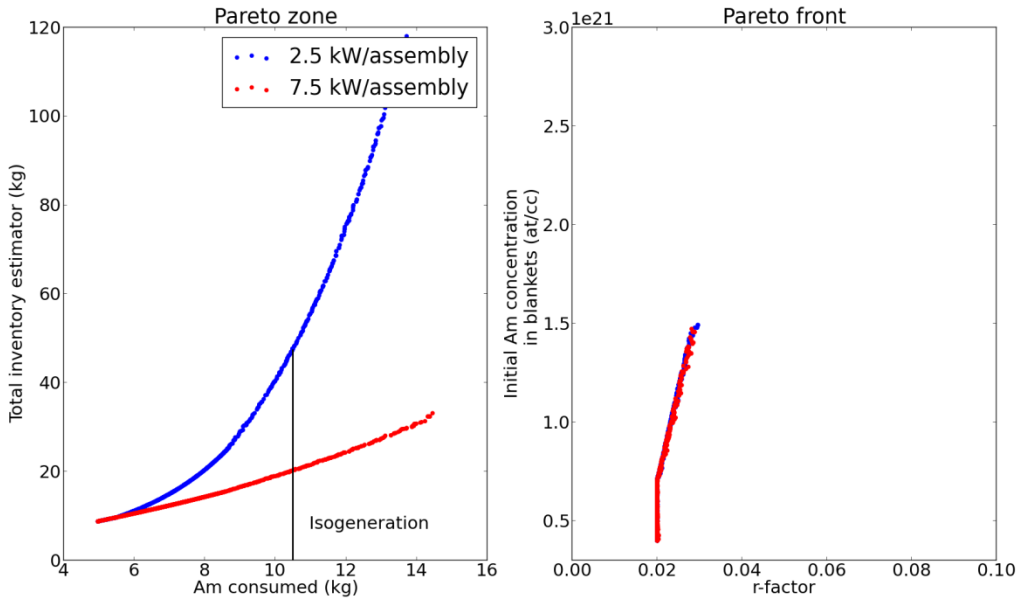

Figure 61 : Pareto front and zone with regards to consumption and americium inventory in the fuel cycle for an oxide core. The irradiation time was maximized at 600 EFPD and the assembly design was optimized with regards to the pellet diameter and gas plenum expansion height.

Neutron source was also found to be a potentially limiting parameter in Chapter 3. We consequently further consider a neutron source limit of 5e9 n/s/assembly, which is approximatively four times the neutron emission of a MOX fuel assembly after 5 years of cooling. It can be seen on Figure 62 that the shape of the accessible domain does not change compared to Figure 58, which was expected as this domain was limited only by design or americium content considerations.

However the total inventory can now reach more than 75 kg per assembly compared to 40 kg for the previous case. This is explained by the major contribution of ^{244}Cm (> 96 %) to the neutron source of the spent assemblies. Consequently, the decrease of the neutron source depends entirely on the decay of this isotope, which has a half life of 18.8 years. For the core considered here, a typical fuel assembly contains 0.12 kg of ^{244}Cm at the end of its life, while a blanket assembly contains 1.77 kg of ^{244}Cm. Consequently, to reach the same level of neutron source, a cooling time of more than 65 years would be required, which is not acceptable. Consequently, it can be seen that improvements in neutron shielding for spent blankets will have to be pursued in order to successfully implement minor actinides transmutation.

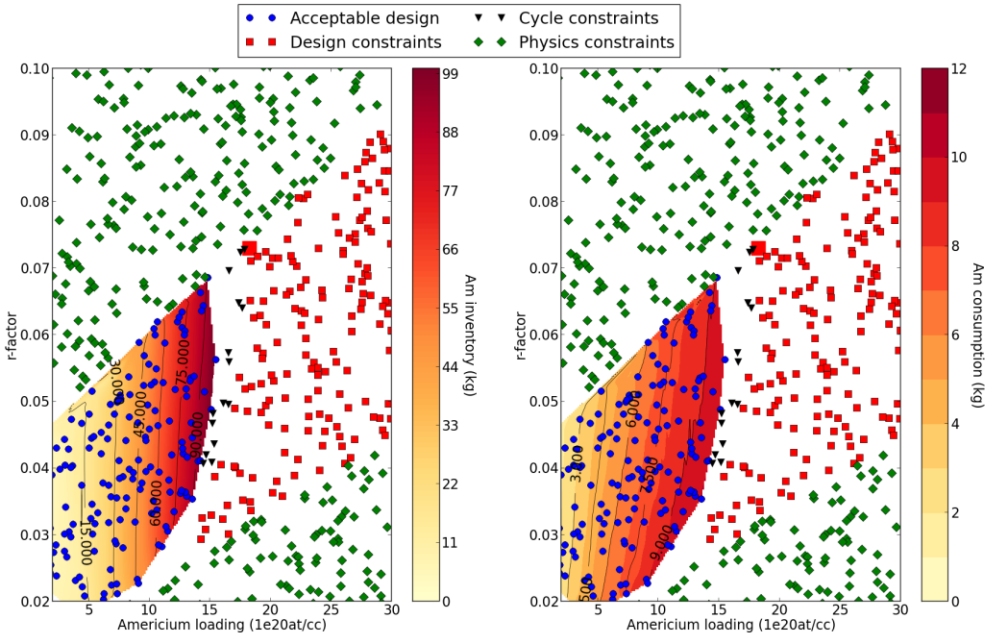

Figure 62 : Americium inventory and consumption for one blanket assembly for a 3600 MWth oxide core conditions. A 7.5 kW cooling limit and a 5e9 n/s neutron source limit were used for this calculation. Only the pellet diameter was modified in terms of geometric optimization. Zirconium hydride was used as moderating material. The big red square corresponds to SFR V2B situation.

As it was shown with the neutron source comparison, cooling times may become unacceptably large if the fuel cycle constraints in terms of decay heat or neutron emission are not decreased. Another approach which is discussed here is to specify the constraint as a maximal level of decay heat and neutrons source at a given time, which is more consistent with the industrial scenarios studies. For instance, if we consider, as it was done in [25], that the maximal cooling time is 5 years, it can be deduced that sodium washing must take place at most after 5 years. Consequently, we can define the following constraint: the assembly decay heat after 5 years cooling must be lower than 5 kW, otherwise the assembly design is not acceptable. The 5 kW limit was taken for illustration purpose The results of this analysis are shown in Figure 63. The domain with acceptable design parameters has shrunk compared to a situation where cooling times are not capped. The portion which is now not feasible corresponds to assemblies which are complying with the pin pressurization and initial americium content constraint, but which decay heat is higher than 5 kW after 5 years. We can conclude from this that limiting the maximal cooling time to reach an acceptable decay heat is going to have strongly negative impacts on the maximal consumption which can be reached using heterogeneous blankets.

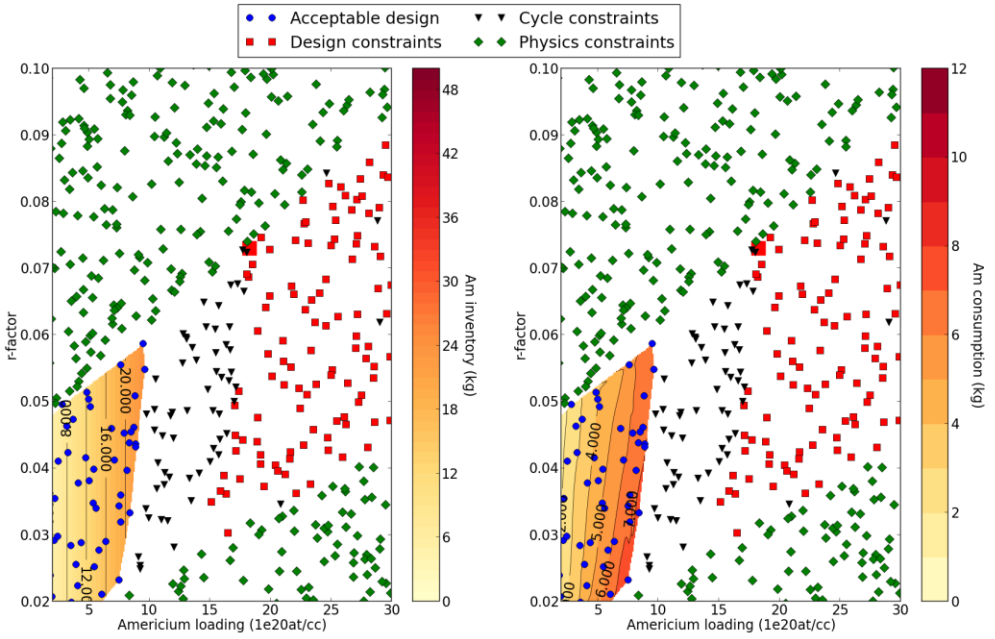

Figure 63 : Americium inventory and consumption for one blanket assembly for a 3600 MWth oxide core conditions. A 5 kW decay heat limit after 5 years of cooling was considered here. Only the pellet diameter was modified in terms of geometric optimization. Zirconium hydride was used as moderating material. The inverted black triangle corresponds to SFR V2B situation.

Using the same tools, it is possible to consider the residence time of the blankets as a free parameter of the model. This is done in Figure 64, which shows the color map of both the inventory in the fuel cycle and the americium consumption per assembly of a SFR V2B core with a constant r-factor of 0.05 in the blankets. This r-factor corresponds to a loading of a few volume percent of ZrH_2. Cases in the upper right corner correspond to solutions where the helium production over the irradiation exceeds the cladding resistance criterion. It can be observed that the transmutation performances of the system increases both with the americium loading and with the residence time, as expected from the results of Chapter 3.

If we observe the inventory behavior, it can be seen that, while the inventory increases with the loaded mass, it decreases with the residence time. This means that the enhanced curium production due to longer irradiation times and the associated longer cooling times are counterbalanced by the americium mass reduction. For longer residence times, the production of ^{244}Cm reaches or overcomes a maximum value after which it slowly decreases, this is the so-called Curium Peak introduced in Chapter 3. Consequently, an increase in the irradiation time will only lead to a reduction of the final ^{241}Am content while having a limited impact on the ^{244}Cm final content, thus leading to a lower final specific decay heat and a lower total inventory. We can thus conclude here that increasing the residence is not only a good solution to increase the transmutation performances, but also reduces the impact on the fuel cycle as the additional consumption of ^{241}Am compensates the increased production of heat emitting nuclei.

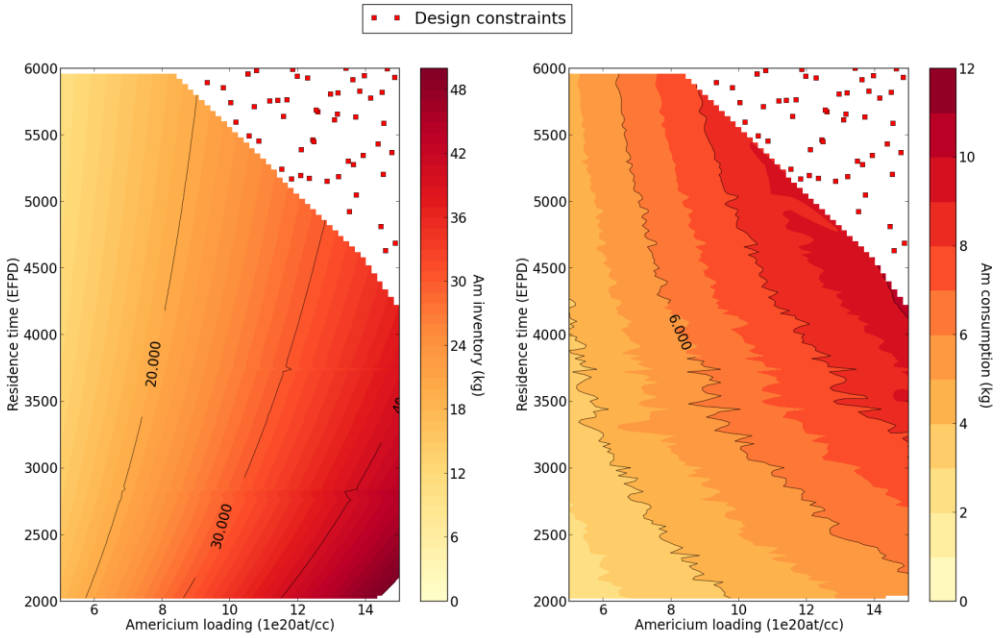

Figure 64 : Americium inventory and consumption for one blanket assembly for a 3600 MWth oxide core conditions with regards to the americium loading the blankets and to their residence time. The r-factor was set at 0.05. A decay heat limit of 7.5 kW was considered here and the plot range was adapted to keep only acceptable cases in terms of designs. Zirconium hydride was used as moderating material.

Finally, it is possible to use all the parameters of the model shown in Table 29 as input variables and then to obtain the optimal assembly which can be obtained using a pin bundle design with 20 at% of Americium. This is done below in Figure 65. Consumption in excess of 15 kg per assembly, which is equivalent to 8.8 kg/TWhe can be reached here, with the americium content being the main limiting factor. The optimized assemblies obtained by the optimization process are characterized by high pellets diameter with thick cladding and high expansion plenum to accommodate pin pressurization.

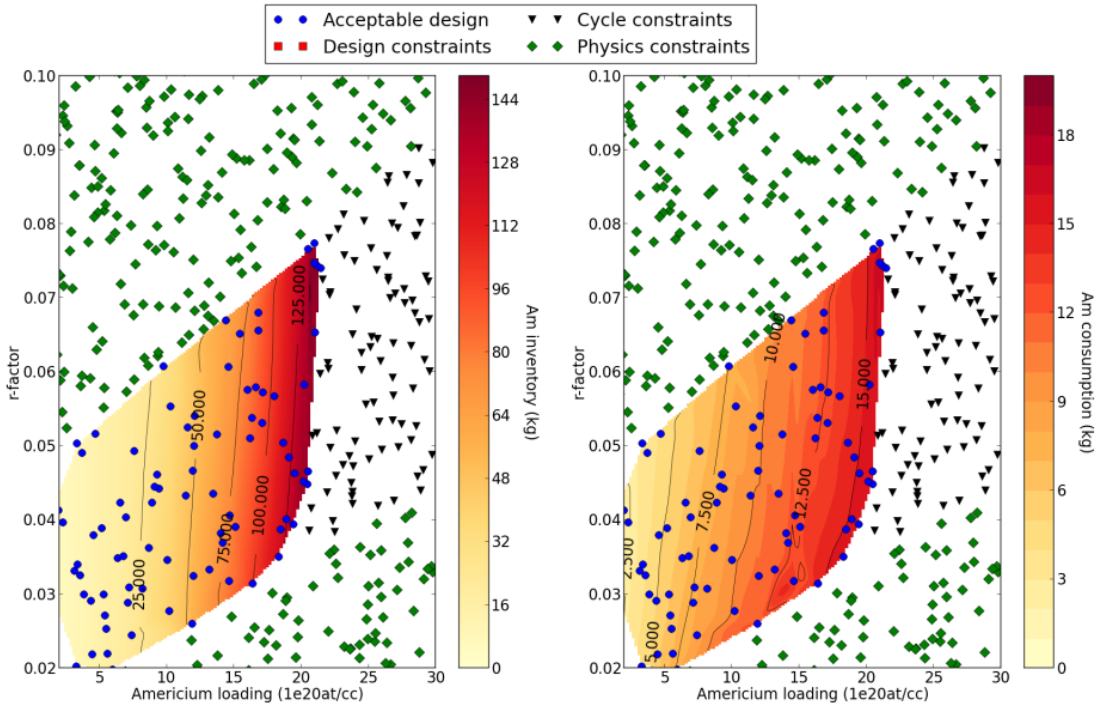

Figure 65 : Americium inventory and consumption for one blanket assembly for a 3600 MWth oxide core conditions. A 7.5 kW decay heat limit was considered here. All the parameters of the assembly design model were used as free parameters. Zirconium hydride was used as moderating material.

b) Comparison between metal and oxide approach

Another possible use of this methodology is to investigate the impact of core production on the total minor actinides transmutation strategy. Indeed, in terms of available neutron spectrum, it has been observed in Chapter 3 that a softer neutron spectrum in the minor actinides bearing blankets yielded better results in terms of transmutation performances with lower associated inventories. However, it was also shown that a fast spectrum limited the production of minor actinides from plutonium isotopes in the core.

A comparison was made here by considering both the oxide core and the metallic core described in Table 30. Zirconium hydride was considered as moderating material in both cases. As the addition of moderating material in the blankets did not excessively impact the minor actinides production in the core (less than 2 %), an average value over the entire possible blankets configurations was considered. The corresponding specific MA productions are given below in Table 34. Considering these productions, the metallic core exhibits a net advantage compared to the oxide one in terms of minor actinides production due to its inherent spectrum.

Table 34 : Specific production of minor actinides in two 3600 MWth oxide and metal cores with MABB

kg/TWhe	Oxide + ZrH	Metal + ZrH	Oxide + MgO	Metal + MgO
Np	0,42	0,54	0,42	0,54
Am	4,22	1,75	4,16	1,75
Cm	0,55	0,20	0,56	0,20

If we now take into account the contributions of the core/targets system, we can obtain the following results, as shown in Figure 66. Geometric optimization for the metallic fuel was done by considering sodium bonding of the pins to a 75 % smeared density in order to account for the high swelling in metallic fuels. Given the scarcity of data on the thermal conductivity of the UAmZr compound, a thermal conductivity of 20 W.m/K was used for the assembly design calculations [69]. Similarly to the oxide case, the fuel temperature was not found to be a limiting factor in this case.

If we consider the total consumption of minor actinides in the blankets and the core expressed in kg/TWhe, the same maps as in the previous part can be plotted for both the oxide and the metal case. This is done in Figure 66 and Figure 67 for the oxide and metal cores respectively. Only the pin diameter was used as an optimization parameter for the assembly design. The range available for the metallic case is extended towards higher r-factor as it is possible to obtain more energetic spectrum using this fuel. Additionally, the design is less constrained due to the lower production of helium in the blankets.

The equilibrium between production in the core and consumption in the blankets is reached for lower loaded mass in the metal case than for the oxide case. This is explained by the higher production of the oxide core due to the less energetic spectrum. Consequently, it appears that a metallic core with metallic blankets has better transmutation performances than an oxide core with oxide blankets. Even though moderated oxide blankets are better to consume americium, this better performance is offset by the high production of minor actinides in the core. On the other hand, metallic blankets are less effective at transmuting americium, but this is compensated by the lower core production.

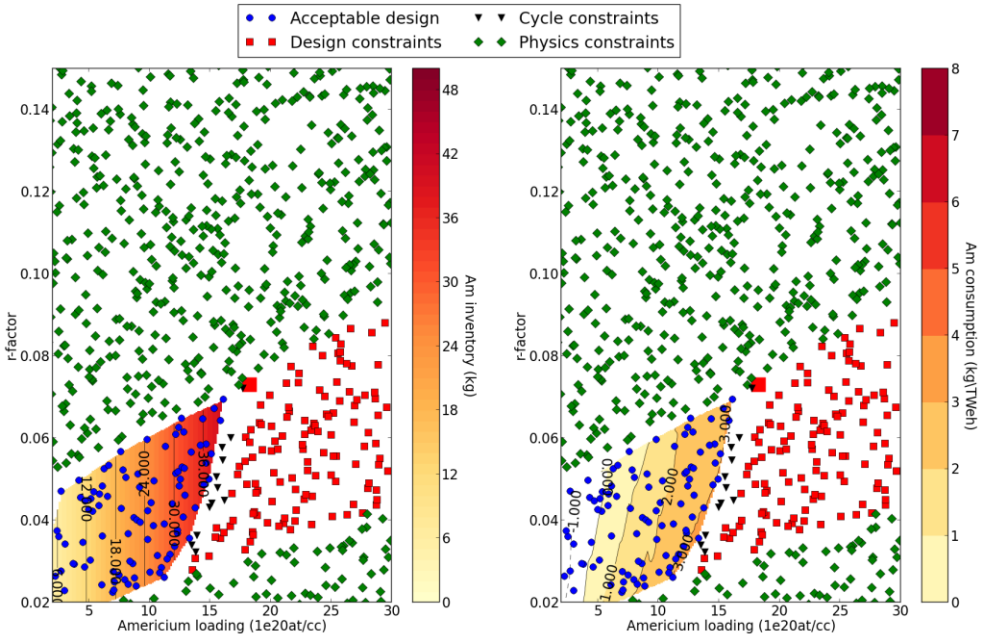

Figure 66 : Performances of the core and blankets for a 3600 MWth oxide with 4100 EFPD of irradiation with a 7.5 kW reprocessing limit and only a pellet diameter optimization for the assembly design

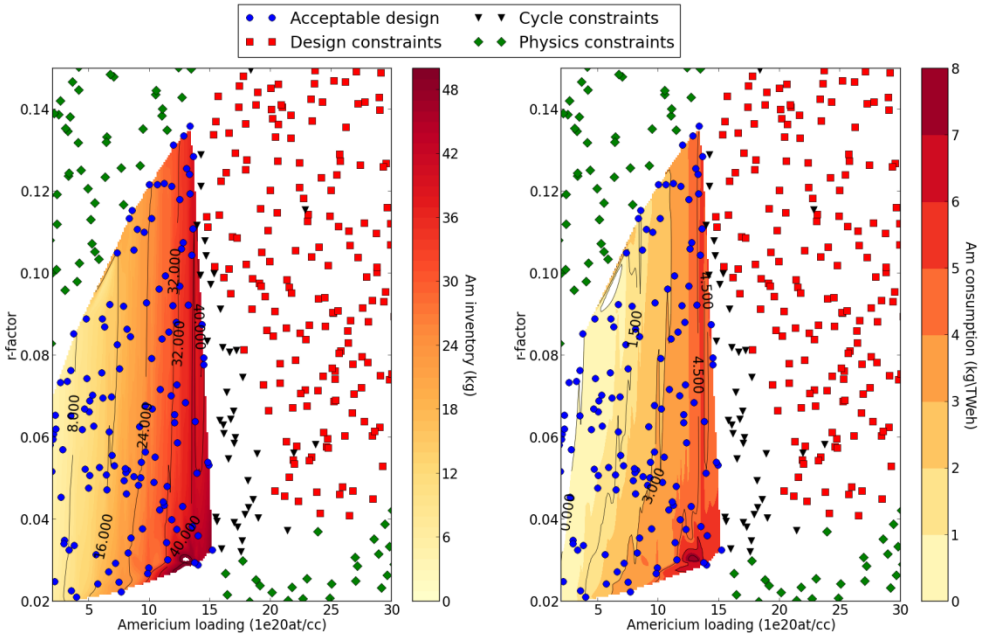

Figure 67 : Performances of the core and blankets for a 3600 MWth metal with 5156 EFPD of irradiation

It should be mentioned here that this result is highly dependent on the plutonium isotopic vector considered for the irradiation. Indeed, if we consider a plutonium isotopic composition as shown in Table 35, which corresponds to a possible vector obtained after multi recycling in a SFR as described in [25], the higher initial quality of plutonium leads to a final americium consumption of 2.63 kg/TWhe for the oxide core and 1.19 kg/TWhe for metal. In this condition, the advantage of the metallic option is slightly lower and the oxide case is again competitive. As this problem is non-trivial and heavily depends on the assumptions made on the plutonium multi-recycling, no further studies were carried out on this topic. Indeed, they would have required a complete industrial scenarios analysis which would have been beyond the scope of this study.

Table 35 : Isotopic composition of a plutonium isotopic vector obtained after multi recycling in a SFR

Isotope	Pu238	Pu239	Pu240	Pu241	Pu242	Am241
Mass %	0,61	62,89	30,46	2,54	3,05	0,45

c) A NEW APPROACH: ADDING FISSILE MATERIAL TO THE TARGETS

Considering the input parameters of the model, it can be observed that only two of them have been modified directly at the design stage, e.g. the americium concentration in the blankets and the neutron spectrum, while the flux level to which the blankets are submitted is calculated from these two parameters depending on the core design. However, it was shown in Chapter 3, where the flux level and irradiation time were considered separately, that the optimal cases for americium transmutation could also be obtained with a maximization of both parameters, either together or separately.

Residence time of the blanket assemblies is mainly limited by the cladding damage rate and helium production during irradiation, along with the increase in the decay heat due to the

additional curium production. However, as it was shown in Chapter 3, curium production tends to show a maximum – the so-called curium peak – after a fluence corresponding to the expected residence time of minor actinides bearing blankets in fast reactors (≈ 4000 EPFD in a 3600 MWth, or around 2 10^{23} n/cm^2). For fluences higher than this, any increase in the residence time will decrease the final curium concentration and increase the americium consumption and thus improve the considered strategy, However, as it is related to technological constraints linked to assembly irradiation behavior, this approach was not studied here. It can be related to the once-through approach detailed previously in which the residence time is maximized in order to achieve the best transmutation performances without recycling the blankets.

A limited range of options exists to tune the flux level to which the blankets are submitted. Their position in the core can be modified by moving them closer to the core center, however this will negatively impact core feedback coefficients, as it will be discussed in the next chapter. The core layout can be modified in order to increase radial neutron leakage; however this goes against the heterogeneous "philosophy" of not modifying the core layout. Another possibility, which will be discussed, would be to add "fissile" material to the target fuel. This exhibits several advantages, as it increases the flux level in the blankets while hardening the neutron spectrum, effectively increasing the absorption rate while limiting production of curium by capture and thus the increase on targets decay heat and neutron source. It also increases power production in the blankets and limits the S/A power shift with irradiation. This may also be beneficial for helium release in the pins free volume, thus limiting fuel swelling rate. However, an increase in the transmutation may lead to an increase in Helium production from alpha decay, which creates additional constraints in term of assembly design. Finally, it may provide a temporary solution to immobilize available fissile material and thus reduce proliferation risks [70] [71].

Various fissile materials can be considered for such a use:

- ^{235}U, which is readily available as PWR fuel
- ^{239}Pu, which is available in a nearly pure form as weapons-grade material
- Any isotopic vector of plutonium coming from reprocessed fuel. Two vectors were considered in this work, Pu2035 and Pu2100 which are deemed representative of the available plutonium stocks in France in 2035 and 2100 in different deployment scenarios. The first one has already been discussed in Chapter 3 and has a lower amount of ^{239}Pu as it is coming from MOX fuel irradiated in PWRs while the second one is representative of the plutonium that could be obtained in a closed fuel cycle with sodium fast reactors [25]. The actual composition of these two vectors can be found in Table 36.

%	Pu238	Pu239	Pu240	Pu241	Pu242	Am241
Pu2035	3,57	47,39	29,66	8,23	10,37	0,78
Pu2100	0,61	62,89	30,46	2,54	3,05	0,45

Table 36 : Composition of the considered isotopic vectors for plutonium

A quick breakdown of the results of this study will be given here. The core used for this approach was the reference oxide core used in the previous description. A comparison the impact of the addition of up to 5 at% of the various fissile nuclei considered above on the core parameters was completed using an RZ model of the core.

The addition of fissile material to the blankets has two impacts. The combination of the two effects is shown below in Figure 68, which shows the evolution of the Americium consumption with regards to the fissile content added in the blankets. Firstly, the increase in the flux level in the blankets increases the consumption in this region of the core. Secondly, it decreases the production of minor actinides from the core itself due to power redistribution towards the outer part of the core and the blankets in which minor actinides consumption takes place. This effect is however rather limited with a maximal value around 3 % here for a case where 5% ^{239}Pu is used.

It can be observed in Figure 68 that the addition of 5 % of pure ^{239}Pu in the blanket assemblies, leads to a twofold increase the total specific consumption. This comes from the very good quality of this isotope as a fissile element. Using either ^{235}U or Pu2100 yield slightly lower results, with a 73 % increase in the total consumption. These two elements yields similar results, with the difference with ^{239}Pu explained either by the lower fission cross section of ^{235}U in a fast spectrum or the lower quality of the plutonium isotopic vector considered. Finally, it can be observed that Pu2035 case exhibits the lowest increase of the four materials compared, but still leads to a 55 % increase in the total specific consumption. This is explained by the lower quality of this plutonium isotopic vector, which leads to a smaller increase in the flux level and to a small amount to the production of minor actinides from the plutonium itself.

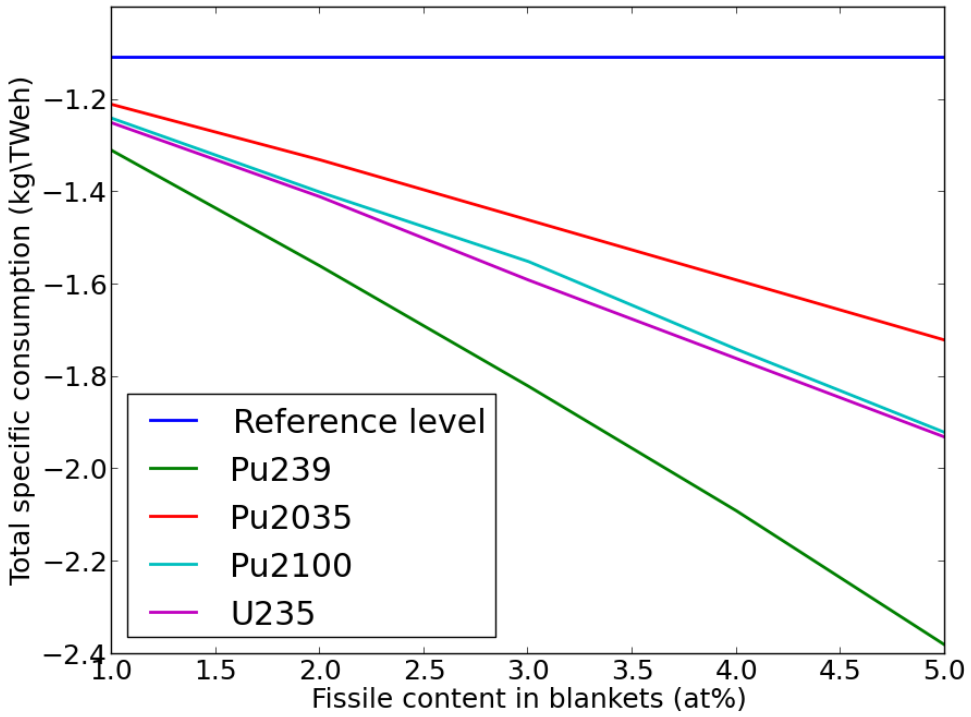

Figure 68 : Specific consumption of minor actinides in blankets vs content in fissile material for various fissile materials

The impact on plutonium inventory in the core and the blankets was also assessed and it was observed that the initial inventory in the core slightly decreases due to the higher fissile content in the blankets. The additional Pu mass required at loading here is at most 546 kg in the Pu 2035 case, or around 5% of the total core Pu content in the core. A similar impact is found at

EOL (End Of Life). In the ^{235}U case, 624 kg of additional ^{235}U is required at the beginning of irradiation. However, due to the lower breeding gain in the cases where plutonium is loaded in the blankets, the final increase in the plutonium core inventory is closer to 2.5 %. Overall, the increase in plutonium content is around one ton per blanket irradiation period.

Considering fuel cycle impacts, the required cooling time to reach 7.5 kW is plotted in Figure 69 with regards to the fraction of fissile material loaded. It can be observed that adding fissile material in the blankets increases the cooling time by up to 2.5 years when 5% of fissile is added. This increase can be divided by two contributions, the main one being from the increase in transmutation performances and thus production of heat emitting isotopes such as ^{244}Cm. The second contribution is directly due to the isotopes of plutonium added in the blankets and increase with the fissile content. This contribution can be easily evaluated by comparing the cooling time for the ^{235}U and Pu2100 cases, which have the same transmutation performances but a different cooling time. The difference can be attributed to the contribution of plutonium isotopes remaining in the blankets at the end of irradiation. An interesting point to note here is that the cooling time associated with Pu2035 is as long as the one required for pure ^{239}Pu, even if the performances are much lower. This is explained by the increased production of ^{244}Cm due to successive captures on ^{242}Pu and then ^{243}Am in the Pu 2035 case. This phenomenon is less obvious for the Pu2100 case as the ^{242}Pu fraction is lower. Neutron source of the irradiated blankets increases to a very limited extent due to the competition between spectrum hardening and fluence increase.

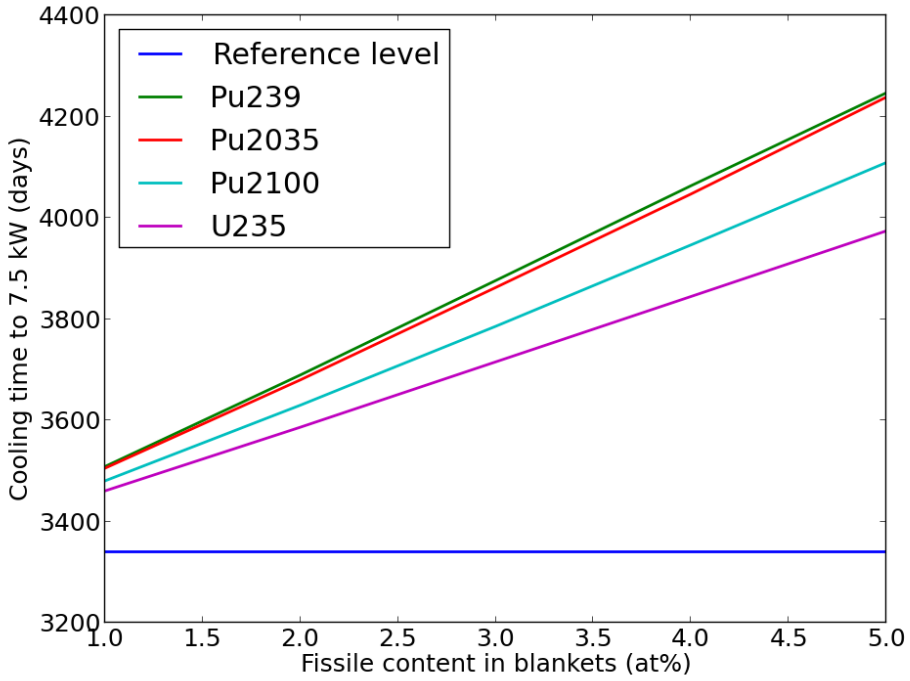

Figure 69 : Cooling time to reach 7.5 kW per assembly vs fissile content in the MABB

The impact on core feedback coefficients was assessed by evaluating core Doppler and sodium void worth coefficient at the end of one representative core cycle and at the end of the blankets irradiation time. Core power distribution at the end of the blankets irradiation time was also studied and it was verified that no power inversion took place between the inner and outer core

during irradiation. The ratio of power production in each zone of the core during irradiation was computed and it was checked that blankets did not generate more than 10 % of the core total production. Addition of fissile material in the blankets also leads to a flux and power redistribution which tends to a power decrease at the core center.

The maximal variation of sodium void worth was estimated as +0.05 $ and the total Doppler Effect (core + blankets) was not modified by the addition of fissile material in the blankets. This result is consistent with the low power level in the blankets and their position at the core periphery. It was observed that the addition of fissile material in the blankets leads to a small power redistribution towards the outer part of the core. However, the power in the peak assembly is not affected by this redistribution. The higher the amount and quality of fissile material loaded, the higher the redistributed fraction of the power is. Nevertheless, for the cases studied here, this fraction of redistributed power remains below 8 %.

3D calculations were carried out for cases loaded with 5 % of fissile material. Using 2D-RZ calculations, an assessment of the helium and gaseous fission products was done. It was verified that the reference design described corresponding to a V2B assembly could be used for each calculation. Each case was evaluated with regards to the relative and absolute power variations during irradiation. In order to limit constraint on the upper part of the core structures and to smooth the temperature distribution in the upper sodium, it is necessary to limit the increase in power in order not to over cool the targets assemblies at the beginning of irradiation. The linear heat rate in the blankets was always below 200 W/cm.

The same values were given for comparison for the “hottest” and “coldest” assembly in the reference core. Depending on their positions in the core, target assemblies can be placed next to 1, 2 or 3 fuel assemblies and consequently exhibit important variations in power produced. As it is shown in Figure 70 for a third of core, one of each case was considered at each step.

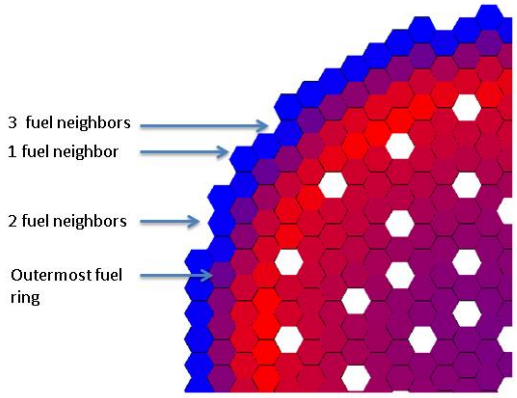

Figure 70 : Position of the various MABB assemblies considered

Table 37 : Comparison of the power variations during irradiation for various fissile in 5 at% amount in the MABB

		Reference value	^{239}Pu	Pu2035	Pu2100	^{235}U
1 fuel neighbor	Power BOL (MW)	0,36	1,33	0,94	0,99	1,24
	Power EOL (MW)	0,94	2,26	1,74	1,84	1,99
	Flow BOL (kg/s)	4,95	11,9	9,16	9,69	10,48
	ΔT BOL (K)	57	88	81	81	93
2 fuel neighbors	Power BOL (MW)	0,62	1,91	1,41	1,48	1,79
	Power EOL (MW)	1,57	3,12	2,54	2,66	2,8
	Flow BOL (kg/s)	8,3	16,4	13,4	14	14,7
	ΔT BOL (K)	59	92	83	83	96
3 fuel neighbors	Power BOL (MW)	0,83	2,37	1,79	1,87	2,25
	Power EOL (MW)	2,08	3,88	3,22	3,36	3,49
	Flow BOL (kg/s)	11	20,4	17	17,7	18,4
	ΔT BOL (K)	60	92	83	83	97

Using the classical formula $\dot{m}\, c_p \Delta T = \dot{Q}$, the mass flow required to achieve a 150 K temperature difference at EOL was computed. Considering this mass flow, the ΔT at BOL was computed using the same approach. Considering the design of the SuperPhénix reactor, it can be considered that the temperature difference between two neighboring fuels should be below 50 °C at anytime. As the power produced in the outermost ring of fuel assemblies decreases during irradiation, the mass flow per assembly is adjusted to achieve a ΔT of 150 K at BOL. As a consequence, it can be seen that this criterion is not fulfilled for any of the cases above mentioned. The corresponding results are shown in Table 37.

It also appears from this analysis that ^{235}U is the best fissile isotope to limit the power variation in the blankets assemblies. The power variation observed in the reference case corresponds to the contribution of plutonium produced during the transmutation process and bred. Adding ^{235}U increases the initial power without adding initial plutonium. This means that part of the plutonium production will compensate for the consumption of ^{235}U, thus limiting the power increase. On the other hand, for the cases where plutonium is used, the power variation is explained by an important production of ^{238}Pu and ^{239}Pu which comes on top of the initial amount loaded. It is higher for the Pu2100 and 2035 cases as the initial amount of ^{239}Pu is comparatively lower.

It appears from this analysis that in order to limit the power variation in the blankets assembly, ^{235}U is the best fissile element, and that only 5.5 % are necessary to fulfill the constraint that the difference of temperature between two neighboring assemblies should be below 50 K.

A short comparison can finally be done to compare the addition of 5 % of fissile material (here, ^{239}Pu) with the addition of moderating material. Two have been selected here: MgO, which is readily available and usable for sodium cooled reactors, and ZrH_2, which use may be more of an

issue due to possible dissociation in case of accidental transients. 5 vol% of fuel in the assembly were replaced by the same amount of moderating material here. As it can be seen below in Table 38, MgO is not efficient enough as moderating material to compensate for the decrease in loaded fuel volume fraction. Consequently, its use will not be further considered here. On the other hand, with ZrH_2, it can be seen that the total Am consumption is close to the one of the fissile-loaded case. However, it can also be seen that the curium production in the blankets and in the core is 12 % higher than the reference configuration, which will have negative impacts on the cooling time and neutron source.

Indeed, the cooling time necessary to reach 7.5 kW per average sub-assembly for the ZrH_2 moderated case is close to 6300 days; which is more than 5 years longer than the case with fissile material, for a similar specific consumption of americium. This is explained by the degraded spectrum in the moderated blankets which leads to a higher capture rate on americium isotopes.

Table 38 : Comparison of the performances of two moderated cases with 5 vol% of moderator and one with 5 at% of 239Pu. Consumptions are expressed in kg/TWhe.

		5 at% ^{239}Pu	5 vol% MgO	5 vol% ZrH_2
Core	Np	0,54	0,55	0,54
	Am	2,66	2,72	2,76
	Cm	0,69	0,74	0,73
Total Core		3,89	4,01	4,03
Blankets	Np	0,14	0,13	0,1
	Am	-7,91	-6,11	-8,01
	Cm	**1,5**	1,24	**1,72**
Total	Np	0,68	0,68	0,64
	Am	-5,25	-3,39	-5,25
	Cm	2,19	1,98	2,45
Total		-2,38	-0,73	-2,16

In terms of inventory, as it is shown in Table 39, the final inventories in plutonium are similar while the moderated case exhibits a lower total americium mass due to the lower initial mass in the blankets. Overall, the two cases are similar as the increase in the cooling time for the moderated case is compensated by the decrease in the loaded mass. Overall, it appears that the addition of 5 at% Pu 239 is similar to the addition of 5 vol% of ZrH_2 in terms of minor actinides consumption, and that the higher fuel cycle impacts of the moderated cases are counterbalanced by the lower loaded mass and thus inventory.

Table 39 : Comparison of the inventories at BOL and EOL for the moderated and fissile loaded cases

	^{239}Pu		ZrH_2	
kg	BOL	EOL	BOL	EOL
Pu core	11786	11831	12037	12127
Pu blankets	631	1557	0	1256
Am core	93	331	94	344
Am blankets	2413	1277	2100	957
Total Pu	12418	13389	12037	13383
Total Am	2506	1608	2194	1301

It is also possible to compare the approach using ZrH_2 with the fissile-loaded approach at equal performances. The reference taken is the consumption of americium in regular blankets which is equal to -6.61 kg/TWhe. The results are shown below in Table 40. The inventory was estimated using the standard formula given in Chapter 3.

Table 40: Comparison of the moderated and fissile loaded cases at similar performances

kg/TWhe	Reference value		5 at% 239Pu	5 vol% ZrH_2
Blankets	Np	0,15	0,12	0,10
	Am	-6,61	-6,61	-6,61
	Cm	1,34	1,26	1,39
Cooling time to 7,5 kW (days)		3339	2193	3907
Am at BOL (kg)		2507	2060	1984
Am at EOL (kg)		1800	1351	1293
Estimated fuel cycle inventory (kg)		4995	3528	4228

It can be observed in Table 40 that, at equal consumption, the cooling time associated with the fissile-loaded approach is reduced due to the faster spectrum and the lower curium production compared to a moderated approach. As the initial loaded mass and consumption are very close, the final inventory in the fuel cycle is lower in the fissile loaded case as the irradiated targets are less active. It can be concluded from this that, for the performances considered, using pure fissile material is a better option in terms of fuel cycle impacts than using moderated material. It is likely that the difference in performances is much less when degraded fissile such as Pu2035 or 2100 is used. However, it has been shown that the two approaches were equally similar in terms of performances increase compared to the basic approach (unmoderated and without fissile material)

An interesting way to visualize the various impacts of the addition of fissile material in the minor actinides bearing blankets is to use radar plots. This is done in Figure 71 where five estimators have been selected:

- Transmutation performances, which are expressed compared to the reference case
- Neutron source after 5 years of cooling, which is a measure of the shielding required for handling the assembly
- Cooling time compared to a regular assembly
- Americium inventory in the reactor (core + blankets) at the end of irradiation
- Temperature difference with the neighboring assemblies

This visualization allows to compare effectively the various approaches and to observe the opposition between the fissile-loaded approach and the moderated approach. The former increases the transmutation performances without modifying the assembly design while only slightly impacting the neutron source and decay heat. The latter increases the transmutation performances while strongly increasing the decay heat and neutron source, but compensate this by a lower inventory in the blankets and thus during cooling. It also to compare the various fissile materials available for such approach, and notably to verify that no material is the best for all the considered parameters.

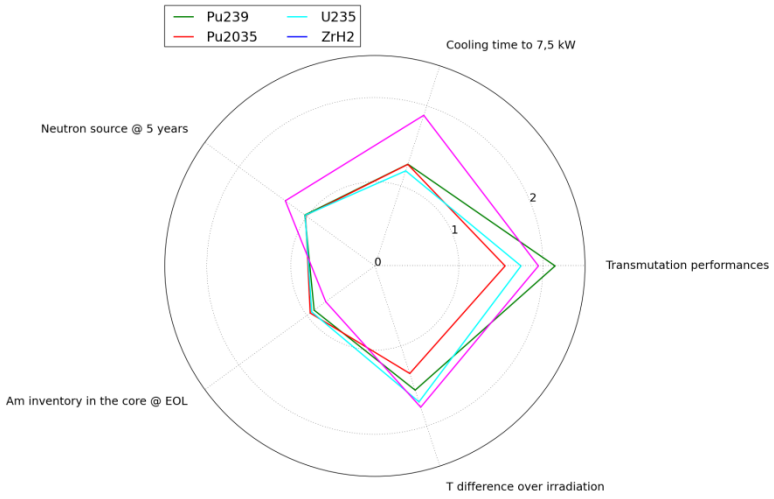

Figure 71 : Radar plot showing the various impacts of the fissile material studied here.

This short study exhibit one of the interests of the methodology developed here: it was observed that a possible optimization path could be an increase in the flux level and the prospect was analyzed using a specific example. It was shown that adding 5 at% of ^{239}Pu in the blanket fuel was relatively similar as adding 5 vol% of hydrogenated material in the blanket assembly in terms of performance increase. Considering the inherent difficulties of handling and loading inside the core each of this material, neither can be directly selected as a “perfect” candidate.

d) IDENTIFICATION OF LIMITING CONSTRAINTS

It is possible to use the tools developed here to evaluate the various constraints relatively to each other and thus establish a “hierarchy” in the constraints. This can be done and viewed in a simple manner by taking a constant r-factor, here 0.05 for instance and a given core, here the oxide core SFR V2B, and then exploring all the americium loading possibilities, and for each

case, looking at the first constraint reached. This will of course depend on the constraints considered here.

An example is shown below in Figure 72. This figure plots the evolution of the mass loaded and consumed in the corresponding optimal assembly depending on the constraints. The blue part of the line corresponds to the feasible cases, while the red zones correspond to assembly not respecting the expected constraints. The black part corresponds to physically not feasible assemblies.

In the first case (upper left figure), even with relatively light fuel cycle constraints after 4100 days of cooling (≈ 11 years or one complete irradiation cycle of a MABB), it can be observed that the fuel cycle constraints linked to neutron source and decay heat are the first limitations to be reached. The neutron source limit considered here of 5e9 n/s/assembly corresponds to four times the neutron source of a spent fuel assembly. This highlights the fact that efficient neutron shielding of the fuel cycles facilities will be necessary for successful fuel cycle implementation. If these constraints are removed, for instance by technological developments related to the fuel cycle back end, it can be observed (upper right figure) that the consumption per assembly can be doubled without modifying the assembly design.

The third constraint which appears in the lower left figure is linked to the manufacturing of the fuel pellets: it was considered here that a maximal Am content of 20 % was allowed during fabrication of the pellets. This constraint can be understood from a radioprotection point of view, as if we consider a standard powder fabrication scheme, the specific activity of the initial powder ($U_xAm_{1-x}O_2$) will depend on the americium content in the compound. There is thus an incentive to minimize the americium content in the fuel. However, due to the high helium emission in the targets, it is necessary to use smaller pins at high americium content, which reduces the fuel volume fraction in the assembly. Consequently, to keep the americium concentration in the assembly constant, it is necessary to increase the americium content in the ($U_xAm_{1-x}O_2$) compound. These effects of this limitation were also shown on Figure 60.

Finally, in the lower right figure, the set r-factor was lowered at 0.03. This corresponds to a strong slowing down of the neutrons in the blankets, which can only be achieved using high content in moderating material. Consequently, the physically acceptable space is smaller due to limitations in the amount ZrH_2 that can be loaded in the blankets. In this case, the americium content is no longer constraining.

One of the main information which can be extracted from this analysis is that the assembly design constraint is a secondary constraint compared to the fuel cycle ones, which means that the pin bundle technology currently in use for fast reactors fuels can also be used for transmutation targets up to high transmutation performances and that the main focus of research activities should be put on fuel cycle related activities which are the main limiting factors here. A more detailed analysis of the hierarchy of these constraints will be done in part 3 where the methodology described here will be applied to industrial scenarios with constraints based on current technological feasibility hypothesis.

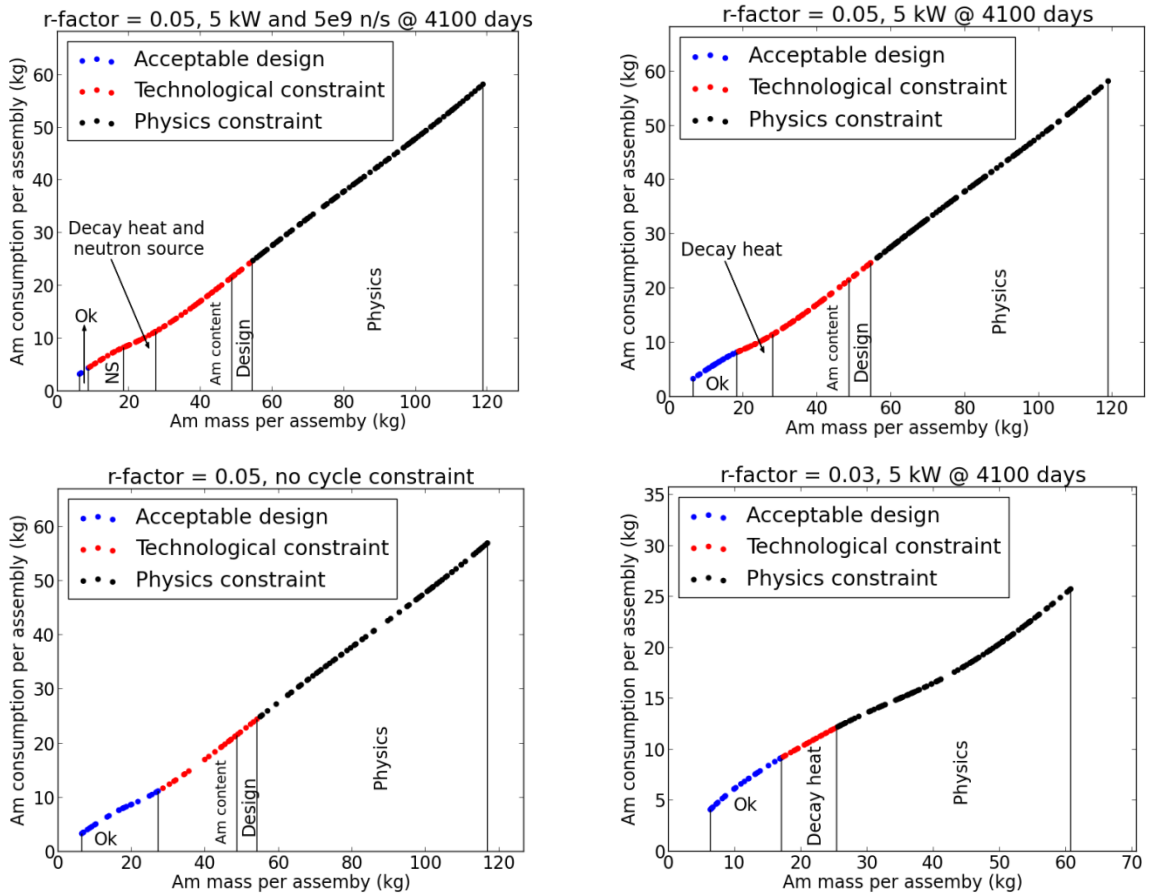

Figure 72 : Am consumption versus loaded mass with various limiting factors indicated. The title of each figure corresponds to the set r factor considered and the maximal decay heat and neutron source at the end of cooling (4000 days here, or one cycle). NS means neutron source.

e) UNCERTAINTY ANALYSIS OF THE META-MODEL APPROACH

The uncertainties on the inventory and consumption can be linked to two main sources:

- The uncertainties on nuclear data, which will be discussed in the next chapter
- The uncertainties on the ANN outputs as shown in Table 28

It is possible to propagate the errors on the artificial neural networks to the estimators by using a so-called "brute" force approach, where the input parameters are modified according the uncertainties associated with the ANN and the distribution of output analyzed. In a first time, the decay heat and neutron sources values were changed and the resulting cooling times distribution was fitted with a Gaussian function. The corresponding errors bars can be seen on Figure 73, the two cases V2B and Mod corresponding to the cases detailed in Table 33. It can be seen that the error increases with the cooling time for both neutron source and decay limits, but stabilizes and decreases cooling time longer than 70 years in the neutron source case. Nevertheless, it can be observed that for cooling time lower than 50 years, the error on the cooling time is lower than 2 years, which will be taken as the bounding value of the error on the cooling time.

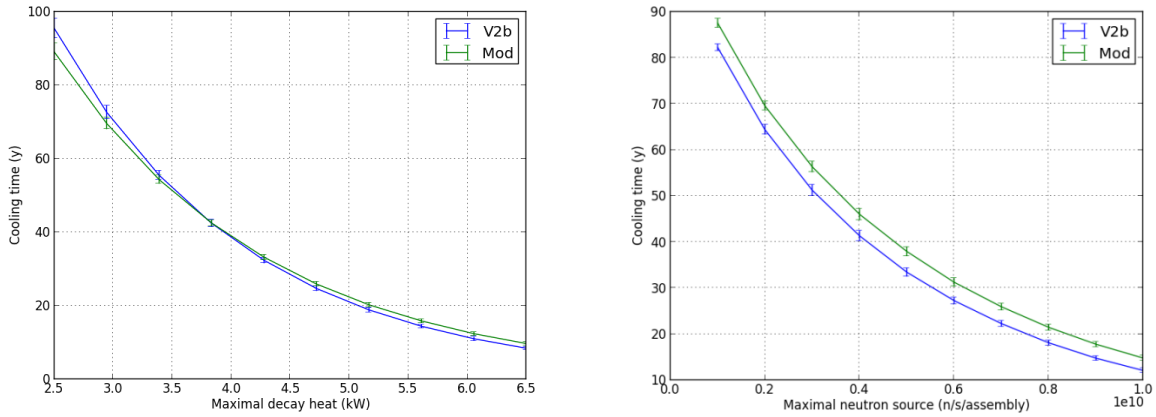

Figure 73 : Evaluation of the errors due to the meta-models approximation on the cooling time for two representative cases based on the V2b assembly design with or without ZrH_2, designed V2b or Mod

The error on the americium mass in the assembly is due to the uncertainties on the actual assembly design. Helium production in the target being the main dimensioning parameter for this design, the error on the ANN was propagated to the assembly mass using the same brute force approach. The actual value of the error depends on the acceptable design constraints due to the discrete nature of the problem. Indeed, if only pin diameter and plenum height are considered as free parameters, a small increase in the helium production may require a decrease in the pin diameter and thus lead to the addition of a new ping ring and changing the fuel volume in a discrete way. On the other hand, if gap and cladding thicknesses can be modified, the fuel volume variation is smoother, as it can be seen below in Figure 74. In this case, the assembly mass is obtained with a 1σ uncertainty of 0.8 kg. This value can be translated into an uncertainty on the Am concentration in the pins of 0.4 %. Considering the wider possible variations of the loaded mass which depend on the set of constraints, this value was raised to 2%.

The optimization process was then carried out using 2 % dispersion around the values corresponding to a V2b core. The dispersions of the inventory and fuel cycle are shown in Figure 75.

A crude approximation of the total uncertainty on the inventory and fuel cycle can then be obtained using Equation 25 and Equation 26, which neglects the correlations between the various uncertainties sources. *T* represents the cooling time, *m* the loaded mass in the assembly and τ the transmutation rate. It is also clear that the value of the uncertainty depends on the constraints set on the optimization process, as the cooling time depends on the limiting value and decay heat. It can be estimated that, all sources taken into account, the uncertainty on the consumption is 3 % and the uncertainty on the inventory is close to 5 % and decreases with the cooling time. This rather simple analysis is consistent with the standard deviation obtained in Figure 75. The main contributor to the uncertainty on the inventory is the high relative uncertainty on the cooling time for short cooling periods. Considering the various approximations used in this methodology and its intended use for scoping studies, these uncertainties estimations are considered acceptable.

$$\frac{\delta I}{I} = \sqrt{\left(\frac{\delta \tau}{\tau}\right)^2 + \left(\frac{\delta m}{m}\right)^2 + \left(\frac{\delta T}{T}\right)^2}$$

Equation 25 : Definition of the uncertainty associated to the inventory

$$\frac{\delta C}{C} = \sqrt{\left(\frac{\delta \tau}{\tau}\right)^2 + \left(\frac{\delta m}{m}\right)^2}$$

Equation 26 : Definition of the uncertainty associated to the consumption

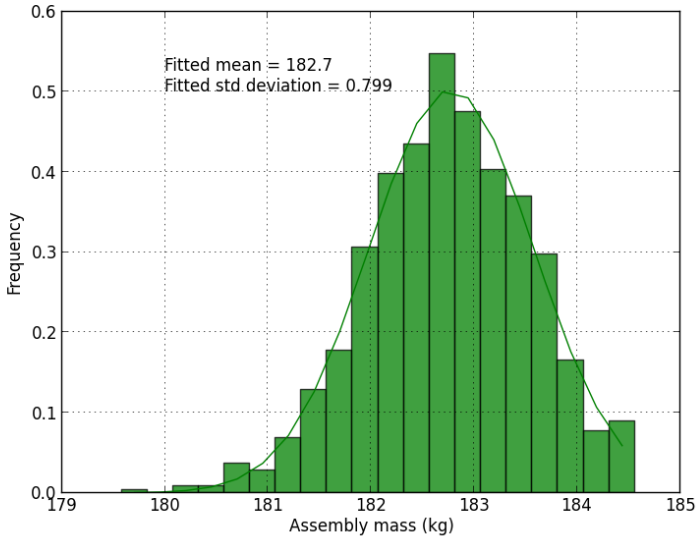

Figure 74 : Dispersion of the assembly mass due to the uncertainties on the helium production

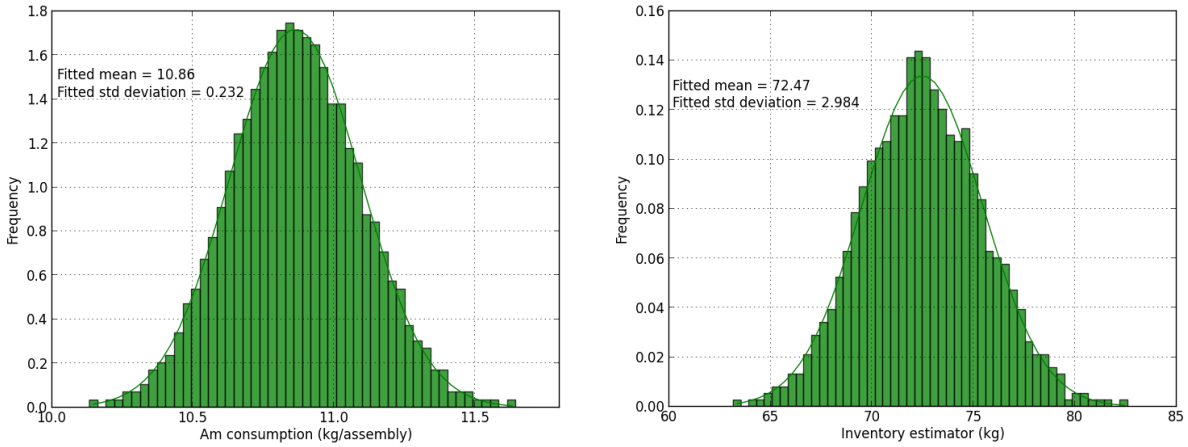

Figure 75 : Dispersion of the Am inventory and consumption per assembly due to the uncertainty on helium production

3) APPLICATIONS TO INDUSTRIAL SCENARIOS

In this part, we will consider only an oxide scenario with a 3600 MWth core. Based on available industrial constraints, the aim of this part is to provide an optimal assembly design for each of the considered constraints, and then to evaluate the one which is the most limiting in order to

highlight potentially interesting research directions. The assembly design was only optimized with regards to the pin diameter, with constant plenum height of 98.9 cm. The maximal Am content in the fuel was set at 20 %, in accordance with the previous studies.

a) MANUFACTURING AND FRESH TARGETS TRANSPORTATION CONSTRAINT

Fuel manufacturing can take place either in gloveboxes or in hot cells. Current MOX fuel for PWRs in France is produced in gloveboxes in the MELOX plant. MOX fuels for the French past reactors in the past have been fabricated at the Plutonium Workshop in Cadarache (ATPu) using gloves boxes, thus demonstrating the feasibility of the manufacturing of pins with high Pu content without hot cells. However, even low americium content in the fuel strongly increases extremities dose rate and overall gamma and neutron emissions, mainly due to (α,n) reaction on oxygen for the latter [72]. If we further consider that curium is likely to be present in very small quantities in the initial americium feed due to the difficulties associated with complete separation of these two elements during reprocessing, dose rates at manufacturing may be unacceptably high and requires the use of a fully automated process in hot cells. Considering the uncertainties existing on the acceptable dose rates during manufacturing, which depends highly on the technological options selected here, this research direction was not further detailed.

Regarding transportation of the fresh fuels, which has to be carried out by road, two industrial limitations can be taken [73] :

- A 550 Watt per assembly with 6 assemblies per transportation cask
- A 800 Watt per assembly with 4 assemblies per transportation cask

For a (75 % ^{241}Am, 25% ^{243}Am) isotopic vector, the specific decay heat production is 87.3 W/kg, with americium generating most of the heat, which means the maximal mass of americium per assembly to be loaded is respectively 6.3 kg or 9.16 kg per assembly.

For such low americium loading, the total inventory in the fuel cycle is not dependent on the neutron spectrum, as it was shown previously in Figure 64. As the constraints on the back end of the fuel cycle are not met, the optimal case for these two applications corresponds to the moderated cases with exactly 6.3 or 9.16 kg of americium in the blankets. The associated performances of each case are given in Table 41. It can be observed that the mass loaded in the assemblies is relatively low, with americium content below 10 %.

Table 41 : Comparison of the performances of the two optimal assemblies with only the constraint on fresh fuel transportation considered

	550 W	800 W
ZrH_2 vol% fraction	4,54	5,24
Assembly mass (kg)	144,5	142,6
Americium mass (kg)	6,3	9,16
Americium consumption (kg/Twhe)	2,78	3,93
Americium production in the core (kg/Twhe)	4,22	4,22
Decay heat after 5 years (kW)	2,29	2,99
Cooling time (y)	5	5
Inventory in the fuel cycle (kg)	10,2	14,9

b) IRRADIATED FUEL HANDLING AND COOLING

Considering the hypothesis taken in this work, especially the fact that a minimum cooling time of 5 years was considered, it is not possible to compute the decay heat of the target assemblies before this time limit. Knowing the decay heat shortly after the end of irradiation may be of interest if systems with passive cooling are used to transfer the irradiated targets from their position in the core to storage under sodium. However, it should be mentioned here than in the reactors Phenix et Superphenix, a sodium revolving drum was used to transfer assemblies under sodium, and thus no constraints on the minimal time for assembly in-core handling existed.

At the end of in-core cooling, it is necessary to drain sodium from the assemblies and then use a chemical process to remove all residual sodium before they can be stored in cooling pools. Two limits can be taken here, which are 2.5 kW and 7.5 kW. If we consider a maximal cooling time of 5 years, which is the time which has been considered in French scenarios studies, it is possible to obtain two other assembly design which are satisfying for these limits.

Table 42 : Comparison of the performances of the two optimal assemblies with only the constraint on sodium washing considered

Maximal cooling time (y)	5	
Maximal decay heat at end of cooling (kW)	2,5	7,5
ZrH_2 vol% fraction	4,75	4,04
Assembly mass (kg)	142,6	116
Americium mass (kg)	7,2	23,4
Americium consumption (kg/Twhe)	3,15	6,87
Americium production in the core (kg/Twhe)	4,22	4,22
Decay heat after 5 years (kW)	2,5	5,53
Cooling time (y)	5	5
Inventory in the fuel cycle (kg)	11,69	38,07

The results of this optimization are given in Table 42. It can be seen that for the 2.5 kW case, the decay heat for sodium washing is the actual limiting parameter. However, for the 7.5 kW case, the decay heat after 5 years is only 5.53 kW, which is below the considered limit. This is explained by the 20 % maximal americium content in the fuel, which prevents further loading of the assembly with americium. Indeed, due to helium production, the fuel volume fraction is limited, in this case at 34 %, and 4.04 % of this fraction are further removed by the addition of ZrH_2. Consequently, only 30 % of the assembly fraction is available for the fuel, which limits the total mass which can be loaded. One important point to be noted here is that it is not possible to reach equilibrium between the production of minor actinides in the core and the consumption in the blankets with the 2.5 kW limit.

c) SPENT FUEL TRANSPORTATION AND REPROCESSING

Regarding transportation, it is here assumed that spent fuel assemblies are transported by rail and not by road, which means that the corresponding constraint is weaker. An extrapolated limit based on current industrial hypothesis will be set at 4 kW per assembly with 6 assemblies

per transport cask. As during transportation, the assemblies are passively cooled and thus sodium-free, it is obvious that if an assembly complies with the 2.5 kW limit exposed previously, it will comply with the transportation limit. For the 7.5 kW, we will arbitrarily consider here that the targets must be reprocessed in a time equal to their irradiation time. With a 4100 EFPD irradiation, five years of in-sodium cooling and two years of manufacturing, this leaves around 4 years in cooling pools before transportation can occur. The constraint taken here will be that the assembly decay heat must be below 4 kW after 9 years of cooling.

Table 43 : Comparison of the performances of the two optimal assemblies with only the constraint on sodium washing considered

Maximal cooling time (y)	5	9
Maximal decay heat at end of cooling (kW)	7,5	4
ZrH_2 vol% fraction	4,04	6,12
Assembly mass (kg)	116	135
Americium mass (kg)	23,4	16,6
Americium consumption (kg/Twhe)	6,87	6,05
Americium production in the core (kg/Twhe)	4,22	4,22
Decay heat after 5 years (kW)	5,53	4,63
Decay heat after 9 years (kW)	4.77	4.00
Cooling time (y)	5	9
Inventory in the fuel cycle (kg)	38,1	32,9

The results for this constraint are given in Table 43. Contrary to the 7.5 kW sodium washing case which is reminded in the table, it can be seen that the transportation constraint is the limiting one here. Compared to the 2.5 kW sodium washing case, equilibrium can be reached with regards to americium production and consumption.

Concerning reprocessing itself, it is not yet possible to give a limiting value in terms of activity of the spent fuel regarding its impact on the process. It is likely that more active fuels will lead to longer process time due to the necessity to limit the activity per batches or solvent radiolysis. However, insufficient data are available to accurate model this, so these considerations were not taken into account.

d) CONCLUSIONS ON THE INDUSTRIAL CONSTRAINTS

Considering the results discussed in the previous parts, it is possible to build a hierarchy of the constraints on heterogeneous transmutation on minor actinides and to represent it on a single figure, as it is done in Figure 76. If we consider that to progress along the x-axis, it is necessary to clear all the constraints encountered, it can be seen that if transportation is carried out in 6 assemblies' casks, this constitutes the first constraint limiting heterogeneous minor actinides. The second one is the cooling limit for washing residual sodium in the assembly, followed by transportation again. The characteristics of the assembly permitting equilibrium between core production and blankets consumption was also plotted on the figure with the details given in Table 44.

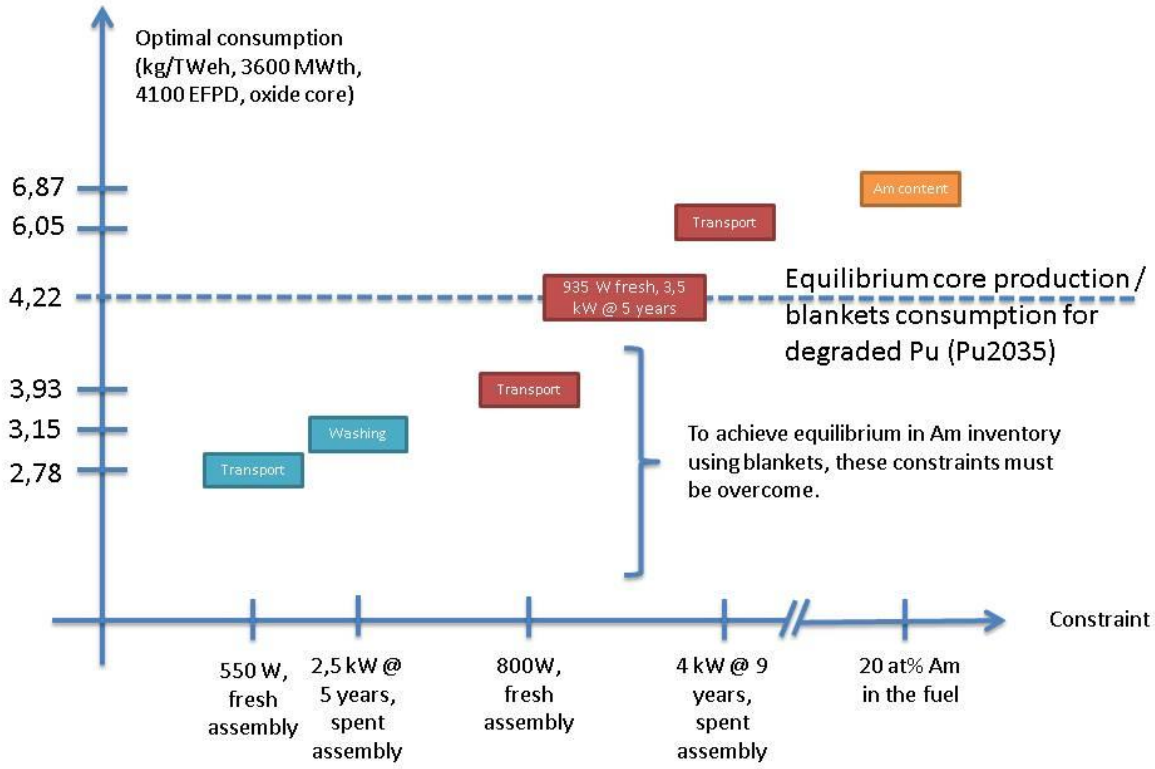

Figure 76 : Hierarchy of the constraints linked to the fuel cycle for one minor actinides bearing blanket

Table 44 : Optimized assembly with regards to inventory and consumption with minimal constraints on the fuel cycle and with prospective constraints

Case	Equilibrium	7,5 kW at 5 years
ZrH_2 vol% fraction	4,31	6,2
Assembly mass (kg)	142,6	127,54
Americium mass (kg)	10,75	25,65
Americium consumption (kg/Twhe)	4,22	7,25
Americium production in the core (kg/Twhe)	4,22	4,22
Fresh assembly heat load (W)	935	2231
Decay heat after 5 years (kW)	3,53	7,43
Cooling time (y)	5	5
Inventory in the fuel cycle (kg)	17,44	41,64

In terms of industrial development of heterogeneous minor actinides transmutation, it can be observed that the main constraints lies not with the design of the assembly itself, but with its transportation and handling, both fresh and irradiated. For the reactor discussed here, it is necessary to raise the fresh assembly transportation limit to 935 W per assembly and the sodium washing limit to 3.5 kW in order to reach equilibrium between core production and blankets consumption. On the other hand, if we consider the current limitations (2.5 kW for

sodium washing), the maximal consumption that can be obtained is 3.15 kg/TWhe, corresponding to the assembly given in Table 42.

It was further observed that due to the Am content and pin pressurization limit, the 7.5 kW limit at 5 years could not be reached. If we postulate such a washing limit and allow higher plenum height (up to 168.9 cm) to accommodate higher Am concentration, we can derive the optimal assembly given the prospective constraints, as shown in Table 44. In this case, the plenum height has been extended close to the limit of 168.9 cm and it is interesting to note here that both the constraint on the Am content and the washing limit are nearly reached here, with an Am content of 20 % and a decay heat after 5 years of 7.43 kW. This assembly is a good illustration of the "best" performances that could be obtained by relatively limited modifications of the fuel cycle and assembly design concepts. In this case, a specific consumption of 7.25 kg/TWhe would be reached in the blankets, or 3.03 kg/TWhe for the entire reactor.

4) CONCLUSIONS ON THE HETEROGENEOUS APPROACH

Several features have been added to the methodology developed in this work, with the main point here being the complete modeling of the assembly. The specificities of minor actinides bearing blankets design were taken into account to obtain a realistic assembly design. This allowed us to generate assembly models for any given case and to evaluate constraints based on fuel cycles parameters evaluated over the entire fuel assembly. The core parameters, mainly its minor actinides production were also evaluated and added to the methodology.

The optimality of the moderated approach with regards to americium consumption and fuel cycle impacts, already highlighted in the previous chapter, was confirmed here even while taking into account the addition of moderating material into the assembly design. However, it was also shown that when the americium core production is taken into account, a metallic approach is more interesting. Indeed, even if the consumption performances of the metallic blankets are lower than the one of the moderated oxide ones, the production of americium in the metallic cores is much lower than in the oxide core. This last point strongly depends on the plutonium isotopic vector considered for the study, and thus would require further detailed analysis coupled with scenarios studies to factor in the fuel isotopic vector at any given time.

An innovative approach the heterogeneous minor actinides transmutation was also presented, with the incorporation of fissile material in the blankets. By increasing the flux level in the blankets while hardening the spectrum, it was shown that this approach yielded similar results as the moderated one for oxide blankets. It was consequently highlighted as potential alternative to the use of hydrogenated moderating material.

Finally, this methodology was used to identify the limiting constraints for transmutation, first in a general approach, and then for a selection of industrial constraints. Given the limiting constraints, the optimal assembly for each case was obtained and a hierarchy of the constraints was given. It was shown that the main constraints related to heterogeneous minor actinides were related to fuel cycle, either transportation of the fresh target of handling of the irradiated ones. Assembly design constraints were secondary in this problem.

CHAPTER 5: THE HOMOGENEOUS APPROACH

Highlights:

- ✓ **Homogeneous loading of minor actinides leads to modification of the core feedback coefficients and thus of the core transient behavior.**
- ✓ **A new core design with geometrical axial heterogeneity is described here and its behavior during three reference transients is detailed.**
- ✓ **The coupling of the methodology developed in the two previous chapters with a transient analysis code is discussed.**
- ✓ **It is shown that minor actinides loading has very limited effects on the core behavior during a loss of flow event, either in the primary or the secondary circuit.**
- ✓ **Reactivity insertion transient behavior is the most affected by minor actinides loading due to the associated decrease in Doppler feedbacks.**
- ✓ **Optimized cores with regards to these parameters are detailed.**
- ✓ **Fuel cycle constraints remain also a limiting factor for homogeneous minor actinides transmutation.**
- ✓ **It is shown that homogeneous transmutation appears as a better solution than heterogeneous transmutation for the set of estimators considered.**

In this chapter, the homogeneous approach of minor actinides transmutation in which the minor actinides are directly mixed with the fuel will be characterized. In a first time, the philosophy of the study and the approach used for core safety analysis will be detailed. It will be shown that considering only the global sodium void worth of the core is not sufficient to conclude on its safety, and the core behavior during three representative transients will be analyzed. The three selected transients correspond to a loss of flow in the primary circuit or the secondary circuit, and a reactivity insertion due to an inadvertent rod withdrawal.

Then, the methodology associated with the optimization will be described, along with the approximations performed to achieve an acceptable calculation time. An optimization process similar to the one used in Chapter 3 will be applied to the various core parameters and objectives, with a focus on each of the three transients. Finally, an uncertainty analysis of the methodology designed in this work will be carried out with regards to the tools, nuclear data and approximations used.

1) PHILOSOPHY OF THE STUDY AND CORE DESIGN PARAMETERS

Complete core design is a complex exercise which requires input from various physics and engineering fields ranging from neutron science, thermal hydraulics, mechanics and economics. Such process can take several years and implies hundreds of people. Considering this and the uncertainties associated with the effective constraints and objectives for a given core, the scope of this study was narrowed at answering the question: "what are the impacts of homogeneous minor actinides loading in a fast reactor and which solutions are the best candidates to improve core response to minor actinides loading?" rather than obtaining a complete core design suitable for transmutation purpose.

The general objective is thus, in this section to start from a design of a core without minor actinides and to state that that core has a sufficiently robust safety review which could act as a reference. Hence, any addition of minor actinides in the core will lead to changes in the core behavior during transients and subsequent core modifications should be implemented, if necessary, so as to recover from penalties introduced by minor actinides loading..

Indeed, various studies related to minor actinides loading in an industrial core have been performed such as [74] or [75] in which the decrease in safety margins due to modification of the feedback coefficients was computed and it was proposed to lower core power in order to recover the lost margins. The general idea of the approach developed here is to start from a non-optimized core and obtain general data on the constraints associated with minor actinides loading, both on the core itself and on the associated fuel cycle and to highlight potentially interesting design options for minor actinides transmutation.

In opposition to what was mentioned in the previous chapter, in which the information required on the actual reactor core was limited to the flux level in the blankets region and the core production of minor actinides itself, it is necessary here to add significantly more parameters to describe the core in its entirety with a sufficient level of details. Considering the new developments in core design with geometrical axial heterogeneities to enhance sodium thermal dilatation feedback and thus improve core behavior during transients [54], several design features were also considered here in addition of assembly parameters.

Heterogeneous cores such as the one described in [54] are designed to achieve a near zero or even negative sodium void worth at the end of cycle by increasing the neutron leakage term during loss of coolant accidents. These features can be seen on Figure 77. A sodium plenum was added in order to increase neutron leakage in the upper part of the core. In case of voiding, this part of the core will be voided first and thus significantly increase axial neutron leakage. This effect is reinforced by the use of an upper absorbing neutron shielding which prevents neutron from backscattering into the core in voided conditions. During normal operations, the sodium plenum zone acts as a neutron reflector.

Axial neutron leakage is also enhanced by the addition of an inner fertile zone which increases the flux level in the upper part of the core and thus the importance of the neutrons in this region. During voiding, this importance decreases sharply thus contributing negatively to the reactivity. Finally, the outer core part was designed slightly taller than the inner core, which increases the core interface with the sodium plenum without increasing core radius. All these effects were taken into account during the core design phase in this work. The following parameters were considered here:

- Core power
- Core radius
- Fuel volume fraction in the assembly
- Sodium volume fraction in the assembly
- Moderator volume fraction in the assembly
- Americium content in the fuel
- Outer core height
- Inner core height (expressed as a fraction of outer core height)
- Thickness of the inner fertile zone

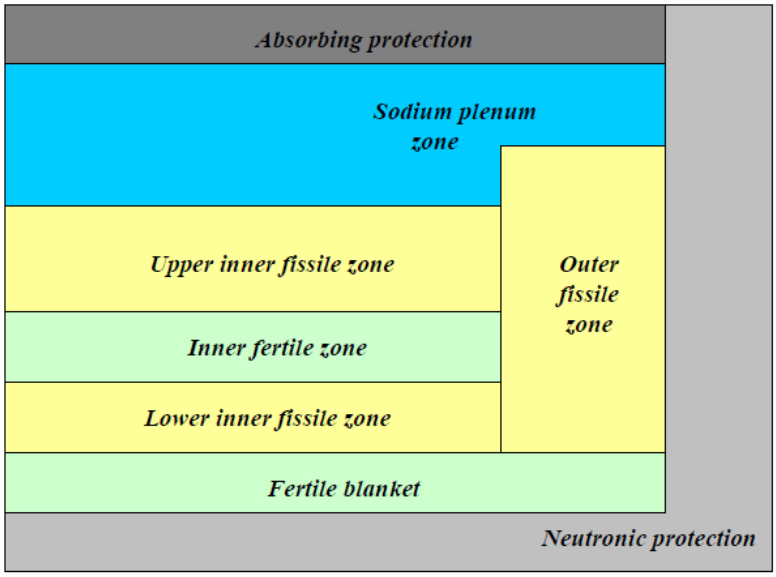

Figure 77 : Core geometry of the CFV design

The number of parameters considered here is relatively small compared to other studies which have been performed using the same approach which can be found for instance in [76]. This was done considering the goal of the study and the available time frame.

a) Approach used for safety aspects

Various approaches can be used to evaluate the "safety" of the cores considered here. For instance, looking at the value of the sodium void worth is a very simplified approach, with cores having the lowest negative sodium void worth being the "safest". However, no clear conclusions can be drawn from this approach which is too simplistic, as it was highlighted in [77]. At the other end of the characterization spectrum, it is also possible to consider full transients calculations of the core based on complete modeling of both the primary and secondary cooling circuits using dedicated codes such as CATHARE or SIMMER. However, this approach requires a high level of details regarding the reactor design and may require excessively long computation time, a feature which is not adapted to optimization calculations.

To carry out this study, it was decided to use an intermediate method based on the MAT4DYN code developed by S. Massara at the beginning of the 2000's [39]. This code is a simplified core dynamics code which couples a point-kinetics model with a hot or average channel thermal hydraulics calculation to simulate flow or reactivity transients. This code was written in

FORTRAN and can perform the evaluation of a given transient in a time frame compatible with a high number of evaluations for multi objective optimization.

Based on the experience accumulated operating French fast reactors [78], the three transients detailed in Chapter 1 were selected here as representative transients. The behavior of a reference core for each of this transient will be detailed below and the parameters which were monitored will be explained.

i) ULOF (UNPROTECTED LOSS OF FLOW)

An Unprotected Loss of Flow (ULOF) can be caused by an abrupt stop of the primary pumps thus leading to a decrease in the primary coolant flow without insertion of the safety rods. The pump coastdown itself is a complex function which depends on the core pressure drop and on the pump characteristic itself. It will not be modelled here and the pump coastdown will be characterized using two values : the time to a reduction of 50 % of the flow and the final flow (which is supposed to be established due to the operation of the pump pony motors or by natural convection).

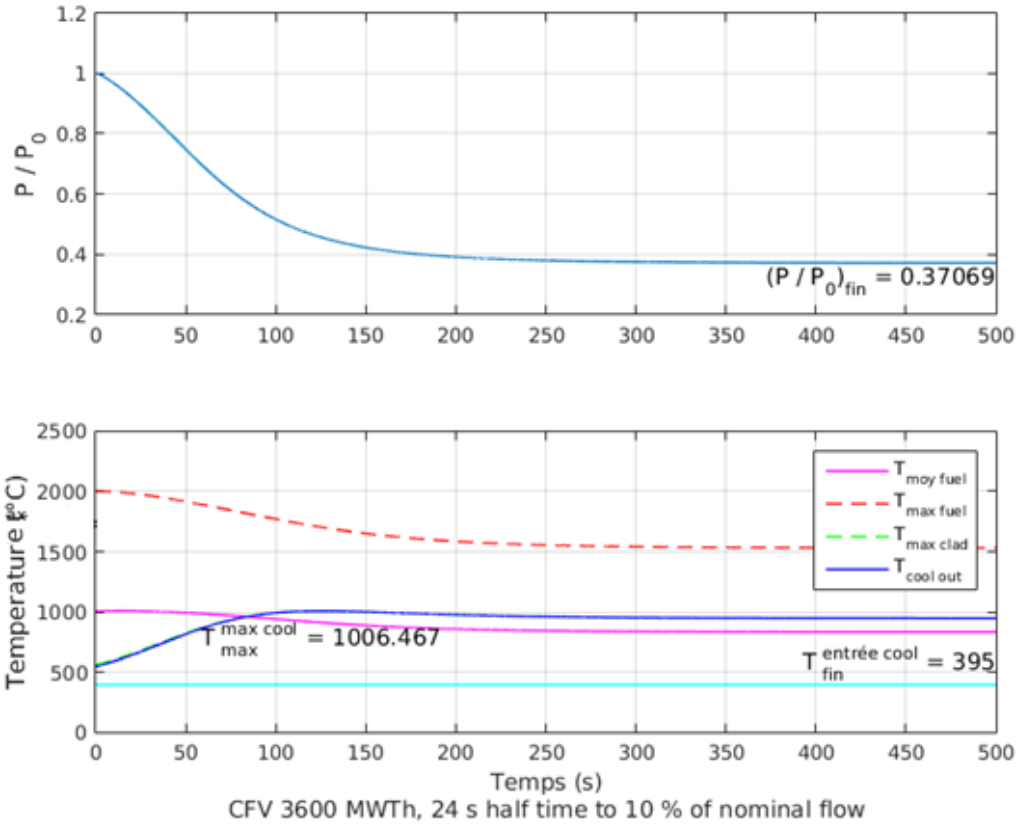

Figure 78 : Evolution of core power and core temperature for an ULOF with a reduction of 90 % of the flow with a half time of 24 s and a 3600 MWth core

The evolution of the various core temperatures is given in Figure 78. Following the pumps trip, the sodium temperature increases up to a maximum due to the lack of exchange with the secondary system, and then stabilizes once the core power has reached an equilibrium value.

The secondary system is assumed to continue operating durig the transient. During such a transient, the main aim is to avoid sodium boiling at the temperature peak, which means keeping at sodium temperature below 883 °C . MAT4DYN is not able of modelling sodium boiling in the core, however it can be reasonably assumed that any boiling situation will worsen the transient outcome.

To investigate natural core behaviour, the reactivity evolution during the transient in the core was plotted in Figure 79. Due to the power decrease, a positive Doppler reactivity is inserted. This is counterbalanced by the negative sodium expansion effect which is favored by the increase in sodium temperature close to the top of the core where this effect is the strongest. Cladding heating by the sodium leads to a positive reactivity insertion. Due to the sodium heating, a differential expansion of the core and the control rods is observed, leading to a negative reactivity insertion. For the transient considered here, it can be observed that the final sodium temperature is above 883 °C, meaning that boiling takes place.

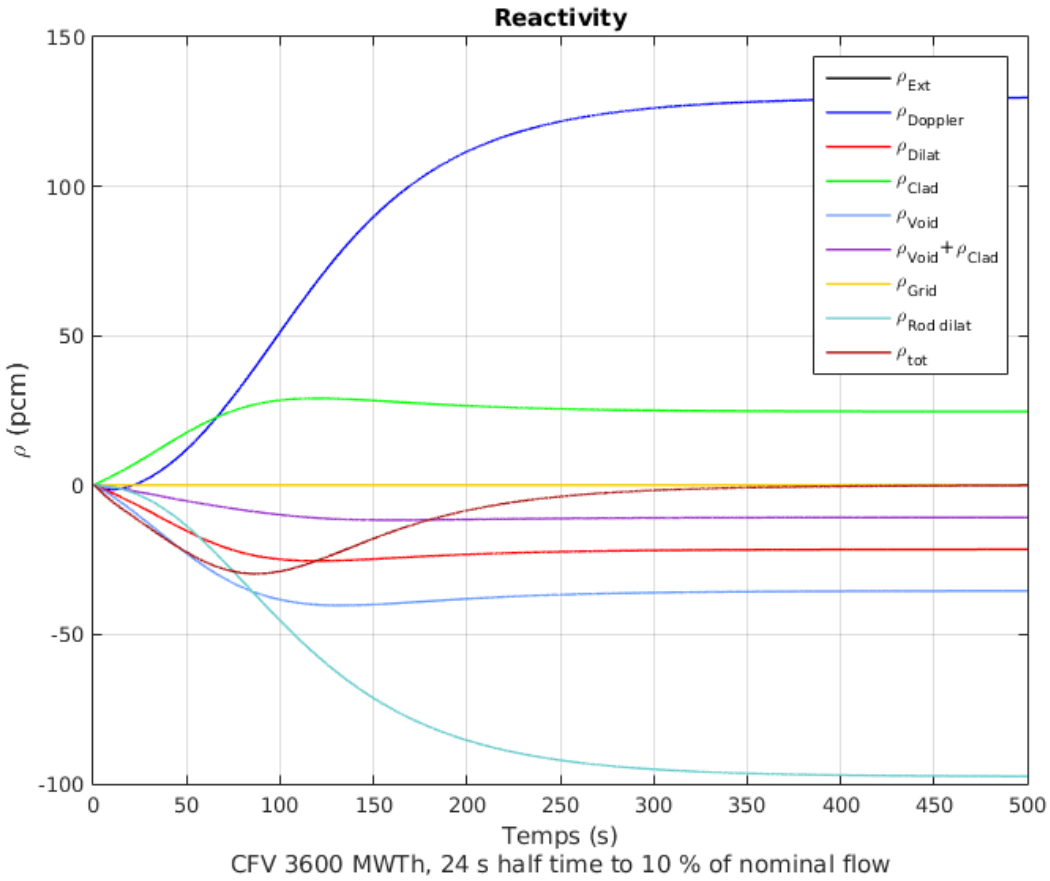

Figure 79 : Evolution of the reactivity in the core during an ULOF with a reduction of 90 % of the flow with a half time of 24 s and a 3600 MWth core

If we use sodium boiling as a limiting criterion, the core used to calculate this transient would not lead to a viable design. As this core is not loaded with minor actinides, it can be observed that the entire problem would be overly constrained by considering this limit. In order to avoid this, it was considered that passive systems such as hydraulically suspended control rods [79] were fitted into the core to insert negative reactivity in the case of a loss of primary flow. If we consider a -400 pcm reactivity insertion when the sodium flow falls below 50 % of the nominal

flow, as it is shown below in Figure 80, the core power falls drastically and sodium boiling is averted. However, due to uncertainties on the actual design and implementation of these passive systems, it was not possible to build a criterion based on sodium boiling while taking into account the use of these systems. Consequently, the maximal sodium temperature during the transient was considered as the estimator of interest to minimize for the study of this transient, even when boiling was reached and the subsequent result is not physical anymore. Indeed, it can be reasonably assumed that if two cases exhibit at 150 °C difference in their peak sodium temperature, this difference will remain if passive systems are used, thus increasing the margin to boiling during the transient.

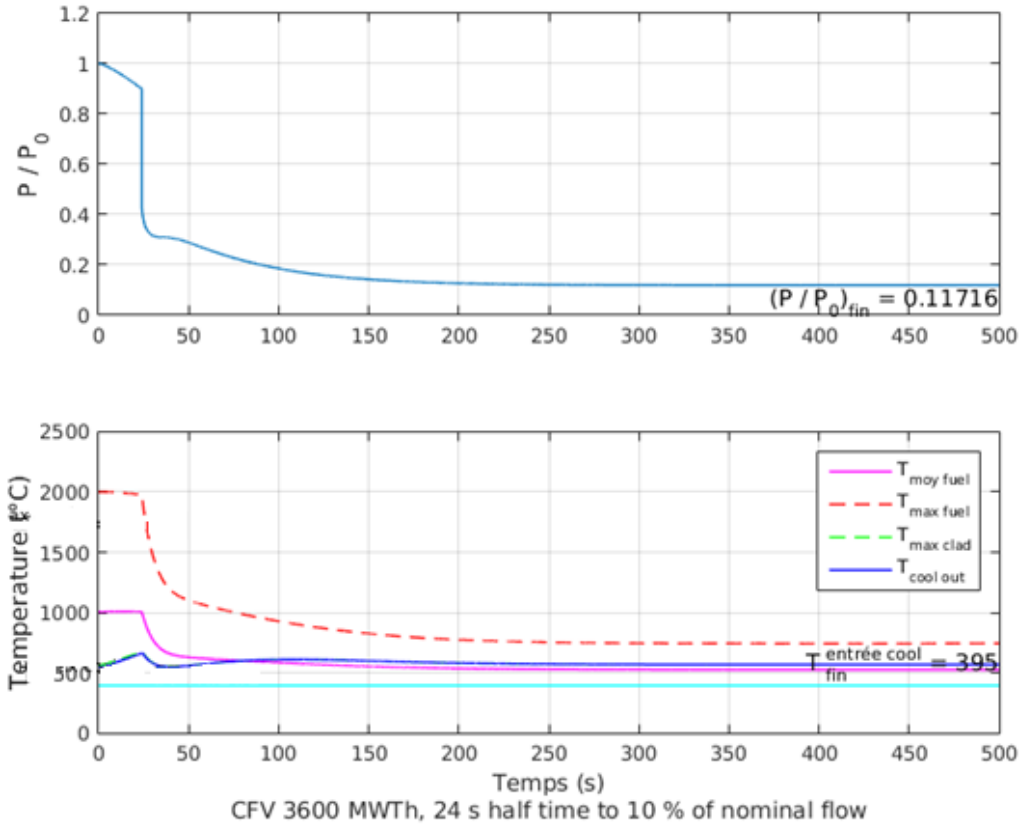

Figure 80 : Evolution of core power and core temperature for an ULOF with a reduction of 90 % of the flow with a half time of 24 s and a 3600 MWth core. An insertion of -400 pcm at 24 s was considered.

ii) ULOHS (Unprotected Loss Of Heat Sink)

During an ULOHS, the secondary pumps fail while the primary pumps continue to operate. Consequently, the sodium inlet temperature increases and the outlet temperature correspondingly increases. The increase in the global core temperature leads to a negative reactivity insertion which leads to the stabilization of the core temperature at the so-called "neutronic shutdown temperature", at which point the nuclear chain reaction stops by itself. The design objective here is to ensure that this temperature remains first below sodium boiling, and secondly, below cladding and structures failure temperature, which will be taken at 700 °C in this study, following recommendations made for the ASTRID project [80].

As it can be seen in Figure 81, the fuel temperature decreases while the sodium inlet temperature increases due to the lack of heat extraction in the secondary circuit. If we look at the evolution of reactivity in Figure 82, it can be observed that the main contributor to negative reactivity is the grid feedback effect. As the sodium inlet temperature increases, the diagrid supporting the core expands thus lowering the reactivity. A positive Doppler insertion can be seen due to the decrease in fuel temperature. Sodium expansion leads to a positive reactivity insertion as the thermal expansion of sodium during an ULOHS is uniform, thus not favoring the upper parts of the core with a negative sodium expansion feedback contrary to the ULOF case.

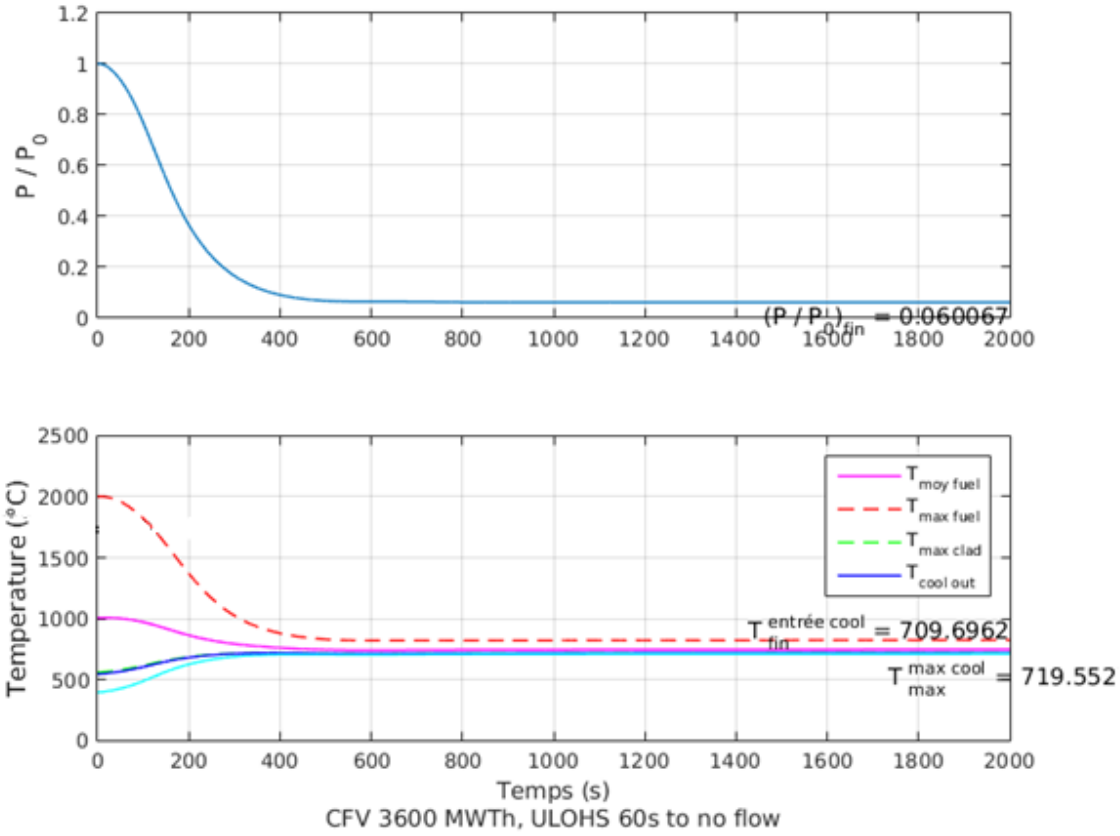

Figure 81 : Evolution of core power and main temperatures during an ULOHS corresponding to a reduction to 0% of the secondary flow within 60 s

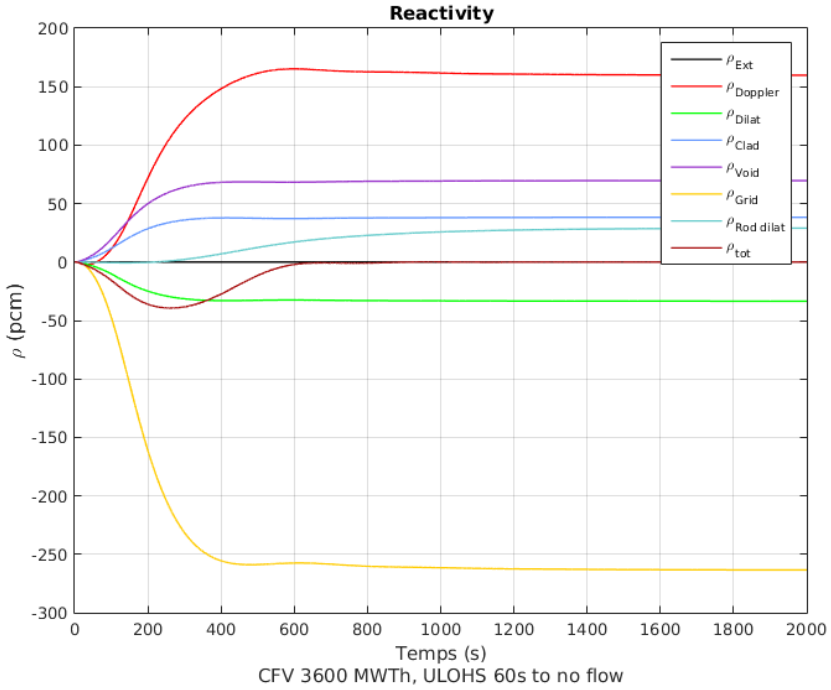

Figure 82 : Evolution of the reactivity during an ULOHS corresponding to a reduction to 0% of the secondary flow within 60 s

iii) UTOP

Unprotected Transients Over Power (TOP) are produced by the sudden insertion of positive reactivity in the core without simultaneous activation of the safety systems. This positive insertion can be explained by various phenomena, such as a hypothetical gas bubble going through the core, an earthquake causing a core compaction or the ejection of a control rod due to the malfunction of its drive mechanism. In this study, we will only consider relatively slow transients corresponding to a rod ejection.

Complete design of the control rods system of the a given core is a task which requires a wide range of information ranging from the reactivity loss to the individual positioning of each control rods and their respective drive mechanisms. This amount of information being not available during this pre design study, a simplified approach was taken. Based on the design of the ASTRID control rod system, the extraction of a given control rod from the entire height of the inner core with an extraction speed of 4 mm/s corresponding to 150 pcm was considered as the reference reactivity insertion here. For a 1m core, this corresponds to a reactivity increase of 0.6 pcm per second within 250 s.

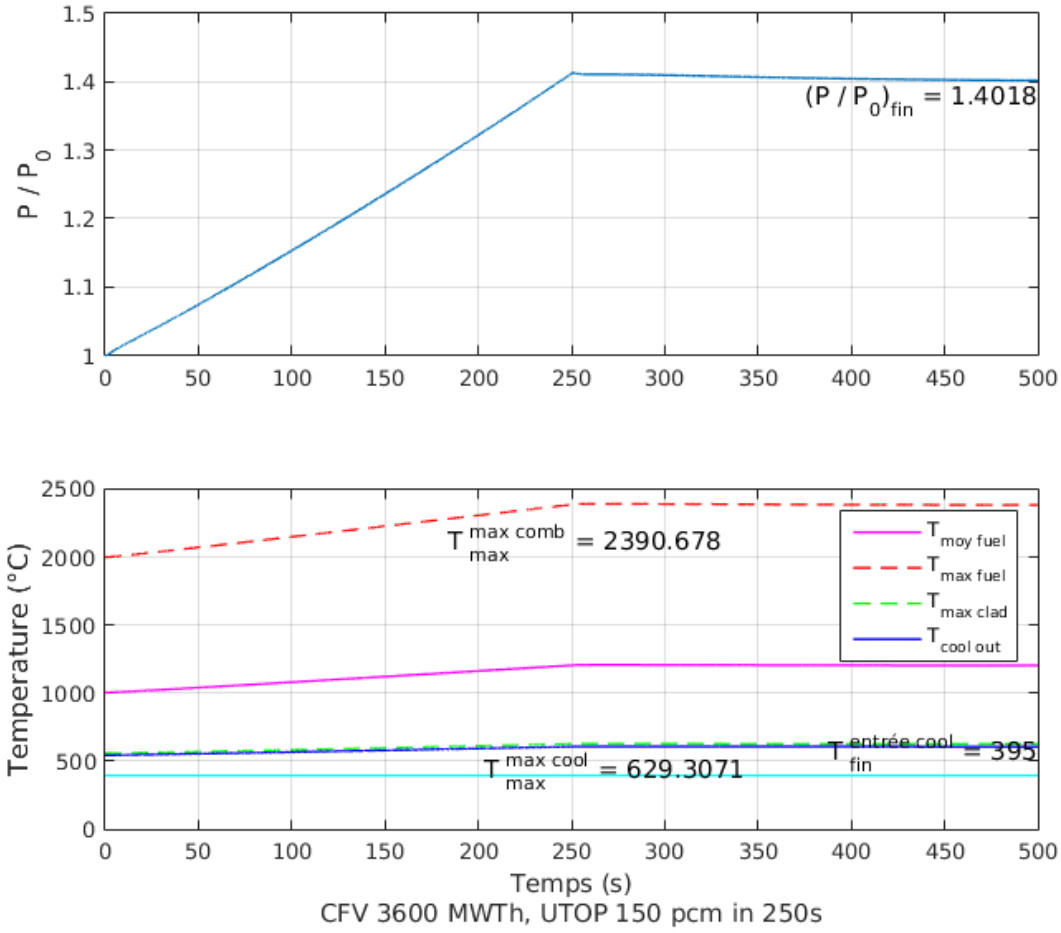

Figure 83 : Evolution of core power and main temperatures during an UTOP corresponding to the insertion of 150 of positive reactivity in 250 s.

During this postulated UTOP, the core power and thus the fuel maximal temperature increases with the reactivity insertion and then stabilizes and start to slowly decrease once the reactivity insertion has ended, as it can be seen in Figure 83. In terms of feedback effects, the Doppler effect is the main feedback limiting the increase in core power here, as shown in Figure 84. Except the control rod differential dilatation which inserts negative reactivity as the rods are inserted by this dilatation (Figure 84), the other feedback effects play a negligible effect on the core behavior during the transient.

The main parameter to be considered during such a transient is the maximal fuel temperature reached, which has to be kept below fuel melting temperature. This temperature depends on the fuel burn-up and design and would have been unpractical to calculate here. Consequently, based on previous studies carried out on fast reactor, a maximal temperature of 2650 °C was considered for the oxide fuel. This value was taken by comparison with the maximal temperature taken for the ASTRID project.

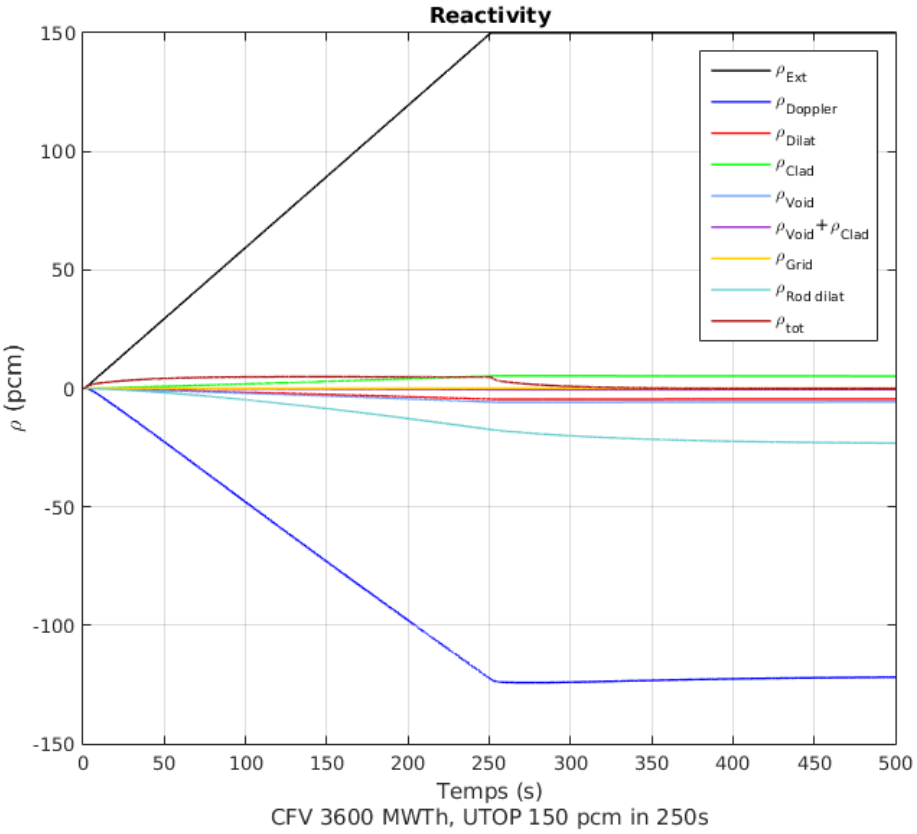

Figure 84 : Evolution of the reactivity during an UTOP corresponding to the insertion of 150 of positive reactivity in 250 s.

It should be noted here that during such a transient, the increase in core reactivity leads to an increase in core power and thus fuel temperature, but also that the local flux map is deformed due to the rod extraction. Due to limitations of the MAT4DYN code system, this local deformation was not taken into account here during the UTOP calculations (point kinetic approach).

iv) INCORPORATION OF MINOR ACTINIDES IN THE CORE

The homogeneous addition of minor actinides in the reactor core leads to various effects on the core feedback coefficients, which will be discussed here. These effects are mainly due to the spectrum hardening already discussed in Chapter 3. A comparison of the spectrum of the same core with 3 wt. % of Am added is shown below in Figure 85. Due to this spectrum hardening, various kinetic parameters are decreased, mainly the effective delayed neutrons fractions, which decreases due to the lower delayed neutron fraction of heavier actinides and due to the important captures of americium isotopes in the epithermal range [81]. The mean lifetime of a neutron generation is also decreased due to the lower delayed neutron fraction.

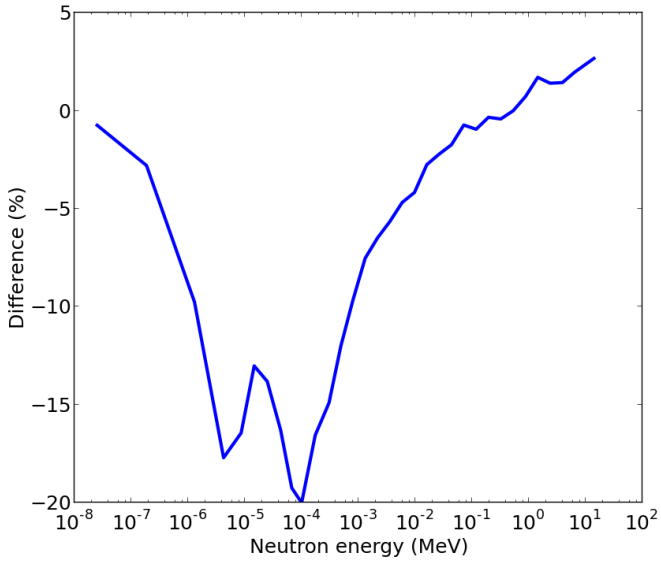

Figure 85 : Spectrum difference between a reference core and a core with 3 % Am (3600 MWth oxide core)

Regarding feedbacks coefficients, the impacts can be decomposed as follows:

- Due to the spectrum hardening, the neutron population in the low energy resonances is lowered when minor actinides are introduced in the core, which in turns decreases the efficiency of the Doppler broadening of these resonances. Consequently, the total Doppler Effect in the core decreases. This effect is reinforced by the decrease in ^{238}U content in the core.
- The sodium thermal expansion feedback increases due to the addition of americium isotopes, which have a lower fission threshold than ^{238}U as it was shown in Chapter 1, which increases the spectrum component of the void effect. In the case of a CFV-like core, this effect is mitigated by the increase in the leakage due to the increase in the neutron mean free path.
- As the cladding and hexagonal wrapper dilatation effect can be interpreted as a decrease of the sodium fraction in the assembly, these two effects are also going to slightly increase.
- The fuel expansion feedback coefficient will slightly decrease due to the harder spectrum.
- Finally, the grid effect is going to decrease due to the increase in neutron mean free path while the fuel dilatation effect will also decrease.

Regarding fuel behavior itself, a decrease in the thermal conductivity and heat capacity of the fuel is going to play a role in the fuel mechanical resistance during any given transient; however limited data is available on these impacts. These phenomena were not considered here but it is likely that they will lead to a decrease in the various temperature margins considered in the event of high loaded fractions (> 5 %). The experience feedback from some in-core experiments leads to think that small fractions of minor actinides may not overly impact fuel behavior (METAPHIX, SUPERFACT).

v) *COMPARISON WITH A HOMOGENEOUS CORE:*

One of the arguments advanced against homogeneous transmutation in the 2012 French report on nuclear waste ([44], page 30) is the negative impact of minor actinides addition to the fuel on the Doppler feedback, sodium void worth and effective delayed neutron fractions (β_{eff}). The studies carried out to compile this report were made using a homogeneous core design, as shown below in Figure 86. The use of the methodology discussed previously showed that the addition of minor actinides in a heterogeneous core led to no significant impacts for flow transients, with only a negative impact for an UTOP. It is then of interest to explain this difference in core behavior. In this part, the effect of minor actinides incorporation in a homogeneous or heterogeneous core design will be discussed.

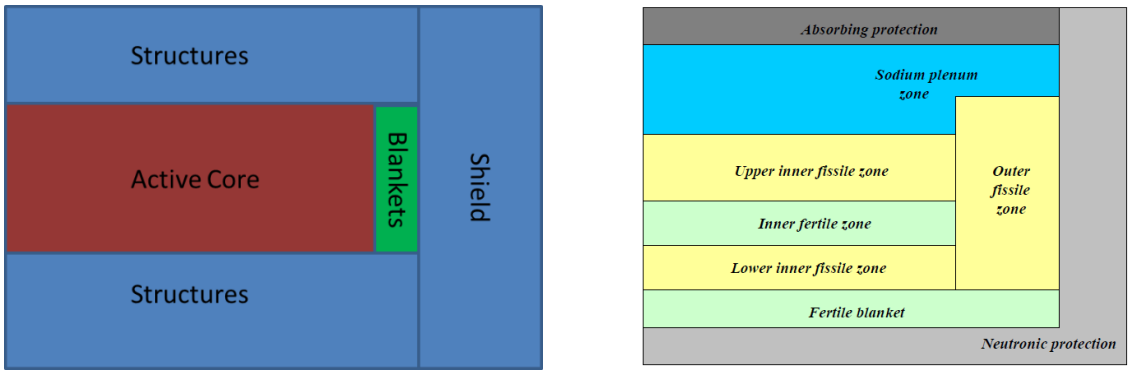

Figure 86: Comparison of the core layout of a homogeneous and heterogeneous core

We will consider here a 3600 MWTh homogeneous core as described here [51] and compare it with the reference core described in Table 52. If we compare the sodium void worth, Doppler feedback and β_{eff} for both cores with or without minor actinides, as it is done in Table 45, we observe a decrease in the three coefficients. However, considering that transient analysis requires more information on the core feedback coefficient that just Doppler and total void worth, it can be concluded that such simplified approach based on these feedback coefficients is not sufficient to evaluate the core behavior when minor actinides are loaded.

Table 45 : Comparison of the main feedback coefficients for a homogeneous and a heterogeneous core

Sodium void worth (pcm)	0 % Am	5 % Am
V2B	1919	2055
CFV	-524	-297

Kd (pcm)	0 % Am	5 % Am
V2B	-767	-561
CFV	-957	-794

β_{eff}	0 % Am	5 % Am
V2B	364	338
CFV	353	333

The core behaviors during the three reference transient used before are shown in Table 46. For the ULOF, the americium loading has a highly negative impact on the homogeneous core

behavior, while it has barely any on the heterogeneous core. For the ULOHS and UTOP, both cores behave similarly: the ULOHS final temperature slightly decreases while the maximal fuel temperature during an UTOP increases. It should be mentioned here that this comparison was done by considering a constant rod worth for the four cases. Due to the spectrum hardening, it is likely that control rods efficiency will be lower when minor actinides content is higher. However, engineering solutions such as a higher enrichment in ^{10}B can be found to keep a constant rod worth.

Table 46 : Comparison of the transient behavior between a homogeneous and heterogeneous core

ULOF max temperature (°C)	0 % Am	5 % Am
V2B	1332	1557
CFV	1027	1026

ULOHS final sodium temperature (°C)	0 % Am	5 % Am
V2B	825	810
CFV	709	703

UTOP max fuel temperature (°C)	0 % Am	5 % Am
V2B	2180	2330
CFV	2390	2446

It is possible to explain the difference in ULOF behavior by comparing the evolution of reactivity during the transient. As it can be seen in Figure 87, for a homogeneous core, the positive sodium thermal expansion feedback leads to a positive reactivity insertion from the start of the transient. This leads to an increase in the fuel temperature and then a negative contribution from the Doppler Effect. Consequently, adding minor actinides will negatively impact both effect, as it will increase the sodium thermal expansion feedback while decreasing the magnitude of the Doppler Effect.

On other hand, for a heterogeneous core as it can be seen in Figure 79, the sodium temperature increases first at the top of the core where the sodium thermal expansion local contribution is negative. This leads to a decrease in core power and a positive reactivity insertion from the Doppler. Adding minor actinides will have a negative impact on the sodium thermal expansion by increasing it, but this will be compensated by the decrease in the Doppler feedback magnitude, which will limit the reactivity inserted due to core power reduction.

Concerning the ULOHS, the two cores behave similarly for the same reason as discussed before: the increase in sodium thermal expansion is compensated by the decrease in fuel expansion feedback, Doppler Effect and grid expansion feedback. Finally, the maximal fuel temperature during an UTOP increases for both cases, but this increase is more limited in the case of the heterogeneous core.

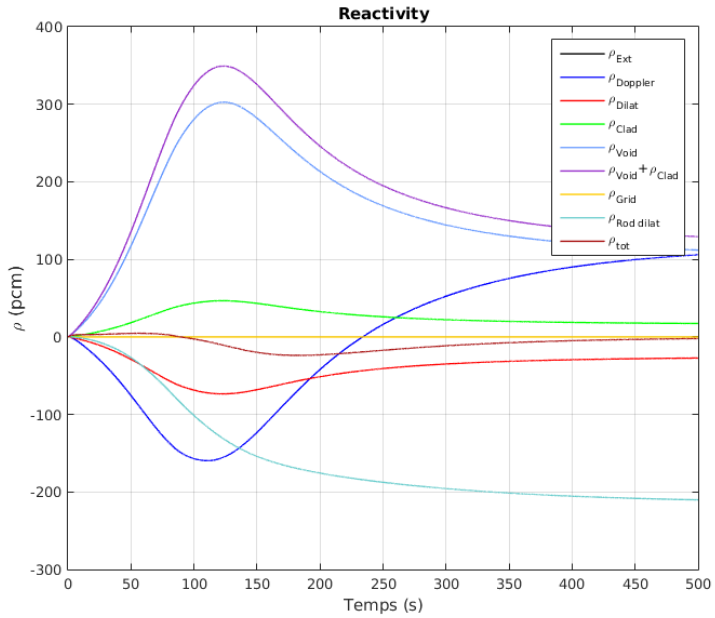

Figure 87 : Evolution of the reactivity during an ULOF ($T_{1/2}$ = 24s, final flow of 10 % of nominal flow) of an homogeneous core loaded with 5 at% of americium

b) METHODOLOGY USED

Following the approach developed in the previous chapters, we will make use of meta-models to limit the calculation time and be able to evaluate a large number of cases in a quick way. First, a test case was generated to train Artificial Neural Networks. This test case was generated using the parameters described in 1) with the following variation ranges:

Table 47 : Variation ranges of the core parameters considered for this study

Parameter	Unit	Min	Max
Core power	MWth	600	3600
Core radius	cm	160	320
Fuel volume fraction in the assembly	Vol%	20	50
Sodium volume fraction in the assembly	Vol%	20	40
Moderator volume fraction in the assembly	Vol%	0	10
Americium content in the fuel	At%	1	10
Outer core height	cm	80	140
Inner core height (expressed as a fraction of outer core height)	/	0.5	1
Thickness of the inner fertile zone	cm	15	25

SN 2D RZ calculations were carried out for each case. It was considered that a 30 cm axial fertile blanket was located below the core. It was verified that the existence of this fertile layer did not significantly modify the core behavior. The height of this blanket can be used in a second design step in order to tune the core breeding gain. Indeed, plutonium self-breeding in a CFV like core is achieved through the addition of these blankets. As minor actinides loading increases the breeding gain in the core, it will be necessary to reduce the blankets height in order to limit the increase in the breeding gain. It was verified that for the minor actinides loading and blanket height considered, it was possible to successfully tune the breeding gain.

Considering the time scales for transmutation deployment, a voluntarist approach was used in which a max burn-up of 200 GWd/t was taken as a reference value for residence time calculations with a 1.5 power peak factor. Burn ups of this magnitude have been reported in the past, with metallic fuels reaching 17.5 at% at EBR II in the seventies and eighties [82] and oxide fuels reaching up to 23 at% at the PHENIX plant using the so-called Quasar fuel pins (small pins with central hole) [83]. Consequently, it was assumed that further technological developments would lead to such achievable burn ups.

An average irradiation scheme was used for these calculations, in which the entire core is irradiated once for the duration of a sub-assembly residence time. This is not representative of what happens in real core management, as fuel assemblies are reloaded by batches during reactor operation. However, completely modeling the fuel reloading scheme would lead to an unacceptable increase in the calculations complexity. Nevertheless, it is necessary to characterize the core at equilibrium that is to say during normal operation. To do so, the assumption that each cycle contributed to the same burn up was made. Consequently, it we consider for instance a *n*-batch management scheme, the state of the average core at the end of an equilibrium cycle (EOC) can be written as shown in Equation 27. The core total burn up can be written as the sum of the burn up of each batch, with b the burn-up corresponding to one batch. For the core calculated with the once through irradiation scheme, the core burn up B at the end of irradiation can be written $B = nb$. Consequently, we obtain the relation between the burn up at the end of an equilibrium cycle and the burn up of the core at the end of a once-through calculation given in Equation 27.

$$BU_{EOC} = \frac{1}{n}(b + 2b + \cdots + (n-2)b + (n-1)b + nb) = \frac{n+1}{2}b = \frac{n+1}{2n}B$$

Equation 27 : Burn-up equivalence formula

In this study, a reference residence time of 400 EFPD was considered, with a maximal number of batches of 8. If the total residence time was higher than 3200 EFPD (which is the case for cores with small power densities), the duration of a batch was calculated for 8 batches. The core main feedback coefficients and power profiles were computed at the end of an equilibrium cycle, along with kinetic parameters such as the delayed neutron fraction and the life time of the neutron population in the core.

For fuel cycle analysis, the specific decay heat and neutron source of the fuel after irradiation were computed using the Darwin code system [38], similarly to what was done for the heterogeneous approach. Helium production was also computed and used for assembly design purposes. Gas production in both axial blankets (lower and middle) was also computed as there is a non-negligible fission gases production in the blankets due to plutonium breeding under irradiation.

Knowing the main assembly geometry parameters (height of the fissile stack, of the fertile layers, volume fraction of fuel and coolant, presence of moderating material), power profiles and the associated helium production at the end of irradiation, it is possible to design an assembly based on the following assumptions :

- The fuel centerline temperature is below 2650 °C, which was taken as the fuel limit in this study.

- The Hoop stress on the cladding is below the cladding resistance, similarly to the heterogeneous approach
- The fuel, coolant and moderator volume fractions are equal to the parameters specified at the beginning of the process. If not, the feedback coefficients are re calculated for the new fraction. Adequate tuning of the volume fractions in the assembly is obtained through slight variation of the hexagonal duct thickness and inter-assembly sodium thickness. The pin diameter, cladding thickness and gap are allowed to variate between the same boundaries as the ones which were used for the heterogeneous approach.

Gas production in the blankets was found to be low enough not to warrant significant modification of the gas plenum. For extreme cases, the expansion plenum height was considered as the adaptation margin. It should be noted here that some design margins exists regarding the lower expansion plenum. As minor actinides loading increases the breeding gain, the lower axial blanket can be shortened thus leaving more room for the lower expansion plenum and limit the pin pressurization. This option was not considered in the optimization methodology.

After establishing the design of the core subassembly based on the previously mentioned assumptions, it was possible to use this design to compute core's response to the three transients mentioned in the previous part. However, several simplifying hypothesis with regards to power and feedback profiles were made.

Indeed, two options were available to compute the core response to the transients. The first one implies selecting a system code such as CATHARE or SAS4, running a large number of calculations and creating metal-models based on the output of the system. Such an approach has been implemented at CEA and can be found in [76] for instance.

In the second approach, which was chosen here due to time constraints and philosophy of the study, artificial neural networks were used to reproduce the output of the ERANOS core calculations which were then fed to the MAT4DYN transient code. Considering the relatively short computation time and ease of use of MAT4DYN, this solution was retained and used in this work. The advantages of this approach is that it allowed more flexibility in the description of the transients, as it will be shown later in this chapter and led to a slightly quicker generation of the learning database.

The description of the power, Doppler and sodium thermal expansion axial profiles was also simplified. An axial power profile from the inner 60 cm of the core was extracted and the average power per region (inner fuel, lower axial blanket, inner axial blanket) was computed. The power profile was then flattened over the assembly height so as to keep the same total power but averaged per medium. However, in the mesh corresponding to the higher fuel temperature (usually slightly above the top of the inner axial blanket), the power was adapted so that the ratio of the maximal power to the average of the fissile part was conserved. This was done to keep the information about the fuel maximum temperature, which is primordial for UTOP behavior. A graphical description of the process done is shown below in Figure 88.

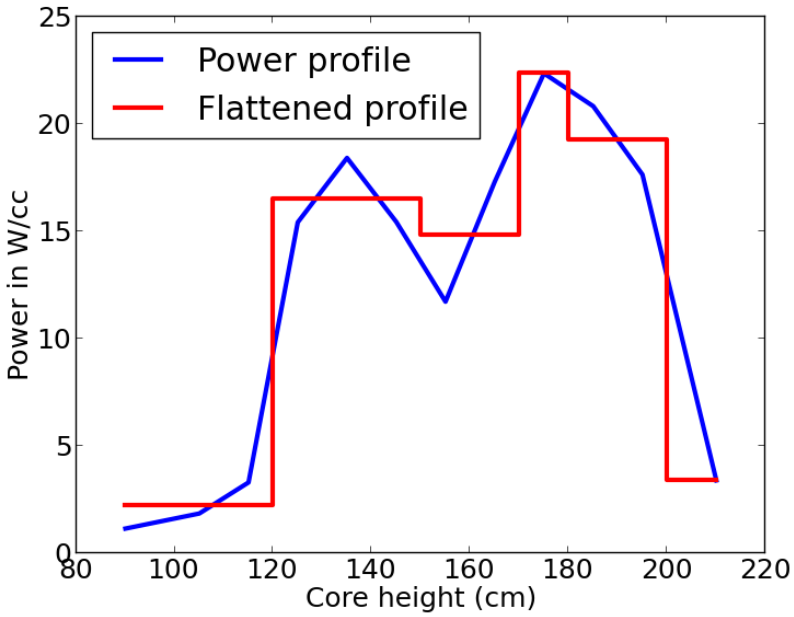

Figure 88 : Comparison of the real power profile and the flattened profile considered for this study. LAB and IFB are the lower and central fertile layer while C1 is the fuel.

Doppler and sodium thermal expansion profiles were similarly averaged over each medium, with the sodium and plenum sodium thermal expansion behind added in an extra mesh on top of the fissile stack with zero power generation. The impacts of these approximations are shown in Table 48. It can be seen that the main changes created by the flattening of the various profiles is limited to 3.3 % here for the final power during an UTOP. Regarding maximal temperature, the impact of this simplification is negligible, however it can be observed that it is necessary to take into account the position of the peak of power density to obtain an accurate maximal fuel temperature.

Table 48 : Comparison of a 1500 MWth CFV core responses to three transients depending on the axial description of power distribution, Doppler and sodium thermal expansion

	Scenario	Final power (%Pn)	Max Sodium Temp (°C)
ULOF (24s to 10% nominal flow	1)Complete profiles	0,419	823,8
	2)Flattened power profile	0,418	824,3
	3)Flattened Doppler and sodium profile	0,416	823,5
	4)All profiles flattened	0,417	824,5
	5) Relative error between 1 and 4 (%)	0,5	-0,1

	Scenario	Final power (%Pn)	Max Sodium Temp (°C)
ULOHS (60s to 0% nominal flow)	1)Complete profiles	0,128	651,2
	2)Flattened power profile	0,128	651,7
	3)Flattened Doppler and sodium profile	0,125	646,5
	4)All profiles flattened	0,126	647,4
	5) Relative error between 1 and 4 (%)	1,6	0,6

	Scenario	Max Power (%Pn)	Max fuel Temp (°C)
UTOP (200 pcm in 100 s)	1)Complete profiles	1,453	1759
	2)Flattened power profile	1,448	1693
	3)Flattened Doppler and sodium profile	1,4815	1778
	4)All profiles flattened	1,475	1711
	5)All profiles flattened with max	1,476	1768
	6) Relative error between 1 and 5 (%)	1,6	0,5

Finally, with the knowledge of core feedback coefficients and with the previously mentioned treatment of the power, Doppler and sodium expansion profiles, the core behavior during an ULOF, ULOHS and UTOP was characterized and an optimization process similar to the one used in the heterogeneous approach was carried out. A graphical overview of the complete methodology can be seen in Figure 89. Rejection of the non-feasible cases (due to exceedingly high linear power density or residence time for instance) was done *a posteriori* during the optimization process.

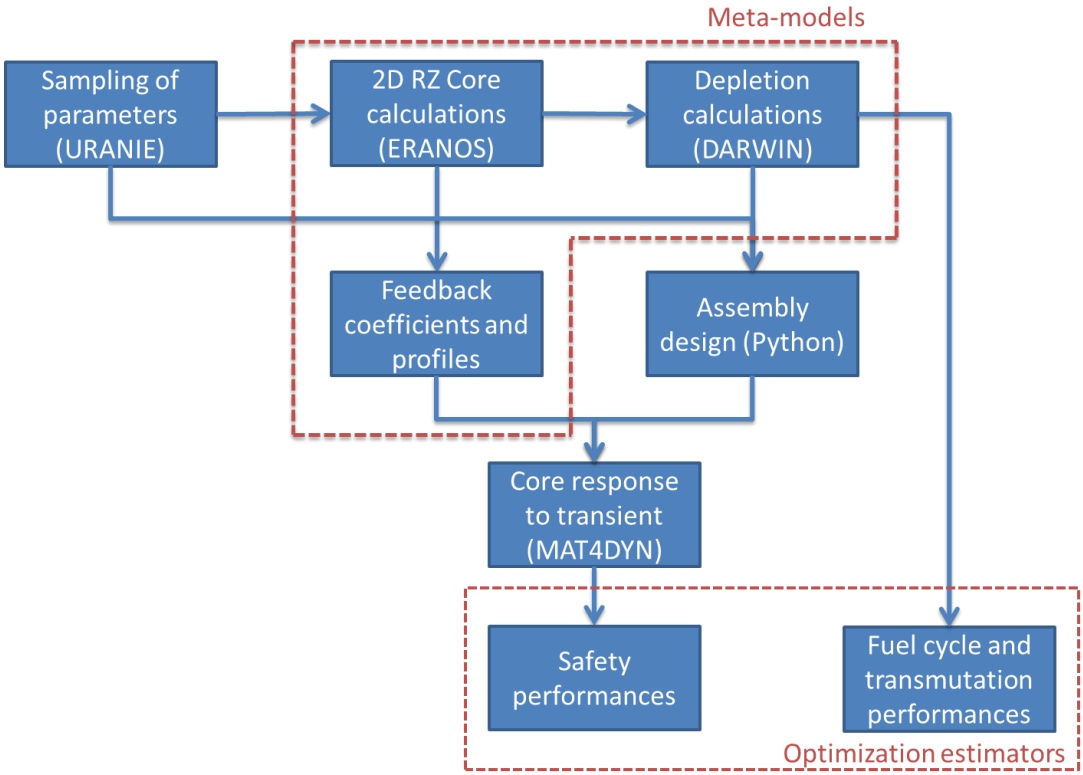

Figure 89 : Graphical description of the methodology developed for the analysis of homogeneous minor actinides transmutation

The performances of the artificial neural networks can be seen in Table 49, with standard deviation generally below 3%, which is deemed sufficient for the applications envisioned here. LAB designates the Lower Axial Blanket while IAB designates the Inner Axial Blanket. It should be mentioned here that for the control rod differential insertion was taken at 2 mm/s, which corresponds to the control rod worth for a homogeneous core. In a heterogeneous core, as the flux level is displaced toward the upper part of the core, it is possible to modify the control rod worth at the start of the insertion by changing its parking position above the interface between the core and the plenum. This approach was not considered here.

Table 49 : Rundown of the errors associated with the artificial neural networks

Parameter	Mean error (%)	Standard deviation (%)	Parameter	Mean error (%)	Standard deviation (%)
Pu inventory	0,05	2,61	Helium production	0,01	4,15
Initial Am content	0,04	3,21	Neutron source @ 5 years	0,05	3,05
Final Am content	0,01	2,61	Neutron source @ 10 years	-0,20	3,03
Pu enrichment	-0,03	2,39	Neutron source @ 20 years	0,10	3,20
Cladding expansion feedback	-0,17	3,69	Neutron source @ 30 years	0,12	3,12
Wrapper expansion feedback	-0,04	3,75	Neutron source @ 50 years	0,04	3,17
Fuel expansion feedback	-0,22	3,22	Neutron source @ 100 years	0,04	3,02
Diagrid expansion feedback	-0,02	1,00	Doppler LAB	-0,07	2,42
Power density	0,03	2,01	Doppler fuel	-0,22	3,81
Delayed neutron fraction	0,00	0,59	Doppler IAB	-0,14	2,17
Neutron lifetime	-0,13	3,92	Sodium thermal expansion fuel	0,24	3,20
Decay heat @ 5years	0,04	2,18	Sodium thermal expansion IAB	0,29	3,39
Decay heat @ 10years	0,00	1,20	Sodium thermal expansion upper plenum	0,05	2,90
Decay heat @ 20years	-0,01	1,28	Sodium thermal expansion sodium plenum	0,17	3,48
Decay heat @ 50years	-0,01	1,26	Power lower fuel	-0,02	3,25
Decay heat @ 100years	-0,02	1,58	Power LAB	-0,40	5,04
Max power	-0,37	3,49	Power IAB	-0,51	5,49
Position of max power	0,15	3,40	Power upper core	0,27	3,27

In the same fashion as in the two previous chapters, the Q^2 estimator was computed for each ANN. The results are shown in Table 50. The Q^2 for nearly all the parameters is above 0.95, except for three parameters which are the fraction of the power in the upper and lower part of the core and the position of the power peak, with a minimal value of 0.53012 for the power in the upper part of the core. Nevertheless, considering both the low standard deviation of the error for these parameters and the low maximal error on the training set (below 11 % for the power in the upper core and below 8 for the two others estimators), the ANN were considered usable in this work. Furthermore, for the UTOP calculation, the most important data is the value of the power peak, which is well predicted by its associated ANN.

Table 50 : Q^2 values for the parameters used in the calculations

Parameter	Q^2	Parameter	Q^2
Pu inventory	0,99412	Helium production	0,99582
Initial Am content	0,99933	Neutron source @ 5 years	0,99578
Final Am content	0,99849	Neutron source @ 10 years	0,99599
Pu enrichment	0,99228	Neutron source @ 20 years	0,99542
Cladding expansion feedback	0,99196	Neutron source @ 30 years	0,99588
Wrapper expansion feedback	0,99211	Neutron source @ 50 years	0,99589
Fuel expansion feedback	0,97536	Neutron source @ 100 years	0,99593
Diagrid expansion feedback	0,99551	Doppler LAB	0,98868
Power density	0,99944	Doppler fuel	0,95325
Delayed neutron fraction	0,99149	Doppler inner blanket	0,96992
Neutron lifetime	0,96615	Sodium thermal expansion fuel	0,98469
Decay heat @ 5years	0,99485	Sodium thermal expansion FCAM	0,98006
Decay heat @ 10years	0,99801	Sodium thermal expansion SVES	0,98960
Decay heat @ 20years	0,99786	Sodium thermal expansion SPLN	0,98400
Decay heat @ 50years	0,99791	Power lower part of the core	**0,71283**
Decay heat @ 100years	0,99660	Power LAB	0,97744
Max power	0,98424	Power MAB	0,96942
Position of max power	**0,88739**	Power upper core part of the core	**0,53012**

Various estimators were used for the optimization process similarly to what was done for the heterogeneous approach. They can be sorted into 4 categories. The first one is related to transmutation performances, with the total consumption of minor actinides during irradiation and the specific consumption which was introduced earlier in this work. The second category is linked to the fuel cycle and an inventory estimator similar to the one used in Chapter 4 was considered here.

The last two categories are specific to homogeneous minor actinides transmutation. The third one is the behavior of the core during the three transients described at the beginning of this chapter. Various margins to boiling or fuel failure were considered:

- For the ULOF case, the maximum sodium temperature during the ULOF was used, even for the cases where it was higher than the sodium boiling temperature.
- For the ULOHS case, the core equilibrium temperature was used as an estimator
- For the UTOP case, the maximum fuel temperature reached was used.

Finally, estimators linked to the core itself were used, such as the plutonium inventory in the core, the pressure drop in the assemblies, which was computed using the Novendstern correlation for sodium-cooled assembly [84] and the power density. The pressure drop is not the entire pressure drop for the assembly, which depends on the mechanical design of the assembly feet and top, but only an estimation of the pressure drop in pin bundle. These estimators can be associated with the economic cost of the core and cycle associated, as an increase in the pressure drop will require additional pumping while higher plutonium inventories leads to a higher fuel cycle costs. Plutonium inventory and pressure drop should be minimized to limit the mass of plutonium in the fuel cycle and the core pumping power, while

power density should be maximized to keep the core as small as possible. All these estimators are summarized in Table 51.

Regarding fuel cycle constraints, in order to focus the analysis on the core behavior, a washing limit set a 7.5 kW per assembly will be considered throughout the study, with an additional separate analysis for the fuel cycle constraints. All the cores were calculated with a burn-up of 200 GWd/t with the irradiation time being calculation to reach this target depending on core geometry and minor actinides loading.

Concerning the geometrical design of the assemblies, it was shown that the additional production of helium due to minor actinides incorporation in the fuel did not modify the design in terms of pin pressurization. Considering that the modelling assumptions taking for the fuel thermomechanical behavior were too limited to appropriately describe and optimized fuel assembly, especially in the description of the temperature field in the pin, it was decided to use a standard assembly design with 42 % of fuel volume fraction, 28 % of sodium and 20 % of structural materials. The pin diameter was computed to achieve a maximal fuel temperature of 2250 °C, which corresponds to an average temperature of 1000 °C. Globally speaking, to limit the sodium thermal expansion feedback, it should be necessary to decrease as much as possible the sodium volume fraction in the assembly, but actual determination of the minimum achievable fraction is out of the scope of this study.

Table 51 : Summary of the estimators considered in this work

Category	Estimator	Formula	Optimization direction
Transmutation performances	Mass consumed	$C = \Delta Am_{irr}$	Maximization
	Specific consumption	$S_c = \frac{\Delta Am_{irr}}{T_{irr} * P_{el}}$	Maximization
Fuel cycle	Total inventory in the fuel cycle (for one assembly of the inner and one of the outer core)	$I = m_0(Am)(1 + (1 - \tau)\frac{T_{reprocessing}}{T_{irr}})$	Minimization
Transient behaviour	Maximal sodium outlet temperature during ULOF	T_{max}^{Na}	Minimization
	Maximal fuel temperature during UTOP	T_{max}^{fuel}	Minimization
	Final sodium temperature at equilibrium during ULOHS	T_{end}^{Na}	Minimization
Core parameters	Plutonium inventory	Calculated by ANN	Minimization
	Power density	Calculated by design	Maximization
	Pressure drop in the bundle	Evaluated using Novendstern correlation from [84]	Minimization

2) APPLICATIONS

The aim of this part is to apply the methodology discussed above to various cases and to identify trends or behaviors of interest regarding homogeneous minor actinides transmutation. An important attention will be paid to the physical analysis of the optimization results. The core detailed below in Table 52 will be used as a reference core throughout the study.

Table 52 : Parameters describing the reference core

Core power	MWTh	3600
Inner core height	cm	80
Inner axial blanket	cm	20
Outer core height	cm	100
Core radius	cm	319,4
Americium content	at%	1
Moderator fraction	vol %	0
Assembly fuel fraction	vol %	42
Assembly sodium fraction	vol %	28
Assembly structural fraction	vol %	30

a) ULOF

Considering the core behavior during an ULOF transient as shown in Figure 79, it can be postulated that the effect of minor actinides loading in the fuel will be limited as the positive contribution of the Doppler effect to the reactivity will decrease while the negative contribution of sodium thermal expansion will increase, thus limiting the total reactivity variation due to the addition of minor actinides.

A preliminary optimization process was performed for such a transient with the following characteristics:

- Parameters : core power, inner and outer core heights, americium content
- Estimators : americium consumption, maximal sodium temperature during ULOF, americium inventory in the fuel cycle
- Constraints : maximal decay heat reprocessing of 7.5 kW
- Transient: 90 % decrease of the flow with a half time of 24 s.

The results are shown in Figure 90. This figure shows the results as a “Cobweb” of the various cases, with the parameters on the left and the performances on the right. A given case is represented by the broken line linking all the four input parameters and three outputs. Generally speaking, the power level is inversely correlated to the minor actinides content. “Optimal” cases can be found with content up to 8 % and correspondingly high minor actinides consumption and inventory. These two quantities are strongly correlated as it can be observed on the right most part of the figure. It can also qualitatively be observed that the ULOF temperature appears to be strongly dependent on the core inner height rather than on the minor actinides content. No general behaviour can be deduced from this optimization, with however two sub sets of cases being identifiable :

- A first one with relatively low Am content, high power and low ULOF maximal temperature which yields small consumption and inventory. In this case, the algorithm minimizes the inventory and the ULOF temperature at the expense of the americium consumption (Figure 91)
- A second one with high Am content and low power, with similar ULOF maximal temperature, which yields higher consumption and associated inventory. In this case, the algorithm minimizes the ULOF temperature and maximizes the consumption at the expense of the inventory.

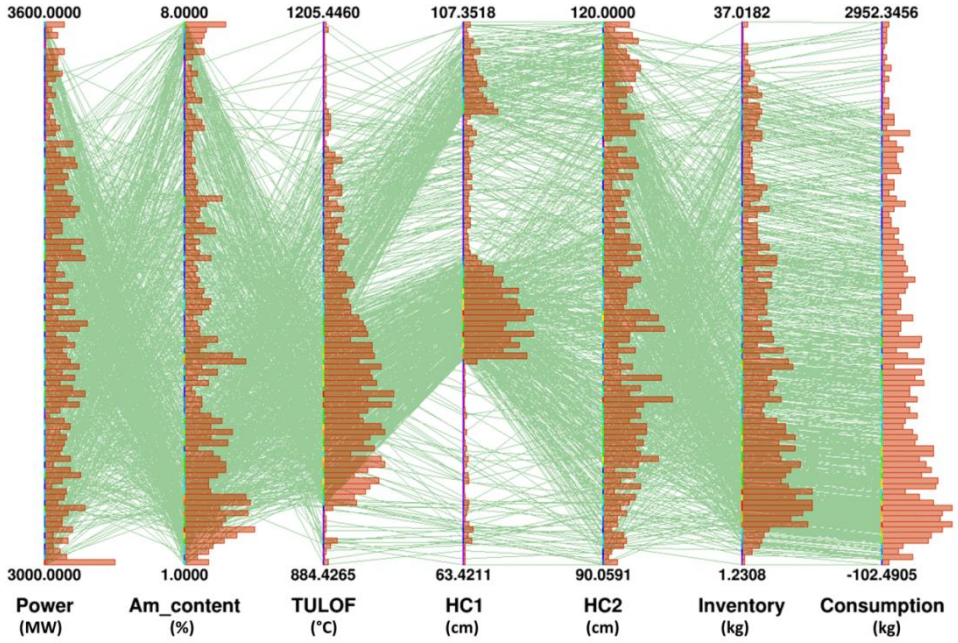

Figure 90 : Optimal cases for the ULOF cases.

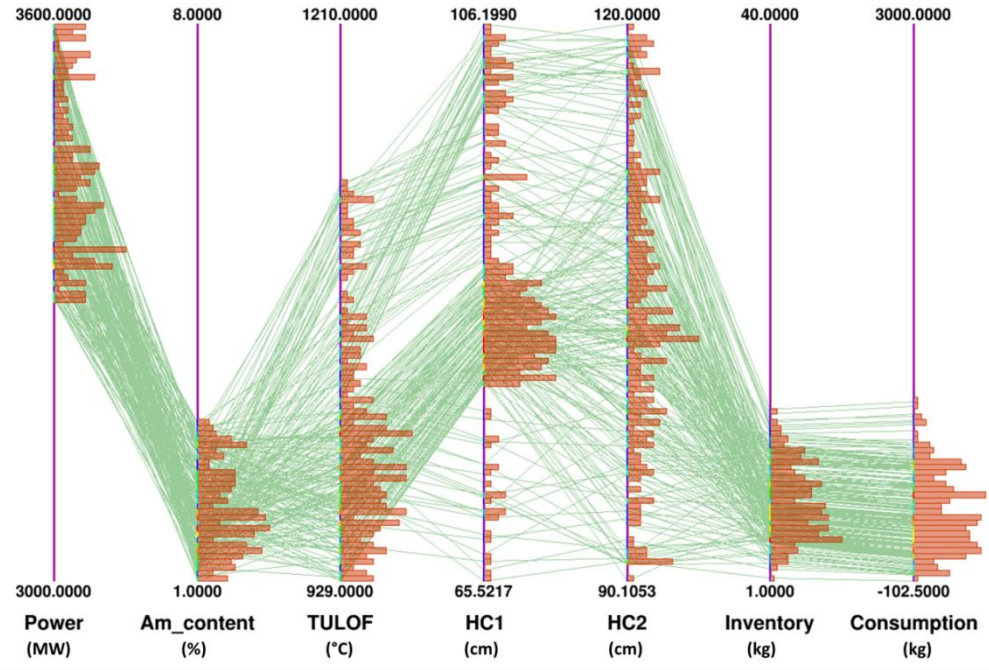

Figure 91 : Subset of the ULOF optimal set corresponding to cores with high power and low minor actinides content

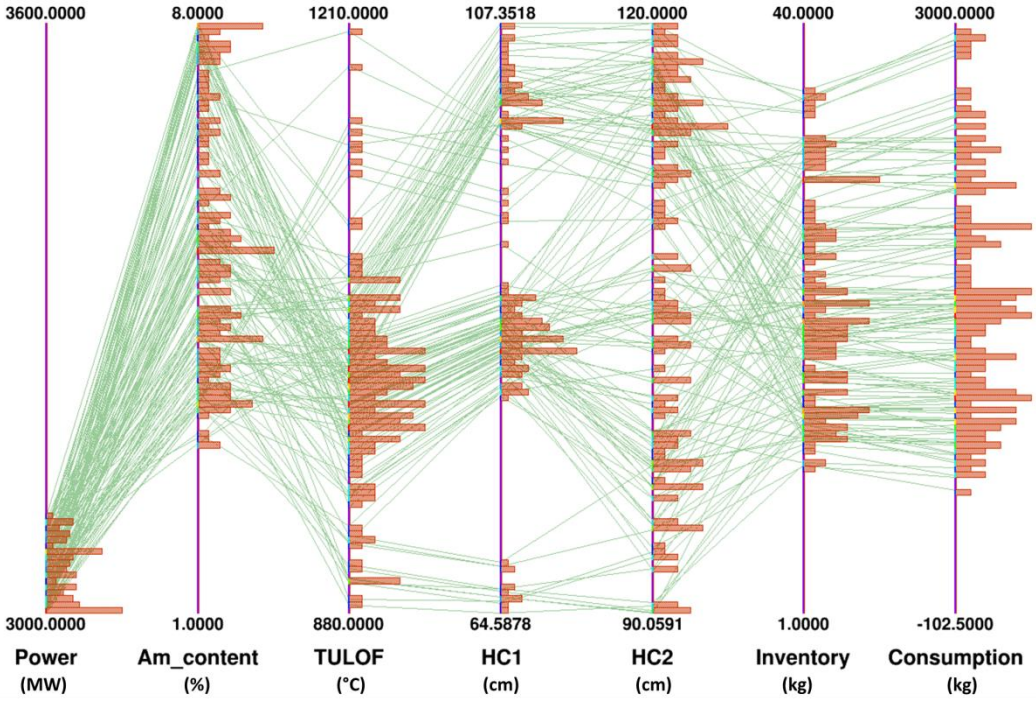

Figure 92 : Subset of the ULOF optimal set corresponding to cores with low power and high minor actinides content

To refine this analysis, it is possible for the reference core to evaluate the impact of each parameter separately on the various estimators using a so-called One at a time method. This is done in Table 53, where it can be observed that the inner core geometry has the most important impact on the transient behavior, while having only a limited impact on the total inventory. The Am content has a limited impact on the transient behavior. The amplitude of the corresponding

variation will be compared to the uncertainties of the optimization process in the following parts.

Table 53 : Evaluation of the impact of each parameter on the output estimators for the reference core during an ULOF

		Estimator		
		TULOF (°C)	Consumption (kg)	Inventory (kg)
1 < Am content < 8 %	Min	1055	-1,7	3,2
	Max	1076	2547	33,7
70 < HC1 < 90 cm	Min	952	684	13,3
	Max	1050	1061	15,9
3000 < Power < 3600 MWth	Min	911	910	14,5
	Max	946	940	15,3

To refine this analysis, the Morris screening method [85] will be used. This method was chosen as it required a limit number of iterations compared to the calculations of more refined indices such as the Sobol indices. [86]. In this method, the initial parameters' set is explored using trajectories obtained by changing one parameter at time. Then, the elementary effects are computed along these trajectories using the following definition, with Δ the difference taken along the trajectory for a given variation and y the function representing the code output.

$$EE_i = \frac{y(x_1, x_2, \dots, x_{i+\Delta}., x_n) - y(x_1, x_2, \dots, x_i., x_n)}{\Delta} \quad (2)$$

Then, a statistical analysis is carried out on the set of elementary effects to obtain their mean $\boldsymbol{\mu}$ and their variance $\boldsymbol{\sigma}$. Considering these two values, it is possible to classify the inputs parameters in three categories:

- The parameters with low mean and low variance, to which the model is not sensitive
- The parameters with low variance, to which the model is sensitive but in a linear fashion with limited interaction with the other parameters
- The parameters with high variance, to which the model is sensitive with non-linear effects and/or interactions between the various parameters.

The Morris coefficients were computed for the consumption and inventory estimators and are shown below in Table 54.The core height has a limited impact on the inventory and consumption while the americium content has a strong impact with non-linear effects according to the above classification. What is interesting to note and was not observed using the simple analysis done in Table 53 is the influence of the core power on its parameters, in both cases with a significant contribution from interactions with other parameters. Concerning the ULOF, the core power and height significant impacts on the core behavior while the am content has very little influence.

Table 54 : Morris coefficients for the consumption, inventory and ULOF estimator

Consumption	μ	σ
C1	42	50
Am content	16500	1800
Core power	2000	650

Inventory	μ	σ
C1	0.2	0.4
Am content	230	6.4
Core power	75	6

ULOF estimator	μ	σ
C1	6500	600
Am content	10	50
Core power	14500	1900

As it was observed in Figure 90 that the minor actinides content and the core power were correlated, it is possible to use the specific consumption as the transmutation estimator, as it includes the core power in its definition. Additionally, the plutonium inventory and the pressure drop in the pin bundle were used as estimators to obtain a complete view of the core designs obtained. The following optimization was then launched:

- Parameters : core power, inner and outer core heights, americium content
- Estimators : americium consumption, maximal sodium temperature during ULOF, americium inventory in the fuel cycle; plutonium inventory, bundle pressure drop
- Constraints : maximal decay heat reprocessing of 7.5 kW
- Transient: 90 % decrease of the flow with a half time of 24 s.

The corresponding optimal cases can be found in Figure 93. The optimal cases can once again be split between the two subsets described before. However, the main difference to be noted with the optimization made in Figure 90 is that the inner and outer core heights have been minimized in order to limit the total plutonium inventory in the core and the associated pressure drop.

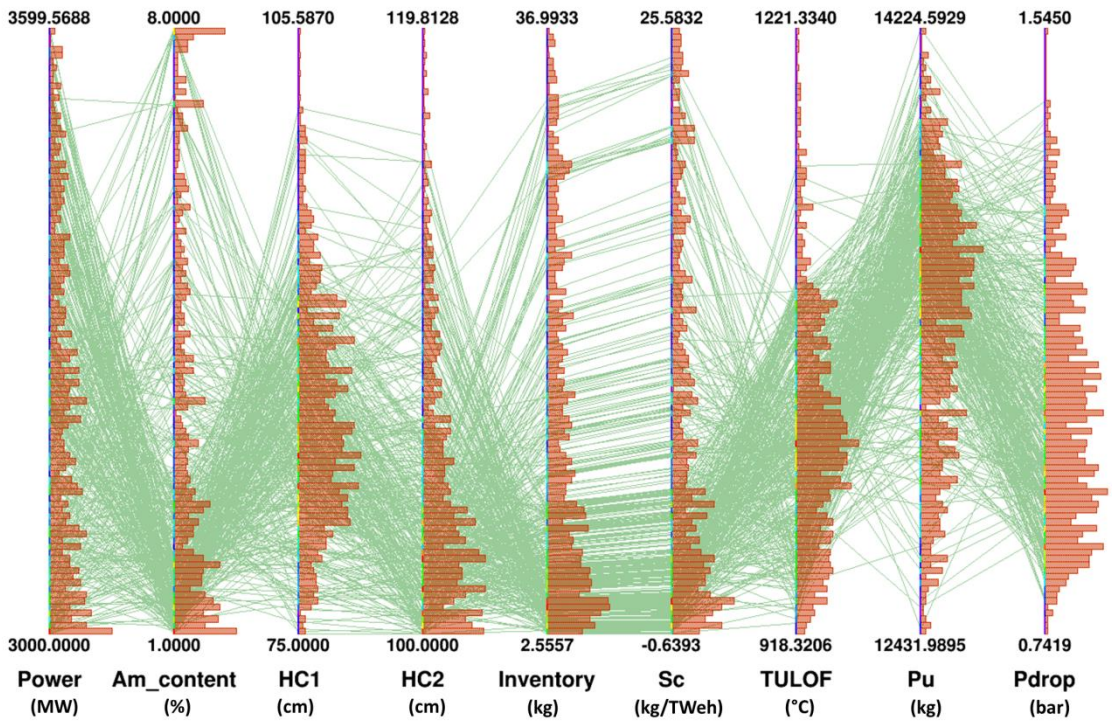

Figure 93 : Optimal cases for the ULOF transient with the Pu inventory and pressure drop considered as estimators to be minimized.

It is finally possible to use additional parameters to extend the optimization process. The following optimization was then launched:

- Parameters : core power, inner and outer core heights, americium content, core radius, moderating material content, inner axial blanket height
- Estimators : americium consumption, maximal sodium temperature during ULOF, americium inventory in the fuel cycle; plutonium inventory, bundle pressure drop
- Constraints : maximal decay heat reprocessing of 7.5 kW
- Transient: 90 % decrease of the flow with a half time of 24 s.

This is done in Figure 94. **The obtained optimal cases correspond to cores with low power, small assemblies and high minor actinides content**. The amount of moderating material in the core appears to be correlated to the amount of minor actinides. Indeed, adding moderating material has the following impacts on the core:

- Increase in the total Doppler feedback
- Decrease in the sodium thermal expansion and slight increase in the plenum sodium expansion feedback
- Increase in the cladding feedback coefficient
- Decrease in the grid feedback coefficient

Consequently, this addition will have negative impact on the ULOF transient by increasing the Doppler reactivity inserted while decreasing the amount of negative reactivity inserted by the plenum voiding. On the other hand, moderating material in the core increases the consumption of minor actinides by modifying the neutron spectrum. There is thus equilibrium between the minor actinides effect and the moderating material effect on the Doppler. We also observe here

a limitation of the core fissile height while no meaningful conclusion can be drawn on the inner fertile layer optimal thickness.

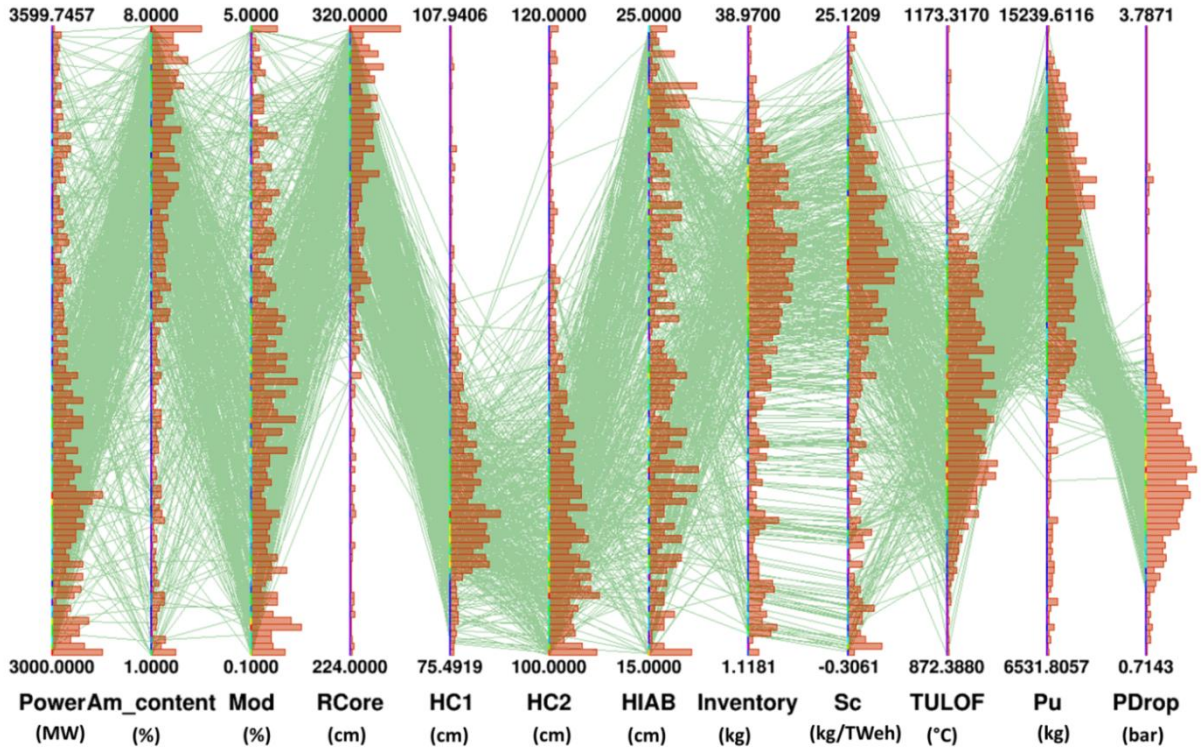

Figure 94 : Optimal cases for the ULOF transient where all the parameters unrelated to assemblies' geometry are considered

The last point which can be analyzed using this methodology is the impact of the transient definition on the core behavior. As mentioned previously, the UTOP transient can be parametrized by the half-time of the pumps coast down and the final flow in the system, which is either established through natural convection or secondary pumps used during transients. For the reference core of Table 52 loaded with 4 % of americium, the evolution of the maximal ULOF temperature with both parameters was plotted in Figure 95. When either of this parameter decreases, the core maximal temperature increases. This is consistent with the idea of increasing the inertia of the primary pumps as discussed in the GEN IV report [3], in order to limit the sodium temperature increase.

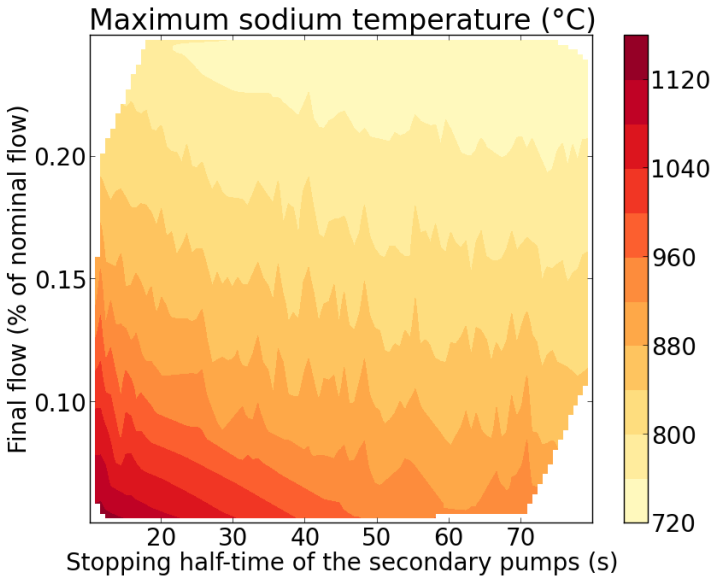

Figure 95 : Evolution of the maximal sodium temperature during an ULOF with regards to the halving time of the pumps and the final flow in the primary circuit

It is also possible to consider the evolution of the maximal sodium temperature during an ULOF with regards to the sodium flow at the end of transient and the americium content. As it can be seen in Figure 96, the maximal sodium temperature does not depend on the minor actinides loaded in the core but almost only the final flow. The same conclusion can be reached regarding the pump inertia.

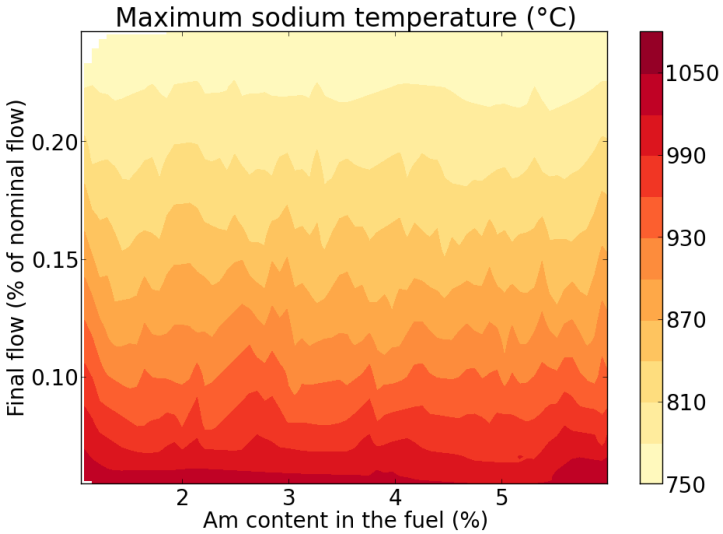

Figure 96 : Maximum sodium temperature during an ULOF with regards to the final flow and the am content in the fuel

Regarding the ULOF transient, **it can thus be concluded that a heterogeneous core such as the CFV core is nearly not impacted by minor actinides loading.** Consequently, optimization must be carried out with regards to other estimators, such as the plutonium inventory or the fuel cycle minor actinides inventory. In this case, relatively small cores loaded with limited

amounts of minor actinides are to be preferred; for such cores it appears not necessary to load the core with moderating material.

b) ULOHS

As it was exposed in the first part of this chapter in Figure 82, during an ULOHS the grid expansion feedback is the main contributor to the negative reactivity inserted in the core while Doppler Effect is the main contributor to the positive reactivity insertion as the fuel cooldowns. When minor actinides are loaded in the core the grid effect increases while the Doppler Effect magnitude decreases due to the spectrum hardening. Then, the reactivity increase due to the fuel cooling down will be lower. Consequently, it can be postulated that for any given core, as long as the sodium thermal expansion effect increase is limited, the impact of minor loading on the ULOHS behavior will be limited or even beneficial.

A preliminary optimization with genetic algorithm was performed with a limited number of parameters and optimization objectives:

The following optimization was then launched:

- Parameters : core power, inner and outer core heights, americium content
- Estimators : americium consumption, final sodium temperature during ULOHS, americium inventory in the fuel cycle
- Constraints : maximal decay heat reprocessing of 7.5 kW, maximal ULOHS final temperature of 700 °C
- Transient: Total linear decrease of the secondary flow in 40s

The optimal cases which combine the best consumption with the lowest sodium temperature are shown in Figure 97. It can be seen that the optimization algorithm maximized the minor actinides fraction loaded in the core (up to 8 % here) while minimizing the inner core height. Furthermore, there is direct correlation between the height of the core, the maximum sodium temperature and the americium consumption. When the americium content increases, the consumption increases and the ULOHS temperature estimator decreases. It can also be seen that for the transients considered and the core here, the core final state is below the temperature limit of 700 °.

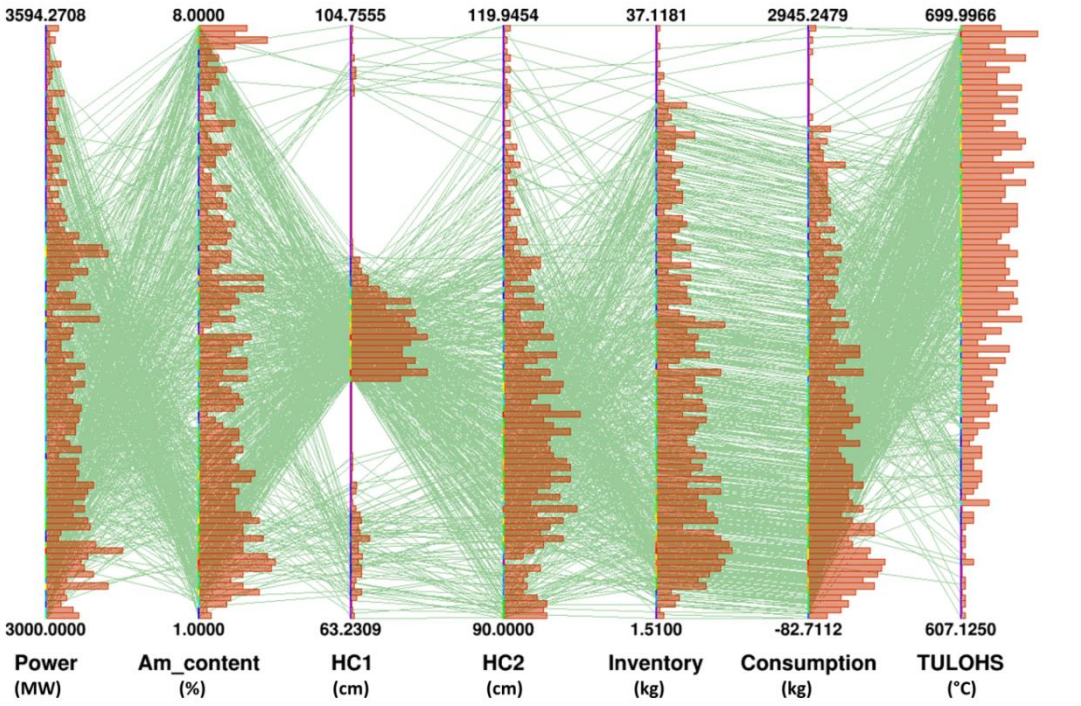

Figure 97 : Optimal cases for ULOHS transient.

Various effects can explain this behavior. Considering that the optimization algorithm tends to maximize the minor actinides content in the fuel, it can be inferred that a decrease in this content will have a negative impact on both the sodium temperature at equilibrium and on the consumption. It is pretty straightforward to see that, with an almost constant transmutation rate, a decrease in the loaded mass of americium will lead to a decrease in the americium consumption during irradiation. However, it is less straightforward to explain the relationship between the final sodium temperature and the minor actinides loaded fraction.

Two cores were then compared, with the geometrical design corresponding to one of the optimized core, e.g. with a small inner and outer core shown in Figure 97. One was loaded with 8 wt% of americium and one with only 2%. For the first one, the final sodium temperature observed was 627 °C compared to 648 °C for the second one. After investigation, it was found that the main explanation for this behavior is the decrease in Doppler Effect due to spectrum hardening. Indeed, the lower Doppler Effect leads to a lower reactivity insertion in the core during cooldown, which limits the required rise in sodium temperature to counterbalance this increase. The other feedbacks parameters are slightly impacted by the spectrum hardening but only have a small impact on final sodium temperature. Kinetics parameters are however modified, with a 7.5 % decrease in the effective delayed neutron fraction. However, this only modifies the time evolution of the transient but not its final state.

It should also be observed that the optimal cores are corresponding to the cores with the lowest height. This is explained by various factors. The first one is the fact that, as the total core height was considered constant here, an increase in the fuel stack height leads to a decrease in the plenum height, which in turns decreases the negative component of the sodium thermal expansion feedback. The lower grid feedback in the larger core also leads to an increase in the final sodium temperature. Finally, the higher Doppler coefficient in the bigger core leads to a more important positive reactivity insertion during the ULOHS. Due to a combination of these

three effects, we can conclude that small cores are better suited for transmutation of minor actinides with regards to the ULOHS. We can also conclude that minor actinides loading has a beneficial impact on the ULOHS behavior of a CFV-like core. As it can be observed on Figure 98, this conclusion holds true regardless of the ULOHS considered.

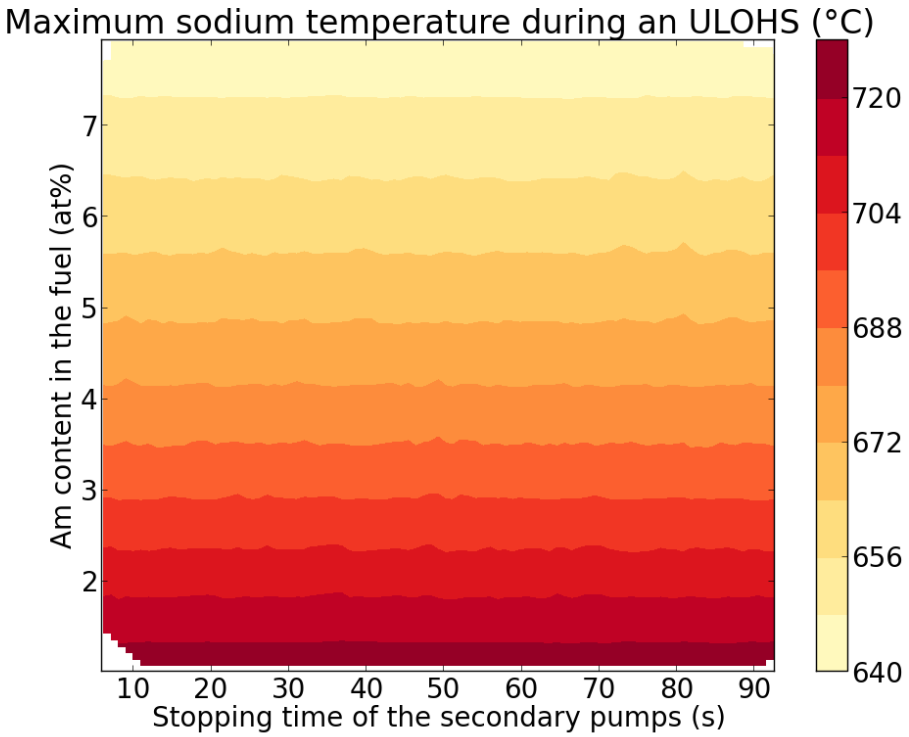

Figure 98 : Maximum sodium temperature during an ULOHS vs americium content in the fuel and stopping time of the secondary pumps

It is also possible, as it was done for the ULOF case, to split the impacts of the each parameter on each estimator as it is done in Table 55. Similarly to the previous case, the inventory is mainly dependent on the americium content, while the consumption is slightly impacted by the core height variation which modifies the total mass loaded. However, the ULOHS final sodium temperature appears to depend on each of the three parameters considered here. The Morris coefficients were computed in Table 56 and it can be observed that the core height and power have more influence on the core behavior than the americium content.

Table 55 : Evaluation of the impact of each parameter on the output estimators for the reference core during an ULOHS

		Estimator		
		TULOHS (°C)	Consumption (kg)	Inventory (kg)
1 < Am content < 8 %	Min	646	-81,7	1,6
	Max	720	1216	24
70 < HC1 < 90 cm	Min	667	524	11,6
	Max	718	972	15,2
3000 < Power < 3600 MWth	Min	614	513	11,5
	Max	680	699	13,1

Table 56 : Morris coefficients for the ULOHS temperature estimator

ULOHS estimator	μ	σ
C1	2500	1900
Am content	200	40
Core power	16000	1000

It is now possible to consider additional parameters, such as plutonium inventory and the pressure drop in the assembly. The following optimization process was then launched:

- Parameters : core power, inner and outer core heights, americium content
- Estimators : americium consumption, final sodium temperature during ULOHS, americium inventory in the fuel cycle; plutonium inventory, bundle pressure drop
- Constraints : maximal decay heat reprocessing of 7.5 kW
- Transient: Total linear decrease of the secondary flow in 40s

This is done in Figure 99. The set of optimal cases is similar to the one obtained with Figure 97. It is interesting to note here the inverse relation between the specific consumption and the ULOHS temperature estimator: the highest specific consumption, which corresponds to high americium content with a low core power yields the lowest temperature, where as the lowest consumption leads to the highest temperature. This is consistent with the results obtained previously about the impact of minor actinides on the ULOHS transient. The core plutonium inventory is correlated to the specific consumption: higher specific consumption leads to higher plutonium inventory due to the necessity to compensate for the neutronic penalty due to high minor actinide loading.

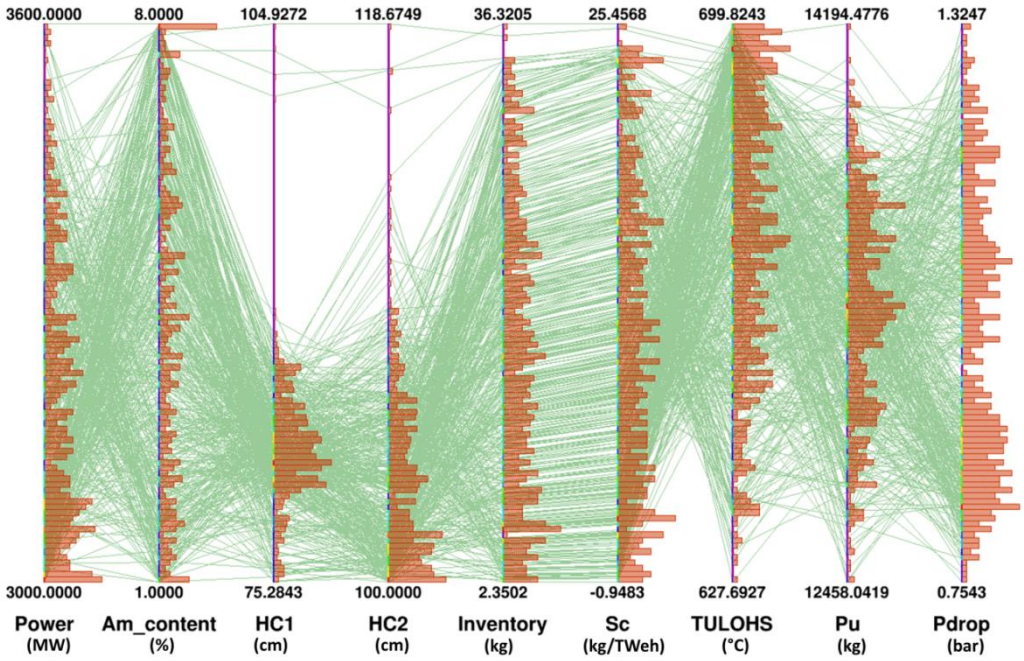

Figure 99 : Optimal cases for ULOHS transient with the Pu inventory and pressure drop considered as estimators to be minimized.

Similarly to the ULOF case, the following optimization was finally launched, which takes into account all the model parameters:

- Parameters : core power, inner and outer core heights, americium content, core radius, moderating material content, inner axial blanket height
- Estimators : americium consumption, maximal sodium temperature during ULOF, americium inventory in the fuel cycle; plutonium inventory, bundle pressure drop
- Constraints : maximal decay heat reprocessing of 7.5 kW
- Transient: 90 % decrease of the flow with a half time of 24 s.

The corresponding results are shown in Figure 100. The overall core behavior is similar to what was observed before for the ULOF and the ULOHS: the amount of minor actinides is maximized while the core height is minimized. The amount of moderating material loaded here is significantly lower than in the ULOF case. This is explained by the fact that in the ULOHS case, the only feedback of interest is the Doppler feedback, which is increased when moderating material is loaded, while it should be decreased to improve the ULOHS behavior. Consequently only a small amount is added to the fuel to slightly increase transmutation performances, but to a lower extent than in the ULOF case, where the sodium thermal expansion feedback also plays a role in the transient behavior. No conclusion can be drawn on the inner axial blanket, and big cores are favored in order to minimize the power density here.

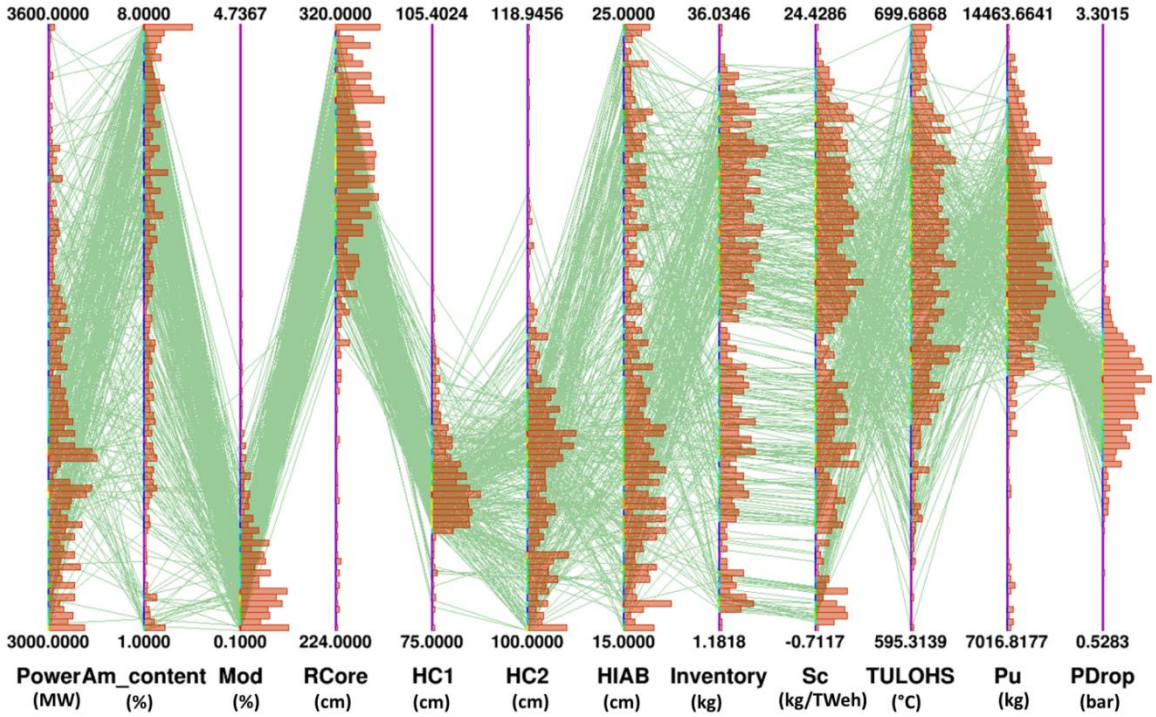

Figure 100 : Optimized cases for the ULOHS case where all the parameters unrelated to assemblies' geometry are considered

Overall, it can be concluded here that minor actinides loading in a CFV-like core has a beneficial effect on its ULOHS behavior, and as such, a given core does not need to be modified to accommodate minor actinides loading with regards to the ULOHS transient. Optimized cores are relatively similar to the ULOF case, with small inner cores and high minor actinides content with however a more limited amount of moderating material.

c) UTOP

Starting from the reference UTOP described in paragraph 2.c (150 pcm inserted in 250 seconds), a similar preliminary optimization is run, with the same free parameters and objectives as for the two previous cases, e.g.:

- Parameters : core power, inner and outer core heights, americium content,
- Estimators : americium consumption, maximal fuel temperature during UTOP, americium inventory in the fuel cycle
- Constraints : maximal decay heat reprocessing of 7.5 kW
- Transient: 150 pcm inserted in 250 s

Considering that minor actinides addition in the fuel decreases the Doppler Effect and that this feedback is the main one for a reactivity transient, it follows that the core behavior during an UTOP will be negatively impacted.

As it can be seen in Figure 101, the optimized cores correspond mostly to cores with a very low amount of minor actinides, close to the required fraction necessary to achieve a positive consumption over the irradiation (around 1.3 %) and with maximized core height. The maximization of the core height has two positive impacts on the UTOP behavior. First, it increases the amount of ^{238}U in the core, thus increasing initial Doppler feedback magnitude. Second, it decreases the linear heat rate of the fuel, thus limiting peak core centerline temperature and its corresponding increase during a transient. It can thus be observed that the final fuel temperature is inversely related to the height of the inner core.

On the other hand, the minor actinides content is kept relatively small in the optimization process in order to limit the decrease in the Doppler feedback coefficient. Due to this small americium content, the associated inventory is also relatively low. Finally, the core power decreases when the minor actinides content increases, in order to decrease the linear power rate. Two conclusions related to homogeneous minor actinides loading can be drawn from this analysis:

- Regardless of the americium loading, the linear power rate should be minimized in order to lower the maximal fuel centerline temperature reached during an UTOP. This can be done either by increasing the core height or by decreasing the core power.
- Minor actinide loading has a negative impact on the UTOP regardless of the loaded amount thus it should be minimized.

As the UTOP temperature obtained for the core studied here are below the limiting value of 2650 °C, the algorithm also proposed cores with low power and high americium content as optimal cores. Indeed, these cores maximize the consumption at the expense of the inventory and the maximal fuel temperature.

Splitting the various impacts of the different parameters on each estimator, it can be observed in Table 57 that the minor actinides loading in this case has a rather small impact on the maximal fuel temperature during an UTOP. As previously, it has a strong one on the consumption and inventory estimators. On the other hand, power and core height have a strong impact on the UTOP estimator has they both change the linear power rate of core, which is the main parameter. The Morris coefficients for the UTOP temperature estimator are given in Table 58 and it can be observed that the main parameter influencing the core behavior is the core

height, followed by the power level, to which the estimator has a strong linear dependency. The minor actinides content has very little influence on the final UTOP temperature.

Table 57 : Evaluation of the impact of each parameter on the output estimators for the reference core during an UTOP

		Estimator		
		TUTOP (°C)	Consumption (kg)	Inventory (kg)
1 < Am content < 8 %	Min	2236	124	4,61
	Max	2286	3036	37,96
70 < HC1 < 90 cm	Min	2077	1042	16,65
	Max	2519	1345	18,08
3000 < Power < 3600 MWth	Min	2091	1326	17
	Max	2368	1358	18

Table 58 : Morris coefficients for the UTOP temperature estimator

UTOP estimator	μ	σ
C1	12000	400
Am content	950	500
Core power	120000	8000

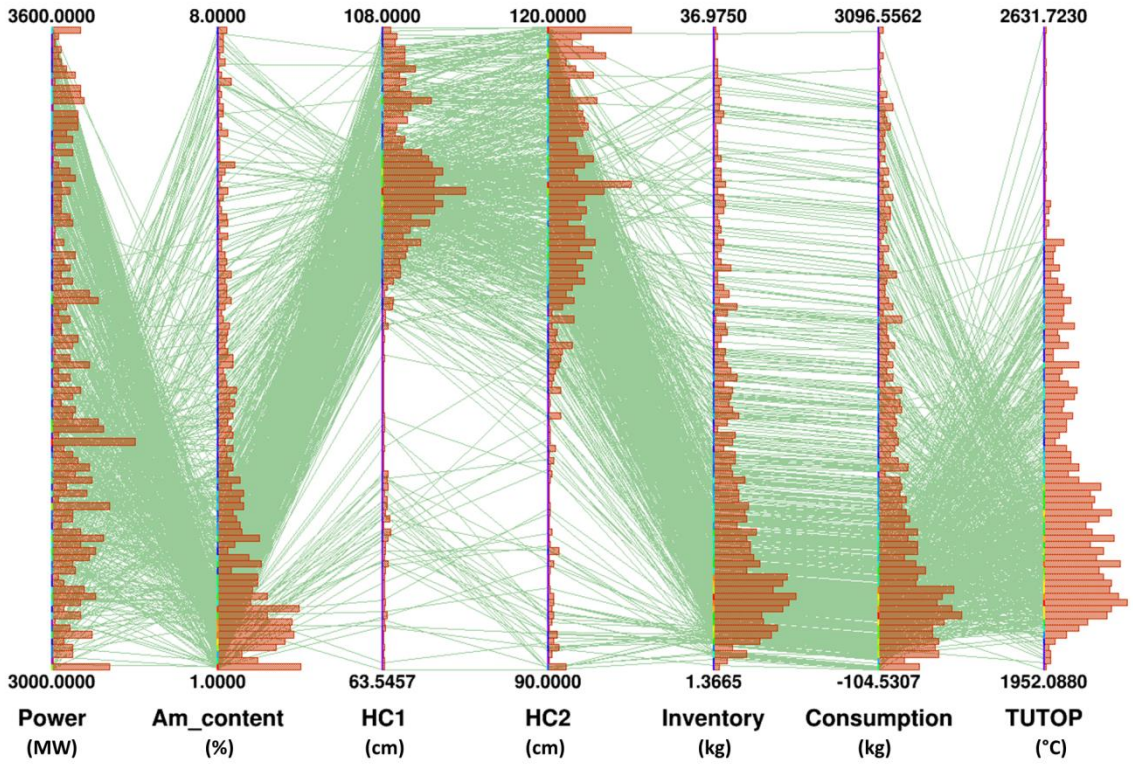

Figure 101 : Optimal cases for the UTOP transient.

The impact of the transient parameter can also be studied here to evaluate the sensibility of a given core to the amount of reactivity inserted and the corresponding speed of insertion. A core with an outer height of 117 cm, an inner height of 105.3 cm and an americium content of 1.62 % for a power of 3500 MWth was selected in in the optimal set to investigate this sensibility. As shown in Figure 102, the core response to an UTOP is linear. It improves with the UTOP length and degrades with the reactivity inserted. Considering this, it can be considered that the conclusions obtained for the reference UTOP stay true for any kind of slow UTOP (e.g., corresponding to a rod withdrawal).

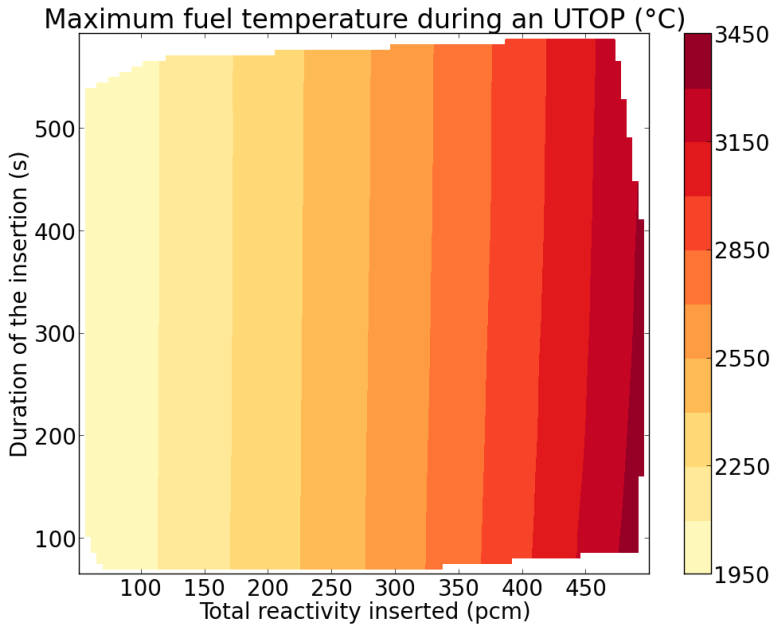

Figure 102 : Maximum fuel temperature during an UTOP depending on its duration and on the reactivity inserted

A secondary optimization process can be run considering the conclusions obtained here. Indeed, increasing the core height has a negative impact on core pressure drop and on the total plutonium inventor in the fuel, two quantities which should be minimized chiefly due to economic considerations. Similarly, decreasing core power is an option with negative impact on the core production. Consequently, a second optimization process was run where the specific consumption was used to estimate the transmutation performances, in order to integrate core production in the process, and where plutonium inventory and pressure were used as estimators to be minimized. The following optimization was considered:

- Parameters : core power, inner and outer core heights, americium content
- Estimators : americium consumption, maximal fuel temperature during UTOP, americium inventory in the fuel cycle; plutonium inventory, bundle pressure drop
- Constraints : maximal decay heat reprocessing of 7.5 kW
- Transient: 250 pcm inserted in 150 s

The corresponding optimized cases are shown below in Figure 103. For readability purpose, only the cases with the highest weight were shown in this figure. The weight of the cases is defined by the plotting algorithm during the binning process of the results. Overall, two subsets can be found in the optimized cases:

- One subset which maximizes the power while minimizing the americium content. The core height is relatively tall, limiting the maximal temperature during an UTOP at the expense of the plutonium inventory and pressure drop.
- A second one which minimizes the power while maximizing the americium content. The core height is smaller, which has a negative impact on the maximal temperature during an UTOP but limits the total plutonium inventory and pressure drop.

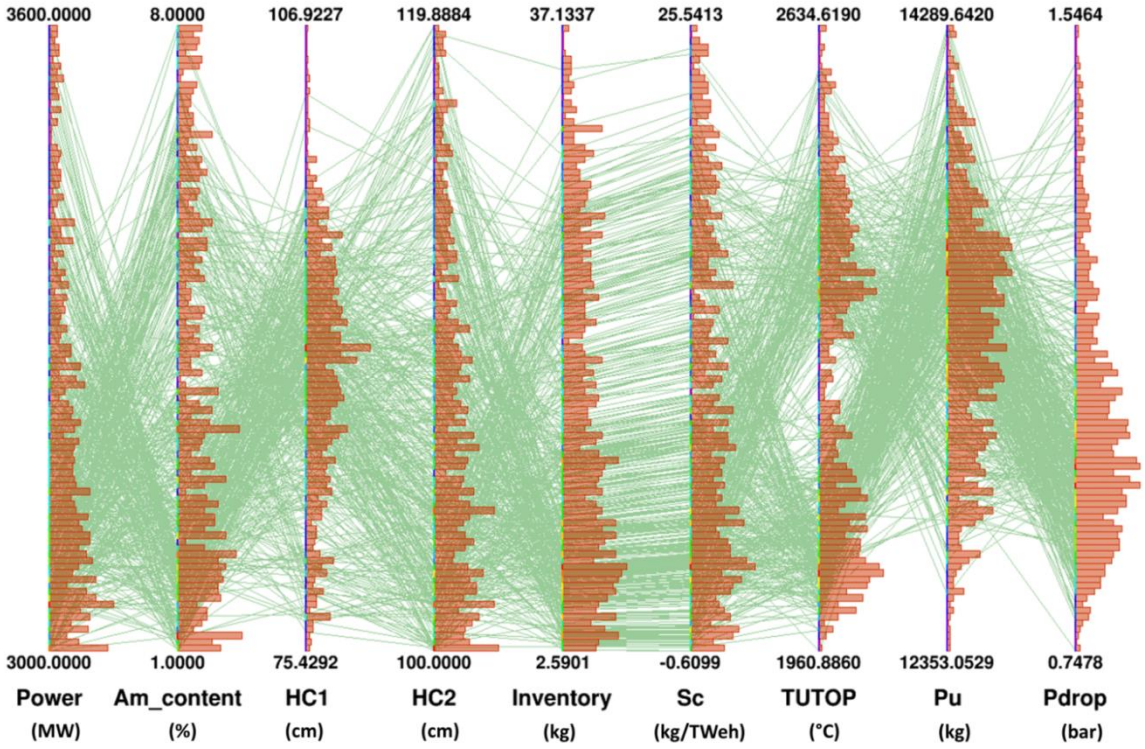

Figure 103 : Optimal cases for the UTOP transient with the Pu inventory and pressure drop considered as estimators to be minimized.

A final analysis of the UTOP transient was carried out while considering all the parameters of the model except the geometrical design of the assemblies. The following optimization was then launched:

- Parameters : core power, inner and outer core heights, americium content, core radius, moderating material content, inner axial blanket height
- Estimators : americium consumption, maximal fuel temperature during UTOP, americium inventory in the fuel cycle; plutonium inventory, bundle pressure drop
- Constraints : maximal decay heat reprocessing of 7.5 kW
- Transient: 150 pcm inserted in 250 s.

The results are shown in Figure 104. Similarly to the optimized cases obtained for this scenario for the ULOF and ULOHS cases, the cores obtained are characterized by a high americium content, low power and relatively small cores, with moderating material added to compensate for the minor actinides loading by increasing the Doppler feedback in the core. Increasing the height of the inner axial blanket increases the Doppler feedback and thus the UTOP behavior.

It can be concluded that for the UTOP, the core optimization will be closely related to the reference transient used for the design and the constraints on other estimators such as the pressure drop or the core production. Any increase in the amount of minor actinides loaded leads to a penalty on the core power or geometry due to Doppler feedback decrease caused by minor actinides loading. It can also be observed that the behavior of the inner axial blanket is opposite between the ULOF and UTOP transient. Considering this, a complete optimization taking into account the three parameters will have to be carried out.

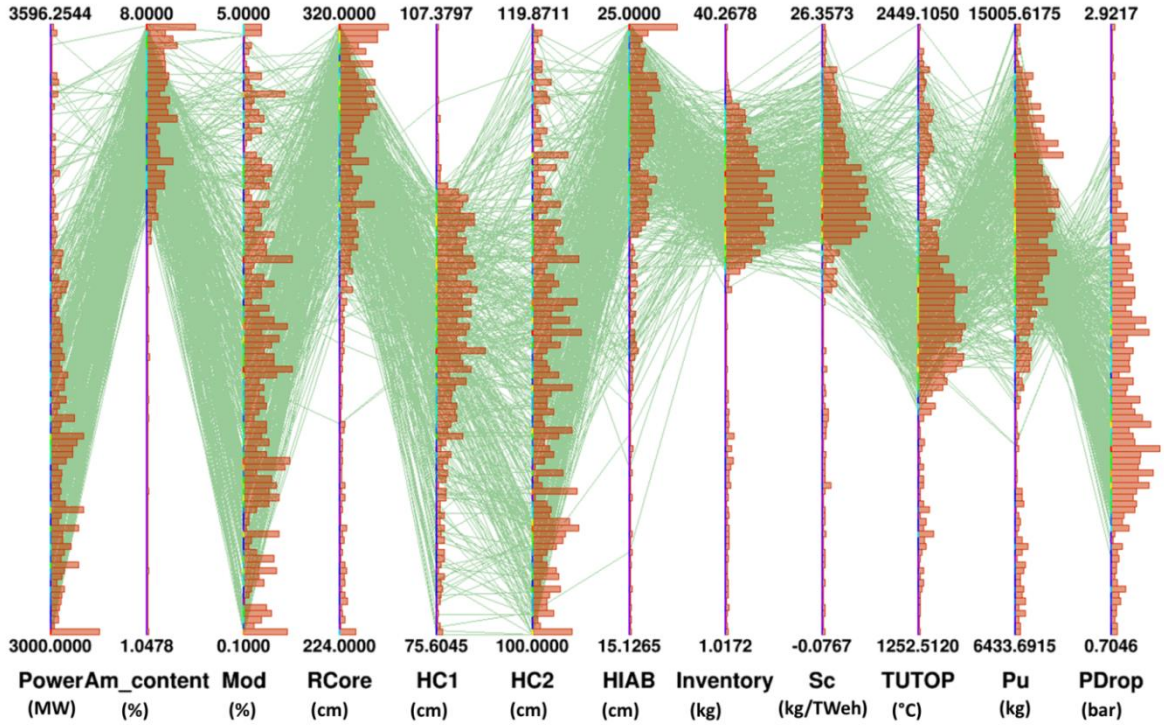

Figure 104 : Optimal cases for the UTOP transient where all the parameters unrelated to assemblies' geometry are considered

d) COMPLETE OPTIMIZATION

The next step in the optimization process is to run it while considering the minimization of the three reference transient response along with the minimization of the inventory and the maximization of the americium consumption, especially considering the opposite behavior of the ULOHS and UTOP optimization. The following optimization was launched:

- Parameters : core power, inner and outer core heights, americium content
- Estimators : americium consumption, maximal sodium temperature during ULOF, americium inventory in the fuel cycle; final sodium temperature during ULOHS, maximal fuel temperature during UTOP
- Constraints : maximal decay heat reprocessing of 7.5 kW
- Transient: 90 % decrease of the primary flow with a half time of 24 s for the ULOF, total linear decrease of the secondary sodium flow for the ULOHS and 150 pcm inserted in 250 s for the UTOP

The corresponding results are shown in Figure 105. The opposite behavior of the power and the minor actinides content is clearly visible, which comes from the UTOP part of the optimization. The inner core height is limited, in order to keep acceptable performances for an ULOHS

transient. A wide range of consumption can be achieved, with a maximal consumption of nearly 2.8 tons of americium over the irradiation. The opposition between the ULOHS optimized core and the UTOP optimized one is visible, with the cores yielding the highest ULOHS temperature corresponding to the cores with limited UTOP fuel temperature. Overall, the dimensioning transient here appears to be the ULOHS transient.

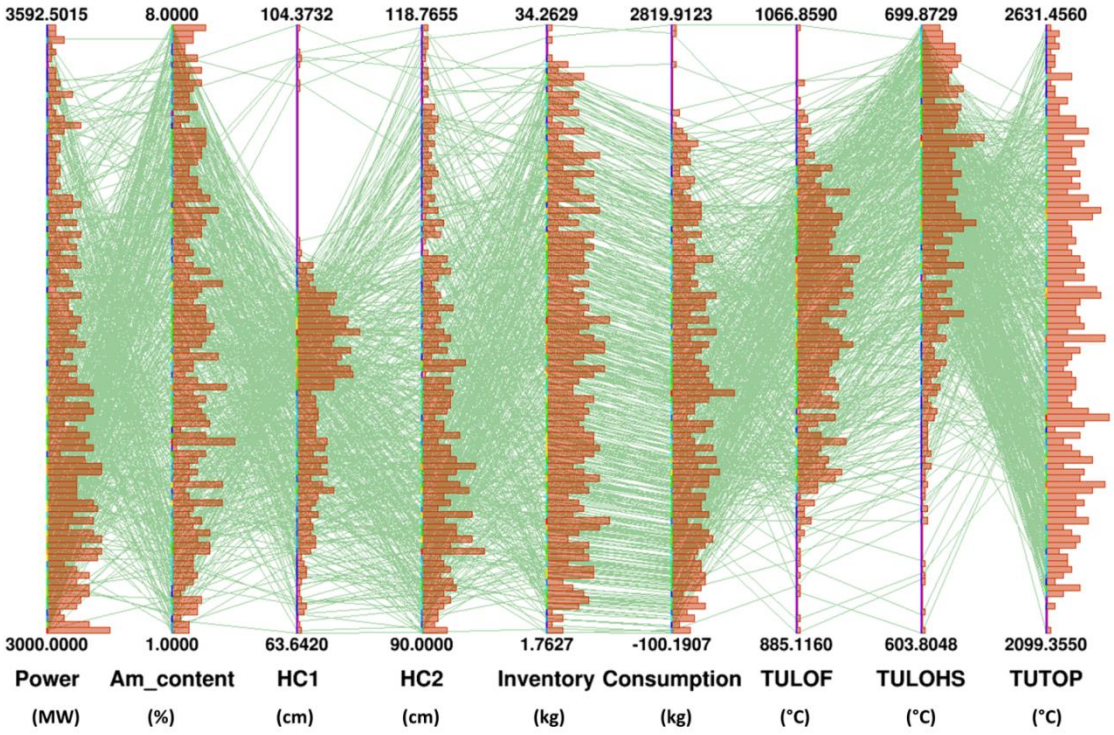

Figure 105 : Optimal cases obtained when considering all transients.

In a similar fashion as with the three previous transients, the following approach was then used:

- Parameters : core power, inner and outer core heights, americium content
- Estimators : americium consumption, maximal sodium temperature during ULOF, americium inventory in the fuel cycle; final sodium temperature during ULOHS, maximal fuel temperature during UTOP, plutonium inventory in the core and pressure drop in the assembly
- Constraints : maximal decay heat reprocessing of 7.5 kW
- Transient: 90 % decrease of the flow with a half time of 24 s.

The results are shown in Figure 106. As the plutonium inventory and pressure drop were added to the estimators of interest, the optimization process favored smaller cores in order to limit these two quantities. This specificity apart, the opposition between ULOHS and UTOP is still observable in this case. The next step is to run a complete optimization with all the parameters and estimators used here. The results are shown in Figure 107 are similar to the results obtained for the ULOHS, with small inner cores, high minor actinides content and low amount of moderating material with large cores. No conclusion can be reached regarding the role of the inner fertile layer.

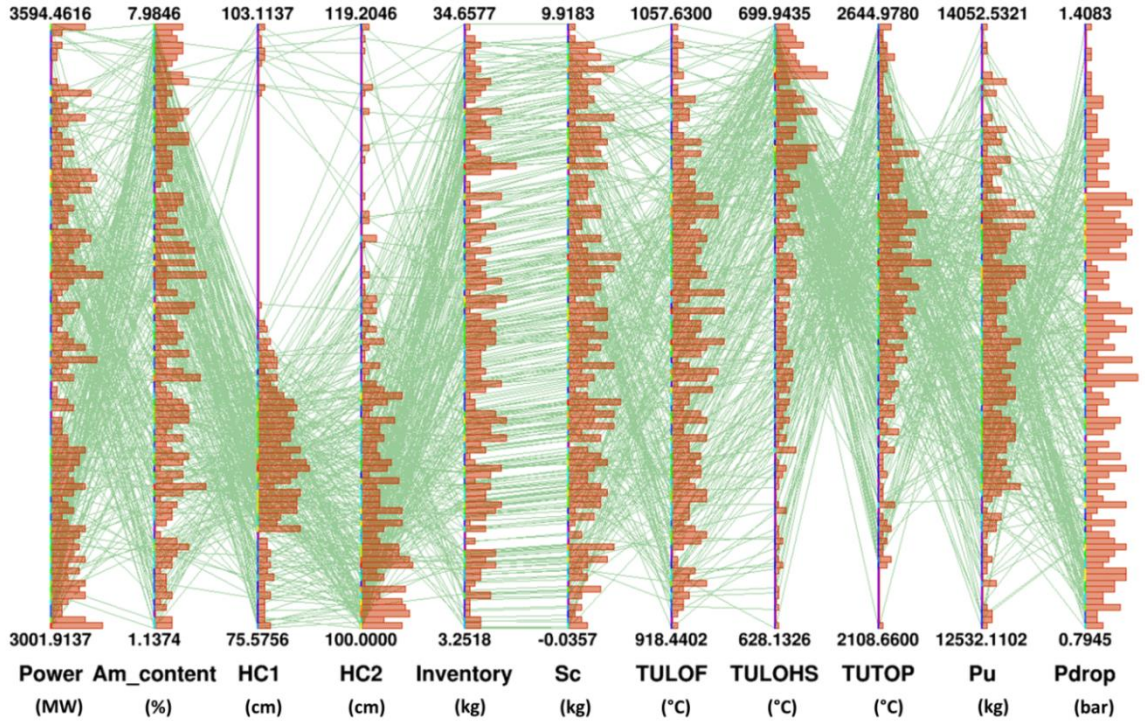

Figure 106 : Optimal cases obtained when considering all transients along with the plutonium inventory and pressure drop

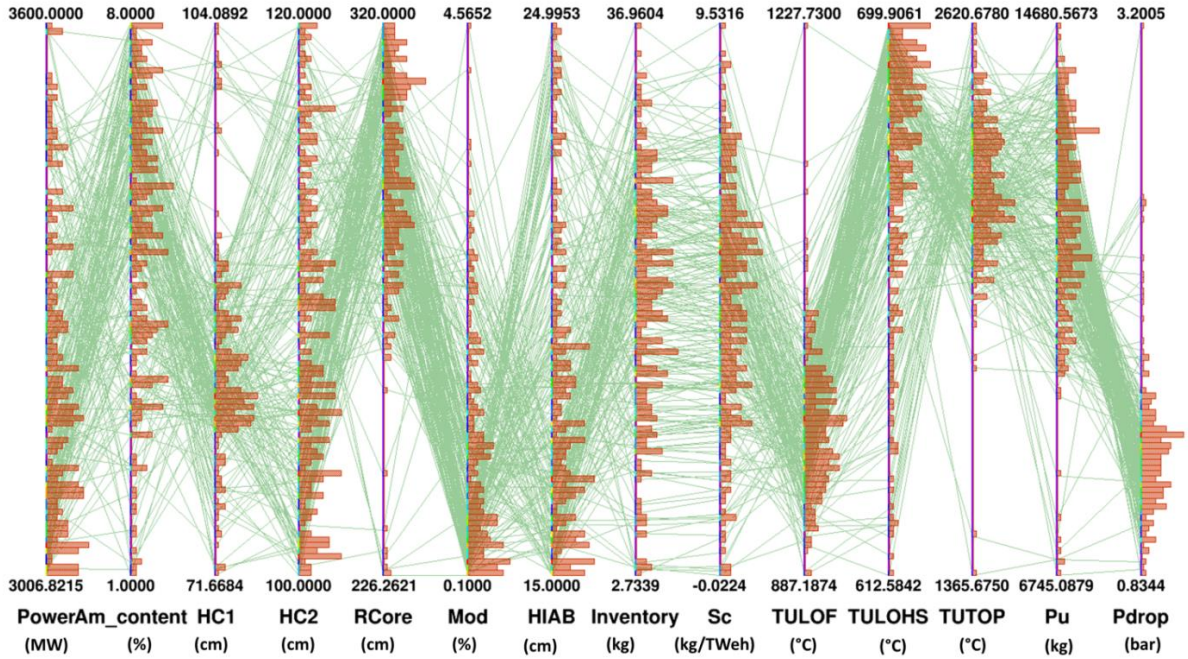

Figure 107 : Optimal cases obtained when considering all transients and considering all the parameters of interest.

As a final point of this part, it can be concluded from this analysis that:

- **Axially heterogeneous cores with relatively low power and high minor actinides content are optimal for minor actinides transmutation, with small inner cores and high outer cores.**
- **It appears not necessary to add moderating material to the core to achieve this result.**
- **The ULOHS transient behavior appears to be the limiting factor regarding the core design, given the transients considered here.**

Further refinements are necessary here, specifically to achieve a more accurate treatment of the UTOP transient. However, the objectives of the study, which were to identify trends which regards to core design and minor actinides incorporation have been reached. It is planned in the future to select an optimal core obtained using this methodology and to qualify it using more refined neutronic and thermal hydraulics tools.

3) UNCERTAINTIES

The uncertainties concerning the results obtained here can be linked to three sources, which are :

- The nuclear data uncertainties associated with the core calculation
- The uncertainties coming the use of the meta-models
- The uncertainties coming from the simplified approach implemented in the MAT4DYN (along with the approximations also made in the code compared to a more detailed code such as CATHARE)

These sources will be discussed and evaluated to the extent possible.

a) NUCLEAR DATA UNCERTAINTIES

The JEFF 3.1 nuclear data library [37] was used for all the calculations carried out in this work. The nuclear data found in these libraries are associated with uncertainties coming from the physical experiments carried out to obtain these data. Using the EGPT theory [87], it is possible to compute the sensitivity of a reactivity variation to a given cross section as defined in Equation 28. This sensitivity represents the relative variation of the integral value Δρ due to a variation of the $\sigma_{r,i,g}$ parameter, where $\sigma_{r,i,g}$ represents the cross section for the reaction *r* on the isotope *i* in the energy group *g*.

$$S(\Delta\rho, \sigma) = \frac{\frac{\Delta(\Delta\rho)}{\Delta\rho}}{\frac{\Delta\sigma_{r,i,g}}{\sigma_{r,i,g}}} \quad (2)$$

Equation 28 : Definition of the sensitivity coefficient of a reactivity variation to a cross section variation

Knowing the sensibilities of a reactivity change with regards to the cross sections, it is possible to derive the associated uncertainties by applying the so-called “Sandwich Formula” given in Equation 29 to the sensibilities matrix S. The M matrix in this formula represents the covariance

matrix of the uncertainties on the cross sections. The COMAC V0 matrix developed at CEA was used for this study [88].

$$U(\Delta\rho) = \sqrt{S^{+}MS} \quad (3)$$

Equation 29 : "Sandwich" formula

This approach was used to compute the uncertainties associated with the sodium void worth and Doppler Effect of the whole core. It was then considered that this uncertainty could be applied to the complete Doppler and sodium thermal expansion and it was propagated using a brute force approach to evaluate the spread of the temperature estimators due to the uncertainties on the nuclear data.

These uncertainties were computed for the ULOHS optimized core described in the next paragraph in Table 62 because it presented the highest minor actinides content. They are shown in Table 59 and Table 60 for the Doppler Effect and sodium void worth respectively. In both cases, ^{238}U is the main contributor to the total uncertainty, with ^{239}Pu adding a similar contribution for the sodium void worth case. The contribution of the two americium isotopes loaded is relatively limited in both cases.

Table 59 : Nuclear data uncertainties on the Doppler Effect of the ULOHS optimized core. The total uncertainty is expressed in % of $\Delta\rho$

Nuclide	Capture	Fission	Elastic	Inelastic	N,XN	Nu	Total
^{235}U	0,13	0,01	0,01	<0,01	<0,01	0,01	0,13
^{238}U	3,03	0,08	0,17	0,58	0,01	0,09	3,09
^{238}Pu	0,11	<0,01	0,01	<0,01	<0,01	0,08	0,14
^{239}Pu	0,55	0,72	0,04	0,04	<0,01	0,12	0,91
^{241}Am	0,50	0,02	0,02	0,06	<0,01	0,01	0,50
^{242m}Am	<0,01	<0,01	<0,01	<0,01	<0,01	<0,01	<0,01
^{243}Am	0,35	0,03	0,01	0,04	<0,01	<0,01	0,36
^{237}Np	<0,01	<0,01	<0,01	<0,01	<0,01	<0,01	<0,01
^{243}Cm	<0,01	<0,01	<0,01	<0,01	<0,01	<0,01	<0,01
^{244}Cm	<0,01	<0,01	<0,01	<0,01	<0,01	<0,01	<0,01
^{245}Cm	<0,01	<0,01	<0,01	<0,01	<0,01	<0,01	<0,01
^{23}Na	0,07	<0,01	0,64	0,01	<0,01	<0,01	0,64
^{56}Fe	0,14	<0,01	0,65	0,05	<0,01	<0,01	0,66
TOTAL	3,14	0,72	0,92	0,59	0,01	0,18	3,41

Table 60 : Nuclear data uncertainties on the sodium void worth of the ULOHS optimized core. The total uncertainty is expressed in % of $\Delta\rho$

Nuclide	Capture	Fission	Elastic	Inelastic	N,XN	Nu	Total
^{235}U	0,12	0,08	0,02	0,02	0,00	0,04	0,15
^{238}U	4,86	6,25	1,12	4,89	0,04	0,72	9,26
^{238}Pu	0,37	0,10	0,04	0,03	<0,01	0,18	0,43
^{239}Pu	2,17	9,02	0,15	0,09	<0,01	1,22	9,35
^{241}Am	1,68	0,44	0,17	0,40	<0,01	0,54	1,87
^{242m}Am	<0,01	<0,01	<0,01	<0,01	<0,01	<0,01	<0,01
^{243}Am	0,94	0,59	0,09	0,35	<0,01	0,10	1,17
^{237}Np	<0,01	<0,01	<0,01	<0,01	<0,01	<0,01	<0,01
^{243}Cm	<0,01	<0,01	<0,01	<0,01	<0,01	<0,01	<0,01
^{244}Cm	<0,01	<0,01	<0,01	<0,01	<0,01	<0,01	<0,01
^{245}Cm	<0,01	<0,01	<0,01	<0,01	<0,01	<0,01	<0,01
^{23}Na	2,22	<0,01	2,72	2,52	0,01	<0,01	4,32
^{56}Fe	2,03	<0,01	2,78	1,04	<0,01	<0,01	3,59
TOTAL	6,42	11,00	3,72	5,62	0,04	1,53	14,50

The Doppler Effect and sodium thermal expansion profile were then modified by considering a normal distribution of the thermal expansion and Doppler profile around their calculated value and with a standard deviation equal to the total uncertainty due to the nuclear data. A thousand calculations are then performed to evaluate the corresponding error on the transients' estimators. The results are show below in Table 61. The corresponding standard deviation for each estimator is relatively low, with the biggest being obtained for the ULOF transient.

Table 61 : Comparison of the mean value and standard deviation of the transient behavior estimators when nuclear data uncertainties are taken into account

	Max sodium temperature ULOF	Final sodium temperature ULOHS	Max fuel temperature UTOP
Mean value (°C)	965	670	2521
Standard deviation (°C)	25	14	20

b) META-MODELS UNCERTAINTIES

Regarding the meta-models uncertainties, two approaches were considered. First, the optimized cores using the methodology were calculated using the ERANOS code system and the results compared with the Artificial Neural Networks output. In a second time, a brute force approach was used to compute the dispersion of the results around the optimized cases.

For the ULOF transient, an arbitrary core from the optimal set of cores was selected with consumption close to 1 ton of americium per cycle. This core is also part of the optimal set of cores obtained for the UTOP transient, as it can be seen on Figure 101. The corresponding core is shown in Table 62. These core parameters were calculated using either the methodology

artificial neural networks or a full ERANOS calculation. The results are compared in Table 63. A globally very good agreement between the two calculations can be observed, with a maximal error of 3.8 % for the outputs of interest (transient behavior and americium consumption).

Table 62 : Optimal cores selected for comparison with ERANOS for the three references transient

Parameter	Unit	ULOF & UTOP Core	ULOHS core
Core power	MWth	3600	3600
Outer core height	cm	115,2	94,3
Inner core height	cm	103,2	66
Am	at%	3,43	8
Inner axial blanket thickness	cm	20	20
Core radius	cm	320	320
Fuel volume fraction	%	42	42
Sodium volume fraction	%	28	28
Moderator fraction	%	0	0

Table 63 : Comparison between the meta-models and ERANOs of the output and core parameters for the optimized ULOF & UTOP core

Parameter	Unit	ERANOS	ANN	Difference (%)
Maximal sodium temperature during ULOF	°C	1255	1288	-2,6
Final sodium temperature during ULOHS	°C	835	840	-0,6
Maximal fuel temperature during UTOP	°C	2125	2130	-0,2
Am consumption	kg	1102	1060	3,8
Pu inventory	kg	14049	13896	1,1
Initial Am	kg	2479	2512	-1,3
Final Am	kg	1377	1452	-5,4
Mean Pu content	%	19,5	19,76	-1,3
Beta eff	pcm	342	355	-3,8
Lambda	s	3,54E-07	3,73E-07	-5,4
Grid feedback	pcm/K	-7,26E-01	-7,16E-01	1,4
Structural feedback	pcm/K	9,60E-02	1,01E-01	-5,1
Fuel expansion feedback	pcm/K	-1,52E-01	-1,66E-01	-8,9
Doppler LAB	pcm/K	-5,91E+01	-5,71E+01	-3,5
Dopp fuel	pcm/K	-2,25E+02	-2,52E+02	10,7
Dopp IAB	pcm/K	-1,90E+02	-1,83E+02	-4,2
Sodium thermal expansion fuel	pcm/K	1,43E+01	1,41E+01	-1,4
Sodium thermal expansion IAB	pcm/K	4,80E+00	4,80E+00	0,1
Sodium thermal expansion gas expansion plenum	pcm/K	-6,13E-01	-6,00E-01	-2,2
Sodium thermal expansion sodium plenum	pcm/K	-3,51E+00	-3,20E+00	-9,6
Fraction of power in LAB	% of total power	1,94E-02	1,92E-02	-1,3
Fraction of power in lower fuel	% of total power	4,95E-01	5,03E-01	1,6
Fraction of power in IAB	% of total power	3,63E-02	3,47E-02	-4,6
Fraction of power in upper core	% of total power	4,49E-01	4,38E-01	-2,6
Power in the most active mesh of ERANOS calculation	% of total power	3,30E-02	3,07E-02	-7,5
Position of the most active mesh	cm	1,61E+02	1,56E+02	-3,3

A similar exercise was carried out for the optimized ULOHS core described in Table 63, which lies at the far end of the core designs investigated with a very small inner core and high americium content. The corresponding results are shown in Table 64. Similarly to the ULOF case, the difference between the ERANOS calculations and the meta-models one is very limited, with once again the biggest error being observed on the americium consumption.

Table 64 : Comparison between the meta-models and ERANOs of the output and core parameters for the optimized ULOHS core

Parameter	Unit	ERANOS	ANN	Difference (%)
Maximal sodium temperature during ULOF	°C	960	961	-0,1
Final sodium temperature during ULOHS	°C	665	663	0,3
Maximal fuel temperature during UTOP	°C	2520	2535	-0,6
Am consumption	kg	1632	1708	-4,7
Pu inventory	kg	13101	13022	0,6
Initial Am	kg	3651	3682	-0,8
Final Am	kg	2019	1973	2,3
Mean Pu content	%	28,4	26,8	5,6
Beta eff	pcm	323	326	-0,9
Lambda	s	2,55E-07	2,81E-07	-10,3
Grid feedback	pcm/K	-9,01E-01	-8,97E-01	0,5
Structural feedback	pcm/K	7,61E-02	7,80E-02	-2,5
Fuel expansion feedback	pcm/K	-1,56E-01	-1,56E-01	0,2
Doppler LAB	pcm/K	-8,96E+01	-8,25E+01	8,0
Doppler fuel	pcm/K	-1,01E+02	-1,01E+02	-0,2
Doppler IAB	pcm/K	-1,76E+02	-1,70E+02	3,6
Sodium thermal expansion fuel	pcm/K	8,69E+00	8,40E+00	3,3
Sodium thermal expansion IA	pcm/K	5,13E+00	5,10E+00	0,6
Sodium thermal expansion gas expansion plenum	pcm/K	-1,09E+00	-1,10E+00	-0,8
Thermal expansion sodium plenum	pcm/K	-7,14E+00	-7,40E+00	-3,7
Fraction of power in FCAI	% of total power	2,61E-02	2,31E-02	-13,0
Fraction of power in lower fuel	% of total power	4,94E-01	4,90E-01	-0,7
Fraction of power in IAB	% of total power	3,96E-02	3,81E-02	-3,9
Fraction of power in upper core	% of total power	4,40E-01	4,46E-01	1,4
Power in the most active mesh of ERANOS calculation	% of total power	5,39E-02	5,06E-02	-6,7
Position of the most active mesh	cm	143,8	143,4	-0,3

These selected cases yielded very good agreement with a complete ERANOS calculation. To further refine the analysis of the uncertainties associated with the meta-models, a brute-force approach was used where the feedbacks coefficients, kinetic parameters and core power profiles were randomly sampled following a normal law with a mean corresponding to the calculated value for the reference ULOHS core and with a standard deviation corresponding to the ANN standard deviation. The dispersion of the results is given below in Table 65. The final and maximal sodium temperatures are very slightly impacted by the meta-modelling uncertainties, while the UTOP transient exhibit an important uncertainty on the maximal fuel temperature. It was verified that the uncertainty on the helium production did not modify the

assembly geometry and thus the core behavior. It actually appears that helium production is not a limiting factor for assembly design in the case of homogeneous transmutation.

Table 65 : Comparison of the mean value and standard deviation of the transient behavior estimators when meta-models uncertainties on the feedback coefficients is taken into account

	Max sodium temperature ULOF	Final sodium temperature ULOHS	Max fuel temperature UTOP
Mean value (°C)	965	670	2521
Standard deviation (°C)	7	4	46

c) TRANSIENT CALCULATION UNCERTAINTIES

It was shown in Table 48 that the use of flattened profiles for power, Doppler Effect and sodium thermal expansion feedback introduced a limited error to the transient calculations. However, it is of interest to evaluate the difference between the MAT4DYN, which is a mono-channel with simplified hypothesis on the core behavior and a more detailed code. Since it was not possible to carry out complete CATHARE calculations of the optimized core, the MACARENA code was used for comparison purpose. This tool is an analytical tool recently developed by CEA for statistical studies of the ULOF transient and validated against experimental data and the SIMMER system code [89].

Validation was carried out by comparing the output of the code for the core given in Table 64. The results are plotted below in Figure 108 and it can be seen that there is a limited discrepancy of 35 °C between the two approaches on the maximal sodium outlet temperature obtained during an ULOF. The core behavior after the peak exhibits a slightly smaller difference. Overall, the time evolution of the transient is very similar. A point of interest here is that the MAT4DYN calculated temperature is higher than the MACARENA one. Considering the MACARENA takes into account additional physical models, it can be assumed that the calculations carried out in this work are conservative.

Regarding the evolution of the core power and reactivity as shown in Figure 109 and Figure 110, a very good agreement is achieved between the two codes. The slightly higher power in MAT4DYN is consistent with the higher sodium peak temperature. Looking at the evolution of the reactivity during the transient, the difference in core behavior can be explained by a different modelling of the control rods drive mechanisms, which is done with additional details in MACARENA. Overall, this hints at the reproducibility of the calculations using another calculation tool for the transient part and their accuracy, although it does not add more information about the trueness of the results obtained.

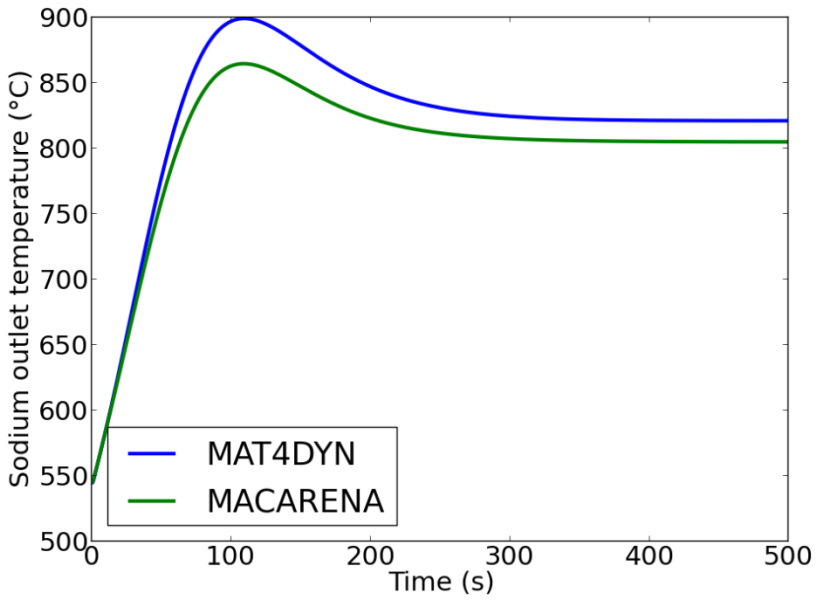

Figure 108 : Comparison of the sodium outlet temperature during an ULOF with MACARENA and MAT4DYN

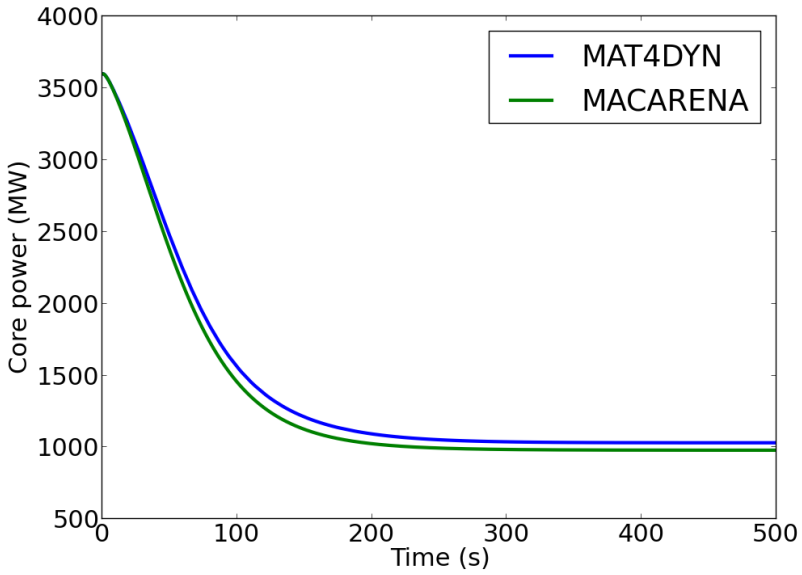

Figure 109 : Comparison of the core power during an ULOF with MACARENA and MAT4DYN

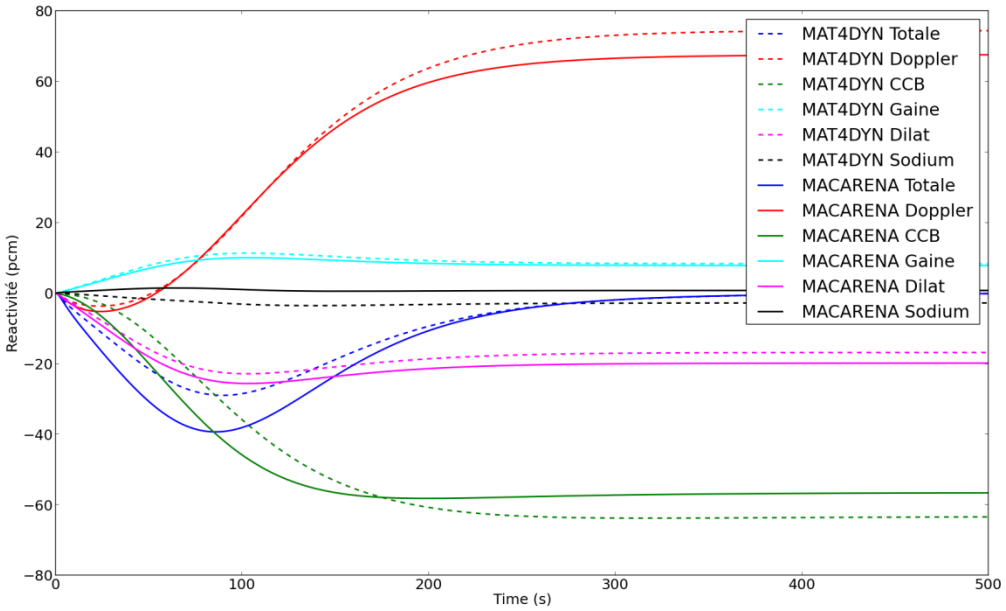

Figure 110 : Comparison of the reactivity evolution during a n ULOF with MAT4DYn and MACARENA

d) Conclusions on uncertainties

Considering the high number of approximations used in this work, several comments can be made on the actual uncertainties associated with the results:

- The overall precision (e.g. dispersion of the results due to meta-modelling uncertainties) is relatively good for ULOF and ULOHS transients but higher for the UTOP.
- The uncertainties associated to nuclear data has been roughly evaluated and is higher than the one associated to meta-models for ULOF and ULOHS transients.
- There is a good agreement between the complete ERANOS calculations and the ANN-made calculations for two tests cases with “extreme” geometry.
- Very limited differences were observed during the comparison of the MAT4DYN and MACARENA code.

Overall, the methodology developed here exhibits a good precision but its accuracy with regards to the real transient behavior of a core is unknown. Nevertheless, its use for tendency analysis and evaluation of trends appears as good compromise between simplified calculations and full transients evaluation.

4) Comparison with the heterogeneous approach and application to industrial constraints

Similarly to the heterogeneous case, a hierarchy of the industrial constraints can be drawn using the methodology developed here. A reference heterogeneous case was considered as a comparison point to design two homogeneous cores with acceptable transient performances

and same consumption or same inventories as the reference core, as shown in Table 66. However, this hierarchy is strongly dependent on the actual transients. For instance, the cores shown in Table 66 are acceptable with regards to the reference transients but may not be acceptable for more penalizing transients.

For similar consumption, the heterogeneous approach requires a much longer irradiation time compared to the homogeneous approach. This is explained by the lower flux level in the blankets previously mentioned. The shorter residence time in the homogeneous case leads to a much greater specific consumption, which a difference which increases when the core production in the heterogeneous case is taken into account. The associated fuel cycle inventory in the homogeneous case is slightly higher as it is necessary to load more americium to consume the same mass due to the lower transmutation rate. Nevertheless, in terms of specific consumption, the homogeneous approach yields a clear advantage.

For comparison purpose, a second core with a similar inventory in the fuel cycle was designed. In this case, the specific consumption is slightly lower than the heterogeneous case (without core production taken into account) at 5.8 kg/TWhe. However, it is still twice as high if the core production if also considered, for a similar inventory and for acceptable transient behaviors. It can be concluded from this analysis that the homogeneous approach with heterogeneous core yields significant advantages compared to the heterogeneous approach. Nevertheless, a second point which was not considered in this work is the fact that the dilution of minor actinides in the fuel leads to a contamination of the entire fuel cycle and then to the treatment of a bigger volume of fuel, albeit with a lower specific activity than in the heterogeneous case.

The actual selection of a strategy thus requires economical appraisal of the choice between a unique facility treating a small number of assemblies with a high content of minor actinides or a dilution of the same mass of minor actinides in the entire facility but to a much lower content, thus requiring a shielding upgrade of the reprocessing facilities.

Table 66 : Comparison of an optimized heterogeneous strategy and a homogeneous approach with a similar consumption

Strategy	Heterogeneous	Homogeneous same consumption	Homogeneous same inventory
Total consumption (kg)	**1428**	**1422**	608
Residence time (EFPD)	5950	3019	3019
Am content in the fuel (at%)	20	4.9	2.7
Initial loading (kg)	1896	3143	1794
Specific consumption (kg/TWhe)	6.9 (2.7 with core production)	13.5	5.8
Fuel cycle inventory (kg)	**2710**	4936	**2719**
Maximal sodium temperature during ULOF (without DCS) (°C)	/	999	998
Final sodium temperature during ULOHS (°C)		664	673
Maximal fuel temperature during UTOP (°C)		2258	2227

As the transient performance comparison is not relevant for heterogeneous transmutation, this part will be focused on fuel cycle constraint. We will consider the core given in Table 66 with similar consumption as the optimized heterogeneous core. As in Chapter 4, we will evaluate the decay of the fresh and irradiated assembly and find the limiting constraints. The decay heat of the inner fertile blanket and lower fertile blanket will be neglected in this work as they are much lower as the one of the fissile part of the assembly.

The assembly parameters for this core are given for the inner and outer core in Table 67. None of the constraints described in Chapter 4 are verified here, to know:

- A maximal heat load of 550 W per fresh assembly if the transport is carried in casks of 6 assemblies
- A maximal sodium washing limit of 2.5 kW after 5 years of cooling for irradiated assemblies.

As for the heterogeneous case, transportation of the fresh assemblies is the first limiting point, followed by sodium washing. Implementation of minor actinides transmutation with 4.9 % of minor actinides in the fuel would require going from 6-assemblies casks to 4 assemblies-casks in order to raise the maximal heat for fresh assembly to 800 W per assembly. This would mechanically lead to a 50 % increase in the total number of fuel movements.

Regardless of the case, the washing limit of 2.5 kW per assembly is always exceeded. Similarly to the heterogeneous case, it will thus be necessary to raise this limit to implement homogeneous minor actinides transmutation. In conclusion, it can be said that the same constraints are limiting for the homogeneous and heterogeneous approach here, but the extent to which they need to be raised differs.

Indeed, to achieve the same total consumption, it is necessary to reach the washing transportation limit to nearly 2 kW and the washing limit to 5.5 kW in the heterogeneous approach, while using it is possible to transport fresh assemblies for homogeneous transmutation with available transportation casks and to reprocess them with a washing limit of around 4.2 kW.

Table 67 : Fuel cycle data for the optimized core shown in Table 67

	Heterogeneous	Homogeneous same consumption		Homogeneous same inventory	
		Inner core assembly	Outer core assembly	Inner core assembly	Outer core assembly
Fissile mass (kg)	116	132	181	132	181
Am content (%)	20	4,9	4,9	2.7	2.7
Heat load of fresh assembly (W)	**2040**	**565**	**774**	311	426
Decay heat after 5 years of cooling (kW)	**5,53**	**3,92**	**4,22**	**2,9**	**3,1**
Cooling time to 2,5 kW (days)	19000	8020	12921	3202	4886

5) CONCLUSIONS

Compared to the heterogeneous approach, the homogeneous loading of minor actinides in a reactor differs mainly by the modification of the core feedback coefficients, which in turns modifies the core behavior during selected transient. The aim of this chapter was to design an optimization methodology taking into account these modifications to obtain a core design suited for minor actinides transmutation with acceptable transient behavior.

A core with axial heterogeneity was selected as the starting point for this study and it was first shown that the impacts of minor actinides loading in such a core was much lower compared to an homogeneous core as designed in the past. From this, a methodology based on the coupling of ANNs with a mono channel transient code was developed to optimize the core geometric parameters with regards to transient and fuel cycle impacts.

It was shown that the transient behavior of such cores during a loss of flow in the primary or secondary circuit was barely affected by the incorporation of minor actinides in the fuel. This was explained for the ULOF by the compensation effect between the decrease in the Doppler feedback and the increase in the sodium thermal expansion feedback, as the Doppler feedback inserts positive reactivity during this transient. For the ULOHS, the addition of minor actinides even had a positive impact on core behavior as the Doppler feedback is the main contributor to positive reactivity insertion during this transient. Consequently, reactivity transients were the most impacted as the Doppler feedback is main contributor to negative insertion for this transients.

Nevertheless, it was shown that the addition of minor actinides in the core did not prevent the design of acceptable cores with a wide range of consumption available. Generally speaking, two opposite trends were identified:

- Tall cores with low minor actinides content, which were more favorable for the UTOP transient due to their lower linear heat rate and higher Doppler feedback
- Small cores with high minor actinides content, which were more favorable for the ULOHS transient due to their lower Doppler feedback and higher grid expansion feedback.

Considering the uncertainties associated with this work and the tools used, it is not possible to give a detailed design of a “perfect” core. However, it is possible to use the results to highlight several trends in the core behavior while exploring the entirety of the acceptable design space. Additionally, this work was limited by the definition of the reference transient, which depends on industrial parameters out of the scope of this study. It is still possible to conclude that an actual core design will result in a tradeoff between ULOHS and UTOP performances which will depend on additional considerations.

Such an optimized core (for the reference transients considered) was compared with the optimal heterogeneous solution obtained in Chapter 4 and it was shown that the homogeneous approach was more interesting in terms of specific consumption or of inventory compared to the heterogeneous one. However, it should be mentioned that the current industrial fuel cycle constraints were still too strong to allow significant homogeneous loading.

CHAPTER 6: CONCLUSION

1) POSITION OF THE PROBLEM

Minor actinides represent a very limited part of the spent fuel unloaded from nuclear reactors, but in the situation of a closed fuel cycle where plutonium is recycled as MOX fuel, they represent the main contributor to long-term radiotoxicity of the nuclear waste. Additionally, they become the main nuclei present in the waste packages emitting significant heat and thus one of the dimensioning factors of the deep geological storage facilities.

A transmutation strategy represents the entire process of recovering the minor actinides from the spent fuel through an adequate reprocessing scheme and to submit them to a neutron flux in order to achieve fission of these nuclei and turn them into shorter-lived fission products. A 100% efficient transmutation strategy would thus lead to a decrease of the long-term radiotoxicity of the fuel by two orders of magnitudes and would divide by three the storage area of a deep geological facility.

Various options exist to irradiate minor actinides, with the most promising currently being the use of sodium fast reactors. This work focus on this reactor design for two main reasons:

- Light-water reactors and more generally thermal reactors are not suited for minor actinides transmutation due to their neutron spectrum, which prevents closure of the fuel cycle and exhibit unfavorable fission to capture ratios.
- Among the fast reactor designs currently envisioned, sodium cooled fast reactors are the ones with the highest industrial experience. With the ASTRID project, France is definitively committed sodium cooled fast reactors, which have been chosen as the best candidate for GEN IV reactors.

Nevertheless, loading minor actinides in SFRs might have negative impacts on the core feedback coefficients which change its behavior during various incidental transients. Additionally, their necessary multi-recycling “pollutes” every step of the fuel cycle with minor actinides which are generally more radioactive than regular fuel.

This work was mainly dedicated to the development of an optimization methodology aiming at designing an optimal reactor core with regards not only to its minor actinides consumption but also to the associated negative impacts on the fuel cycle and on its natural behavior for a selection of transients. Additional work was carried out to explore innovative solutions for minor actinides transmutation.

In a first stage, an historical review of the transmutation studies have been carried out and two main approaches have been selected, namely the heterogeneous transmutation, in which minor actinides are loaded in dedicated targets generally located at the core periphery, and the homogeneous transmutation, in which minor actinides are directly diluted in the fuel. The physics processes and specificities of both approaches were analyzed and it was verified that no threshold effect appeared related to the minor actinides content and that a limited number of variables were sufficient to characterize the entire transmutation process, namely the minor

actinides content in the fuel and the neutron spectrum, along with the irradiation time and associated flux level.

Then, industrial constraints related to fuel cycle and core behavior were identified. Concerning the fuel cycle, two strong limitations were found, to know:

- A maximal heat load of the fresh assembly limited from 550 W to 800 W in order to limit the number of transports of minor actinides loaded assemblies, with the actual limit depending on the type of casks used (available or foreseen technologies).
- A maximal heat load of the spent fuel assembly limited from 2.5 to 7.5 kW due to limitations on the washing device necessary to remove residual sodium left in the assemblies before transportation and reprocessing can take place.

Finally, an analysis of the constraints linked to the assembly design of minor actinides bearing targets was carried out in order to obtain mechanically acceptable assembly design. The problem was thus entirely characterized and an adequate optimization methodology was developed. **The aim of this methodology was to be versatile enough to explore the entire range of physically realistic configurations at a reasonable computation cost and to identify general trends for minor actinides transmutation optimization.**

2) OPTIMALITY OF TRANSMUTATION STRATEGIES

Considering the scope of the study, meta-models were used to supplement full core calculations, which would have required prohibitive calculation time. Artificial neural networks were trained and validated to compute physical estimators related to minor actinides transmutation performances (specific consumption), fuel cycle impacts (cooling time or inventory in the fuel cycle) or core performances during transient (maximal temperature for sodium or fuel). A genetic algorithm was then used to evaluate a great number of cases and select the optimal ones with regards to the estimators described above.

In a first stage, heterogeneous transmutation was analyzed. Using this strategy, the perturbations on the core transient behavior can be considered as negligible. Using the approach described in the previous section, it was shown that **the use of moderating materials in radial blankets was an optimal solution, even when considering their negative impacts on the production of heat-emitting nuclei such as curium.**

Additional results were obtained for this transmutation approach. Namely, it was demonstrated that the use of metallic fuel in the core and blankets yields better performances than the corresponding oxide option, as the faster spectrum in the metallic core limits the production of minor actinides in the fuel. An innovative approach where small amount of fissile material is loaded within the targets was also characterized and it was shown that it was equivalent to the “moderated” approach.

A hierarchy of the industrial constraints associated with this strategy was also produced and it was shown that design constraints were of secondary order compared to fuel cycle constraints and **that it was not possible to achieve equilibrium between core production and blankets consumption with the current set of constraints**. This should drive R&D program to lift such constraints if MA transmutation is planned in a fast reactor deployment strategy.

Concerning the homogeneous approach, the core behavior during three selected transients (loss of flow in primary or secondary circuit and slow reactivity insertion) was taken into account in addition to the transmutation performances and fuel cycles impacts. Axially heterogeneous cores were considered and it was shown that in opposition to homogeneous cores, **the addition of minor actinides in the fuel did not negatively impact the core behavior during loss of flow transients.** This was explained by compensation between the decrease in the Doppler feedback and the increase in the sodium void worth of the core due to minor actinides loading.

On the other hand, the core behavior during a reactivity insertion was still negatively impacted by the addition of minor actinides due to the Doppler feedback decrease. Various options were proposed to counteract this effect, such as an increase in the core height at the expense of the plutonium inventory, or the addition of moderating material in the core in limited amounts to compensate for the Doppler decrease. It was also shown that fuel cycle constraints were also limiting minor actinides loading in the homogeneous case and that **significant loading of minor actinides still requires improvements on the different fuel cycle stages.**

Finally, two optimized cases for both strategies were compared and it was shown that it was possible to design cores with high minor actinides content and similar acceptable transient behavior than the original core which exhibit better transmutation performances than optimized blankets assemblies.

3) RESEARCH PERSPECTIVES

Various research avenues have been opened by the results obtained using the methodology developed here, along with additional options to be implemented to further refine the analysis. For instance, if the homogeneous approach using geometrical heterogeneous core design has been shown as more interesting than the use of minor actinides bearing blankets, its implementation requires the modification of the entirety of the fuel cycle facilities in order to accommodate minor actinides loading, which may have a prohibitive economic cost. It would thus be necessary to add to the methodology a cost analysis function which could be used to compare two strategies with regards to their associated costs and then draw a more general conclusion.

A second point of interest would be to refine the analysis of the optimized cores for homogeneous transmutation using complete systems codes such as CATHARE or SIMMER and additional industrial design constraints coming from the plant engineering or the control rods design. In a similar fashion, design and qualification of assemblies and fuels for the moderated heterogeneous approach should be carried out.

Finally, the observation that low-void effect cores are suitable for homogeneous minor actinides transmutation opens a new range of possibilities, especially with coupling of both the heterogeneous and homogeneous approaches.

Coupling to scenarios studies might also be envisioned. Indeed, during this study, a conservative plutonium isotopic vector was considered but this vector will in fact change depending on the industrial strategy adopted. Consequently, the optimal cases which were obtained using a given vector may be further refined to adapt to the new isotopic vector. A consistent coupling with scenarios would allow qualification of a transmutation strategy at the scale of a reactor fleet

rather than for an individual reactor. Additionally, adequate tuning of the breeding gain of the reactor was not considered here but would be required for a complete characterization of the core performances at the scenario scale.

Similarly to the scenarios studies, fuel constraints definition could be refined. Indeed, integrated constraints based on the assembly handling were taken, however additional constraints exist on dose rates, decontamination factors during reprocessing and thermomechanical behavior during irradiation at high minor actinides content or specific heat production of the powdered fresh fuel during manufacturing. Such constraints may be dimensioning but it was not possible to take them into account due to limited available data.

Further options could be added to the optimization methodology after analyzing their specific associated constraints, such as the use of carbide or nitride fuels along with helium cooled or lead cooled fast reactors. Similarly, the use of innovative assemblies departing from the canon bundle design could be implemented, such as the fissile loaded approach described in Chapter 4 or the use of inert matrix fuels.

It was also observed that the minor actinides isotopic vector (and especially the americium one) could be adapted with regards to the specific fuel cycle constraints in order to optimize cooling time of the assemblies. As such a variation would also impact the helium production in the assembly, a detailed analysis could be carried out with the ratio $^{241}Am/^{243}Am$ as an additional parameter of optimization depending on the limit considered.

ANNEX 1: NEPTUNIUM AND CURIUM TRANSMUTATION

Highlights:

- ✓ **Neptunium is a long-lived minor actinide which transmutation is more easily feasible than for americium or curium.**
- ✓ **Its impacts on the fuel cycle are limited while its impacts on the core transient behavior are similar to americium.**
- ✓ **The main curium isotopes are short-lived minor actinides with very strong impacts on the fuel cycle, especially manufacturing.**
- ✓ **Homogeneous transmutation should be preferred for Curium as its impacts on the core behavior are lower than americium and the corresponding dilution in the fuel limits the impacts on the fuel cycle.**

The main part of this work was dedicated to the transmutation of americium, which is the most suitable candidate for early implementation of transmutation in fast reactors. The aim of this annex is to detail the specificities of neptunium and curium transmutation, both in the heterogeneous and homogeneous approach and to compare them with the americium case.

1) NEPTUNIUM TRANSMUTATION

The element neptunium has one isotope with a half-life greater than 3 days, which is $^{237}_{93}Np$. With a half life of 2.144 million years, it is a long-lived radionuclide which is a by-product of nuclear reactors operation. ^{237}Np (or neptunium as it will be referred to henceforth) has two main production routes:

- Successive neutron captures on ^{235}U, which yields ^{236}U and ^{237}U, which finally decays with a half-life of 6.75 days to ^{237}Np. This reaction is preponderant in thermal reactors (Equation 30) .
- (n,2n) reaction on ^{238}U which is a threshold reaction around 6 MeV. This reaction is preponderant in fast reactors, where it makes up to 90 % of the neptunium production (Equation 31).

$$^{235}_{92}U + n \rightarrow {}^{236}_{92}U + n \rightarrow {}^{237}_{92}U \xrightarrow{\beta} {}^{237}_{93}Np$$

Equation 30 : Neptunium formation route from ^{235}U

$$^{238}_{92}U + n \rightarrow {}^{237}_{93}Np + 2n$$

Equation 31 : Neptunium formation route from ^{238}U

The cross sections corresponding to these formation reactions are shown in Figure 111.

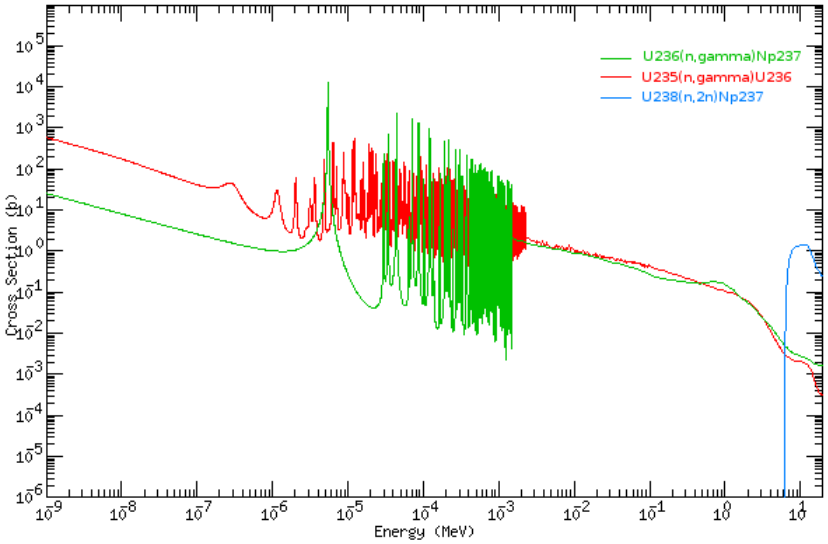

Figure 111 : Cross sections for main production reactions of neptunium (ENDF B-VII library [90])

Considering these two routes, we can deduce that neptunium production is going to be higher in a thermal reactor using uranium dioxide as fuel than in a fast reactor. A comparison of the production and share of neptunium in various reactors is given in Table 68.

Table 68 : Orders of magnitude of neptunium production depending on the reactor type

Reactor type	Neptunium production (kg/TWhe)	Np fraction of the minor actinides output of the reactor after 5 years cooling (%)
900 MWe UOX	1.5	50
EPR 1600 MWe UOX	2.0	50
EPR 1600 MWe 100 % MOX	0.3	5
SFR CFV 3600 MWth	0.3	10

It appears that neptunium amounts around half of the minor actinides production of a current UOX reactor. According to the IAEA, neptunium will represent up to 57 % of the total minor actinides discharge of the world by 2050 [91]. For the French nuclear fleet, with an average electrical production of 400 TWhe, the yearly production of neptunium is in range of 600-800 kg. If neptunium was transmuted with 100 % efficiency in fast reactors, this would decrease the mass of minor actinides in the waste by 50 %.

Neptunium incorporation in the fuel has several impacts in fast reactors, which are:

- A decrease in the absolute value of the coolant void worth, due to an earlier increase in the fission cross section of neptunium compared to uranium with regards to the neutron energy. Consequently, during a coolant voiding accident, the hardening of the spectrum leads to a reactivity increase. [34]
- A decrease in the absolute value of the Doppler feedback, which is explained by an increased capture in the 30 keV range by neptunium nuclei. This leads to a reduction of

the flux in the lower energy region below 1 keV which contributes the most to the Doppler Effect. [34]
- An increase in the breeding gain due to higher neptunium capture cross section level compared to uranium.
- A slight decrease in the delayed neutron fractions (around to 3%).

These effects are similar to those observed with ^{241}Am. As such, the study of neptunium transmutation is representative of the study of americium or curium transmutation.

Neptunium-bearing pins have already been irradiated, in Russia in the DOVITA experiment [92] and in France during the SUPERFACT experiment [93]. The pins containing 2 vol % of Neptunium in SUPERFACT and 5 vol % in DOVITA did not exhibit any significant differences in terms of behavior under irradiation compared to the regular MOX pins. From these results, we can consider that neptunium volume fractions up to 5 % in the fuel can be considered without extensive modifications of the fuel design.

Furthermore, sample pins containing 45 % of Neptunium irradiated in SUPERFACT did not show extensive modification of their behavior compared to standard pins. Although there are not enough data to draw final conclusions on the behavior of pins containing a high fraction of neptunium, we assumed here that manufacturing and irradiation of such pins is possible.

Under irradiation, neptunium either undergoes fission or yields ^{238}Pu by neutron capture following the reaction:

$$^{237}_{93}Np + n \rightarrow {}^{238}_{93}Np \overset{\beta}{\rightarrow} {}^{238}_{94}Pu$$

Equation 32 : Neptunium transmutation route

^{238}Pu is a strong alpha-emitter with a half-life of 87.75 years and an associated specific decay heat of 567 W/kg. This high level of thermal activity will increase the complexity of manipulation and reprocessing of the irradiated neptunium-containing fuel. However, ^{238}Pu can be directly mixed with the existing plutonium feed and be reused as fuel as it is a net neutron provider in a fast spectrum.

Separation of the neptunium from the spent fuel has already been demonstrated and can be implemented industrially with a good expected separation factor [94]. As neptunium exhibits low specific activity level, it can be readily manipulated and manufacturing of neptunium-bearing pellets does not require additional precautions compared to MOX pellets.

The critical mass of a bare sphere of neptunium is estimated to be around sixty kilograms [95]. As such, separated neptunium from nuclear spent fuel can lead to a proliferation issue, which would be lessened by the transmutation of neptunium. However, leaving some of the ^{238}Pu produced with the separated neptunium would greatly diminish the proliferation risk as it would prevent its use for military purposes in a way similar to plutonium denaturation as discussed in [71]

Neptunium impact on the thermal load of the waste package, which is the main parameter influencing the repository size is nearly inexistent, as it has a very low specific activity. However, the amount of ^{238}Pu lost during reprocessing may increase the heat load of the waste packages. In terms of radiotoxicity, neptunium contribution is negligible up to several millions

years, as it can be seen on Figure 112. This figure only shows the heavy nuclides radiotoxicity. The fission products radiotoxicity being negligible compared to the minor actinides contribution after a few centuries, they were not taken into account for this application.

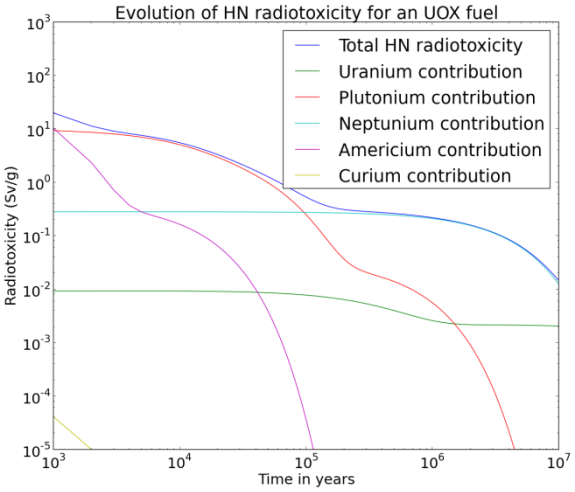

Figure 112 : Radiotoxicity by ingestion from ICRP 119 [16] for the MA vector of an irradiated UOX fuel at 33GWd/t from [17]

Neptunium in the waste comes from two streams: the neptunium originally present in the waste and the decay of ^{241}Am which has a half-life of 432.2 years. Considering the relative proportion of neptunium and ^{241}Am presents in the waste at the final casting into glass, removal of the first production stream would decrease the mass by a factor seven at the million-year time scale, as shown in Figure 113. This corresponds to a reduction of the total radiotoxicity by a factor 3 at the same timescale.

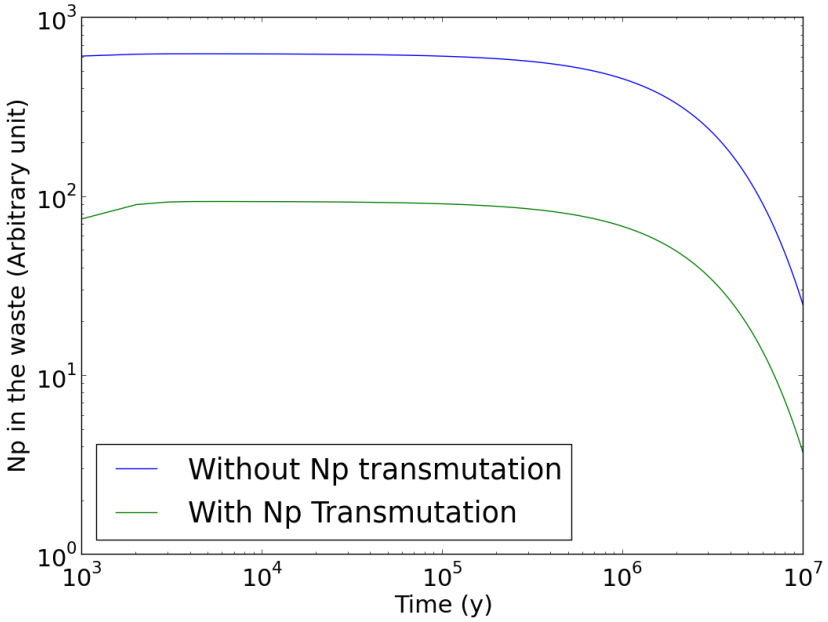

Figure 113 : Evolution of the neptunium concentration in the waste depending on the implementation of Np transmutation

It should also be mentioned that Neptunium has been found to be prone to diffusing in the some types of proposed rocks, as it was observed in Yucca Mountain [96]. Consequently, decreasing neptunium content in the waste would contribute to reduce the potential risk of radionuclides diffusion in the biosphere.

We can conclude from all these considerations that neptunium transmutation is of interest as it would reduces the volume of minor actinides sent to the final repository. Additionally, it would also be a practical first step towards transmutation of harder-to-handle americium and curium. Now these preliminary points have been considered, various transmutations of neptunium will be discussed in the next part.

2) CURIUM TRANSMUTATION

Curium is created by successive capture on plutonium and americium isotopes as shown in the equation below

$$^{242}_{95}Am \xrightarrow{\beta} {}^{242}_{95}Cm + {}^{1}_{0}n \rightarrow {}^{243}_{95}Cm$$

Equation 33 : ^{243}Curium formation route

$$^{243}_{95}Am + {}^{1}_{0}n \rightarrow {}^{244}_{95}Cm + {}^{1}_{0}n \rightarrow {}^{245}_{95}Cm + {}^{1}_{0}n \rightarrow {}^{246}_{95}Cm + \cdots$$

Equation 34 : ^{244}Curium and heavier isotopes formation routes

^{244}Cm is the main curium isotope found in the spent fuel, as it is produced from ^{243}Am which is readily available for neutron capture and as its absorption cross-section is low leading to its accumulation in the fuel. Similarly to ^{242}Cm, it is a strong thermal and neutron emitter with a specific heat load of 2.84 W/g. With its longer half-life, it is going to be more of an issue with regards to the storage in the final repository. It also has a high spontaneous fission probability, leading to a high intrinsic neutron source.

^{245}Cm is also produced in kilogram quantities as it comes from ^{244}Cm which is present in significant quantities in the fuel. It shares a significant neutron emission with its parent isotope ^{244}Cm. However, heavier isotopes of Curium are not found in significant quantities in general (up to a few grams each in fast reactors) as they require numerous successive captures to be produced. Nevertheless, they have a non negligible contribution on the neutron source of the spent fuel as they usually have a high spontaneous fission rate.

Curium production is less than 10 % of the total minor actinides production but it drives the short-term radiotoxicity along with fission products (up to a few hundred years) and is the main contributor to decay heat and neutron source. Curium has very limited applications, the main one being the construction of X-ray spectrometer for space probes such as Curiosity.

In terms of radiotoxicity, its short term contribution is relatively important but its long term contribution is close to zero as most of the isotopes produced during irradiation are short lived. This is illustrated in Figure 114, where the radiotoxicity of the minor actinides vector from a MOX fuel is plotted.

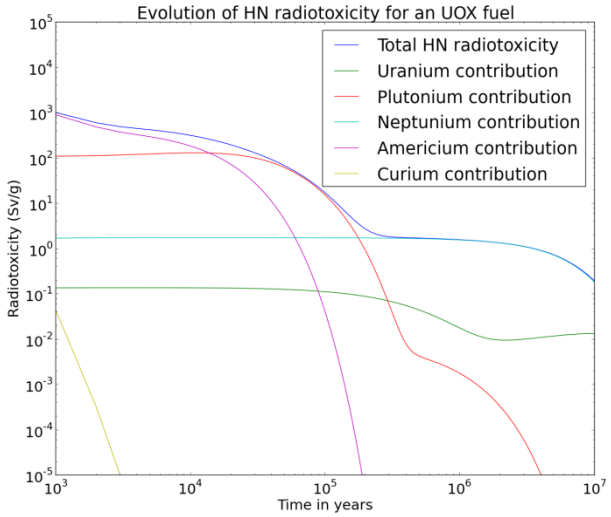

Figure 114 : Radiotoxicity by ingestion from ICRP 119 [10] for the MA vector of an irradiated MOX fuel at 48 GWd/t

The main rationale behind curium transmutation is the decrease of the final waste package heat load. Indeed, curium is a very strong contributor to final decay heat of the waste. Higher spacing between the waste packages is necessary to maintain adequate temperature in the deep geological repository if curium is loaded into the waste package. The current approach is to store the packages containing curium for 120 years in order to await its natural and then send them underground. A reduction in the curium amount in the waste would allow a reduction of this storage duration, and thus limit the inventory of waste stored on surface. It would also limit the final volume to be excavated underground and the total size of the storage facility as discussed in [97].

3) THE HETEROGENEOUS APPROACH

In this part, the transmutation performances and fuel cycle impact of a « standard » blanket will be compared for each of the three minor actinides. As in Chapter 4, a 4100 EFPD irradiation in an homogeneous core 3600 MWth SFR V2B will be considered here [51]. A fuel volume fraction of 38.6 % will be considered with 20 at% of minor actinide loaded in the blanket assemblies. The minor actinides isotopic vector considered in this study are shown in Table 69. The curium vector corresponds to the composition of the curium expected to be available around 2035 in the industrial scenarios considered in [25]

Table 69 : Composition of the minor actinides feed used in this study

Element	^{237}Np	^{241}Am	^{243}Am	^{242}Cm	^{243}Cm	^{244}Cm	^{245}Cm	^{246}Cm
Mass Fraction (%)	100	0	0	0	0	0	0	0
Mass Fraction (%)	0	75	25	0	0	0	0	0
Mass Fraction (%)	0	0	0	0,30	1,07	78,23	19,18	1,22

a) BACK END

The first point to study is the characterization of the fresh blanket. Their decay heat level and neutron source level are summarized in Table 70. The main conclusion to draw here is that neptunium is not an issue from the back end point of view, while a fresh curium-loaded assembly is nearly thirty times hotter than americium assembly, while its neutron source is equivalent to the one of a freshly irradiated americium target.

Table 70 : Decay heat and neutron source of the fresh blanket assemblies for neptunium, americium and curium loading

	Specific power (W/kg)	Total power per assembly (kW)
Curium	0,52	74,08
Americium	0,02	2,47
Neptunium	0,00	0,00

	Specific neutron source (n/s/g)	Total neutron source per assembly (1e10 n/s)
Curium	1,80E+06	25
Americium	0	0
Neptunium	0	0

b) TRANSMUTATION PERFORMANCES

The second point of interest is the study of the transmutation performances through the specific consumptions and the mass balances in the blankets. The results are shown in Table 71. In terms of consumption, americium and neptunium behave similarly, with the only difference that neptunium transmutation does not produce americium or curium but only plutonium. On the other hand, Curium transmutation appears more efficient. This is due to the fact that during the 11 years irradiation, a significant part of the ^{244}Cm will decay considering its 18.8 half-life, thus adding to the total consumption of curium. Interestingly enough, a small production of americium and neptunium can be noted. Neptunium production is due to (n,2n) reactions on ^{238}U nuclei, the fast neutron necessary for this reaction to take place being supplied by fissions of ^{245}Cm, while the americium is produced by capture on ^{240}Pu coming from the decay of ^{244}Cm.

Table 71 : Specific consumption in the blankets for neptunium, americium and curium loading

Specific consumption in kg/TWhe | Loaded minor actinide	Np	Am	Cm
Pu	8,55	7,56	9,64
Np	-6,7	0,2	0,04
Am	0	-6,61	0,13

Cm	0	0,99	-10,52

In terms of mass balance, similar conclusions can be reached as it is shown in Table 72. In all cases, a strong plutonium production can be observed. The production has two sources, namely breeding on ^{238}U and the actual transmutation process. Its isotopic composition is of interest regarding both the proliferation resistance of the blankets and their cooling behavior.

Table 72 : Mass balance in the blankets for neptunium, americium and curium loading

		Np	Am	Cm
Initial composition (kg)	Am	0	2375	0
	Np	2370	0	0
	Cm	0	0	2378
	Pu	0	0	0
Final composition after 5 years (kg)	Am	0	1433	19
	Np	1413	29	5
	Cm	0	141	878
	Pu	1220	1079	1376

The isotopic composition of the final plutonium is shown in Table 73. Significant differences can be observed in this table. Breeding from ^{238}U represents mostly fifty percent of the produced plutonium, in the form of ^{239}Pu and a small part of ^{240}Pu, with the remaining part being strongly different between the cases. For neptunium, it is mostly entirely composed of ^{238}Pu coming from captures on ^{237}Np. ^{238}Pu is also produced in the americium case through captures on ^{241}Am and the following decay of the produced ^{242}Cm. A small amount of ^{242}Pu is produced, mainly through decay of ^{242g}Am. Finally, for the curium case, an important production of ^{240}Pu can be observed due to the decay of ^{244}Cm. These differences will have an impact on the front end of the blanket fuel cycle, as it will be discussed in the next paragraph.

Table 73 : Plutonium isotopic vector in the blankets for neptunium, americium and curium loading

Plutonium isotopic vector (%)	Np	Am	Cm
^{238}Pu	50	33	0
^{239}Pu	46	49	55
^{240}Pu	4	9	42
^{241}Pu	0	0	3
^{242}Pu	0	8	0

Finally, a last point to be discussed here is the gas production in the blankets during irradiation, which plays an important role in the design of the blanket assemblies. As it can be seen in Table 74, the gas production in the neptunium case is relatively limited compared to the Am or Cm cases. For neptunium, gas production comes from fission of ^{238}Pu or ^{239}Pu and to a lower extent from alpha-decay of ^{238}Pu. On the other hand, for the americium case, most of the gas production comes from the alpha-decay of ^{242}Cm. Finally, for the curium case, the gas production is evenly distributed between fission gases coming mainly from ^{245}Cm fissions and helium coming from ^{244}Cm and ^{242}Cm decay. Overall, the design margin for the curium case is

more limited due to the increased gas production. For the neptunium case, the gas production is not an issue in terms of design.

Table 74 : Gas production in the blankets for neptunium, americium and curium loading

Gas production	Np	Am	Cm
Fission gases (cm^3/g)	0,99	0,84	3,35
Helium (cm^3/g)	0,26	4,19	3,83
Total (cm^3/g)	1,25	5,02	7,18

c) FRONT END

The evolution of the decay heat of the assembly during cooling is shown in Figure 115. Neptunium exhibits a lower level decay heat as it comes mostly from ^{238}Pu which has a low specific decay heat. However, consequently, the target assembly can be handled without any limitations (if we consider a 40 kW limit for short-term handling). Similarly, sodium washing is not limited if a 7.5 kW limit is considered with a few weeks necessary to reach this limit. However, if this limit is decreased to 2.5 kW, the cooling time jumps to more than 60 years due to the relatively long half life of ^{238}Pu (87 years).

The americium case which was detailed in Chapter 4 exhibits an important short term decay heat followed by a sharp drop due to ^{242}Cm production during irradiation. Long term decay heat is dominated by ^{244}Cm, ^{238}Pu and ^{241}Am and the cooling time to 7.5 kW is close to 10 years. The cooling time to 2.5 kW is similar to the one of the neptunium due to the contribution of the long-lived ^{238}Pu and remaining ^{241}Am

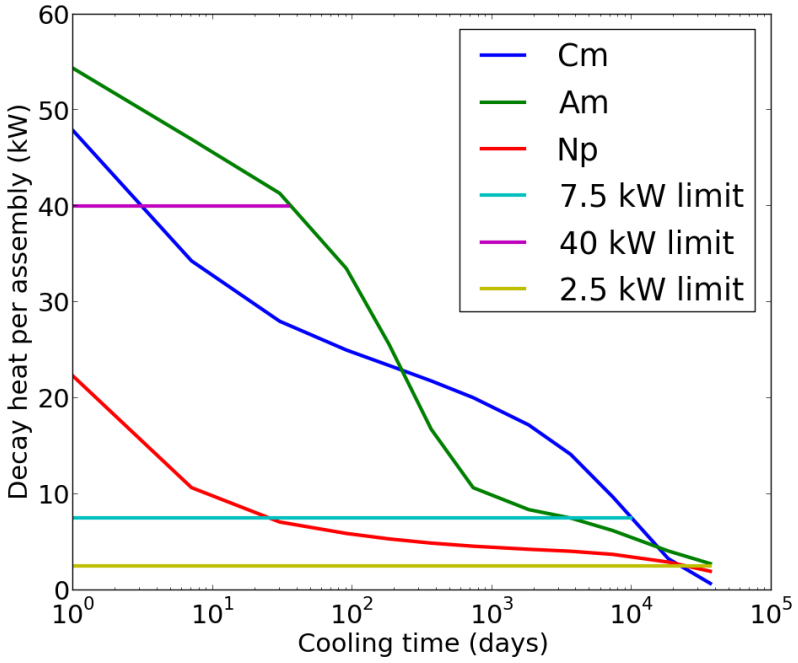

Figure 115 : Evolution of the target assembly decay heat for neptunium, americium and curium loading

Finally, the curium case exhibits a stronger short term decay heat mainly due to ^{244}Cm, which decreases with the decay of this nucleus. Due to important quantities still present in the blankets, the cooling time to 7.5 kW or 2.5 kW is higher than for the americium or neptunium case.

Regarding neutron source, it can be observed in Figure 116 that neptunium loaded targets do not exhibit any neutron source as they do not contain neutron emitting nuclei. On the other and, since ^{244}Cm and heavier curium isotopes are the main responsible for neutron source in the blankets, it can be verified that the curium case yields the highest neutron source. Its neutron source after five years of cooling is nearly fifty times higher than the one of a standard MOX assembly, making its handling significantly harder.

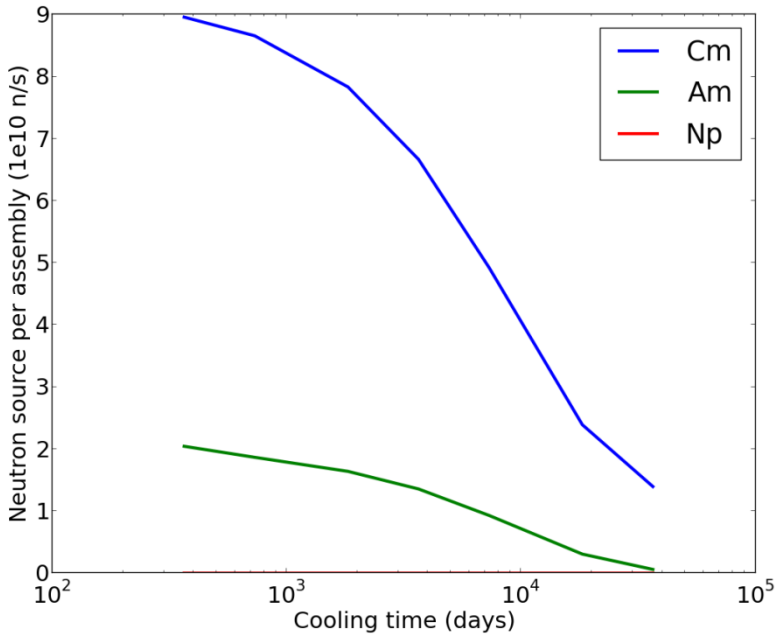

Figure 116 : Evolution of the target assembly neutron for neptunium, americium and curium loading

Regarding the heterogeneous transmutation of neptunium and curium compared to americium, it can be concluded that neptunium is a suitable candidate, even better than americium as the irradiated targets are less active and do not emit neutrons, while curium heterogeneous transmutation cannot be considered realistic due to the high heat load for fresh targets and the very high neutron source of the irradiated targets. Decay heat of the irradiated targets is similar to the americium case, making it a non-limiting factor.

3) THE HOMOGENEOUS APPROACH

For the homogeneous approach, a reference core similar to the one available in [98] was used. The residence time of the fuel was modified to reach a mean burn up of 200 GWd/t . Various geometrical parameters of the core design are given in Table 75. 5 at% of neptunium, americium and curium were loaded in the cores and their respective performances were compared in terms of minor actinides consumption, impacts on the core transient behavior and fuel cycle impacts.

Table 75 : Description of the core used for this comparison

Core description		
Power	3600	MWth
Inner core height	80	cm
Inner fertile layer	20	cm
Outer core height	90	cm
Core radius	320	cm
Assembly fuel volume fraction	40%	%
Assembly sodium volume fraction	30	%
Number of batch	7	-
Cycle length	435	Jepp

a) TRANSMUTATION PERFORMANCES

As previously, the transmutation performances will be analyzed through the specific consumption (Table 76) and the mass balance in the core (Table 77). It can be seen that neptunium consumption is the highest in the homogeneous configuration, while curium and americium consumption are quite similar. The difference between the two can be explained by the very limited neptunium production in the core during irradiation compared to americium or curium. Curium production being more limited than the production of americium during irradiation, curium consumption is consequently higher.

Table 76 : Specific consumptions in the core for neptunium, americium and curium loading

Specific consumption (kg\TWhe) | Actinide loaded	Np	Am	Cm
Np	-14,7	0,3	0,2
Am	3,8	-11,0	3,3
Cm	0,7	2,7	-13,3

Regarding the mass balance, the cases of neptunium and americium are quite similar regarding the plutonium inventory. On the other hand, curium loading leads to a diminution by around 20 % of the initial plutonium content in the core as ^{245}Cm is a very good fissile nucleus. ^{244}Cm also contributes significantly to the core neutron balance by breeding ^{245}Cm during irradiation. Concerning the minor actinides, the conclusions are similar than for the specific consumption.

Table 77 : Mass balance in the core for neptunium, americium and curium loading

		Np	Am	Cm
Initial composition (kg)	Np	2438	0	0
	Am	101	2545	84
	Cm	0	0	2446
	Pu	12835	12927	10640
Final composition after 5 years (kg)	Np	860	33	26
	Am	398	1252	336
	Cm	103	382	1149
	Pu	10475	10288	9033

b) IMPACTS ON THE CORE TRANSIENT BEHAVIOR

The behavior of the core loaded with minor actinides for each of the three reference transients considered in Chapter 5 was analyzed and compared to the behavior of the core without minor actinides loading.

An ULOF corresponding to an exponential decrease of the primary circuit flow rate up to an asymptotic value of 10 % of the nominal flow with a half-time of 24 s was considered, along with an ULOHS corresponding to a linear total cancellation of secondary flow in 40 s. For the UTOP, a 150 pcm insertion in 250 s was considered. The maximal sodium or fuel temperature during the transients was calculated and is recorded in Table 78.

Table 78 : Evaluation of the core transient behavior depending on the minor actinides loaded

	Ref	Np	Am	Cm	Np+Cm
Maximal sodium temperature ULOF (°C)	1044	1052	1049	1056	1055
Final sodium temperature ULOHS (°C)	775	761	763	795	780
Maximal fuel temperature UTOP (°C)	2370	2490	2482	2453	2460

Similarly to what was shown in Chapter 5, americium has a positive effect on the ULOHS transient, barely any effect on the ULOF and an important effect on the UTOP transient. Neptunium shares a similar behavior with americium in this regard. More interesting is the behavior of the core when Curium is loaded, where with observes a degradation of the performances in ULOHS and UTOP along with a lower decrease in the UTOP performances. This is consistent with an actual increase in the Doppler Effect caused by the incorporation of curium in the fuel.

From this analysis, it can be postulated that the production of Curium during irradiation has positive effects on the core behavior during a transient as it behaves like a fissile material and cancels some of the penalties created by the loading of americium. To investigate this possibility, a case was loaded with 2.5 % of ^{237}Np, which has similar behavior as americium but does not lead to curium production, and 2.5 % of Curium. A mitigation of the impacts on each transient can be observed in Table 78, making this approach potentially interesting to optimize homogeneous minor actinides transmutation.

c) IMPACTS ON THE FUEL CYCLE

The decay heat and neutron source of the fresh and irradiated assembly was analyzed here to evaluate the impacts on the fuel cycle. The values for the fresh assemblies are given in Table 79. There is very little difference with the reference case for the neptunium and americium case. However, for the curium case, the decay heat and neutron source of the fresh assembly are significantly higher. This will require improvements in the transportation cask design in order to be able to transport these assemblies. On the other hand, it can be supposed that the three other assemblies can be transported safely using a similar cask design.

Table 79 : Heat load and neutron source of a fresh assembly with neptunium, americium or curium loading

Fresh assembly	Ref	Np	Am	Cm
Heat load (kW)	0,07	0,07	0,11	1,38
Neutron source (n/s)	3,48E+03	3,27E+03	4,45E+03	4,57E+06

Regardless of the minor actinides loaded, the decay heat of the spent assembly will be higher than for a regular one, as it can be seen in Figure 116. This increase is the most limited for the neptunium case, while the short term increase is the most important for the Am case to ^{242}Cm production. The impact on long term decay heat can be analyzed by evaluating the time necessary to reach a 7.5 or 2.5 kW washing limit, as shown in Table 81.

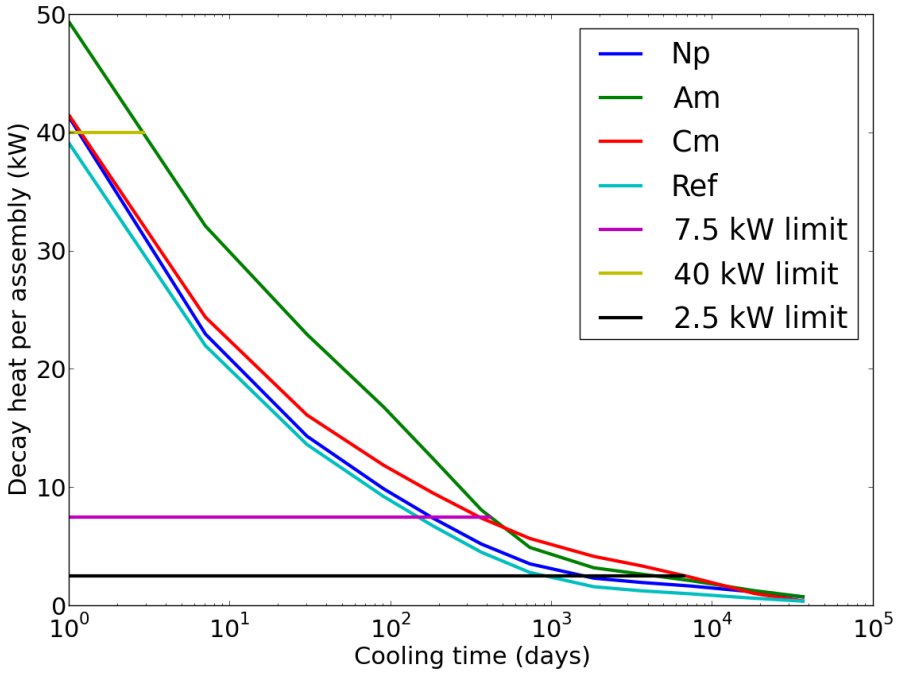

Table 80 : Evolution of the inner fuel assembly decay heat for neptunium, americium and curium loading

For the 7.5 kW limit, the reference case and the neptunium case are relatively similar as the contribution of ^{238}Pu to the decay heat remains smaller compared to the fission products

contribution. The americium and curium case requires much longer cooling time due to the contribution of ^{244}Cm for both cases and ^{242}Cm for the americium case only.

For the 2.5 kW, the effect of the short-lived ^{242}Cm disappears and only the long-lived ^{238}Pu, ^{244}Cm and ^{241}Am are playing a role in the decay heat production. As the final content in ^{244}Cm is the highest for the curium case, this case requires the longest cooling time, followed by the americium case in which ^{244}Cm is produced by captures on ^{243}Am. Overall, if we consider a maximal cooling time of 5 years, minor actinides loading is not an issue if a washing limit of 7.5 kW is feasible. However, if a limit of 2.5 kW is considered, only neptunium loading is feasible in this case.

Table 81 : Cooling time to a given washing limit for neptunium, americium and curium loading

Case	Ref	Np	Am	Cm
Time to 7,5 kW (days)	148	178	416	357
Time to 2,5 kW (days)	932	1620	4611	6840

For neutron source, the neptunium and reference case are similar as neptunium addition does not lead to the production of any neutron emitting nucleus, as shown in Table 82 . On the other hand, the americium case and curium case exhibits higher neutron due to ^{244}Cm production, with the curium case being the case with the highest neutron source. It should nevertheless be mentioned that the neutron reached here in this case corresponds to the neutron source of an irradiated blanket assembly loaded with americium as studied in the previous part. Being able to handle assemblies with such a level of neutron source is consequently necessary both for heterogeneous transmutation of americium or homogeneous transmutation of Curium.

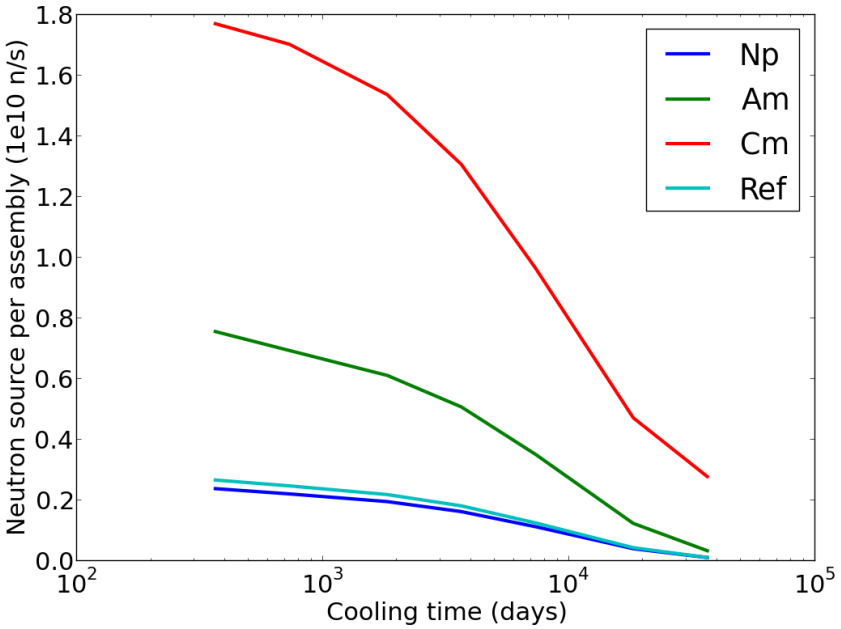

Table 82 : Evolution of the inner fuel assembly neutron source for neptunium, americium and curium loading

4) CONCLUSION

Compared to americium, it was shown that neptunium was a very good candidate for transmutation, either in the homogeneous or the heterogeneous approach. Its impacts on the fuel cycle are lower in each case but it has the same negative impacts on the UTOP transient than americium in an heterogeneous core.

Concerning curium, two main problems can be identified for the heterogeneous approach:

- The very high heat load and neutron source of the fresh assemblies
- The high neutron source of irradiated assemblies

The decay heat of an irradiated curium target is lower than the one of an Americium target, with a slightly lower cooling time. In terms of consumption, the curium is more favorable due to the decay of ^{244}Cm during irradiation.

In the homogeneous case, curium was shown to have a limited impact on the UTOP transient as it behaves as a fissile nucleus. However, as its introduction in the fuel increases the Doppler Effect, it has a slightly negative impact on the flow transients. The fuel cycle impacts are comparable to the ones of an irradiated americium target. Regardless of the option chosen, the main limiting factors towards implementation of minor actinides transmutation remain linked to the fuel cycle.

ANNEX 2: NEUTRONIC AND FUEL CYCLE COMPARISON OF URANIUM AND THORIUM AS MATRIX FOR MINOR ACTINIDES BEARING-BLANKETS

Note : This annex was published in *Annals of Nuclear Energy* **92** (2016) 61–71 with a similar title and in a similar form.

Highlights:

- ✓ **The use of thorium as the support element for heterogeneous minor actinides transmutation is characterized.**
- ✓ **The possibility of in-situ reusing the ^{233}U produced during irradiation is shown as potentially interesting approach to increase transmutation performances.**

ABSTRACT:

Minor actinides transmutation is one of the three main axes defined by the 2006 French law for nuclear waste management, along with long-term storage and use of a deep geological repository. In the heterogeneous approach, minor actinides are loaded in specially designed targets assemblies which are located in the periphery of the core, in order to limit the impacts on core operations. In this paper, we compare the use of uranium and thorium dioxide as support matrix in which minor actinides are diluted in the target assemblies. Both UO_2 and ThO_2 exhibit sufficiently good irradiation behavior to withstand the long residence time associated with heterogeneous transmutation. Five different reprocessing strategies are compared in which some or all the elements in the blankets are reused after reprocessing. The impacts on core safety parameters and fuel cycle parameters are also evaluated for each case and it is found that using thorium as support matrix with reuse of uranium 233 leads to transmutation performances similar to the one obtained with the reuse of plutonium from uranium blankets with slightly lower global impacts on reactor operation and fuel cycle.

1) INTRODUCTION:

Minor actinides are a set of three main elements (neptunium, americium and curium) which are by-products of uranium irradiation in nuclear reactors. These elements are produced in relatively limited quantities [99] but they exhibit long-term radiotoxicity and decay heat levels which complicate the handling of associated nuclear waste.

In the case of a closed nuclear fuel cycle strategies where spent fuel is reprocessed and plutonium reused in fast spectrum reactors, minor actinides are the main contributors to long term radiotoxicity of the spent fuel and to decay heat of the ultimate waste package. Minor actinides transmutation has thus been proposed as a potential solution to decrease the burden of nuclear waste and to reduce the constraint on the final repository. [100]

Transmutation in critical reactors can be done in two different ways:

- Homogeneous transmutation, in which minor actinides are directly mixed with the reactor fuel. This solution exhibits the best performances as the minor actinides are exposed to a high flux level. However, it exhibits the drawback of contaminating the entire fuel cycle with minor actinides and it decreases the "safety" performances of the reactor. Minor actinides content of up to 5 %vol can be loaded depending on the considered core design. Additionally, the residence time of the minor actinides bearing fuels can not exceed the one of standard MOX fuel.
- Heterogeneous transmutation in which minor actinides can be loaded in specifically designed assemblies, usually in the periphery of the core, which are called "Minor Actinides Bearing Blankets" or MABB. The use of such subassemblies helps decoupling minor actinides management from the fuel and thus gives a larger flexibility compared to the homogeneous mode. As these blankets benefit from the neutron leakage from the active zone they have almost no impact on the core neutronic parameters such as delayed neutron fractions or sodium void worth. This allows to load a large minor actinide mass and to reduce the number of MABB to be manufactured. On the other hand, the obtained performances are lower than the previous one as the flux level seen by the assemblies is quite low. Minor actinides content between 10 % and 40 % are expected to be loaded in such cores. As fuel and MABB cycles are decoupled, higher transmutation rates can be expected at the cost of longer irradiation time.

The present paper focuses on heterogeneous transmutation strategies. A thorough analysis of this transmutation approach has been carried out by a NEA task force in 2009 and summarized in [101]. The main points are described below:

- The high content of minor actinides in the fuel requires important fuel design effort, notably in terms of mechanical design. Previous experiments, especially the SUPERFACT experiment in which pins with up to 45 % of americium and neptunium were irradiated in the Phenix reactor core [93] showed that MABB irradiation was accompanied by an important production of Helium due to alpha decay of minor actinides nuclei which has an impact on the mechanical behavior of the pin and on the size of the gas plenum.
- Power production in the MABB assemblies is also very low at the beginning of irradiation which puts tighter constraints on the mechanical design as fuel restructuration does not happen at low temperatures. The important power variation

during irradiation also increases the strain on the fuel pins, possibly leading to thermal cracking. [61]

- Decay heat, gamma and neutron emission of irradiated and refabricated MABB assemblies is significantly higher than for a standard MOX fuel, which leads to additional issues in terms of fuel handling, reprocessing and manufacturing.

When considering minor actinides transmutation, several objectives are usually pursued. Firstly, the transmutation performances, e.g. the amount of minor actinides which are effectively turned into fission products during irradiation is considered, as it is a direct estimator of the performances of the process. The support ratio, which is the number of reactors which production can be absorbed in one minor actinide burner, is also of interest from an economic point of view. The support ratio can be reduced either by decreasing the production of minor actinides in the reactor or by increasing transmutation performances, as discussed here.

It has been proposed to add moderating material in the MABB in order to increase the transmutation performances of the design [102]. Slowing down the neutrons in the blankets has the interest of increasing the absorption cross sections and thus the number of captures or fissions. However, it also increases the amount of curium produced, which is more troublesome than americium on fuel back-end due to a higher neutron source and specific decay heat. This addition is especially interesting in case of once-through transmutation, in which the blankets are irradiated only once and then discarded as waste. We considered here a heterogeneous transmutation scheme in which irradiated blankets are reprocessed to maximize amount of transmuted material.

Similarly to plutonium, minor actinides cannot be loaded *per se* as oxide fuel in a reactor but must be blended with a matrix to produce usable reactor fuel. Several materials have been proposed as potential matrices for MABB fuels. The first one is evidently uranium dioxide (UO_2), which has been tested in the SUPERFACT experiments for instance. UO_2 is a well-known material with a low swelling rate and which can withstand the long residence time associated with heterogeneous transmutation. However, the use of uranium oxide as support matrix comes with a production of plutonium which may cause an issue in terms of proliferation. It also implies a modification of the core to keep a total breeding gain close to unity. An analysis of the impact (or lack thereof) of the use of minor actinides blankets has been done in [41]. Additionally, the irradiation behavior of mixed uranium-minor actinides oxide fuel has yet to be fully characterized [91].

Inert Fuel Matrix, or IMF, has also been discussed for transmutation in heterogeneous mode. A review can be found in [103]. In this concept, the minor actinides are embedded as oxide in either a ceramic material (Cercer concept) or a metallic material (Cermet). This removes the production of plutonium due to capture by uranium 238 in the target but the selection of the matrix is complicated as it should exhibit a good thermal conductivity, acceptable swelling under irradiation and good irradiation resistance behavior to neutrons, alpha and fission products. No matrix has been found featuring all these parameters. However, a possible hybrid matrix of $AmZrO_2$ dispersed in an $MgAl_2O_4$ matrix, which limits damage to $MgAl_2O_4$ by fission products irradiation while making good use of its otherwise good stability has been proposed in [104] . Issues regarding dissolution of the inert matrix must also be addressed (see for instance [105]).

Thorium has been proposed as a potential nuclear fuel in the Th232/U233 fuel cycle, in which fissile uranium 233 is bred from thorium 232. This cycle can be closed in fast or thermal reactors, although it requires an initial stock of fissile material (U235 or Pu239) to start the breeding process. The potential benefits coming from the use of this cycle are listed in [106]. To name but a few, this option virtually removes minor actinides production and increases the reserve in fertile material by a factor three to four as thorium is more abundant than uranium while being intrinsically proliferation resistant due to high gamma production of daughter isotopes of U232. India is currently the leading country for thorium fuel cycle industrialization. Thorium dioxide (ThO_2) or thoria is also a relatively well-known material which performances under irradiation are better than those of UO_2. A detailed study of thorium properties as a nuclear fuel can be found in [107]

Thorium dioxide use has been already discussed as support matrix for heterogeneous transmutation in once-through scheme, for instance in [108]. In this case, advantage is taken of the low solubility of thoria in groundwater for long-term storage. Additionally, this option limits the production of plutonium in the blankets, thus decreasing the total radiotoxicity at disposal. Advantage has also been taken of the lack of plutonium to transmute plutonium and minor actinides without separation during reprocessing, in the case of it being not acceptable. The use of thorium axial blankets in such a case and the related neutronic impacts are discussed in [109].

We elaborate in this paper on the possibility of using thorium dioxide (ThO_2) as a support matrix for minor actinides bearing blankets in the case of a multi-reprocessing scheme in plutonium-fueled fast reactors. We compare the relative performances of uranium and thorium for this application in terms of reactor and fuel cycle impacts. The methodology and tools used are detailed in the first part and the effects of thorium and uranium matrixes on reactors parameters, fuel cycle and transmutation performances are then analyzed in the following sections.

Several cases can be envisioned for transmutation with a thorium support. We considered that thorium was used in combination with a conventional U/Pu fuel cycle. The following possibilities for thorium use which were investigated here are :

- Thorium could be used only as support matrix and the bred uranium 233 can be recovered after reprocessing and used for starting an independent thorium/uranium cycle. As this cycle requires an initial supply of uranium 233 for starting, this solution would allow a reduction of the total inventory of minor actinides during the switch to thorium while producing the necessary uranium 233. Similarly, the uranium production could be incorporated in the reactor core as fuel, thus replacing part of the plutonium and decreasing the minor actinides production. This option was not pursued here.
- Uranium 233 produced during irradiation could be reused as a neutron supplier directly in the blankets, in order not to mix plutonium and uranium 233 in the standard fuel cycle. In this approach, plutonium from the blankets is recovered to be used in the reactor core while uranium, thorium and minor actinides are left in the blankets. The transmutation performances would then benefit from the presence of fissile material in the blanket without requiring plutonium for this purpose, thus limiting the increase in the plutonium inventory.

- Finally, thorium could be used in conjunction with a reprocessing scheme which prevent recovery of potential proliferating materials [4] [110], in which case all the elements produced during irradiation would be recovered together and incorporated again into MABB. This case totally separates the management of the fuel cycle and of the blankets.

We compared those strategies with two similar ones using uranium dioxide as support matrix:

- The direct one in which UO_2 is used as matrix and plutonium is recovered during reprocessing for use in the reactor core. Minor actinides are then reincorporated in fresh blankets. This strategy is currently envisioned in France as discussed in [50].
- The TRU approach in which there is a complete separation of the driver fuel cycle from the blankets fuel cycle. This approach is promoted by the USA in which plutonium and minor actinides are not separated in order to remove any proliferation issues. Plutonium is considered as a minor actinide in this case and treated as such. An example of implementation of this strategy is discussed in [111].

2) METHODOLOGY

Neutronic calculations were performed using the ERANOS code package [36]. The starting point of the calculations was a critical homogeneous SFR core developed jointly by CEA, EDF and Areva and detailed below in Table 83. The core was described using 2D-RZ geometry with a homogeneous description of the various core mediums. Calculations were based on the nuclear data library JEFF 3.1 [42]. A layout of the core is given in Figure 117. The plutonium content was tuned to fulfill a reactivity criteria at the end of cycle (ρ_{FC} = 750 pcm). Calculations were done using with the transport equation with a 33-group energy mesh. The design of the target assembly and fuel pin is still underway so the analysis was done with 38 % in volume of heavy metals in the target assemblies, which is deemed representative of the expected result.

Table 83: Characteristics of the SFR V2b core used for the calculations [51]

Main characteristics of SFR V2b	
Power (MWTh/MWe)	3600/1450
Number of fissile assemblies (Internal core/External core)	453(267/186)
Number of assemblies in the first outer ring (MABB)	84
Residence time	5 x 410 = 2050 EPFD
Volume fractions	43.7 % $UPuO_2$, 27.5 % Na, 8.2 % Wrapper, 11.9 % cladding
Fuel nature	$UPuO_2$
Plutonium content(mean/IC/EC) %vol	15.80%/14.65%/17.44%
Effective breeding ratio	1

Transmutation performances were evaluated using the two following estimators:

- Transmutation rate calculated between the beginning of irradiation and after 5 years of cooling and 2 years of manufacturing : $\frac{\text{initial mass of MA-final mass of MA}}{\text{initial mass of MA}} * 100$
- Support ratio, which is defined as the ratio of the minor actinides consumption in the blankets with 20 % MA loaded, divided by the production in the reactor core alone. This

indicates the number of reactors which minor actinides production can be transmuted using one reactor equipped with radial blankets.

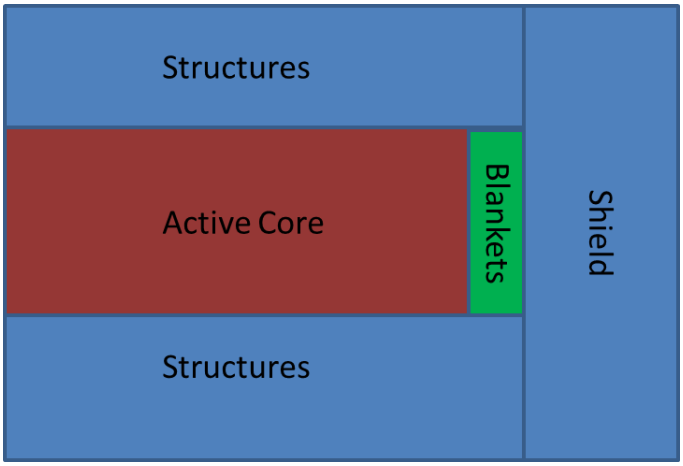

Figure 117 : 2D-RZ representation of the SFR-V2B core with minor actinides bearing blankets

Minor actinides loading was done with a minor actinides vector hereafter labelled "MA2035" and given in Table 84. This isotopic vector is deemed representative of the minor actinides feed available by 2035 in France considering the foreseen evolution of the French PWR fleet. The plutonium vector used for the calculations, given in Table 85 was also considered representative at the same time scale.

Element	Np237	Am241	Am242m	Am243	Cm242	Cm243	Cm244	Cm245	Cm246
Fraction (%mass)	16.87	60.62	0.24	15.7	0.02	0.07	5.14	1.26	0.08

Table 84 : Isotopic vector used for minor actinides

Isotope	Pu238	Pu239	Pu240	Pu241	Pu242	Am241
Fraction (%mass)	3.57	47.39	29.66	8.23	10.37	0.78

Table 85 : Isotopic vector used for plutonium

Minor actinides bearing assemblies were loaded in the first outer ring of the core in substitution of the first reflector ring. Their residence time was twice the one of standard fuel assemblies in order to compensate for the associated low flux level. This amounted to 4100 EPFD, i.e. 10 reactor cycles. In the uranium matrix case, at the end of the irradiation, blankets were reprocessed with 5 years cooling time and 2 years manufacturing time. The plutonium was removed from the blankets and mixed with the core production. Uranium is reused as matrix for the blankets. The minor actinides content in the blankets was recompleted using the minor actinides vector coming from the core production in order to keep the loaded mass constant over two cycles. The external feed of minor actinides is assumed to come from similar reactors without radial blankets. Mass balance is then achieved using uranium. This strategy will be called as U/Pu/MA in the following. It is shown in Figure 118. In the thorium case, blankets were reprocessed on the same time scale with the plutonium being recovered and added to the plutonium of the core. The uranium produced during irradiation, mainly uranium 233, is taken out of the blankets while minor actinides are recompleted using the minor actinides vector from

the core. This strategy will be called Th/U-Pu/MA in the following. The uranium here produced could be mixed with plutonium and used as fuel but this option was not investigated here. It is also shown in Figure 118.

A third strategy was investigated in which thorium is used as support matrix and uranium is left in the blankets along with minor actinides and plutonium is removed for use in the reactor core. This strategy is denominated Th(U)/Pu/MA. The feasibility of thorium/U/Pu separation still yet has to be demonstrated, as discussed in [106], so it is possible that this strategy may incur penalties in terms of reprocessing losses.

A final situation in which the blankets are reprocessed on a Th(U)/TRU basis was also studied. In this case, uranium, plutonium and minor actinides from the blankets are kept in the blankets. Minor actinides with the core isotopic composition are then added to the blankets up to 20 % of minor actinides and mass balance is achieved with thorium. A similar strategy named U/TRU was also studied, which is similar to the Th(U)/TRU one, with all the transuranics being kept in the blanket. As said before, this strategy completely separates the driver and the blankets fuel cycles and reduces the proliferation risks. All these strategies are shown in Figure 119.

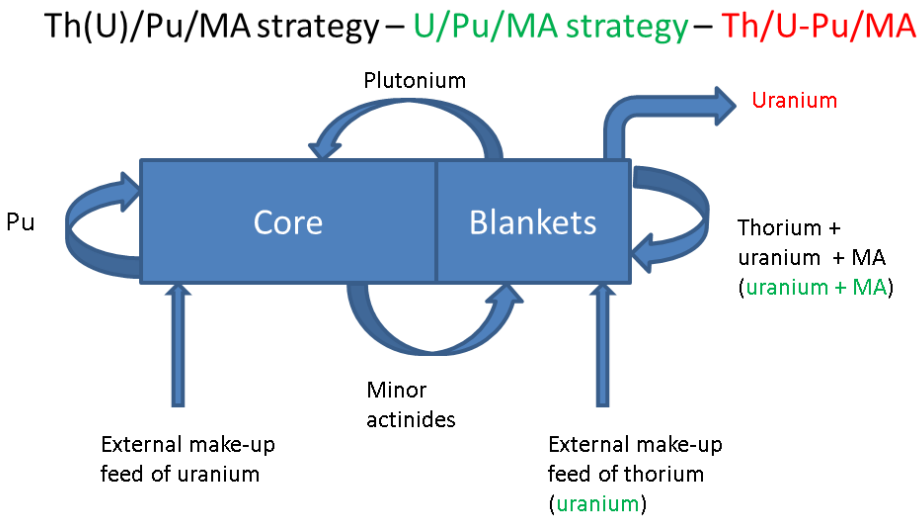

Figure 118 : Outline of the Th(U)/Pu/MA, U/Pu/MA and Th/U-Pu/MA strategies

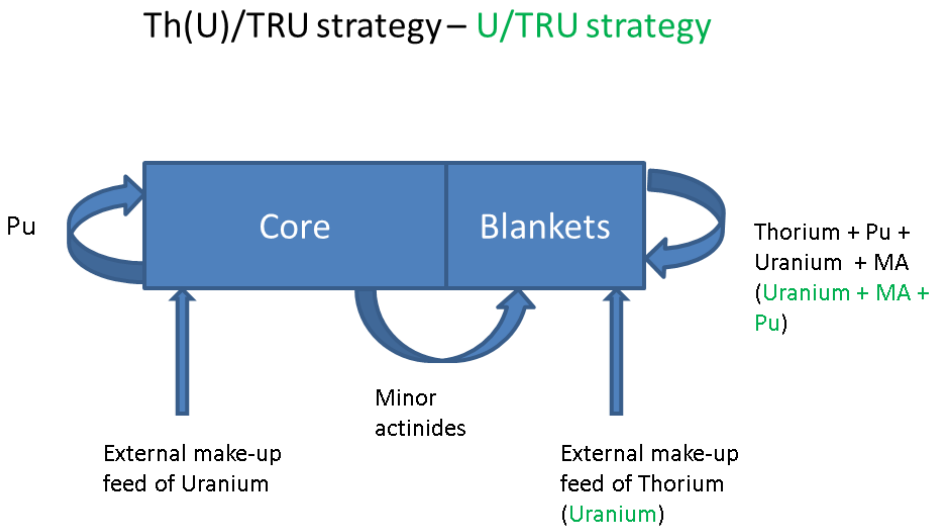

Figure 119 : Outline of the Th(U)/TRU and U/TRU strategies

The whole system was taken to equilibrium and characterized both at the end of the first 10 irradiation cycles and at equilibrium. The equilibrium is reached when the transmutation performances over two consecutive cycles are identical. We denominated as EOEC the end of a MABB equilibrium cycle.

The minor actinides content is stalled to 20% which corresponds to 2375 kg of minor actinides (heavy nuclides mass) in both cases. For perspective, the current minor actinides production of the French nuclear fleet amounts to 1.2 tons a year. The minor actinides isotopic vector of the core production is used as make-up feed to reach the 20 % limit which is currently considered by CEA [41].

The use of thorium as matrix material was analyzed through its impacts on the core parameters such as breeding gain, transmutation performances, sodium void worth and Doppler Effect and on the fuel cycle with neutron and gamma source, decay heat, radiotoxicity estimated.

3) COMPARISON OF URANIUM AND THORIUM AS SUPPORT MATRIX FOR MABB : TRANSMUTATION PERFORMANCES

a) TRANSMUTATION RATE

The first parameter of interest with regards to transmutation performances is the transmutation rate, which can be related to the efficiency of the transmutation process. Several comments can be made on Figure 120. The options U/Pu/Ma and Th/U-Pu/MA, which correspond to the case where only the minor actinides are left in the blankets, yield the lowest transmutation rate. Indeed, for these two strategies, no fissile material is initially present in the blankets. Consequently, the neutron production *in situ* is limited compared to the other cases, which in turn limits the transmutation performances. The thorium case is slightly lower than the uranium one as the thorium mass in the blankets is inferior to the uranium mass due to the thoria density being only 10 $g.cm^{-3}$ compared to 10.95 $g.cm^{-3}$ for uranium dioxide. This leads to a

lower production of fissile material during irradiation and thus a slightly lower transmutation rate.

In all the three other cases, fissile materials are left in the blanket during reprocessing. The transmutation rate is then directly proportional to the amount of fissile material in the blanket. For the Th(U)/Pu/MA strategy, the fraction of U233 in the blanket is 7 % and for the two TRU cases, volume fractions of "fissile" material (U233, U235, Pu239 and Pu241) at the beginning of irradiation at equilibrium are respectively 7.8 % and 8.0 % for Th/U(TRU)) and Th(TRU).

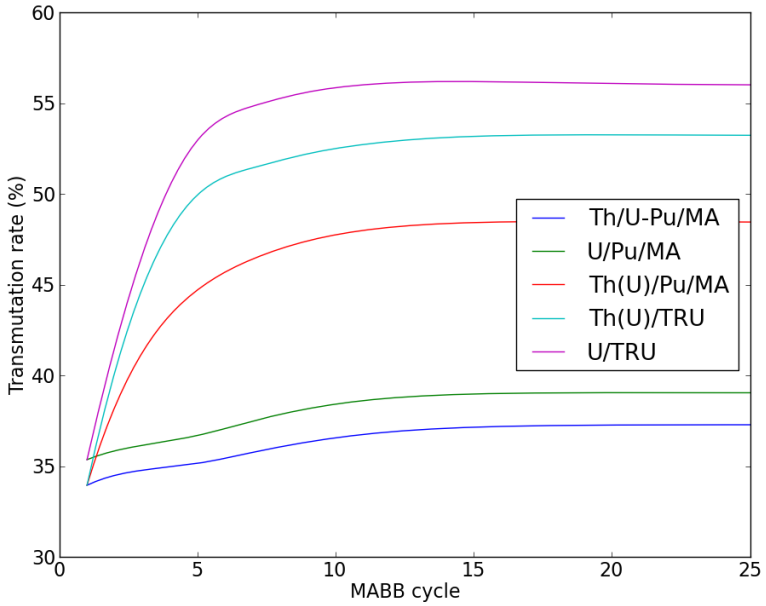

Figure 120 : Evolution of the transmutation rates in the MABB

The increase in the transmutation performances is directly linked to the increase in fissile material in the blanket assembly. The latter has two mutually opposing effects on the neutron spectrum in the blankets. On the one hand, the increase in the flux level leads to a direct increase in the reaction rate, while on the other hand, the spectrum hardening leads to a decrease in the absorption cross section, thus decreasing the transmutation rate.

To evaluate the magnitude of each effect, the same calculations were carried out over 410 EPFD using a simplified depletion equation while varying in turns the spectrum and the flux level. Two calculations were performed with the neutron spectrum from the U/Pu/MA case and two different flux levels and the same jobs were performed again with the Th(U)/Pu/MA spectrum.

Table 86 : Comparison of the one-group cross sections between the uranium and thorium case

Uranium		
Isotope	Capture (b)	Fission (b)
Th232	4.46E-01	1.00E-02
U233	2.69E-01	2.81E+00
U238	2.94E-01	3.96E-02
Pu239	5.77E-01	1.86E+00
Np237	1.72E+00	3.07E-01
Am241	1.96E+00	2.51E-01
Am243	1.76E+00	1.83E-01
Cm244	9.14E-01	3.88E-01

Thorium		
Isotope	Capture (b)	Fission (b)
Th232	3.33E-01	1.17E-02
U233	2.51E-01	2.69E+00
U238	4.06E-01	4.64E-02
Pu239	5.32E-01	1.86E+00
Np237	1.55E+00	3.50E-01
Am241	1.81E+00	2.89E-01
Am243	1.60E+00	2.12E-01
Cm244	8.31E-01	4.38E-01

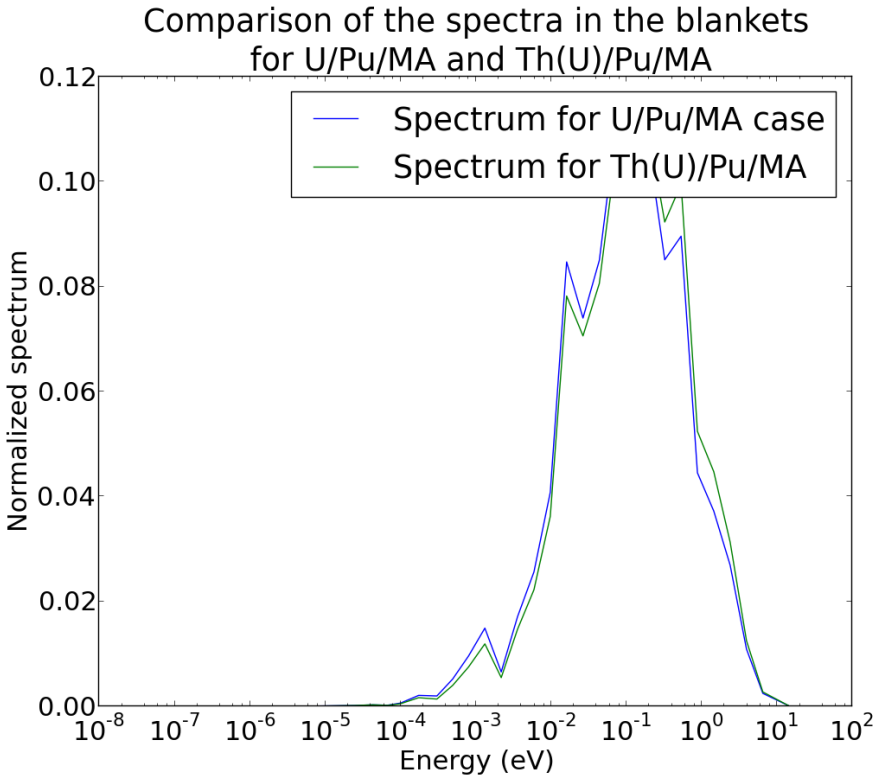

Figure 121 : Difference between the spectrum in the blankets in the thorium case and in the uranium case

Table 87 : Comparison of the effect of cross sections variations and flux levels on transmutation rate over one cycle

Transmutation rate (%)	Flux level of Uranium case : 9e14 n/cm²/s		Flux level of Thorium case : 1,2e15 n/cm²/s	
	Uranium Spectrum	Thorium Spectrum	Uranium Spectrum	Thorium Spectrum
Support U	-5,2	-5,12	-6,39	-6,28
Support Th	-5,27	-5,19	-6,43	-6,33

Looking at Table 87, we can see that the impact of the spectrum hardening is limited to around -0.1 % point in the transmutation rate. Looking at the impact of the flux level, we can see it is dominant compared to the spectrum effect, and that is this effect which explains the increase in transmutation performances.

b) SUPPORT RATIO

The results for support ratio evaluation are given in Table 88. Similarly to what can be seen on Figure 120, obviously the strategies where fissile materials are left in the blankets are more effective than the two strategies without fissile material. We can also see that the U/TRU approach yields the best support ratio. As the core production of minor actinides is nearly not impacted by the presence of minor actinides bearing blankets, the support ratio is proportional to the transmutation rate.

Table 88 : Support ratio for each strategy at equilibrium

Strategy	Th/U-Pu/MA	U/Pu/MA	Th(U)/Pu/MA	Th(U)/TRU	U/TRU
Support ratio	1.61	1.77	2.2	2.55	2.68

4) COMPARISON OF URANIUM AND THORIUM AS SUPPORT MATRIX FOR MABB : IMPACT ON CORE PARAMETERS

a) CORE OPERATION PARAMETERS

The impacts of each strategy on core operation parameters are given in Table 89. The reactivity swing in the thorium case is higher at the beginning of irradiation than for uranium as thorium is more capturing than uranium and the build-up of plutonium 239 and uranium 233 occurs in the first cycles. At equilibrium, the reactivity swing is higher for the case with fissile material in the blankets as these blankets act like fuel assemblies. Conversely, the average burn-up is lower as power production is spread over one more ring of assemblies.

The cases where thorium and uranium 233 are kept in the blankets have a lower impact on the core sodium void worth as the ν-factor (neutron production per fission vs energy) of U233 dependency on the neutron energy is flatter than to the one of plutonium at high energy. Consequently, in case of coolant voiding, the contribution of the blankets to the total sodium void worth is lower. The case with uranium leads to a higher power production in the blankets by 8 % at equilibrium which is due to the higher content in fissile material in this case. During

the first cycles, both cases are equivalent. In both fissile-free cases (U/Pu/MA and Th/UPu/MA), the breeding gain is increased by 0.1 due to the presence of fertile blankets. In the other case, the breeding gain only increase by a factor six to eight as fissile material is already present in the blankets. This residual increase is mainly explained by production of more fissile isotope such as plutonium 238 during the transmutation process.

Table 89 : Impact of the support on core parameters (MA 2035 vector, no moderating material, FC = fifth cycle, EQ = equilibrium cycle)

Parameters	SFR V2B Core (453 S/A)	Th/U-PU/MA	U/Pu/MA	Th(U)/Pu/MA	Th(U)/TRU	U/TRU
Reactivity swing (FC) (pcm)	-450	-518	-419	-518	-518	-419
Reactivity swing (EQ) (pcm)		-153	-108	-151	-240	-241
Mean Burn-up, FC (GWd\tHM)	99	97	97	97	97	97
Mean Burn-up, EQ (GWd\tHM)		93	93	87	83	82
Max DPA (FC)	149	156	156	157	157	156
Max DPA (EQ)		150	149	149	152	155
Sodium void worth (pcm) (FC)	1790	1808	1818	1808	1808	1820
Sodium void worth (pcm) (EQ)		1814	1821	1791	1783	1837
Doppler Effect Magnitude (pcm) (FC)	-441	-430	-440	-430	-430	-434
Doppler effect (pcm) (EQ)		-444	-448	-443	-428	-424
Breeding gain (total/blankets) (FC)	0.009	0.088/0.093	0.086/0.082	0.088/0.093	0.088/0.093	0.086/0.082
Breeding gain (total/blankets)(EQ)		0.106/0.039	0.103/0.058	0.078/0.029	0.063/0.008	0.062/-0.001
Fraction of power in blankets at EOC (%) (FC)	0	2.1	2.4	2.1	2.1	2.4
Fraction of power in blankets at EOC (%) (EQ)	0	5.4	5.64	10.5	13.5	14.7

b) INVENTORY IN THE BLANKETS

The evolution of the heavy nuclides content in the blankets is given in Figure 122. The behavior of each element can be divided into two consecutive patterns constituted of a first irradiation phase of 4100 EPFD followed by a second one of similar-length. Then, the blankets composition is evolved for 2555 days to simulate reprocessing and the blankets are recompleted using the minor actinides vector from the core production (also after 2555 days of decay) to achieve 2375

kg of MA in the blankets. Mass balance is achieved using the support element. Cooling time was omitted on Figure 122 for clarity.

Thorium and uranium in the cases where they are used as support matrix behave similarly. Their mass decreases during irradiation and are stable during decay phase. Both the time necessary to reach an equilibrium situation and the amount of thorium/uranium in the blankets depends on the amount of fissile elements in the blankets. Both Th/U-Pu/MA and U/Pu/MA reaches equilibrium after on complete MABB cycle (10 reactor cycles). Cases where fissile material is present in the blankets require a longer time to achieve equilibrium.

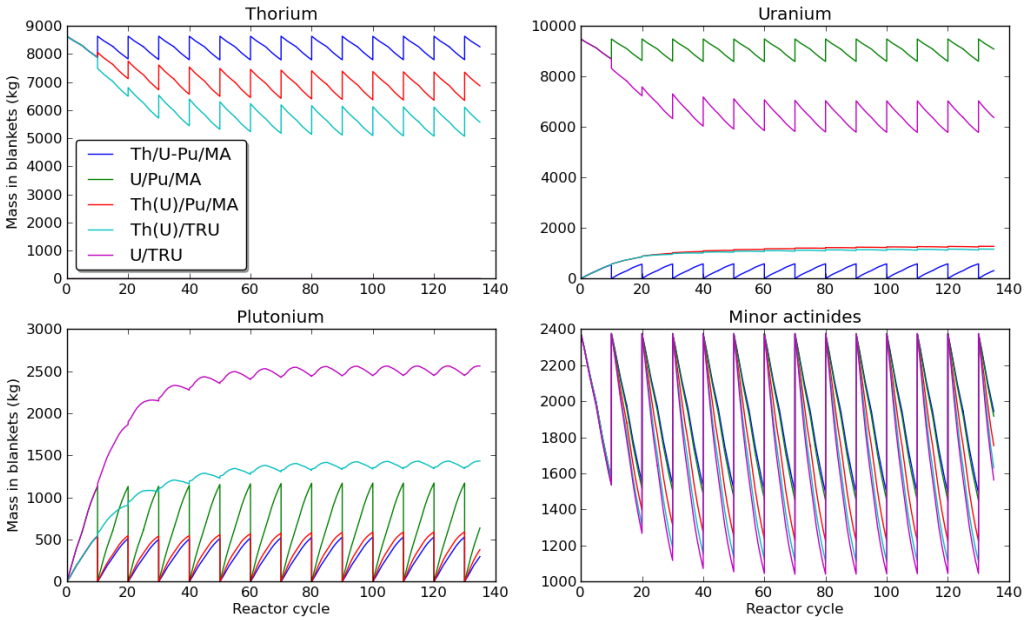

Figure 122 : Evolution of the Th, U, Pu and MA content in the blankets vs reactor cycle. Cooling and manufacturing were not plotted.

Regarding uranium evolution, it should be noted that the uranium mass in the Th(U)/TRU or Th(U)/Pu/MA is remarkably stable during irradiation, which will have a positive effect on power variation in the blankets during irradiation. Considering plutonium production, it is interesting to observe that half of the plutonium production in the U/Pu/MA case is coming from minor actinides transmutation, especially from the reaction ${}^{241}_{95}Am + n \rightarrow {}^{242}_{96}Cm \xrightarrow{\alpha} {}^{238}_{94}Pu$. Using thorium as support matrix consequently halves the production of plutonium in the blankets and the related inventory. Regarding the evolution of minor actinides mass in the blankets, the behavior of each curve on Figure 122 is directly related to the transmutation rate plotted on Figure 120.

The uranium 233 vector is slightly different between the Th(U)/Pu/MA and Th(U)/TRU cases with respectively 63 and 53 % of uranium 233. The exact composition is given in Figure 123 at EOEC. It can be seen that the fraction of U232, which has a strong gamma emitter in its decay chain is the same in both cases.

Figure 123 : Uranium vector at equilibrium loading for Th(U)/Pu/AM and Th(U)/TRU strategies

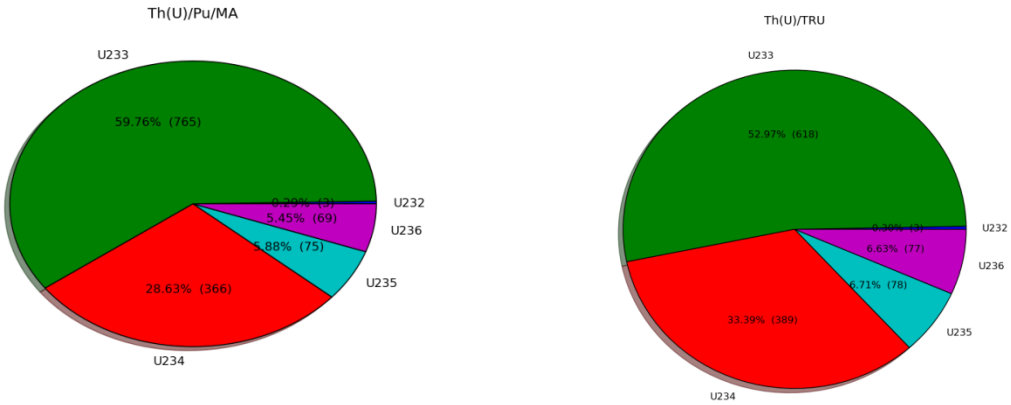

The plutonium isotopic vector is however widely varying between the various cases. As it can be seen in Figure 124, the Pu239 content in the thorium cases is very limited, making the plutonium useless for reactor use without dilution with higher-grade plutonium. This plutonium could for instance be used as denaturing material for military grade plutonium [112] or mixed with high-grade plutonium depending on the considered limits for proliferation resistance. It should be noted that the total mass of plutonium 238, which is the main responsible for decay heat at the reprocessing time-scale is similar between the two cases, as this production is related to the transmutation process and not to the breeding on the support.

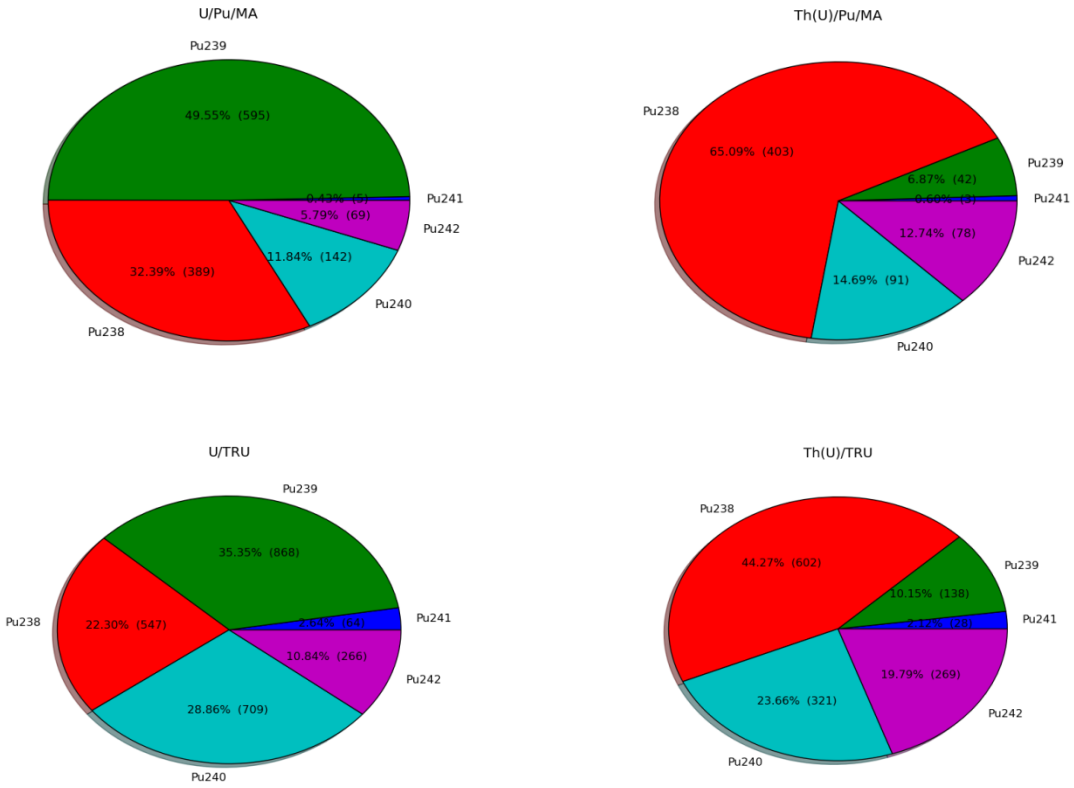

Figure 124 : Plutonium isotopic vector at equilibrium for U/Pu/MA, Th(U)/PuMA, U/TRU and Th(U)/TRU. The case Th/UPu/MA is similar to the Th(U)/Pu/MA in terms of isotopic vector.

mass in kg	Th/U-Pu/MA	U/Pu/MA	Th(U)/Pu/MA	Th(U)/TRU	U/TRU
Np237	211.2	225.8	175.2	137.8	124.4
Am241	694.9	667.0	543.4	458.1	401.1
Am242m	69.5	70.1	57.4	49.6	43.8
Am243	225.3	203.8	176.1	187.6	183.7
Cm242	0.2	0.2	0.2	0.1	0.1
Cm243	2.5	2.6	2.8	2.9	2.9
Cm244	140.2	134.8	135.4	145.7	157.6
Cm245	48.2	47.0	45.3	47.3	52.5
Cm246	36.6	35.9	31.7	31.1	34.5
Cm247	7.5	7.4	6.0	5.7	6.3
Cm248	5.4	5.7	4.8	4.5	4.9
Total	1441.5	1400.3	1178.2	1070.4	1011.7

frac in %	Th/U-Pu/MA	U/Pu/MA	Th(U)/Pu/MA	Th(U)/TRU	U/TRU
Np237	14.65	16.12	14.87	12.87	12.29
Am241	48.21	47.63	46.12	42.80	39.64
Am242m	4.82	5.01	4.87	4.63	4.33
Am243	15.63	14.55	14.94	17.53	18.16
Cm242	0.01	0.01	0.01	0.01	0.01
Cm243	0.17	0.19	0.24	0.27	0.28
Cm244	9.73	9.63	11.49	13.61	15.58
Cm245	3.35	3.36	3.84	4.42	5.18
Cm246	2.54	2.57	2.69	2.90	3.41
Cm247	0.52	0.53	0.51	0.53	0.62
Cm248	0.37	0.41	0.41	0.42	0.48
Total	100.00	100.00	100.00	100.00	100.00

Table 90 : Minor actinides isotopic vector comparison at end of irradiation cycle at equilibrium

Looking at Table 90, the final inventory in minor actinides is directly linked to the transmutation performances of the strategy considered. The strategies with the highest transmutation rates also lead to a shift of the isotopic vector towards heavier curium isotopes, both in terms of mass and in terms of content. This shift is due to the higher level of flux which permits successive capture on curium isotopes and to the reprocessing of curium in the minor actinides. This can be seen while comparing Th/U-Pu/MA and U/TRU strategies for instance. The effect of this shift on fuel cycle parameters such as decay heat or neutron source is evaluated subsequently in this work.

c) POWER LEVELS IN THE BLANKETS

Power level variation in the blankets is due to the build-up of fissile isotopes during irradiation. One part is due to production of fissile material such as Am242m from the minor actinides initially loaded and the other part is explained by the support. Figure 125 shows the evolution of the power level in the blankets. For fissile-free strategies, we can observe an increase in the power level in the blankets due to the production of plutonium 239 or uranium 233. The sharp increase observed after five cycles is explained by the calculation scheme used, which adjusts the enrichment of the entire core to take into account the fissile material in the blankets, thus increasing the flux region. This also explains the behavior of the three other strategies.

Looking at Figure 125, it can be observed that the cases Th/U-Pu/MA and U/Pu/MA are very similar in terms in power level and power variation during irradiation. This is explained by the production of Pu239/U233 during the first phase of irradiation followed by a quasi-equilibrium state during the second irradiation phase. The minor actinides contribution is similar for each case. Power variation in the region is 144 MW over ten reactor cycles for the thorium case and 113 MW for the uranium one, which corresponds respectively to a 218 % and 152 % increase in blanket power.

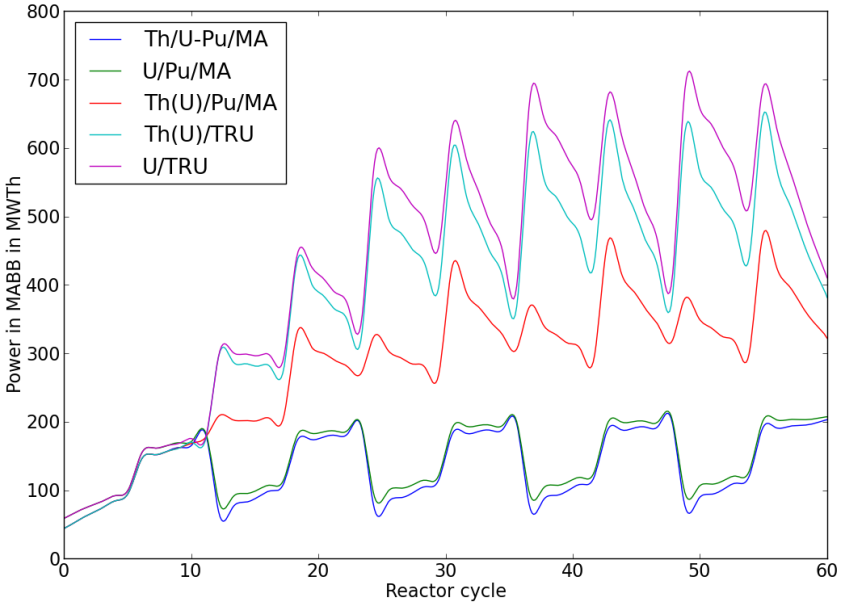

Figure 125 : Evolution of the power level in the blankets during irradiation

For the TRU cases, the power level can reach up to 720 MW due to high fissile content in the blankets. This is equivalent to adding a new ring of fuel assemblies in the periphery of the core. In the case, the blankets assemblies are equivalent to fuel assemblies in terms of power at the end of irradiation but undergo a 45 % increase in their power from 400 to 720 MW, compared to a 20 % maximal increase for standard fuel assemblies. This high power variation may have adverse effects on fuel mechanical behavior, especially for swelling and fission gases release behavior [61].

The Th(U)/Pu/MA strategy is an intermediate one with a higher power level which may be beneficial for pins mechanical behavior compared to fissile-free strategy. The lower power variation limited to 193 MW or a 156 % increase, may also limits the constraints on the assembly design. As such, it may be interesting as a solution which could increase the transmutation performances without hindering assembly conception.

5) COMPARISON OF URANIUM AND THORIUM AS SUPPORT MATRIX FOR MABB : IMPACT ON FUEL CYCLE PARAMETERS

In terms of fuel cycle, the estimators that were selected are the decay heat, gamma source and neutron source of the spent fuel. R&D is currently still required to ascertain the feasibility of handling, reprocessing and manufacturing of minor actinides bearing blankets and we showed here that using thorium instead of uranium does not add new requirements to the fuel cycle part. The depletion calculations were performed using the DARWIN code package [38].

a) MANUFACTURING AND REPROCESSING OF THORIUM OXIDE FUELS

An extensive review of the benefits and challenges associated with the thorium fuel cycle has been done by the IAEA in [106]. Generally speaking, the main challenge associated with thorium reprocessed is the industrial implementation and validation of the THOREX process developed

at Oak Ridge in the fifties. This implementation requires the development of adequate shielding solutions to overcome the issue of high gamma emissions from uranium 232 daughter nuclei such as thallium 208, thorium 228 or lead 212. The presence of hard-to-extract protactinium 233 in the spent fuel is not an issue since its 27 days period means it has completely disappeared from the spent fuel after five years of cooling. A second challenge is the development and industrial validation of a process which can successfully separate and recover U, Pu and the minor actinides from the spent fuel.

It should be noted here that the plutonium obtained from the separation of plutonium from thorium during recycling of the blankets may not be suited for military applications as its Pu 238 fraction is too high according to [112] , as shown in Figure 124.

b) BACK END : DECAY HEAT AND NEUTRON SOURCE

Decay heat per assembly is a dimensioning factor for the reprocessing flowsheet. A "hotter" fuel assembly will require extended cooling time before handling is possible or more expensive handling devices. Similarly, an equilibrium between longer cooling time and decreased reprocessing performances will have to be found as more active fuels degrades reprocessing efficiency [113].

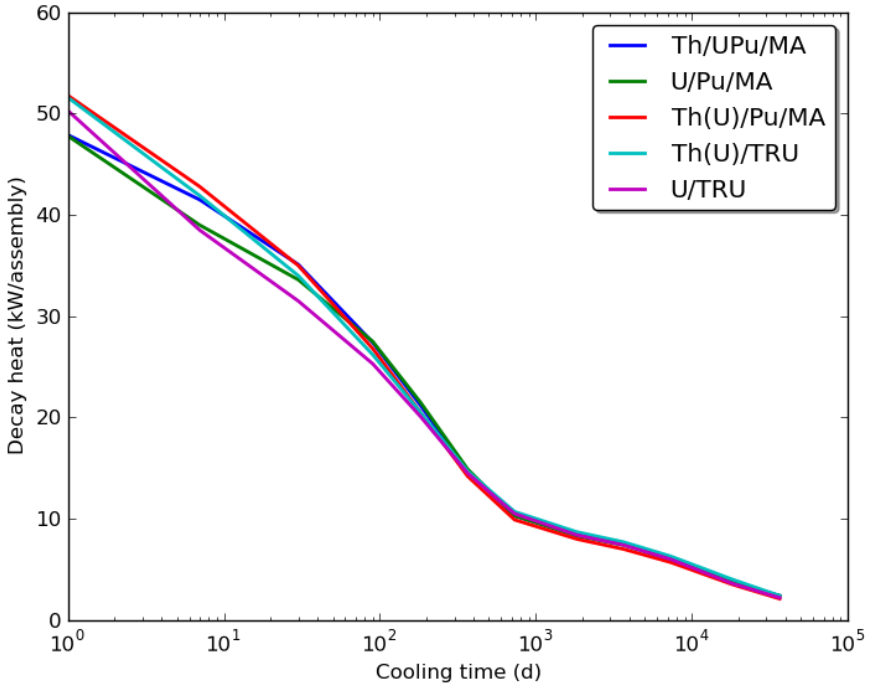

Figure 126 : Evolution of decay heat per assembly for each strategy

Time evolution of decay heat in the spent blanket assemblies can be separated in two steps as seen in Figure 126. The first one, from end of irradiation to about two years is characterized by a rapidly decreasing decay heat mainly fueled by short-lived fission products and curium 242 decay. The U/TRU strategy is the less penalizing in terms of decay heat for this timescale as in this case curium 242 concentration has already peaked and actually started decreasing under irradiation. On the longer time scale, from two years to a century, the decay heat decrease is slower as the main contributors are Pu238 and Cm244, with half lives of 87.8 and 18.1 years.

The decay heat for the Th(U)/Pu/MA strategy is the lowest for this time scale, as more americium 241 has been consumed than in the fissile-free cases and less curium has been produced than in the TRU cases. Irradiated assemblies in the Th(U)/Pu/MA are on the average 10 % less active than those of Th(U)/TRU, which is the most penalizing case.

If the impact of the strategy on decay heat is relatively limited, neutron source can change up to 30 % between the two extremal cases. Neutron source is mainly linked to curium isotopes heavier than curium 244 and is key factor for evaluating transportation and reprocessing feasibility, with regards both to radioprotection and criticality safety. In the U/TRU case, the plutonium accumulation in the blankets creates a reservoir for americium production and curium production onwards, which explains the higher neutron source associated with this strategy. In this case, using thorium as a support matrix leads to a reduction of 10 % in the total neutron source on the short term. In both fissile-free strategies, the neutron source remains lower than 6e10 n/s/assembly due to a low production of higher curium isotopes as it can be seen in in Table 8.

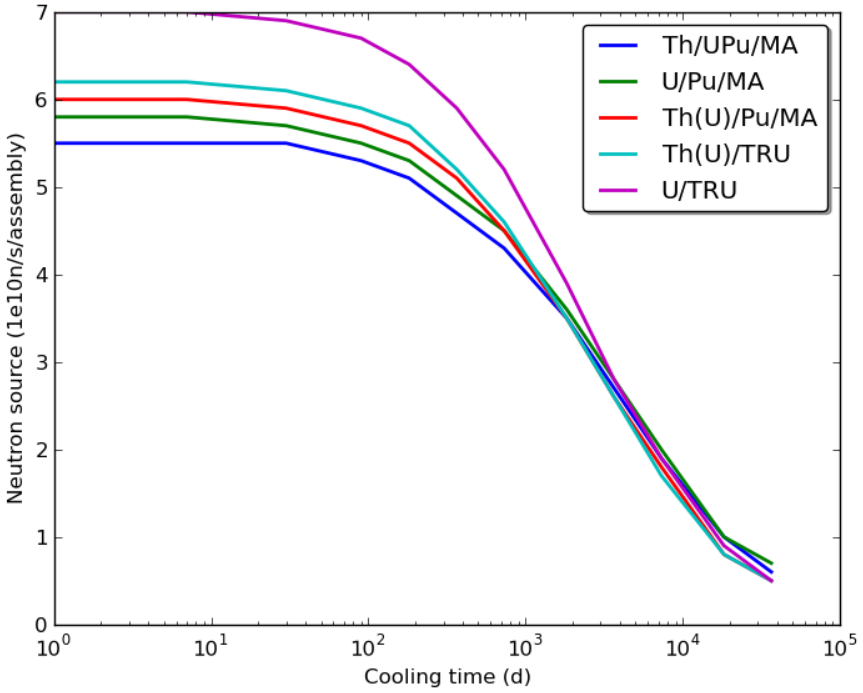

Figure 127 : Evolution of neutron source vs cooling time for each strategy

c) GAMMA EMISSION

A potential issue associated with the use of thorium is the increased gamma emission coming from thorium 228 and its daughter-nuclei or Pa 233, which are strong gamma emitters [106]. The level and spectrum of gamma emission 30 days after the end of irradiation (assembly extraction of the core for relocation) and 5 years (typically expected cooling time) have been evaluated, to assess the shielding requirements both for handling the irradiated assembly during refueling operations and during reprocessing. The results are given in Figure 128 and Figure 129. A comparison of the total level of gamma emissions in each case is also given in

Table 91. It should however be noted that due to the high content in minor actinides, remote handling will be necessary both for manufacturing and reprocessing of transmutation targets.

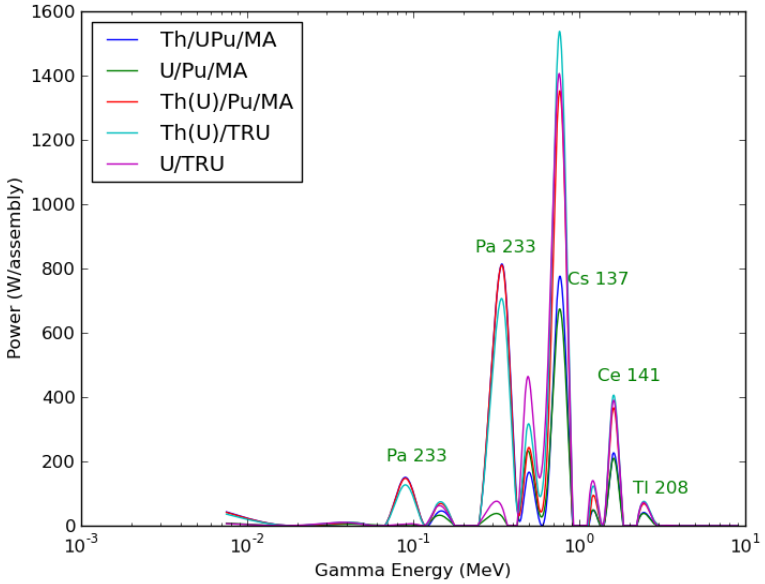

Figure 128 : Gamma spectrum after 30 days of cooling of irradiated CCAM assembly

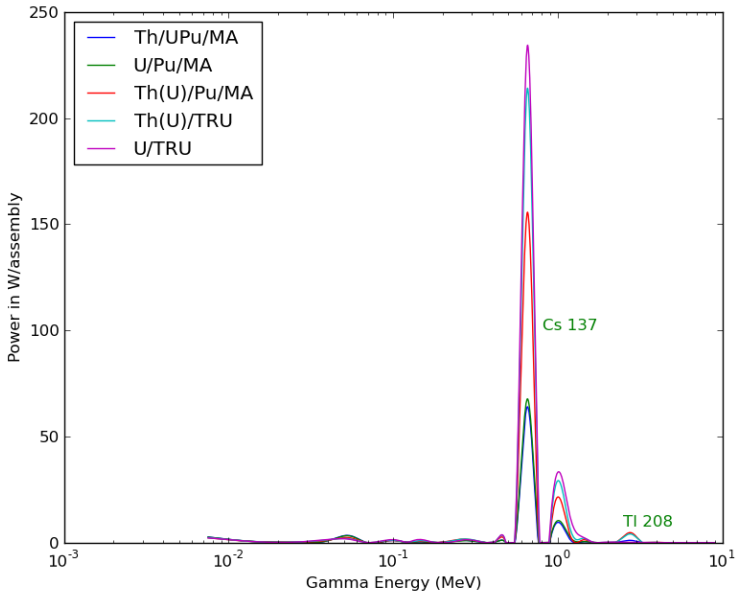

Figure 129 : Gamma spectrum at 5 years of irradiated CCAM with U or Th support matrix

Table 91 : Comparison of the total level of gamma emissions at the end of irradiation

Strategy	Th/U-Pu/MA	U/Pu/MA	Th(U)/Pu/MA	U/TRU	Th(U)/TRU
30 days (W/assembly)	2559	1536	3680	3441	4081
5 years (W/assembly)	89	95	208	327	289

Concerning Figure 128, two remarks can be done. First, the presence of low energetic gammas from Protactinium 233 can be observed along with a small contribution from Thallium 208 in the 2 MeV range. These two contributions are directly due to nuclei produced by capture on thorium or thorium disintegration chain and are thus not visible in the spectrum for the U cases. The second point to make is that several peaks such as for Cs 137 or Ce 141 are corresponding to fissions products. The height of these peaks is linked to the amount of fissile material in the blankets and to the transmutation performances of the strategy.

Contrary to the decay heat and neutron source, it is expected that the evolution kinetic of gamma emission will be different between the two cases as the main emitters are not the same. However, as most of the gamma emissions (more than 70 %) come from fissions products which are roughly the same regardless of the support matrix, the difference in evolution time-scale is limited, as it can be seen on Figure 130.

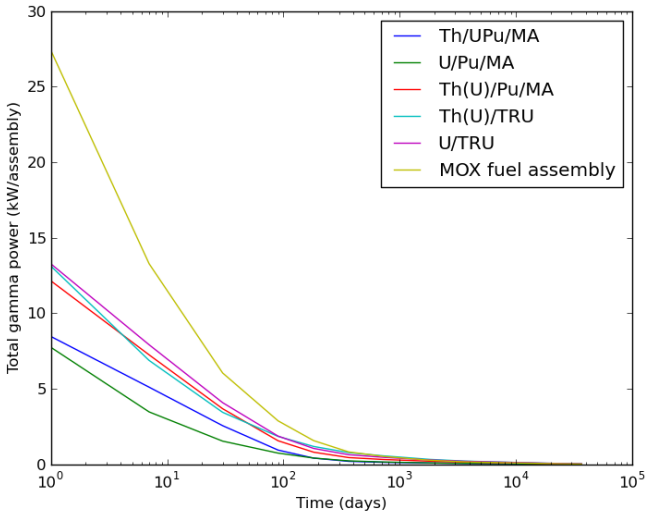

Figure 130 : Comparison of the evolution of gamma emissions for three cases

Regardless of the strategy, the total gamma emission of the blankets assembly is always lower than the one of a standard fuel assembly, as the one of such an assembly is dominated by fission products.

d) Conclusion

The conclusion of this analysis is that the use of thorium instead of uranium as support matrix for MABB will have a limited impact on spent fuel neutron source and decay heat, which means that no additional constraints have to be considered on the conditioning of the waste for final disposal. However, the increased number of fissions in the blanket assemblies in the thorium and TRU cases means that more fission products are going to be found in the assemblies to be reprocessed and thus the gamma emission of these elements will be higher compared to the fissile-free cases. Thorium itself was not found to have a significant impact on the gamma emission of the fuel elements except between 30 and 300 days where Protactinium 233 is responsible for up to 30 % of the emission. The exact impact of the 2.6 MeV gamma emitted by Thallium 208 on the fabrication and retreatment processed should be more thoroughly assessed in the future, notably in terms of additional shielding required. However, the high minor actinides content is likely to induce the need for adequate shielding, thus mitigating the increase in safety requirements for handling thallium 208.

6) Conclusion

We can compare the various strategies with the U/Pu/MA, which is the one currently envisioned in France [114]. This is done in Table 92. We can see that simply replacing uranium with thorium in the blankets and extracting the uranium 233 for use elsewhere yields performances lower than in the reference case, except for the impact on reactor operation due to the flatter ν-value of the uranium 233 compared to Pu239.

Uranium 233 can also be left in the blankets to fasten the transmutation process. In this case, we compared a strategy where only uranium 233 is left to two strategies where all the transuranics elements are left in the blankets with either uranium or thorium support. Again, the thorium impact on core operation is lower. In terms of fissile inventory, the U/TRU case leads to the highest fissile inventory in the blanket while use of thorium leads to a 10 % lower inventory. The neutron sources at 30 days and at five years are also lower in the thorium case due to a lower of production of heavy curium isotopes. In terms of decay heat, thorium is less effective at 30 days but leads to a lower long-term decay heat source.

Table 92: Global comparison of the five strategies previously discussed

Strategy	U/Pu/MA (REF)	Th/U-Pu/MA	Th(U)/Pu/MA	Th(U)/TRU	U/TRU
Transmutation rate (%)	39	37.4	48.5	53.3	56
Sodium void worth (Δ with standard core value, pcm)	+31	+24 (-22.6 %)	+1 (-96.8 %)	-7 (-122 %)	+47 (+153 %)
Reactivity swing (% of the standard core)	24	34 (+41 %)	34 (+41 %)	53 (+121 %)	54 (+125%)
Power in blankets (MW)	5.64	5.4 (+4.4 %)	10.5 (+86.2 %)	13.5 (+139 %)	14.7 (+161 %)
Power variation in blankets during irradiation (MW)	113	144	193	281	324
Assembly residual power at 30 days	33.6	35.1 (+4.5 %)	35,0 (+4.2 %)	34,0 (+1.2 %)	31,5 (-6.3 %)
Neutron source at 30 days	5,46	5,70 (+4.4 %)	5,92 (+8.4 %)	6,10 (+11.7 %)	6,87 (+25.8 %)
Fissile material inventory in the blankets at EOEC (kg)	606	573 (-5.4%)	880 (+45 %)	863 (+42 %)	957.6 (+58 %)

It can be concluded that the use of thorium as a substitute for uranium support in minor actinides bearing blankets does not yield increased transmutation performances if the uranium 233 thus produced is extracted for use outside the blankets. On the other hand, the use of thorium blankets with a 'TRU' scheme in which all the transuranics, plutonium included, are left in the blankets for further irradiation yields similar performances to the uranium one albeit with a lower impact on the core parameters due to better neutronic behavior of uranium 233 and a lower overall fissile inventory by 16 %. The intermediate option of reusing only the uranium 233 produced in the blankets to speed up the transmutation process yields intermediate performances but require fine reprocessing of the irradiated fuel. This approach also increases the transmutation performances compared to a fissile-free approach while limiting the power variation in the blankets which is favorable in terms of assembly design. We can conclude from this work that the choice of thorium instead of as support matrix for heterogeneous transmutation targets cannot be decided in terms of transmutation performances only but requires careful analysis of the potential gains it can bring with regards to the overall fuel cycle.

ANNEX 3: OVERVIEW OF THE EXISTING TRANSMUTATION CONCEPTS

Highlights:

- ✓ **Current reactors (PWRs) appears are less suited for transmutation than fast reactors.**
- ✓ **Transmutation in fast reactors can be done either by mixing the fuel and the minor actinides (homogeneous approach) or using dedicated targets (heterogeneous approach)**
- ✓ **Each approach exhibits specific drawbacks and advantages.**
- ✓ **Experiments have shown that limited loading of minor actinides in the fuel did not change its behavior while further studies were required for the high fractions associated with the heterogeneous approach.**
- ✓ **Fuel cycle impacts appear to be important with higher decay heat level and neutron source both for the fresh and spent fuel.**

An extensive review of the various transmutation systems that have been proposed so far and of the experiments related to transmutation that have been carried out is given here, with the main conclusions outlined. Then, the various solutions for separation and recovery of minor actinides are presented, along with possible technological solutions for manufacturing of transmutation fuels. The aim of this chapter is to present a panoramic view of the possible options for minor actinides transmutation as a basis for improvement.

1) PROPOSED DESIGNS FOR MINOR ACTINIDES TRANSMUTATIONS

a) TRANSMUTATION IN THERMAL REACTORS

Considering that nearly all of the currently operating nuclear reactors are light water reactors, exploring the thermal spectrum transmutation approach seems interesting as a lot of experience is available on this kind of reactors [115]. It would also be implementable within decades, which would limit the size of the minor actinides "buffer" which is stored in glasses. Minor actinides stored this way are unlikely to be transmuted in the near future due to the difficulty of recovering them from the nuclear glasses [22].

This option was studied in depth in France following the 1991 Act on nuclear waste management and it was concluded that minor actinides burning can be achieved in thermal reactors and could be a transitory step towards transmutation in fast reactors which would help validate the fuel fabrication, reprocessing and handling techniques necessary to successful implementation of minor actinides transmutation in FR. Specificities of transmutation in

thermal reactors can be found in more details in [45]. Assembly design for transmutation have been proposed in [116] for instance and studied in details in [117]. Minor actinides recycling in PWR requires first the implementation of an adequate solution to close the plutonium cycle, which has the effect of increasing the minor actinides production. This can be achieved by modifying the standard fuel assemblies to reach a zero mass balance of plutonium, as discussed in [118]. Once this is achieved, minor actinides transmutation can be implemented by homogeneous dilution of the minor actinides in the fuel or by replacing some fuel rods by minor actinides rods. However, in each case, an increased enrichment in uranium 235 is required in order to compensate for the fact that minor actinides are net neutron absorbers in a thermal spectrum. Additionally, loading of plutonium in PWR assemblies is limited to up to 12 at% due to design constraints on the maximal allowable void worth. It is generally considered that a loading of 1 at% of americium is equivalent to 4 at% of plutonium [78], thus limiting the maximal amount minor actinides which can be loaded to 3 at% and making the loading of minor actinides along with MOX fuels more complicated.

The main drawback associated with minor actinides transmutation in thermal spectrum is that the high capture cross sections disproportionately leads to capture rather than fission, and this leads to an important production of curium and heavier actinides with very high neutron dose rate and thermal load, which extensively complicates the reprocessing operations. Curium transmutation and reprocessing in thermal reactors should be avoided to prevent its build-up as it is difficult to handle. ^{245}Cm especially has a critical mass of 54 gr in aqueous solution, which means that using current technical solutions, its reprocessing is not realistic. Consequently, only americium recycling should be implemented in thermal reactors, which implies the separation of Am from Cm which has not yet been demonstrated on the industrial scale for now, which prevents a possible implementation of transmutation in thermal reactors.

However, successful minor actinides transmutation requires the optimization of the consumption in the reactor core but also the minimization of the source and of the inventory. If it is possible to multi-recycle plutonium with the PWR option to reduce the plutonium inventory, it leads to a production of minor actinides several times higher compared to the closed case with fast reactors. This also means that equilibrium inventory of minor actinides in the entire fuel cycle will be much higher in this case. As a consequence, we did not pursue further the study of minor actinides transmutation in thermal reactors in this work.

b) Transmutation in fast reactors

As we have already seen in the previous chapter fast reactors are more adapted to minor actinides transmutation than thermal reactors as they produce less minor actinides and as they have a better neutron balance. The fast spectrum also leads to better fission-to-capture ratio which limits the production of Curium and heavier actinides and leads to smaller inventories. The various technical solutions that have been proposed so far are discussed below.

i) HOMOGENEOUS TRANSMUTATION

In the homogeneous recycling option, the minor actinides are directly mixed with the standard fuel, with up to 10 % of minor actinides in the current propositions, depending on the type of reactor (concept, power, size, etc.…). The interest of this approach is that the transmutation performances are quite interesting as the minor actinides are directly exposed to a high and energetic flux.

However, the introduction of MA in the fuel decreases the Doppler coefficient in absolute value and increases the coolant void worth. This degradation of the reactor coefficients is a safety issue which puts an effective limit on the maximum amount of minor actinides than can be mixed with the fuel. Details on the effect of MA addition the fast reactor fuel can be found in [101]. Solutions to this problem have been proposed, for instance in the form of the BUMPY assembly [4] or heterogeneous design of the core such as in the CFV concept [80]. Addition of heterogeneities in the core decreases the coolant void worth by increasing the leakage coefficient in case of voiding. In order to increase the Doppler contribution, it is possible to add moderating material in the core which would slightly soften the spectrum and thus increase the neutron population in low energy range below 30 keV. However, this degrades the core breeding ratio and fission-to-capture ratio and thus as a negative impact on transmutation performances.

Minor actinides transmutation however requires adaptation of the entire fuel cycle to withstand incorporation of minor actinides with high neutron activity, decay heat and gamma emission. This will complicate both the reprocessing process and the manufacturing of the new pellets, which will at least necessitate glove-boxes if not installation of hot-cells dedicated to fuel manufacturing, as it will be discussed thereafter.

ii) HETEROGENEOUS TRANSMUTATION

In the heterogeneous case, minor actinides are separated of the spent fuel and loaded in dedicated targets. This requires the separation of the minor actinides from the plutonium beforehand, but allows separating the conventional fuel cycle from the minor actinides recycling part. Those targets can be loaded in dedicated positions in the core or at its periphery.

Heterogeneous recycling targets can make use of either an UO_2 matrix, which presents already well known properties and is compatible with transmutation, or an "inert" matrix, which avoids the production of plutonium during the irradiation. However, a suitable matrix with good properties under irradiation must be found for this application. An overview of the requirements for such a matrix can be found in [119]. High melting point, high thermal conductivity, high density, low chemical reactivity with cladding material, low impact on the core reactivity and good stability under irradiation are required, the reference point being uranium dioxide. Reprocessing feasibility may also be necessary if the fuel has to be reused.

The inert matrix fuel approach was initially designed to use the surplus of plutonium without breeding (uranium-free fuel) and was then applied to the transmutation of minor actinides. When transmutation is considered with a closed plutonium fuel cycle, is it possible to tune the breeding gain of the core to take into account the plutonium production in the blankets during the transmutation process and keep a stable plutonium inventory. New IMF designs based on smaller fuel elements and dispersed fuels have been proposed more recently, in [120] for instance but so far, no adequate matrix has been found yet and research efforts in this direction have dwindled. ([48] [121] [47] [122] or the European project FAIRFUELS [123]).

Using an UO_2 matrix and standard assembly design, the concept of minor actinides bearing blankets (MABB), where the targets are directly placed at the periphery of a critical fast reactor core, has been discussed. The insertion of minor actinides bearing blankets in the core does not degrade core safety parameters [41]. This approach is also compatible with multi-recycling of the irradiated targets and reuse of the plutonium produced. However, the transmutation

performances are slightly lower than in the homogeneous case due to a lower level of flux and the fabrication/reprocessing of the targets remains an issue due to the very high heat rate and neutron dose rate of the virgin and irradiated targets (x80 for the decay heat and x5000 for the neutron source [124]).

One possibility with heterogeneous transmutation is the use of moderated targets assemblies. In this approach, pins with a moderating material (typically zirconium or calcium hydride) are inserted in the target to slow down the incoming neutrons. It is then possible to obtain both the cross sections from an (epi) thermal range and the high flux of a fast reactor, thus increasing the transmutation rate in the target while keeping an acceptable fission rate [125] [102]. However, some issues relative to stability of hydrogenated materials inside the core remain to be solved [126].

A variant has also been proposed in which minor actinides bearing fuels (MABF) are loaded into the core in locations where the associated impacts on core voiding or transient will be minimized [41]. This solution allows taking advantage of the higher flux in the core while minimizing the impact on safety parameters. However, it also combines the drawbacks of the two approaches, e.g. it modifies the core behavior while creating highly active assemblies.

iii) OTHER TECHNICAL SOLUTIONS

Transmutation using a fast neutron spectrum can also be achieved using non-critical nuclear reactors. For completeness, we will just present the two main other solutions which have been discussed in the literature, however we will not investigate further these options.

The first one is the so-called ADS concept which stands for Accelerator-Driven System. This kind of concept is designed around a sub-critical core and a high-energy proton accelerator. The proton beam from the accelerator hits a spallation target located inside the core and produce neutrons to feed the nuclear reaction. As the neutron source can be easily stopped, this kind of reactor is inherently safe for reactivity insertion event, but loss of flow events are still a concern and require that decay-heat removal must be ensured even if the core chain reaction has stopped [127].

Several engineering challenges must be met before an industrial ADS can be built, mainly with the design and operation of the high-intensity proton accelerator which must have a very high industrial reliability. The design of the spallation target requires also a lot of attention. Anticipating a solution to these various issues, the SCK-CEN in Belgium has planned to build a complete demonstrator named MYRRHA by 2021 [128] [129].

The use of such a system for minor actinides transmutation has several advantages, as it removes the safety penalties stemming from minor actinides addition in a critical reactor and detailed in the first chapter. More neutrons are also available for transmutation purposes in such systems. A detailed analysis of transmutation possibilities of such a device will be found in [130].

The second device which has been discussed for transmutation purposes is the so-called FFH, or fission-fusion hybrid in which the 14-MeV neutrons from a fusion reactor are used as an external neutron source for transmutation. The very high energy of these neutrons means that they will predominantly trigger fissions in the minor actinides target and thus be very effective in terms of transmutation. However, the practical feasibility of such a device remains

hypothetical and they will not be included in the scope of this study. More details on this solution can be found in [131].

iv) ONCE-THROUGH OR MULTI-RECYCLING STRATEGIES

Uranium and plutonium reprocessing is routinely carried out in the reprocessing plants of La Hague or Sellafield and the associated technical challenges have been mastered. However, as it was presented in Chapter 1, minor actinides severely complicates reprocessing and manufacturing or minor actinides containing fuels. Considering the issues associated with reprocessing fuels with high minor actinides content, the once-through (OT) solution has been proposed, in which targets are loaded at set positions in the core and irradiated until 90 % of the minor actinides have been transmuted. However, this approach requires very long irradiation times (8700 Equivalent Full Power Days (EFPD) in [102]) which are not achievable using current technologies, mainly due to mechanical constraints on the assembly behavior during irradiation.

v) THE CHOICE OF ELEMENT SEPARATION OR TRU RECYCLING

Regardless of the heterogeneous or homogeneous approach, various solutions are available for the global strategy related to reprocessing and transmutation. The simplest option, which is also the most proliferation-resistant, is to adopt TRU-recycling. TRU stands for *TRansUranics* and represents all the heavy nuclides in the fuel which are not Uranium. In this case, only a separation U/TRU is carried out during reprocessing and the TRU fuel is directly reused. Proliferation resistance is achieved through the mixing of plutonium with highly active minor actinides, making it improper for military handling. This approach is obviously not compatible with heterogeneous transmutation which requires selective recovery of the minor actinides.

It was first discussed in the US in the framework of the Integral Fast Reactor project, which was fueled with metal fuel and built along a pyro processing plant for treatment of the spent fuel. [132] [133]. In a pyro-processing plant, the spent fuel is molten in chloride and fluoride bath and electrochemical technics are used to selectively recover actinides from fission products. Compared to the PUREX process, which is carried out in water, there is no limit on the spent fuel activity as the process is operated at high temperatures. With this design, the plutonium is not separated and does not have to leave the facility, which decreases the risk of diversion. In terms of transmutation performances, the homogeneous approach combined with a metal fuel with a more energetic spectrum than an oxide fuel leads to interesting performances. The fast spectrum leads to a reduced inventory while the homogeneous strategy allows important consumption. Finally, the use of metallic fuel exhibits some interests in terms of safety, as for instance a stronger stored Doppler reactivity for instance, which is due to the low temperature of the fuel in operating conditions and its good thermal conductivity compared to oxide fuels. The important thermal expansion of the metal fuel is also an added benefit in terms of safety. However, the IFR project was cancelled in 1994 and experimental research was halted on this topic. This approach was well-suited to the strategy envisioned at that time in the US, e.g. a closure of the fuel cycle using only fast reactors without reprocessing irradiated UOX fuels from LWRs.

If element separation can be implemented, several ways are open. Neptunium and plutonium selective recovery is already achievable on an industrial basis using the PUREX process. Consequently, we consider that if extraction of plutonium is carried out, neptunium extraction can also be carried out with a limited number of extra steps. Neptunium transmutation being

relatively straightforward, as it yields plutonium by neutron capture; we focused on the americium and curium here. Two cases can be differentiated here: either only Americium is recovered during reprocessing while Curium is discarded as waste with fissions products or Americium and Curium are extracted together. The first solution reduces the constraint on the fabrication as Curium is not present in the fresh fuel, but requires further R&D in order to design an effective Am/Cm separation process. We explain some notations used in this report along with the different flows of radioactive materials in Table 93. The elements between parentheses can be found indifferently in the blankets or in the core depending on the chosen strategy. We will review that current progress on the various reprocessing strategies in the next part.

Table 93 : Description of various reprocessing options

Notation	To reactor core	To reactor blankets	To waste
U/TRU	U,(Pu+MA)	Nil	FP
U/Pu/MA	U,Pu,(MA)	U,(MA)	FP
U/Pu/Np/Am+Cm	U,Pu,(Np),(Am+Cm)	U,(Np),(Am+Cm)	FP,Np
U/Pu/Am+Cm	U,Pu,(Am+Cm)	U,(Am+Cm)	FP,Np
U/Pu/Am	U,Pu,(Am)	U,(Am)	FP,Np,Cm

2) TRANSMUTATION EXPERIMENTS REVIEW

Several experiments on transmutation have been carried out in the past years, notably in the fast reactor Phenix in Marcoule. Among the objectives of these experiments was the observation of the mechanical behavior of the minor actinides loaded fuel under irradiation and the validation of calculation codes in accordance with one of the objectives of the 1991 French Law, namely the demonstration of the feasibility of minor actinides transmutation . An overview of the experimental work carried out in CEA from 1993 to 1997 can be found in [134]. We selected the most relevant ones performed in France and abroad and their conclusions are presented below. An extensive list of the transmutation experiments can be found in [91].

a) SUPERFACT EXPERIMENT (1986-1988)

This experience was carried out by CEA and ITU between 1986 and 1988. One assembly, shown in Figure 131, containing various fuel pins was irradiated for 360 EFPD in the PHENIX reactor core and the irradiated pins were then analyzed by the two participants. Four different fuel pins composition were used:

- $(U,Pu,Am)O_2$ with 2 % Am
- $(U,Pu,Np)O_2$ with 2 % Np
- $(Np,U)O_2$ with 45 % Np
- $(Am,Np,U)O_2$ with 20 % Am + 20 % Np

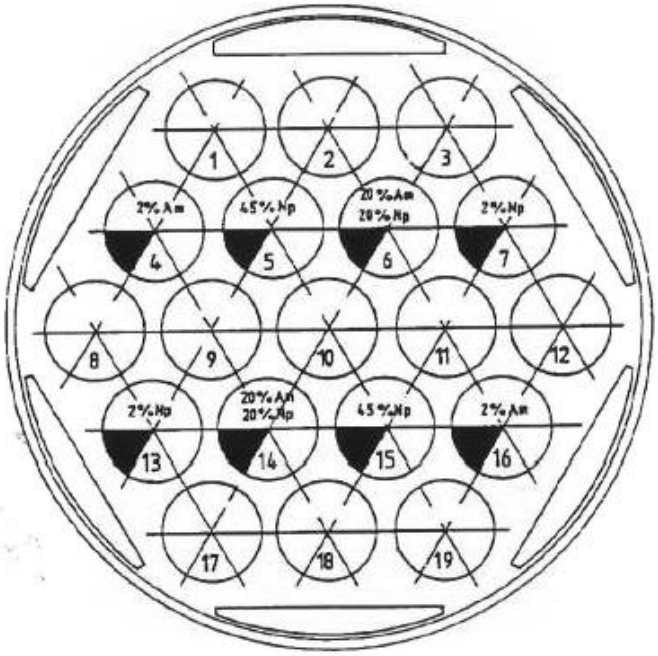

Figure 131 : SUPERFACT experiment assembly with pins positions and compositions [135]

The remaining fuel pins in the assembly were standard PHENIX pins with $UPuO_2$ fuel. The MA-loaded pins were fabricated using the SolGel process [136] which avoids the use of fine powders, thus limiting dust deposition inside the glove boxes. This process also allows a homogeneous distribution of the elements in the fuel.

A point which is interesting to note here is that the linear power of the fuel pins loaded with 45 % of MA increased during irradiation. This is due to the production of elements with a high fission cross section in the fuel by capture on the minor actinides (^{239}Pu from ^{237}Np, ^{242m}Am from ^{241}Am and ^{243}Cm and ^{245}Cm from ^{243}Am). This behavior has to be taken into account in the dimensioning of the fuel pins so as not to exceed the maximum linear power rate to avoid any fuel melting in nominal operation. This will also translate into an increase in the reactivity of some cores when loaded with high minor actinides fraction, increase which should be avoided to prevent a situation where the core would be operated by lowering the control rods.

Extensive post-irradiation analysis was carried out and the following results were obtained [93] :

- A good thermo-mechanical behavior of the fuel pin, except for the americium loaded pins with 20 % of Americium which showed a high helium production coming from the alpha decay of ^{242}Cm. This important helium production increases the strain on the cladding and degrades the thermo-mechanical performances of the fuel. This may limit the residence time or the achievable fluence.
- Transmutation rates around 30 % for all the pins, which was in good agreement with the calculations.
- Spent fuel processing by chromatographic extraction was also demonstrated as a potentially valuable technique to recover U, Pu and potentially Np from the spent fuel.

This experiment hinted towards the feasibility of homogeneous transmutation with loading of a few percent of neptunium or americium and showed the necessity for ulterior developments for americium heterogeneous transmutation in dedicated targets. However, the burn-up was limited at 7 at% and the follow-up experiments which should have taken place in SuperPhénix were never carried out due to the closure of the reactor. However, it is reasonably possible to consider from the experimental data that neptunium transmutation up to reasonably high Np fraction is possible, as the 45%-Np pins did not exhibit any specific behavior. Americium transmutation also seems feasible if the americium content is limited but there are not enough data to refine on this limitation.

SUPERFACT also showed that design modification will have to be carried out for assemblies dedicated to heterogeneous transmutation in order to take into account the high swelling and the increase in pressure due to helium and gaseous fission products release.

b) ECRIX EXPERIMENTS

The ECRIX experiments were a set of two experiments named ECRIX-H and ECRIX-B in which an americium oxide dispersed in an MgO matrix was irradiated for 318 EFPD in the PHENIX reactor. The Am content of the fuel pins was 16.65 % in weight. Moderator material was added to the fuel assembly to speed up the transmutation process, CaH_x in the case of ECRIX-H and B_4C in the case of ECRIX-B. Details on the fuel pin fabrication can be found in [48]. The purpose of the experiments was to study the performances of this new type of fuel and the use of moderated targets for minor actinides transmutation.

Transmutation rate of 94 % were obtained with a fission rate of 25%. These experiments validated the use of moderated targets for transmutation, which leads to nearly full incineration of the Am with a significant fission rate.

Another issue observed in these experiments is the formation of a plutonium oxide phase inside the americium phase which was only partially dissolved during spent fuel reprocessing [47]. This may complicate the full treatment of the fuel in the case of multi-recycling of Am targets.

The conclusion from these experiments and especially from the ECRIX ones is that the use of moderated targets can be considered a possible solution to take advantage of both the high neutron flux in a fast reactor and the high cross sections of a thermalized/degraded spectrum. However, there are some concerns about thermal dissociation of zirconium or calcium hydride in the case of accidents which may prevent the effective use of such materials [46].

c) METAPHIX AND AFC EXPERIMENTS

The METAPHIX set of experiments was carried out in PHENIX from 2003 to 2008 for CRIEPI, a Japanese research institute. The purpose of these tests was to evaluate the feasibility of minor actinides transmutation using metallic fuels and the impact of lanthanides compounds which have to be separated from minor actinides during reprocessing. The following pins were irradiated:

- U-19Pu-10Zr
- U-19Pu-10Zr + 2 % minor actinides + 2 % rare earths
- U-19Pu-10Zr + 5 % minor actinides
- U-19Pu-10Zr + 5 % minor actinides + 5 % rare earths

The minor actinides isotopic composition was 60 % Np, 30 % Am and 10 % Cm while the rare earths were made of 70 % Nd, 10 % Gd,Y,Ce. These compositions are representative of the minor actinides feed from an UOX core and of the main fission products recovered with minor actinides during reprocessing.

Metallic fuel is prepared using injection casting and the presence of rare earths in the liquid feed can lead to segregation of the matrix in two parts, on the one hand U-Pu-Zr-Np and on the other Pu-Am-RE, which degrades the thermo-mechanical properties of the fuel rod. It was shown during the preparatory phase of these experiments that no more than five percent of rare earths can be tolerated in the fuel, which underlines the necessity for efficient minor actinides/lanthanides separation during reprocessing. Additionally, no significant impact on the fuel thermo-mechanical was observed for minor actinides fraction up to 5 % [137]. No critical damage to the fuel rods were observed during irradiation and good overall behavior was reported. Quantitative analysis is being currently performed.

The AFC experiments were conducted at Idaho National Laboratory in the Advanced Test Reactor (ATR) in 2007. It featured metallic and nitride fuels with various Np and Am fractions irradiated at low and high-burn ups. PIE is still ongoing but preliminary results indicate, as for METAPHIX, that such metal fuels with minor actinides behave similarly to conventional fast reactors fuels. The same conclusion was reached for nitride fuels, although the comparison database for nitride fuels is smaller than for metal fuels [138] [139].

These experiments showed that incorporation of minor actinides in a metallic fuel was possible and did not lead to significant modification of the thermo-mechanical behavior of the fuel.

d) THE X501 EXPERIMENT IN EBR-II

This mainly qualitative experiment was carried out in EBR-II where a U-Pu-Zr alloy with 2.1% of Am and 1.3 % of Np was irradiated for 339 EPFD between 1993 and 1994. This experiment showed similar results as the SUPERFACT experiment in terms of helium release. A transmutation rate of 9.1 % was achieved for ^{241}Am. No alteration of the fuel thermo-mechanical due to the addition of minor actinides was observed [140].

One point that arose from the fabrication of the X501 experiment alloy is the high loss rate of americium during injection casting processes due to the high vapor pressure of americium. Nearly 30 % of the total inventory was lost during the fabrication process, which is not acceptable in an industrial setup. Nevertheless, this experiment confirmed the feasibility of using metallic fuel for transmutation purposes.

e) THE MARIOS AND DIAMINO EXPERIMENTS

These experiments were analytical experiments aimed at evaluating the helium release in Americium loaded blankets for heterogeneous transmutation. Irradiation of samples containing 7.5 % and 15 % of Americium with standard or optimized microstructure with increased open porosity to facilitate the release of gases was done in HFR and OSIRIS. The irradiation in a thermal flux allows the effective acceleration of the Helium production compared to a fast reactor case, thus representing a bounding case. Post-irradiation analyses of MARIOS are still ongoing and should be available by the end of 2016 [62]. DIAMINO irradiation is still located inside the Osiris reactor building and is awaiting post-irradiation analysis. Preliminary results

indicate that the fuels did not exhibit a problematic behavior and seems to validate their use in minor actinides bearing blankets with adapted micro structures and the concept itself [141].

f) CONCLUSIONS OF THE EXPERIMENTAL RESEARCH ON TRANSMUTATION

The following conclusions can be drawn from the various experiments presented here:

- Incorporation of a few percent of minor actinides in conventional fuels is possible without alteration of the physical properties of the fuel (SUPERFACT, METAPHIX, AFC, X-501)
- Specific developments are required for highly loaded fuels due to important helium production, as shown in SUPERFACT. Analytical experiments are ongoing to assess more closely the issue and new designs looks promising. (MARIOS & DIAMINO)

Consequently, it appears that in the case of homogeneous transmutation, no specific modification related to the fuel design must be done to accommodate the loading of minor actinides. Thermo-mechanical behavior of the fuel can be reasonably assumed to be the same as the one of standard fuel. On the other hand, in the heterogeneous transmutation case, expansion room for the helium release must be taken into account. However, the results from the MARIOS experiments showed that the new pellets with open micro-porosity did not show significant issues. However the impact of minor actinides addition in the fuel leads to a decrease of its thermal conductivity and melting point. This means that additional care must be taken to qualify transmutation fuels in accidental conditions.

Most of the irradiation experiments were carried out to obtain data on the mechanical and thermal behavior of minor actinides bearing fuels under irradiation. No experiment was done at the assembly level, which means there is no data available for comparison between calculations and experiments at this scale, for instance to evaluate peaking factor in an assembly or the impact of minor actinides during a transient.

3) OTHER ASPECTS OF THE FUEL CYCLE

In-pile irradiation cannot be thought independently from all its surroundings operations such as manufacturing, reprocessing and characterization of the irradiated elements. We saw that the thermo-mechanical behavior observed during the experiments was in good agreement with the behavior of standards fuels. In this part, we focus on the impacts of minor actinides on the other steps of the fuel cycle and present the various experiments and techniques which have been developed so far for minor actinides handling.

a) PARTITIONING OF MINOR ACTINIDES

The PUREX process which is currently in use in reprocessing plants is not adapted to selective recovery of minor actinides as it is designed to extract uranium and plutonium only. However, a variety of methods [142] exist to control the oxidation state of neptunium ions in the various feeds of the PUREX process and to extract it using the same solvent as for plutonium and uranium. Consequently, neptunium can be recovered at a relatively low cost using the so-called advanced PUREX process. [143].

Americium recovery is complicated by the fact that it must be separated from the rare earths presents in the spent fuel as fission products, with which it shares the same chemistry. Good

separation from these elements is required to optimize the transmutation process itself. Various solutions based on the PUREX process have been developed in France as the EXAm process [144]and in Japan as the PARC process [143].

Curium recovery is also complicated by the fact that it shares a similar chemistry with rare earths components from which he must be separated and by the very low critical mass in aqueous solution of its isotopes 245, 54 gr in an optimally moderated case. The high decay heat from isotopes 242 and 244 leads to stronger requirements in terms of temperature control.

Various processes have been developed depending on which output feed was required. To cite but a few, the TRUEX process [12] was designed to separate uranium from TRU from fission products, the SANEX-DIAMEX can selectively recover the trivalent actinides Am and Cm, while the COEX process being designed to recover plutonium and uranium in a single feed [145].

In a general way, partitioning using aqueous reprocessing is feasible but exhibits some drawbacks. Special care to the criticality hazards must be taken, as both ^{242m}Am and ^{245}Cm have very low critical mass of the order of few tens of grams in aqueous medium. In addition, the important specific decay heat and gamma/neutron activity of such fuels either leads to an increase in the number of reprocessing batches or an increase in the cooling time before reprocessing, thus lengthening the entire treatment. Finally, the high alpha and gamma activity of the waste may have a radiolysis effect on the solvent and may degrade its extraction performances. Research is still ongoing on this topic [146] [113]. Early results indicate that a higher gamma and alpha activity decreases the efficiency of the process.

Another possible reprocessing solution is the use of the pyro-processing solution [147], in which the fuel is dissolved in a molten salt and then the elements of interest are recovered by electrochemical means. This approach is very well adapted to metal fueled reactors. However, industrial development of such approaches as yet to be made even if treatment of tons of spent fuel from the EBR-II has been done at INL. Additional research is necessary to increase the efficiency of the process and adapt it to other types of fuel such as oxide or nitride. [148]

Many possible processes for recovering minor actinides from spent fuel, either alone or bundled together or with plutonium have been tested up to the laboratory scale. The ones presented here showed good extractions performances with recovery factor up to 99.9 % for the EXAm process. However, further development is required for industrialization of such processes. Complete evaluation of the impact of spent fuel activity on the extraction process is yet to be made, but early results indicate that an important radiolysis decreases its efficiency. Consequently, we can assume there is an incentive to optimize the activity of the irradiation transmutation fuels in order to limit the losses during reprocessing. However, as not hard data exists on these aspects, it is not easy to select relevant constraints.

b) TRANSPORTATION AND MANIPULATION OF MINOR ACTINIDES BEARING FUELS

Transportation of irradiated nuclear fuels is a complex process which requires safety approval of the cask used to safely isolate the spent fuel from the environment. Cooling of the irradiated elements must also be ensured to prevent local melting of the cladding or loss of integrity of the cask. The heat load of minor actinides bearing fuels is more important than regular oxide fuels due to the higher amount of elements with a strong decay heat such as ^{238}Pu or ^{244}Cm, as outlined in Chapter 1.

This increase in the thermal activity of the irradiated assemblies means that fewer assemblies will be loaded in each cask, thus increasing the number of required trips. Consequently, there is an interest in minimizing the decay heat of each assembly. Setting an upper limit to the thermal activity of an assembly is not easy as it depends on on-going technological developments.

Specific agreements had to be required for transportation of the assemblies containing the experiments described in 2), except for the X-501 experiments which took place directly inside the facility which was an integrated one. For the experiments that took place in the Phenix reactor, post irradiation experiments took place either in the ATALANTE facility in Marcoule, in Cadarache or in the hot cells of the laboratory commissioning the study.

Handling of irradiated assemblies inside the reactor core is also complicated by the presence of ^{242}Cm which has a very high power density. Manipulation of the irradiated assemblies is required during reloading operations and depends on the technological solution chosen. However, high ^{242}Cm content is likely to lengthen the cooling time necessary to start reloading operations, thus decreasing the plant load factor. Consequently, there is an incentive in transmutation studies to decrease the residual decay heat per assembly at the week-to-month time scale in order not to hamper the reloading operations.

c) MANUFACTURING OF ACTINIDES BEARING FUELS

Minor actinides being more radiotoxic than uranium and plutonium, it is very likely that fabrication of minor actinides bearing fuels will have to be carried out in hot cells instead of gloves boxes as it is currently the case for MOX pellets manufacturing. For the experiments presented in 2), manufacturing of the targets was done in gloves boxes as small quantities of minor actinides were involved.

However, in the case of industrial manufacturing of fresh fuels containing more than a few percent of americium or a very limited amount of curium, the increase in the gamma activity of the fuel may prevent the use of glove boxes. Hot-cells with remote capability will be necessary in such a case and should be so in any situation which involves curium reprocessing or manufacturing of fuels with fraction of americium above a few percent. Neptunium being a low gamma emitter, it can be incorporated to MOX pellets without additional requirements.

The current process used for MOX pellets fabrication is also not suited for manufacturing of such fuels as it requires mechanical grinding of the pellets. This would lead to heavy contamination of the operating space with powdered minor actinides. Consequently, new processes are being developed to overcome this difficulty, such as the Sol-Gel process [136] or the Sphere-Pac process [149] to cite but a few. Sol-Gel has been used for the manufacturing of the SUPERFACT experiments pellets. In this process, polymerization of an organic material containing the actinides leads to the synthesis of a ceramic. In the Sphere-Pac process, uranium beads of various sizes are produced by milling and infiltrated with americium. A fuel element is then filled with the beads to the required density and sintered. This approach is flexible enough to allow a vertical gradient of the minor actinides content in the fuel element.

The previous considerations were expressed for oxide fuels. It should be mentioned that minor actinides nitride and carbide have also been fabricated at the laboratory scale and exhibit the same issues in terms of gamma or neutron activity. For metal fuel, it should be added that

americium has a low vaporization pressure which complicates the casting operation. For instance, 30 % of the americium used in the X-501 experiments was lost to vaporization [140].

Similarly to the reprocessing case, many different approaches have been tested for manufacturing of minor actinides bearing fuels but none has been taken to the industrial scale and thus additional R&D is still necessary on this topic. Due to the high activity of minor actinides, hot cells will be required for manufacturing of such fuels in any case. We can consequently conclude that the optimization of the activity at the manufacturing step is secondary compared to transportation or reprocessing.

d) CONCLUSION

It is also relevant to study the out-of-core fuel cycle part for minor actinides transmutation, as minor actinides incorporation in the fuel leads to strong impacts on nearly every step from manufacturing to reprocessing and waste management. The higher neutron source, gamma and alpha emission and decay heat lead to increased safety precautions and decreased performances, which incurs extra-costs.

4) GENERAL CONCLUSION

Considering the data from all the irradiation experiments carried out on minor actinides transmutation, we can conclude that up to a few percent of minor actinides, the fuel behavior under irradiation seems to be acceptable. It is very likely than a specific assembly will have to be designed to take into account the very high swelling rate coming from helium production in fuel elements with significant proportions of minor actinides, as it was outlined in the SUPERFACT experiment.

This does not remove the necessity to develop new core designs to accommodate the effect of minor actinides on the core parameters such as the breeding gain, delayed neutrons fractions or resistance to accidents. No experiments have been done to evaluate the effects of minor actinides on these specific points on the assembly or reactor scale.

Nevertheless, the impact of minor actinides in the entirety of the fuel cycle should not be neglected as it was shown for the manufacturing or transportation step, and the optimization of a transmutation strategy should take into account inputs not only from the reactor-side but from all the fuel cycle, and especially handling and reprocessing of the irradiated fuel. In any case, should minor actinides fuels be fabricated at the industrial scale, hot cells will be required for manufacturing.

However, this approach is complicated by the important technological uncertainties associated with the lack of industrial feedback on minor actinides transmutation. This is both an advantage and a drawback, as technological solutions not yet mature can be considered in the global design process but also as it is difficulty to evaluate realistically the constraints that can exist on transportation or reprocessing for instance. Technological uncertainties evaluation is thus going to play an important role in the optimization process.

Considering this, we will explore two ways for improvements of minor actinides transmutation:

- The optimization of a complete transmutation strategy from fuel manufacturing to reprocessing while taking into accounts constraints from all the fuel cycle steps.
- The development of innovative transmutation systems aimed at improving the efficiency of the in-pile part of transmutation. This approach will evidently be assessed in light of the optimization process.

ANNEX 4: NUMERICAL TOOLS USED FOR THIS WORK

Two numerical tools available in the URANIE code system were used in this work, namely:

- Artificial neural networks, which were used to reproduce the outputs of full core and depletion calculations at a lower computational cost.
- Genetic algorithms, which were used to carry out the actual optimization process of minor actinides transmutation while taking into account various constrains and estimators.

The aim of this annex is to described in details the conditions of use of these tools.

1) ARTIFICIAL NEURAL NETWORKS

The artificial neural networks (ANN) available in URANIE are known as Multi Layer Perceptron (MLP) with only one hidden layer and were used here. Their effective implementation in URANIE is shown below in Figure 132. Starting from the set of input parameters on the left, various weights denominated ω here are adjusted to "activate" a set of hidden neurons in yellow here, which are then used to output a single value. This output is then compared to the expected value and the values of the weights are adjusted to fit the expected value. This process is repeated over a first set of data denominated the training set and the accuracy of the ANN is then checked on a validation set independent from the training set.

The output value is calculated from the weights of the various neurons using an activation function θ and the formula given in Equation 35. The activation function which was considered here, known as a sigmoid is the standard activation function available in URANIE and is given in Equation 36. The β parameter is a slope parameter of the sigmoid function which was not disclosed in the documentation of the code used.

$$s = \theta(\omega_0 + \sum_{i=1}^{n} \omega_i x_i)$$

Equation 35 : Calculation of the ANN output, with ω_0 the weight associated with the inputs parameters and $\omega_i x_i$ the weight output associated to a neuron i

$$\theta(t) = \frac{1}{1 + e^{-\beta t}}$$

Equation 36 : Sigmoid function used here as activation function

The main parameter which determines the quality of the output is the number of hidden neurons. There a no rule of thumb which gives the optimal number of hidden neurons for a given problem. Consequently, a small parametric study was done to find the best solution with regards to calculation and reduction of the error of the ANNs. This is shown in Figure 133. Considering this figure, 10 hidden neurons were used in this work, which were a good compromise between standard deviation of the output error (below 1% here) and computation time (2 to 20 minutes par ANN depending on the approach considered). In the homogeneous case, due to the higher number of parameters and the lower number of points in the training

set, the corresponding standard deviation is slightly higher with a mean standard deviation of 3% compared to 2.5 % of the heterogeneous case.

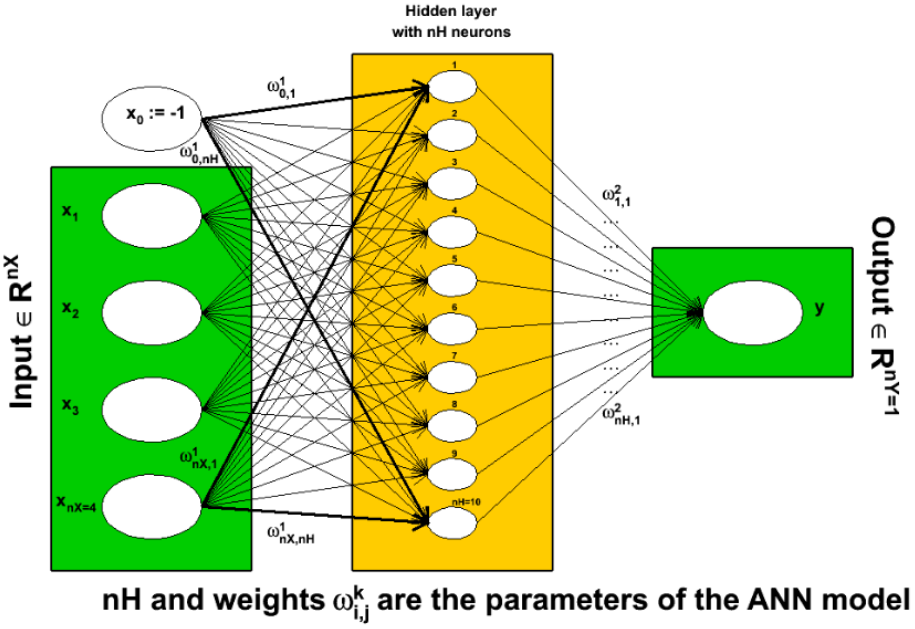

Figure 132 : Schematic description of the ANN implementation in URANIE (from Uranie User Manual)

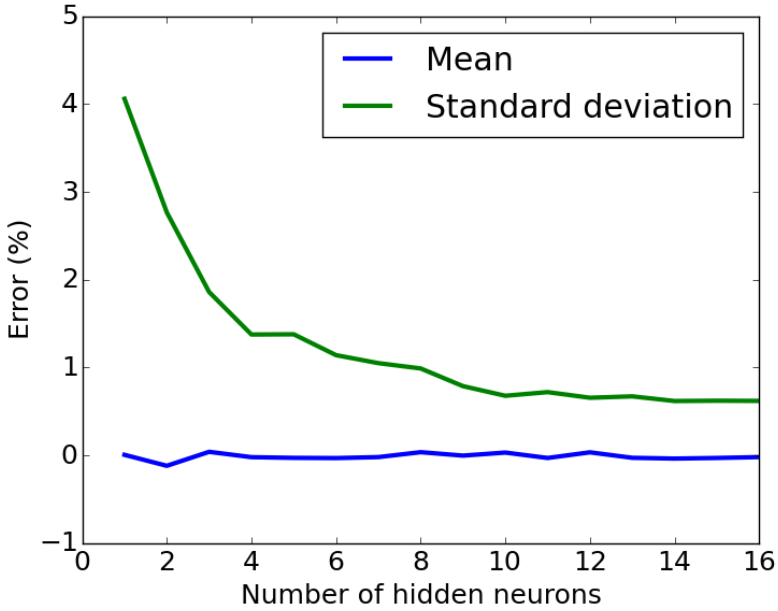

Figure 133 : Evolution of the mean error and standard deviation of the error for the 5 years decay heat ANN used for the heterogeneous case

2) GENETIC ALGORITHM

The genetic algorithm available in the URANIE code system was also used in this work. This algorithm is diploid algorithm with real-coding and true dominance. This means that a given case is represented, similarly as in human genetic code, by two chromosomes. These chromosomes contain the information on the case input parameters, or genes, in the shape of vector of double.

The information encoded in both can be similar or different, corresponding either to a homozygote case or heterozygote case. Different parameters can be set to tune the behavior of the genetic algorithm:

- The total number of evaluations that can be done during one optimization
- The population per generation
- The mutation rate at each generation
- The survival rate of the population at each generation
- The rate of homozygote cases in the population.

The total number of evaluations is by default set at 100,000 in URANIE and was not modified here as convergence of the optimization algorithm was always obtained with less than this number of evaluations.

The optimization algorithm works by first randomly creating one generation of size N with a homozygote rate set at 50 % by default. Using the artificial neural networks, the various estimators of interest are calculated for this first generation. As mentioned earlier, true dominance is implemented in this algorithm, which means that for heterozygote case, one chromosome is designated as dominant while the second once is recessive. The selection of the dominant chromosome is done by randomly selecting it.

The estimators for each case of the first generation being calculated, the N solution are ranked. As the problem is a multi-criterion one, ranking is done by affecting a integer number to each case corresponding to the number of cases which dominates the one considered. A case x_1 is said to dominate a case x_2 all the performances of x_1 are better than or equal to the performances of x_2. The fitness of a case is evaluated by calculating the number of cases dominating it. The best candidates have a rank of 0, which means that they are optimal in the Pareto-sense. They correspond to cases for which a gain in one of the objective estimator is necessarily compensated by a loss for the others.

Convergence of the optimization scheme is then tested and three situations can arise :

- All the cases are non dominated (of rank 0), which means the evaluated generation is optimal
- Not all the cases are non-dominated but the total number of evaluations has been reached. The algorithm stops without reaching convergence. This situation was not encountered here.
- Not all the cases are non-dominated and the total number of evaluations has not been reached.

In the final case, a new generation is drawn. Starting from the previous generation, the best cases are kept up to a fraction of the generation population corresponding to the survival rate

set at 40 % by default. The missing part of the population is then drawn from the previous generation using a process similar to genetics. Starting from a parent case, a child case is created by randomly selecting allele for the first or the second chromosome of the parent case until a full chromosome is obtained, and by repeating the process to obtain a complete case.

Then, a sampling is done to evaluate if the new case is homozygote or heterozygote. If it is homozygote, for each gene of the case, a weighted sum of the alleles of this gene on each of two chromosomes is done to generate a new chromosome which will characterize the homozygote case. The weighted sum is done by affecting a coefficient drawn in [0-ε; 1+ ε] to enhance the exploration of the research space. If the case is considered heterozygote, no modification is done but the dominant chromosome is done by randomly selecting it.

Finally, mutation occurs by randomly selecting a case (with a 1 % default percentage here) and then selecting one gene on each chromosome and replacing the stored value by a new randomly sampled one. Leaving the maximal number of evaluation aside, there are then four parameters that can be used to modify the behavior of the genetic algorithm.

The first one is the population per generation. The default value used in Chapter 5 is a population of 1000 cases per generation. It can be observed on the figure below, which we obtained for an optimization of the ULOF case that the shape of optimal population does not change with the number of cases per generation. The convergence of the problem however increases, with 7 generations needed to reach convergence with population of 100 and 250 individuals compared to 13 generations for a 1000 individual case. This can be seen below in Table 94. The selection of case with a high core and low americium content to limit the decrease in Doppler feedback is found for each case, with a smaller part of the set being comprised of cases with a lower power and high minor actinides content.

Table 94 : Evolution of the optimal set with regards to the number of individuals per generation, all other parameters being equal. (mutation rate = 1 %, survival rate = 40 %, homozygote rate = 50 %)

Parameter	Optimal set	Number of generations
100 individuals per generation	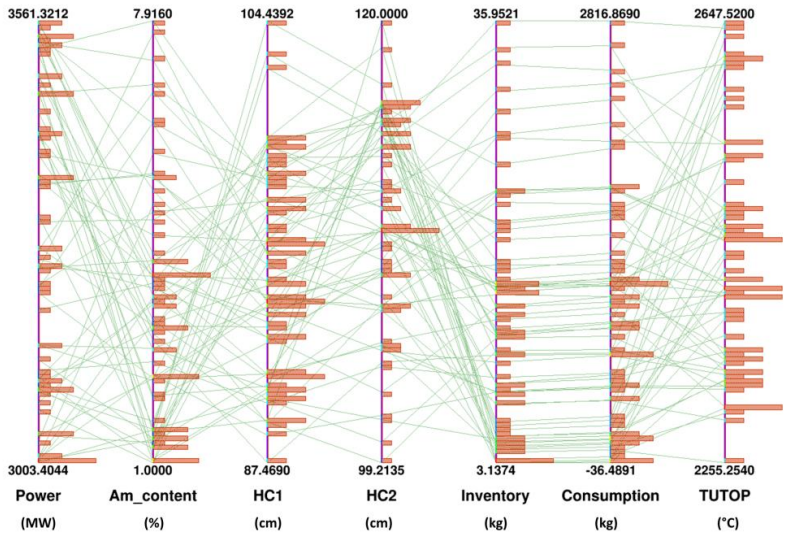	7

250 individuals per generation	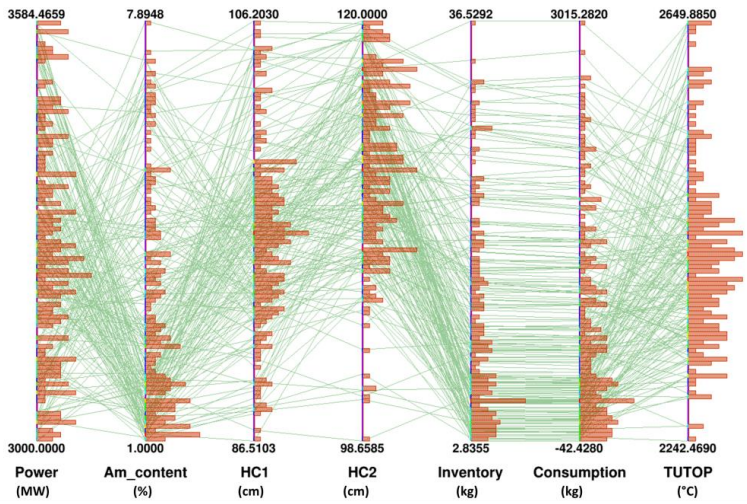	7
500 individuals per generation	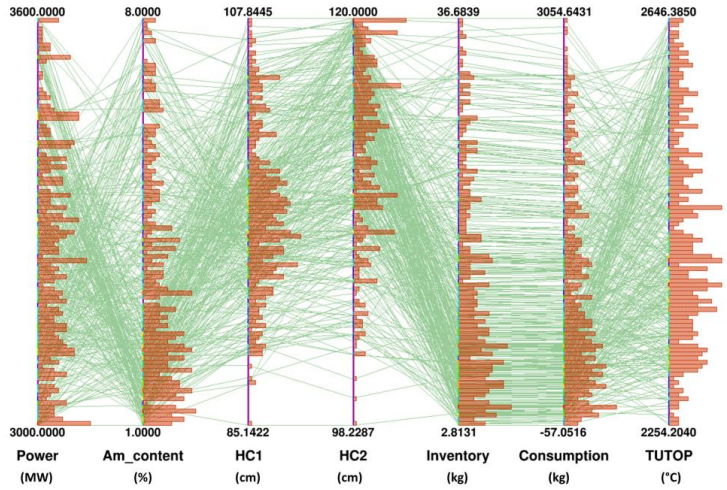	11
1000 individuals per generation	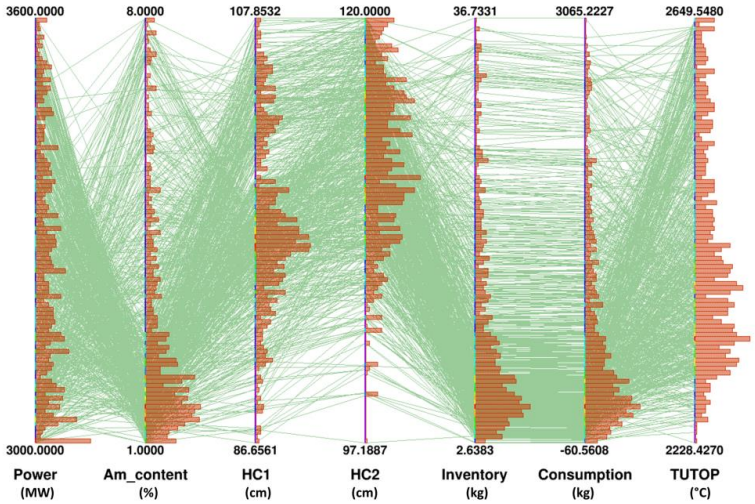	13

Changing the mutation rate from 1 % to 10 % increases the number of generations needed to reach convergence from 11 to 13, which in turn increases the optimization time. However, it does not modify the shape of the optimal set as illustrated below in Table 95

Table 95 : Evolution of the shape of the optimal set with regards to the mutation rate, all other parameters equal (population = 500, survival rate = 40 %, homozygote rate = 50 %)

Parameter	Optimal set	Number of generations
Mutation rate 1 %	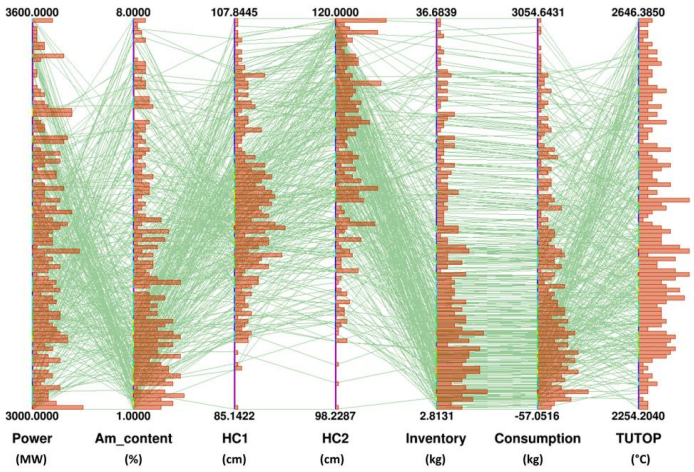	13
Mutation rate 5 %	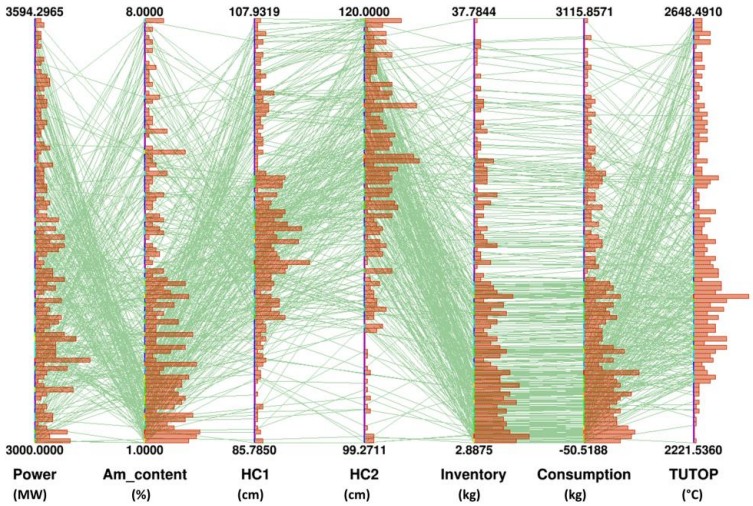	11

Mutation rate 10 %	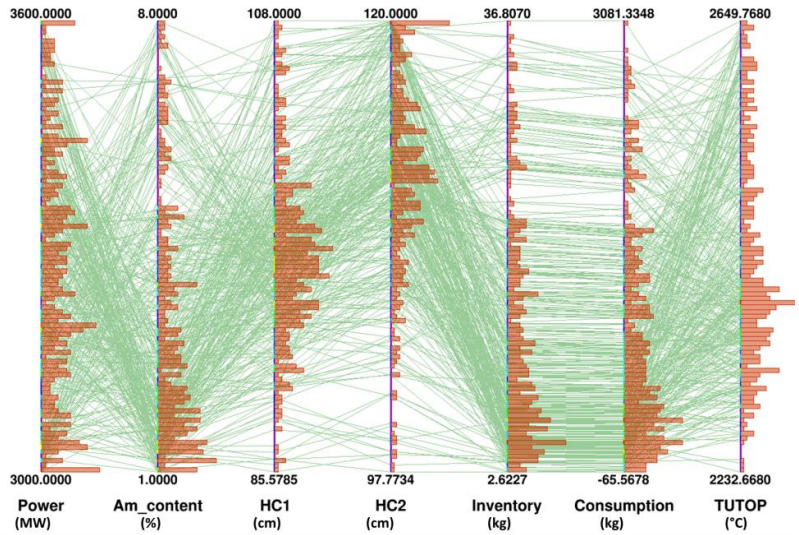	12

Modifying the survival rate appears to increase the number of generation necessary to obtain the optimal set but not the total number of evaluations. Indeed, when the survival rate is increased, less new evaluations must be made at each generation. This increase does not seem to modify the shape of the optimal distribution. It is worth noting here that the default value used by URANIE appears to be optimal, as it can be seen below in Table 96.

Table 96 : Evolution of the shape of the optimal set with regards to the survival rate, all other parameters equal (population = 500, mutation rate = 1 %, homozygote rate = 50 %)

Parameter	Optimal set	Number of generations
Survival rate 30 %	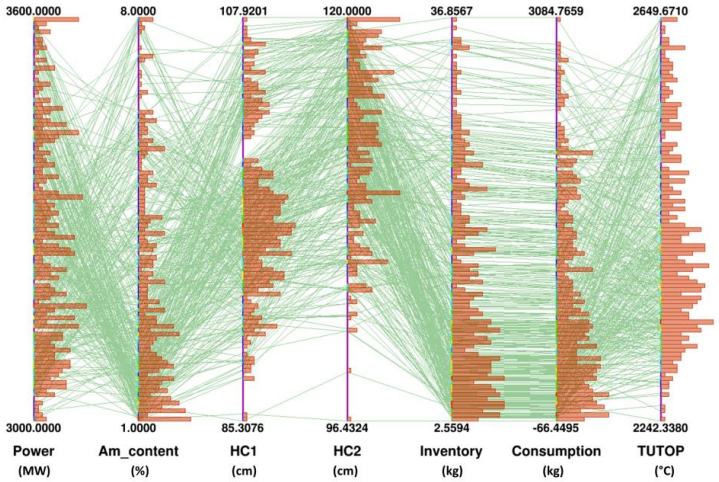	15

Survival rate 40 %	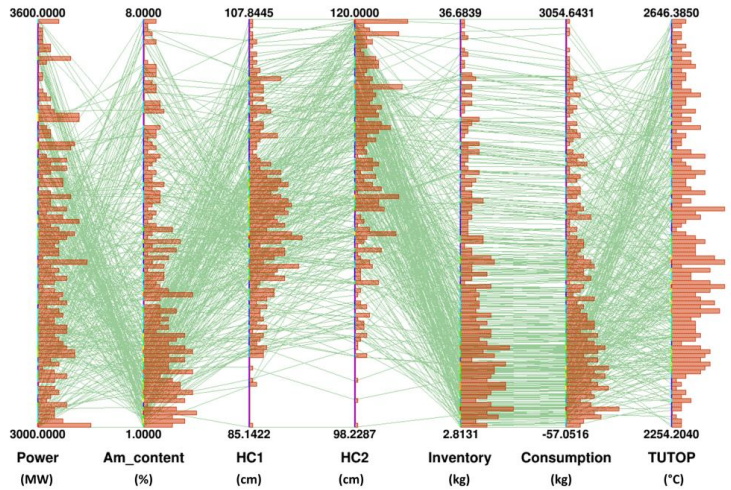	11
Survival rate 50 %	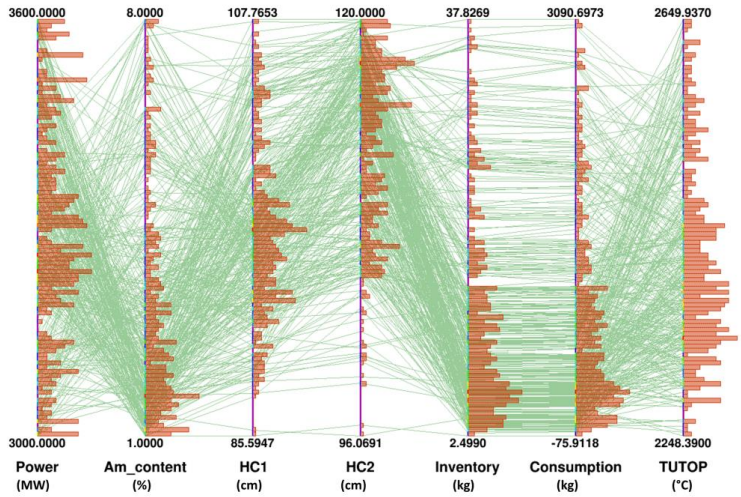	24
Survival rate 60 %	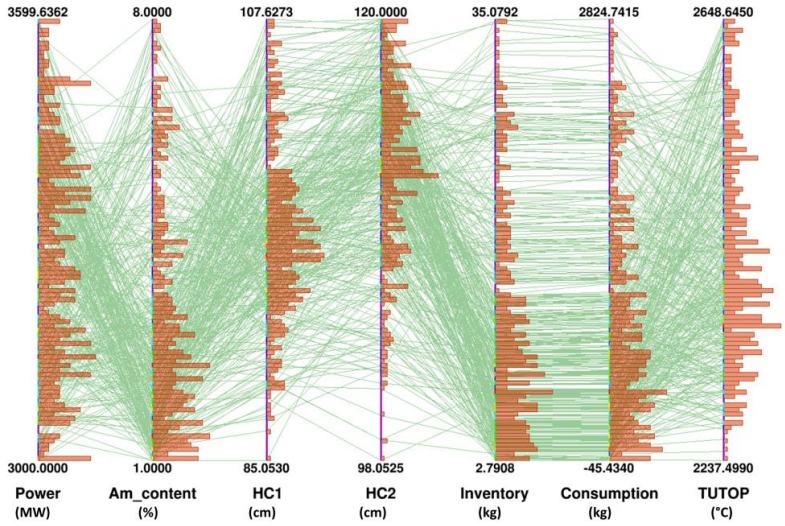	32

Increasing the homozygote rate does not seem to have any significant on the convergence of the genetic algorithm as shown in Table 97. The two expected population sets are still found in each cases.

Table 97 :Evolution of the shape of the optimal set with regards to the survival rate, all other parameters equal (population = 500, mutation rate = 1 %, survival rate = 40 %)

Parameter	Optimal set	Number of generations
Homozygote rate 25 %	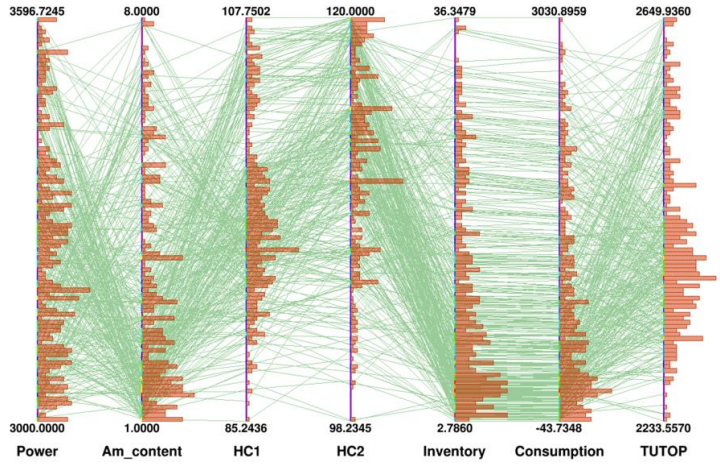	13
Homozygote rate 50 %	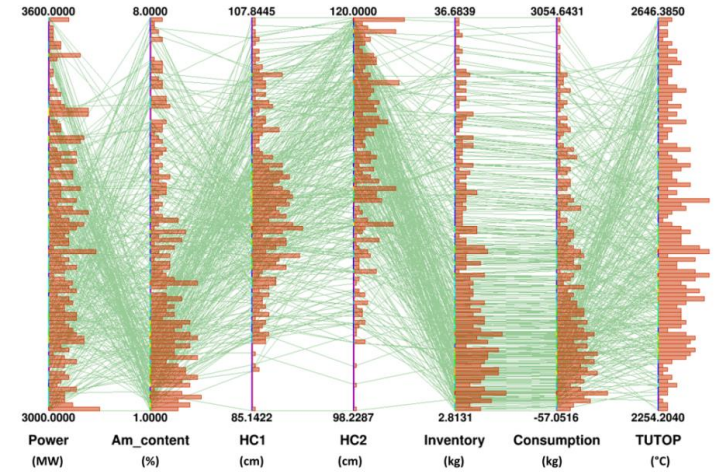	11

Homozygote rate 75 %	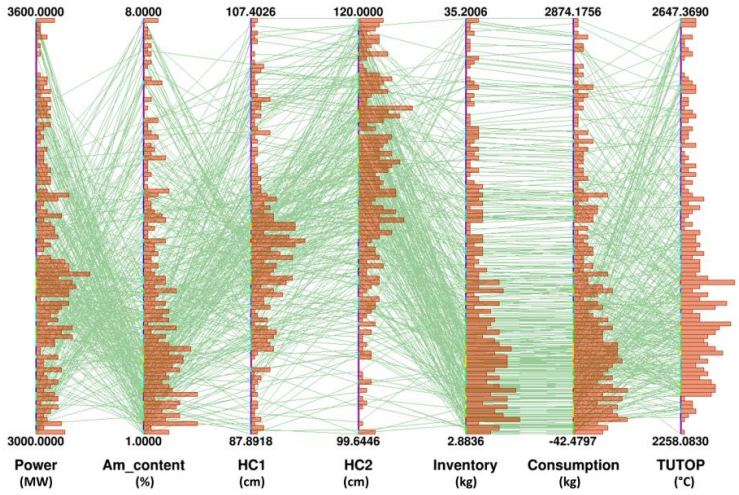	12

CONCLUSION

The numerical tools used to carry out the work performed during this PhD were discussed here. The technical choices behind the ANN and genetic algorithm parameters were justified. The default parameters of the genetic algorithm implementation in URANIE appears to be satisfactory enough to be used.

BIBLIOGRAPHY

[1] NEA, "Forty years of Uranium Resources, production and demand in perspective : the Red Book retrospective," NEA, Issy les Moulineaux, 2006.

[2] A. Baschwitz, C. Loaëc, J. Fournier and M. Delpech, ""GEN IV deployment: Long term perspective"," in *FR09:International Conference on Fast Reactors and Related Fuel Cycles: Challenges and Opportunities*, Kyoto, 2009.

[3] GIF, 2013 Annual Report, 2013.

[4] K. Kawashima, K. Sugino, S. Ohki and T. Okubo, "Design study of a low sodium void reactivity core to accomodate degraded TRU fuel," *Nuclear Technology,* vol. 3, no. 185, pp. 270-280, 2013.

[5] B. Raj, "Carbide Fuel Reprocessing and Fast Reactor Fuel Cycle Development," in *9th IEMPT*, Nimes, 2006.

[6] NEA, "Fuel and Materials for transmutation : a status report," NEA, Issy les Moulineaux, 2005.

[7] D. Plancq, L. Cachon and J.-F. Dirat, "ASTRID French SFR: Progress in Sodium Gas Heat Exchanger development," in *International Conference on Fast Reactors and Related Fuel Cycles: Next Generation Nuclear Systems for Sustainable Development (FR17)*, Iekaterinbourg, 2017.

[8] M. Gerber, "A brief history of PUREX and UO3 facilities," Westinghouse Hanford Company, Richland, Washington, 1993.

[9] H. Escrich, J. V. Geel and E. Detilleux, "Management of fuel reprocessing wastes at Eurochemic plant," in *NEA-IAEA Symposium on the management of radioactive wastes from fuel reprocessing*, Paris, 1972.

[10] M. Arslan, "MOX fuel recycling : present status and prospects," in *GLOBAL*, Paris, 2009.

[11] C. Poinssot, S. Bourg, N. Ouvrier, N. Combernoux, C. Rostaing, M. Vargas-Gonzalez and J. Bruno, "Assessment of the environmental footprint of nuclear energy systems. Comparison between closed and open fuel cycles.," *Energy,* no. In Press, pp. 1-13, 2014.

[12] E. P. Horwitz, D. C. Kalinaa, H. Diamonda, G. F.Vandegrift and W. W. Schulzb, "The TRUEX process - a process for the extraction of the transuranic elements from nitric acid in wastes utilizing modified PUREX solvent," *Solvent Extraction and Ion Exchange,* vol. 3, no. 1-2, pp. 75-109, 1985.

[13] M. Miguirditchian, L. Chareyre, C. Sorel, I. Bisel, P. Baron and M. Masson, "Development of the GANEX process for the reprocessing of Gen IV spent nuclear fuels," in *Atalante* , Marcoule, 2008.

[14] ANDRA, "Comment sont classés les déchets radioactifs ?," 5 12 2012. [Online]. Available: http://www.andra.fr/pages/fr/menu1/les-dechets-radioactifs/comment-sont-classes-les-dechets-radioactifs-r-9.html. [Accessed 17 02 2015].

[15] ANDRA, [Online]. Available: https://www.andra.fr/international/. [Accessed 2017].

[16] "Compendium of Dose Coefficients based on ICRP Publication 60. ICRP Publication 119," *Ann. ICRP,* no. 41, 2012.

[17] P. Reuss, Précis de neutronique, Paris: EDP Sciences, 2003.

[18] ANDRA, "Les recherches de l'ANDRA sur le stockage géologique des déchets radioactifs à haute activite et à vie longue : résultats et perspectives," 2005.

[19] D. Lemasson, J. L. Mer and C. Garzenne, "Scenario of a Symbiotic Nuclear Fleet Composed of PWRs and SFRs," in *20th ICONE*, Anaheim California, 2012.

[20] J. B. Clavel, "Thèse de doctorat :Etude de systèmes et scénarios électronucléaires double strate de transmutation des actinides mineurs en ADS," Nantes, 2012.

[21] D. D. Bruyn, "PATEROS Final activity report," European Commission, Bruseels, 2009.

[22] CEA, "Bilan des recherches conduites sur la séparation-transmutation des éléments radioactifs à vie longue et sur le développement de réacteurs nucléaires de nouvelle génération, Tome1," Paris, 2012.

[23] E. Mcmillan and P. Abelson, "Radioactive Element 93," *Physical Review,* vol. 57, no. 12, p. 1185, 1940.

[24] G. T. Seaborg, R. James and L. O. Morgan, "The New Element Americium (Atomic Number 95)," *National Nuclear Energy Series, Plutonium Project Record,* vol. 14.B, no. 22.1, 1949.

[25] C. Coquelet-Pascal, M. Meyer, R. Girieud, M. Tiphine, R. Eschbach, C. Chabert, C. Garzenne, P. Barbrault, B. Gannaz, L. V. D. Durpel, D. Favet, M. Caron-Charles, B. Carlier and J.-C. Lefèvre, "Scenarios for Fast Reactors Deployment with Plutonium Recycling," in *Fast Reactors*, Paris, 2013.

[26] G. T. Seaborg, R. A. James and A. Ghiorso, "The New Element Curium (Atomic Number 96)," *National Nuclear Energy Series, Plutonium Project Record,* vol. Vol 14 B, no. 22.2, 1949.

[27] B.Forget, M.Asgari, R.Ferrer and S. Bays, "Impact of including higher actinides in fast reactor transmutation analyses," INL/EXT-07-13247, 2007.

[28] L. Buiron, "Mémoire d'HDR : Le potentiel de transmutation des actinides mineurs: états de lieux pour les réacteurs à neutrons rapides refroidis au sodium de quatrième génération," Université Paris Sud, Orsay, 2015.

[29] M. Salvatores, I. Slessarev and M. Uematsu, "A Global Physics Approach to Transmutation of Radioactive Nuclei," *Nuclear Science and Engineering,* vol. 116, pp. 1-18, 1994.

[30] M. Salvatores, I. Slessarev and A. Tchistiakov, "The transmutation of LLFP by neutron irradiation," *Nuclear Science and Engineering,* vol. 130, no. 13, pp. 310-319, 1998.

[31] N. Messaoudi, "Etude d'un réacteur à neutrons rapides (RNR) dédié à l'incinération des actinides mineurs," Université de Provence, Aix en Provence, 1996.

[32] D. Wootan, D. Jordheim and W. Matsumoto, "Irradiation test of 99Tc and 129I transmutation in the Fast Flux Test Facility," *Transactions of the American Nuclear Society,* vol. 64, pp. 125-126, 1991.

[33] W. S. Yang, Y. Kim, R. N. Hill, T. A. Taiwo and H. S. Khalil, "Long-Lived Fission Product Transmutation Studies," *Nuclear Science and Engineering,* vol. 146, pp. 291-318, 2004.

[34] J. Wallenius, Transmutation of nuclear waste, Marstä, Sweden: Leadcold , 2011.

[35] L. R.Morss, N. M. Edelstein and J. Fuger, The chemistry of the actinide and transactinide elements, p2135, Dordrecht: Springer, 2010.

[36] G. Rimpault, "The ERANOS code and data system for fast reactor neutronic analyses," in *PHYSOR*, Seoul, 2002.

[37] NEA/OECD, "The JEFF-3.1 Nuclear Data Library," NEA, Paris, 2006.

[38] A. Tsilanizara, C. Diop, B. Nimal, M. Detoc, L.Luneville, M. Chiron, T. Huynh, I. Bresard, M. Eid, J. Klein, B. Roque, P. Marimbeau, C. Garzenne, J. Parize and C. Vergne, "DARWIN: An Evolution Code System for a Large Range of Applications," *Journal of Nuclear Science and Technology,* vol. Supplement 1, pp. 845-849, 2000.

[39] S. Massara, "Etude et amélioration du comportement cinétique de coeurs rapides dédiés à la transmutation de déchets à vie longue," Université Louis Pasteur, Strasbourg, 2002.

[40] F. Gaudier, "URANIE: The CEA/DEN Uncertainty and Sensitivity platform," *Procedia - Social and Behavioral Sciences,* vol. 2, no. 6, pp. 7660-7661, 2010.

[41] L. Buiron and e. al, "Heterogeneous minor actinides transmutation on a UO2 blanket and on (U,Pu)O2 fuel in sodium-cooled fast reactor. Assessment of core performances," in *GLOBAL*, Paris, 2009.

[42] A. Santamarina, "The JEFF-3.1.1 Nuclear Data Library," OECD, Paris, 2009.

[43] L. Buiron, *Communication personelle,* 2014.

[44] CEA, "Bilan des recherches conduites sur la séparation-transmutation des éléments radioactifs à vie longue et sur le développement de réacteurs nucléaires de nouvelle génération, Tome 2," CEA, Paris, 2012.

[45] NEA, "Minor actinides burning in thermal reactors," Paris, 2013.

[46] K. Terrani, M.Balooch, D. Wongsawaeng, S.Jaiyen and D. Olander, "The kinetics of hydrogen desorption from and adsorption on zirconium hydride," *Journal of Nuclear Materials,* no. 397, pp. 61-68, 2010.

[47] S. Béjaoui, J. Lamontagne, E. Esbelin, J. Bonnerot, E. Brunon and P. Bourdot, "ECRIX-H experiment: Synthesis of post-irradiation examinations and simulations," *Journal of nuclear materials,* vol. 415, no. 2, pp. 158-166, 2011.

[48] Y. Croixmarie, E.Abonneau, A.Fernandez, R. Konings, F.Desmoulières and L.Donnet, "Fabrication of transmutation fuels and targets : the ECRIX and CAMIX-COCHIX experience," *Journal of nuclear materials,* vol. 320, pp. 11-17, 2003.

[49] J. Bussac and P. Reuss, Traité de neutronique : Physique et calcul des réacteurs nucléaires avec application aux réacteurs à eau pressurisée et aux réacteurs à neutron rapides, Paris: Hermann, 1985.

[50] M. M. e. al, "Scenarios for Minor Actinides Transmutation in the Frame of the French act for waste management," IAEA, 2012.

[51] P.Sciora, L.Buiron, G.Rimpault and F.Varaine, "A break even oxide fuel core for an innovative French sodium-cooled fast reactor : neutronic studies results," in *GLOBAL*, Paris, 2009.

[52] L. Buiron and D. Plisson-Rieunier, "Homogeneous Minor Actinide transmutation in SFR : neutronic uncertainties propagation with depletion," in *IEMPT2014*, Seoul, 2014.

[53] Tommasi.J, "Long-lived waste transmutation in reactors," *Nuclear Technology,* no. 111, 1995.

[54] P. Sciora, D. Blanchet, L. Buiron, B. Fontaine, M. Vanier, F. Varaine, C. Venard, S. Massara, A. Scholar and D. Verrier, "Low void effect core design applied on 2400 MWth SFR reactor," in *ICAPP 2011*, Nice, France, 2011.

[55] K. Hornik, M. Stinchcombe and H. White, "Multilayer feedforward networks are universal approximators," *Neural Networks,* vol. 2, no. 5, pp. 359-366, 1989.

[56] T. E. Oliphant, "Python for Scientific Computing," *Computing in Science & Engineering,* vol. 9, no. 90, 2007.

[57] A. Marrel, B.Iooss and E.Volkova, "An efficient methodology for modeling complex computer codes with Gaussian processes," *Computational Statistics and Data Analysis,* vol.

52, pp. 4731-4744, 2008.

[58] T. Kooyman and L. Buiron, "Sensitivity analysis of minor actinides transmutation to physical and technological parameters," in *GLOBAL2015*, Paris, 2015.

[59] C. Chabert, C. Coquelet-Pascal, A. Saturnin, G. Mathonniere, B. Boullis, D. Warin, L. V. D. Durpel, M. Caron-Charles and C. Garzenne, "Technical and economic assessment of different options for minor actinides transmutation : the French case," in *GLOBAL2011*, Tokyo, 2011.

[60] Buiron.L and a. et, "Transmutation abilities of the SFR low void effect core concept CFV 3600 MWth," in *ICAPP2012*, Chicago, 2012.

[61] J.-M. Bonnerot, S.Pillon, S.Béjaoui, E. D'Agata, R. Hania, N. Herlet, A. Jankowiak, M. Auclair, S. Bendotti, T. Lambert and B.Valentin, "Development programme on minor-actinide-bearing blankets at CEA," in *IEMPT11*, San Francisco, 2010.

[62] S. Bejaoui, T. Lambert, S. Bendotti, C. Neyroud, N. Herlet and J.-M. Bonnerot, "Americium-bearing blanket separate-effect experiments. MARIOS and DIAMINO irradiations," in *GLOBAL*, Tokyo, 2011.

[63] R. Klueh, J. Shingledecker, R. Swindeman and D. Hoelzer, "Oxide dispersion-strengthened steels: A comparison of some commercial and experimental alloys," *Journal of Nuclear Materials,* vol. 341, no. 2-3, pp. 103-114, 2005.

[64] M. Le Flem, P. Gavoille, Y. D. Carlan, C.Bisor and J. Seran, "Advanced steel claddings for SFRS: feedback and challenges," in *GEMAT Final Workshop*, 2013.

[65] O. Vălu, D. S. b, O. Beneš, R. Konings and P. Lajarge, "Heat capacity, thermal conductivity and thermal diffusivity of uranium–americium mixed oxides," *Journal of Alloys and Compounds,* vol. 614, pp. 144-150, 2014.

[66] A. Waltar and A. Reynolds, "Chapter 8 : Fuel pin and assembly design," in *Fast Breeder Reactors*, New York, Pergamon Press, 1981, pp. 251-312.

[67] F.Varaine, N.Stauff, M.Masson, M.Pelletier, G.Mignot, G.Rimpault and J. A.Zaetta, "Comparative review on different fuels for Gen IV Sodium Fast Reactors: merits and drawbacks," in *International Conference on Fast Reactors and Related Fuel Cycles (FR09)*, Kyoto, 2009.

[68] T.Kooyman, L.Buiron, B. Valentin, G.Rimpault and F.Delage, "Pre-design optimization of a target assembly for minor actinides transmutation," in *IEMPT2016*, San Diego, 2016.

[69] Y. S. Kim and G. L. Hofman, "AAA Fuels Handbook," Argonne National Laboratory, 2003.

[70] M. Saito, "Advanced core concepts with enhanced proliferation resistance by transmutation of minor actinides," in *GLOBAL05*, Tsukuba, Ibaraki (Japan), 2005.

[71] H. SAGARA, M. SAITO, Y. PERYOGA, A. EZOUBTCHENKO and A. TAKIVAYEV, "Denaturing of plutonium by transmutation of minor actinides for enhancement of proliferation resistance," *Journal of nuclear science and technology,* vol. 42, no. 2, pp. 161-168, 2005.

[72] R. Rainisch, "Effect of Americium-241 Content on Plutonium Radiation Source Terms," *Transactions of the American Nuclear Society,* no. 80, 1999.

[73] A. Allou, *Communication Personnelle,* 2016.

[74] Y. Zhang, J. Wallenius and M. Jolkkonen, "Transmutation of americium in a large sized sodium-cooled fast reactor loaded with nitride fuel," *Annals of nuclear energy,* vol. 53, pp. 26-34, 2014.

[75] Y. Zhang and J. Wallenius, "Upper limits to americium concentration in large sized sodium-cooled fast reactors loaded with metallic fuel," *Annals of Nuclear Energy,* vol. 70, pp. 180-187, 2014.

[76] O.Fabbris, S.Dardour, P.Blaise, J.-H. .. Ferrasse and M. Saez, "Surrogates based multi-criteria predesign methodology of sodium-cooled fast reactor cores - application to CFV-like cores," *Nuclear Engineering and Design,* vol. 305, pp. 314-333, 2016.

[77] G. Palmiotti, M. Salvatores and M. Assawaroongreungchot, "Impact of the core minor actinide content on fast reactor reactivity coefficients," *Journal of nuclear science and technology,* vol. 48, no. 4, pp. 628-634, 2011.

[78] G. Rimpault, *Communication personelle,* 2017.

[79] Y. Bagdarasov, Y. K. Buksha, R. Voznesenski, N. Vyunnikov, V. Kornilov, N. Krayev, L. Mamayev, A. Portianoy and A. Sorokin, "Development of passive safety devices for sodium cooled fast reactors," in *AIEA Technical commitee meeting* , Obninsk, 1995.

[80] F. Varaine, P. Marsault, M. S. Chenaud, B. Bernardin, A. Conti, P. Sciora, C. Venard, B. Fontaine, N. Devictor, L. Martin, A. C. Scholer and D. Verrier, "Pre-conceptual design study of ASTRID core," in *ICAPP2012*, Chicago, 2012.

[81] J. Wallenius, "Physics of americium transmutation," *Nuclear Engineering and Technology,* vol. 44, no. 2, pp. 199-206, 2012.

[82] G. Hofman, L. Walters and T. Bauer, "Metallic fast reactor fuels," *Progress in nuclear energy,* vol. 31, no. 1/2, pp. 83-110, 1997 .

[83] P. Martin, M. Pelletier, D. Every and D. Buckthorpe, "French and United Kingdom experience of high burn-up mixed oxide fuels in sodium-cooled fast breeder reactors," *Nuclear Technology,* vol. 161, no. 1, pp. 35-44, 2006.

[84] A. Waltar and A. Reynolds, "Chapter 10 : Core thermal hydraulics design," in *Fast Breeder Reactors*, New York, Pergamon Press, 1981, pp. 376-377.

[85] M. Morris, "Factorial Sampling Plans for Preliminary Computational Experiments," *Technometrics,* vol. 33, no. 2, pp. 161-174, 1991.

[86] I. Sobol, "On the distribution of points in a cube and the approximate evaluation of integrals," *USSR Computational Mathematics and Mathematical Physics,* vol. 7, pp. 86-112, 1967.

[87] A.Gandini, G.Palmioti and M.Salvatores, "Equivalent Generalized Perturbation Theory (EGPT)," *Annals Nuclear Energy,* 1975.

[88] C. De Saint Jean, P. Archier, G. Noguere, O. Litaize, C. Vaglio, D. Bernard and O.Leray, "Estimation of multi-group cross section covariances of 238,235U, 239Pu, 241Am, 56Fe, 23Na and 27Al," in *PHYSOR2012*, Knoxville, USA, 2012.

[89] J. Droin, N. Marie, A. Bachrata, F. Bertrand, E.Merle and J.-M. Seiler, "Physical tool for Unprotected Loss Of Flow transient simulations in a Sodium Fast Reactor," *Annals of nuclear energy,* vol. 106, pp. 195-210, 2017.

[90] M. Chadwick, M. Herman, P. Oblozinský, M. Dunn, Y. Danon, A. Kahler, D. Smith, B. Pritychenko, G. Arbanas, R. Arcilla, R. Brewer, D. Brown, R. Capote, A. Carlson, Y. Cho, H. Derrien, K. Guber, G. Hale, S. Hoblit, S. Holloway and T. Johnson, "ENDF/B-VII.1 Nuclear Data for Science and Technology: Cross Sections, Covariances, Fission Product Yields and Decay Data," *Nuclear Data Sheets,* vol. 112, pp. 2887-2996, 2011.

[91] IAEA, "Status of minor actinides fuel development," IAEA, Vienna, 2009.

[92] A. Bychkov, O.V.Skiba, M. K. A.A Mayorshin, O. Shishalov, I. Zhemkov, V. Kisly and L. Babikov, "Burning of minor actinides in fuel cycle of the fast reactor : the DOVITA programme - results of the ten years activites," in *7th IEMPT*, Jeju (ROK), 2002.

[93] C. Prunier, F. Boussard, L. Koch and M. Coquerelle, "Some specific aspects of homogeneous Am and Np based fuels transmutation through the outcomes of the superfact experiment in PHENIX fast reactor," in *GLOBAL*, 1993.

[94] Z. Kolarik and R. Schuler, "Separation of neptunium from plutonium and uranium in the PUREX process," in *Symposium on Liquid–Liquid Extraction Science*, 1984.

[95] R. Sanchez, D. Loaiza, R. Kimpland, D. Hayes, C. Cappiello and M. Chadwick, "Criticality of a 237Np Sphere," *Nuclear science and engineering,* vol. 158, no. 1, pp. 1-14, 2008.

[96] D. Efurd, W. Runde, J. Banar, D. Janecky, J. Kaszuba, P. Palmer, F. Roensch and C. Tait, "Neptunium and plutonium solubility in a Yucca Mountain ground water," *Environ. Sci. Tec.,* no. 32, pp. 3893-3900, 1998.

[97] C. Chabert, D. Warin, J. Milot, A. Saturnin and A. Leudet, "Impact of minor actinide transmutation options on interim storage and geological disposal," in *IEMPT*, Prague, 2012.

[98] L.Buiron, B.Fontaine and L.Andriolo, "Transmutation abilities of the SFR low void effect core concept 'CFV' 3600 MWth," in *ICAPP2012*, Chicago, 2012.

[99] NEA, "Status and assessement of fission products and minor actinides partitionning and transmutation," NEA, Paris, 1999.

[100] M. Salvatores, A. Zaetta, C. Girard, M. Delpech, I. Slessarev and J. Tommasi, "Nuclear Waste Transmutation," *AppL Radiat. Isot.,* vol. 46, no. 6/7, pp. 681-687, 1995.

[101] NEA, "Homogeneous versus heterogeneous recycling of transuranics in fast nuclear reactors," NEA, Paris, 2012.

[102] C. De Saint Jean, "Americium once-through of moderated targets in a CAPRA core," in *Seminar Int. CAPRA conf*, Karlsruhe, 1998.

[103] H. Matzke, V. Rondinella and T. Weiss, "Materials research on inert matrices: a screening study," *Journal of Nuclear Materials,* Vols. I-II, no. 274, pp. 47-53, 1999.

[104] N. Chauvin, R. Konings and H. Matzke, "Optimisation of inert matrix fuel concepts for americium transmutation," *Journal of Nuclear Materials,* Vols. I-II, no. 274, pp. 105-115, 1999.

[105] E. L. Ebert, G. Modolo, D. B. M. Cheng, M. Steppert and C. Walther, "Dissolution studies on molybdenum-based inert matrix fuels for the transmutation of minor actinides," in *SACSESS*, Warsaw, 2015.

[106] IAEA, "Thorium fuel cycle — Potential benefits and challenges," IAEA, Vienne, 2005.

[107] P. Hania and F. Klaassen, "Volume 3: Advanced Fuels/Fuel Cladding/Nuclear Fuel Performance Modeling and Simulation," in *Comprehensive Nuclear materials*, 2012, pp. 87-108 .

[108] C. Lombardi, L. Luzzy, E. Padovani and F.Vettraino, "Thoria and inert matrix fuels for a sustainable nuclear power," *Progress in Nuclear Energy,* vol. 50, pp. 944-953, 2008.

[109] W. S. You and S. G. Hong, "A neutronic study on advanced sodium cooled fast reactor cores withthorium blankets for effective burning of transuranic nuclides," *Nuclear Engineering and Design ,* vol. 278, pp. 274-286, 2014.

[110] M. Ozawa, K. Yoshikazu, N. Kazunori and T. Yasumasa, "process, Separation of actinides and fission products in high-level liquid wastes by the improved TRUEX," *Journal of Alloys and Compounds,* Vols. 271-273, pp. 538-543, 1998.

[111] S.Bays, "Heterogeneous transmutation sodium fast reactor," INL, Idaho Falls, 2008.

[112] G. Kessler, "Plutonium denaturing by Pu-238," *Nuclear Science and Engineering,* vol. 155, no. 1, pp. 53-73, 2007.

[113] Y. Gao, W. Zheng, X. Cao and S. Chen, "Influence of alpha and gamma radiolysis on Pu retention in the solvent TBP/kerosene," *Nukleonika,* vol. 59, no. 4, pp. 123-128, 2014.

[114] F.Varaine, L.Buiron, L.Boucher and C.Chabert, "Heterogeneous recycling in SFR core periphery," in *PHYSOR*, Interlaken, 2008.

[115] F. Varaine, C. Chabert, G. Youinou and W. D., "Transmutation in industrial thermal reactors (PWR)," in *European Nuclear Conference*, Versailles, 2005.

[116] H. Golfier, M. Rohart, S. Aniel, J. Bergeron and J.-P. Deffain, "Plutonium and Minor Actinides recycling in PWRs with new APA concepts," in *GLOBAL*, Paris, 2001.

[117] T. A. Taiwo, T. K. Kim, J. A. Stillman, R. N. Hill, M. Salvatores and P. J. Finck, "Assessment of a heterogeneous PWR assembly for plutonium and minor actinide recycle," *Nuclear Technology,* vol. 155, no. 1, pp. 34-54, 2005.

[118] G. Youinou, A.Zaetta, A.Vasile, M. Delpech, M. Rohart and J. Guillet, "Heterogeneous assembly for plutonium multi-recycling in PWRs : the CORAIL concept," in *GLOBAL*, Paris, 2001.

[119] C. Degueldre and J. Paratte, "Concepts for an inert matrix fuel, an overview," *Journal of nuclear materials,* vol. 274, no. 1-2, pp. 1-6, 1999.

[120] K. Lipkina, A. Savchenko, M. Skupov, A. Glushenkov, A. Vatulin, O. Uferov, Y. Ivanov, G. Kulakov, S. Ershov, S. Maranchak, A. Kozlov, E. Maynikov and K. Konova, "Metallic inert matrix fuel concept for minor actinides incineration to achieve ultra-high burn-up," *Journal of Nuclear Materials,* vol. 452, no. 1-3, pp. 378-381, 2014.

[121] Y. Guérin, N. Cocuaud, T.Duverneix, J. Faugère and C.Morin, "Transmutation of minor actinides in PWR : preparation of the actineau experiments," in *GLOBAL93*, Seattle, 1993.

[122] J. Guidez, P. Chaucheprat, B. Fontaine, E. Brunon, L. Martin, D. Warin, A. Zaetta and F. Sudreau, "Phenix: the irradiation program for transmutation experiments," in *8 IEMPT*, Las Vegas, 2004.

[123] R. Hania, "Final Report Summary - FAIRFUELS (FAbrication, Irradiation and Reprocessing of FUELS and targets for transmutation)," European Commision, Brussels, 2016.

[124] C. Fazio, M. Salvatores and W. Yang, "Down selection of partitionning routes and transmutation fuels for P&T strategies implementation," in *GLOBAL*, Boise, Idaho, 2007.

[125] C. de Saint Jean, J. Tommasi, F. Varaine, N. Schmidt and D. Plancq, "Americium and curium heterogeneous transmutation in moderated S/ A in the framework of CNE scenarios studies," in *GLOBAL2001*, Paris, 2001.

[126] D. Olander, E. Greenspan, H. D. Garkisch and B. Petrovic, "Uranium–zirconium hydride fuel properties," *Nuclear Engineering and Design,* vol. 239, no. 8, pp. 1406-1424, 2009.

[127] G. Rimpault, P. Richard, L. Mansani, F. Frogheri, A. Woaye-Hune, S. Ehster-Vignoud, S. Larmignat, A. Mueller, J. Biarotte and e. a. C. Artioli, "General Synthesis Report of the Different ADS Design Status. Establishment of a Catalogue of the R&D needs.," EC-FP6 IP EUROTRANS, 2010.

[128] H. Abderrahim and e. al, "MYRRHA: A multipurpose accelerator driven system for research & development," *Nuclear Instruments and Methods in Physics Research Section A: Accelerators, Spectrometers, Detectors and Associated Equipment,* vol. 463, no. 3, pp. 487-494, 2001.

[129] P. Baeten, M. Schyns, R. Fernandez, D. D. Bruyn and G. V. d. Eynde, "MYRRHA: A multipurpose nuclear research facility," in *3rd European Energy Conference*, E2C, 2013.

[130] F. Lelievre, Stratégies pour l'incinération de déchets nucléaires dans des réacteurs hybrides, Orsay: Université Paris Sud, 1998.

[131] T. Mehlhorn, B. Cipiti, C. Olson and G. Rochau, "Fusion–fission hybrids for nuclear waste transmutation: A synergistic step between Gen-IV fission and fusion reactors," *Fusion Engineering and Design,* vol. 83, no. 7-9, pp. 948-593, 2008.

[132] D. Wade and Y. Chang, "The integral fast reactor (IFR) concept: Physics of operation and safety," in *American Nuclear Society international meeting on advances in reactor physics, mathematics and computation*, Paris, 1988.

[133] Y. Chang, "The Integral Fast Reactor," in *Water reactor safety information meeting*, Gaithersburg, Maryland, 1988.

[134] C. Prunier, Y. Guérin, J. Faugère, N. Cocuaud and J. Adnet, "The CEA SPIN program : minor actinides fuels and targets aspects," *Nuclear science and technology,* vol. 120, no. 2, pp. 110-120, 1997.

[135] N. Chauvin and J. Babelot, "Rapport de synthèse commun CEA/ITU sur l'expérience SUPERFACT1," CEA, Cadarache, 1996.

[136] D. Sood, "The role sol–gel process for nuclear fuels-an overview," *Journal of Sol-Gel Science and Technology,* vol. 59, no. 3, pp. 404-416, 2011.

[137] H. Ohta, T. Ogata and K. N. a. T. Koyama, "Development of minor actinides transmutation by CRIEPI," in *IEMPT*, San Francisco, 2010.

[138] B. Hilton, D. Porter and S. Hayes, "AFC-1 transmutation fuels post-irradiation hot cell examination 4 to 8 at % final report," Idaho National Laboratory, Idaho Falls, 2006.

[139] H. J. M. Chichester, "Postirradiation, Irradiation and Examination of AFC-1Transmutation Metallic Fuels for Fast Reactors," in *Fast Reactors*, Paris, 2013.

[140] M. Meyer, S. Hayes, W. Carmack and H. Tsai, "The EBR-II X501 minor actinide burning

experiment," *Journal of Nuclear Materials,* vol. 392, pp. 176-183, 2009.

[141] E. D'Agata, P. Hania, S. Bejaoui, C. Sciolla, T. Wyatt, M. Hannink, N. Herlet and A. Jankowiak, "The results on irradiation experiment MARIOS on americium transmutation," *Annals of nuclear energy,* vol. 62, pp. 40-49, 2013.

[142] Z. Yoshida, S. G. Johnson, T. Kimura and J. R. Krsul, "Neptunium," in *The Chemistry of the Actinide and Transactinide Elements*, Springer, 2005, pp. 699-785.

[143] G. Uchiyama and H. e. al, "Parc process as advanced PUREX process," in *NUCEF 2001*, Tokai, 2001.

[144] C. Rostaing, C. Poinssot, D. Warin, P. Barona and B. Lorrain, "Development and validation of the EXAm separation process for single Am reprocessing," in *ATALANTE*, 2012, 2012.

[145] C. Poinssot, C.Rostaing, P.Baron, D. Warin and B.Boullis, "Main results of the French Program on Partitioning of minor actinides : a significant improvement towards nuclear waste reduction," in *Atalante 2012*, Marcoule, 2012.

[146] B. J. Mincher, "8 - Radiation chemistry in the reprocessing and recycling of spent nuclear fuels," in *Reprocessing and Recycling of Spent Nuclear Fuel*, Woodhead Publishing, 2015.

[147] J. Laidler, J. Battles, W. Miller, J. Ackerman and E. Carls, "Development of pyroprocessing technology," *Progress in Nuclear Energy,* vol. 31, no. 1-2, pp. 131-140, 1997.

[148] M. F. Simpson, "Developments of Spent Nuclear Fuel Pyroprocessing Technology at Idaho National Laboraty," Idaho National Laboratory , Idaho Falls, 2012.

[149] R. Konings, Comprehensive Nuclear Materials, Newnes, 2012.

[150] J. Wallenius, K. Tucek and W. Gudowski, "Safety analysis of nitride fuels in cores dedicated to waste transmutation," in *IEMPT*, Madrid, 2000.

[151] K. Kawashima, T. Ogawa, S. Ohki, T. Okubo and T. Mizuno, "Fast reactor core design considerations from proliferation resistance aspects," in *FR09*, Kyoto, Japan, 2009.

Résumé en français :
La transmutation des actinides mineurs est une solution inscrite dans la loi de 2006 sur la gestion des déchets nucléaires à long terme. Une approche possible pour implémenter cette technique consiste à récupérer ces noyaux lourds lors du retraitement du combustible nucléaire et à les recharger dans le cœur d'un réacteur pour les faire fissionner et ainsi obtenir des produits de fission à vie plus courte. Cependant, l'ajout d'actinides mineurs dans le cycle du combustible nucléaire entraine l'apparition de pénalités, tant sur le comportement du réacteur associé que sur les différentes étapes du retraitement. On observe ainsi une modification des coefficients de contre réactions du cœur, ou une augmentation de la puissance résiduelle ou de la source neutron des combustibles irradiés.

Après une analyse exhaustive des impacts de la transmutation, une méthodologie d'optimisation du cœur d'un réacteur est ici développée avec prise en compte de l'ensemble des contraintes liées au cycle du combustible et au fonctionnement du réacteur. Pour le mode hétérogène, dans lequel les actinides mineurs sont chargés dans des assemblages dédiés placés en périphérie du cœur, il est démontré que l'utilisation d'éléments légers pour modérer le spectre dans les cibles est une solution optimale, y compris en tenant compte des impacts négatifs sur le cycle.

Pour le mode homogène, où les actinides mineurs sont directement dilués dans le combustible du cœur, il est démontré que les cœurs à faible vidange présentant des hétérogénéités axiales ne sont que peu impactés par le chargement en actinides mineurs pour les transitoires de type perte de débit. On montre également que le design d'un cœur pour le transmutation doit résulter d'un arbitrage entre les performances pour un transitoire de perte de débit et celles pour un transitoire de type insertion de réactivité. Enfin, il a été démontré que quelle que soit l'approche envisagée, les contraintes liées au cycle présentent des défis que seule une importante R&D dans ce domaine pouvait surmonter.

English summary:
Minor actinides transmutation is a solution written in the 2006 law on nuclear waste management. One option to carry out transmutation is to recover these heavy nuclides during fuel reprocessing and load them again in reactor cores to achieve fission and obtain shorter-lived fission products. However, minor actinides loading in the nuclear fuel cycle leads to penalties on core transient behavior and fuel reprocessing, such as a modification of core feedback coefficients or a higher neutron source and decay heat of the spent fuel.

Following a complete analysis of the transmutation impacts, an optimization methodology of the reactor core taking into account all the fuel cycle and core behavior constraints is developed here. For the heterogeneous mode, where minor actinides are loaded in dedicated targets located at the core periphery, it is shown that the use of light elements to locally moderate the neutron spectrum in the blankets is an optimal solution, even when considering the negative impacts on the fuel cycle.

For the homogeneous mode, where minor actinides are directly mixed with the fuel, it is shown that low void cores with axial heterogeneities are not impacted by minor actinides loading for loss-of-flow transients. It is demonstrated that core design results from a balance between core behavior in loss-of flow transient and reactivity insertion transient. Finally, it is shown that regardless of the minor actinides transmutation mode envisaged, fuel cycle constraints were challenging and requires significant R&D in support.